Proceedings of the North American Congress on Biomechanics

combined with
The Tenth Annual Conference of
The American Society of Biomechanics (ASB)
and
The Fourth Biannual Conference of the
Canadian Society for Biomechanics (CSB)/
Société Canadienne de Biomécanique (SCB)

Human Locomotion IV
La locomotion humaine IV

Montréal (Québec), Canada
25, 26, 27 August 1986

Volume II

Proceedings of the North American Congress on Biomechanics

combined with
The Tenth Annual Conference of
The American Society of Biomechanics (ASB)
and
The Fourth Biannual Conference of the
Canadian Society for Biomechanics (CSB)/
Société Canadienne de Biomécanique (SCB)

Human Locomotion IV
La locomotion humaine IV

Volume II

Montreal (Quebec), Canada

Published by the Organizing Committee

P. Allard and M. Gagnon, Co-chairpersons, G. Drouin, M. Duhaime, G. Dumas, C. Gagnon, M. Lamontagne, C. Putman, C.-H. Rivard, B. Roy, C. Sicard

Additional copies of Volumes I and II may be obtained from:

Secretariat ASB
Thomas P. Andriacchi
Secretary-Treasurer
Dept. of Orthopaedic Surgery
Rush - Presbyterian - St. Luke's
Medical Center
1753 West Congress Parkway
Room 1471 Jelke
Chicago, Illinois, 60612

Secretariat CSB/SCB
School of Physical and
Health Education
Queen's University
Kingston, Ontario
K7L 3N6

Price:

$35.00 (U.S.) cheque or money order payable to American Society of Biomechanics to be forwarded to Secretariat ASB.

$50.00 (Can.) cheque or money order payable to Canadian Society for Biomechanics to be forwarded to Secretariat CSB/SCB.

North American Congress on Biomechanics

NACOB

August 25-26-27, 1986
Montréal, Québec, Canada

CO-CHAIRMEN

Paul Allard
Dépt. d'Éducation Physique
Université de Montréal, PQ

Micheline Gagnon
Dépt. d'Éducation Physique
Université de Montréal, PQ

ORGANIZING COMMITTEE

Gilbert Drouin
Dépt. de Génie Mécanique
École Polytechnique
de Montréal, PQ

Morris Duhaime
Dépt. de Chirurgie
Hôpital Sainte-Justine, PQ

Geneviève Dumas
Dept. of Mechanical
Engineering
Queen's University, ON

Carole Gagnon
Dépt. d'Éducation Physique
Université de Montréal, PQ

Mario Lamontagne
Dépt. de Kinanthropologie
Université d'Ottawa, ON

Carol Putnam
School of Physical Education
Dalhousie University, NS

Charles-Hilaire Rivard
Dépt. d'Orthopédie
Hôpital Sainte-Justine, PQ

Benoit Roy
Dépt. d'Éducation Physique
Université Laval, PQ

Claude Sicard
Dépt. d'Éducation Physique
Université de Montréal, PQ

The Executive Boards which have governed the American Society of Biomechanics (ASB) and the Canadian Society for Biomechanics (CSB/SCB) during the past year comprise the following members:

ASB
1986

Savio L-Y. Woo
President
University of California
San Diego

Peter R. Cavanagh
President-Elect
Penn State University

Thomas P. Andriacchi
Secretary/Treasurer
Rush-Presbyterian-St. Luke's
Medical Center

Paul Allard
Meeting Chairperson
Université de Montréal

Carol Putnam
Program Chairperson
Dalhousie University

Richard A. Brand
Nominating Committee
Chairperson
University of Iowa Hospital

Ronald F. Zernicke
Education Committee
Chairperson
University of California

Roger M. Enoka
Membership Committee
Chairperson
University of Arizona

Secretariat ASB
Thomas P. Andriacchi
Secretary-Treasurer
Dept. of Orthopaedic Surgery
Rush-Presbyterian-St. Luke's
Medical Center
1753 West Congress Parkway
Room 1471 Jelke
Chicago, Illinois, 60612
(312) 942-5813

CSB/SCB
1985-1986

J. Gavin Reid
President
Queen's University

Carol Richards
Secretary - Treasurer
Université Laval

Micheline Gagnon
Conference Chairperson
Université de Montréal

Susan Tupling
Newsletter Editor
University of Toronto

Sandy Thorton-Trump
Past Conference Chairman
University of Manitoba

Secretariat CSB/SCB
School of Physical and
Health Education
Queen's University
Kingston, Ontario,
K7L 3N6

ASB
founded 1977
AMERICAN SOCIETY OF BIOMECHANICS

DEPARTMENT OF ORTHOPEDIC SURGERY
Rush-Presbyterian-St. Luke's
Medical Center
1753 West Congress Parkway
Room 1471 Jelke
Chicago, Illinois 60612

May 14, 1986

Dear Colleagues:

The field of Biomechanics is large, and the investigators are from many disciplines. As a result, numerous difficulties in communication develop. In particular, there are too many meetings which touch upon Biomechanics, and they are scattered in many different professional societies. Thus, the founding members of the American Society of Biomechanics (ASB), in 1977, formed our Society to provide a forum for the exchange of information and ideas among researchers in Biomechanics. The term "Biomechanics" is used to mean the study of the structure and function of biological systems by means of methods of mechanics. ASB consists of members from five loosely divided disciplines. They include: biological sciences, engineering and applied physics, ergonomics and human factors, health sciences, and exercise and sport sciences.

It is a great honor for me to write this note to welcome you to the first combined meeting of the ASB and the Canadian Society of Biomechanics (CSB). This meeting also marks the Tenth Annual Conference of ASB and the Fourth Biannual Conference of CSB. I believe this "crossing the border" meeting will greatly enhance the advances of Biomechanics by bringing investigators from North America under one roof. I am certain that this Congress is only the beginning. I anticipate the combined meeting will blossom and attract increasing numbers of quality papers and participants, as well as to become a focal point for discussion of applications of mechanics to biological and biomedical problems in North America.

The 1986 NACOB is particularly exciting, as we have outstanding invited keynote speakers from Europe including Drs. Cappozzo (Italy), Alexander (United Kingdom), and Huiskes (The Netherlands). Other keynote lecturers will include Drs. Chaffin, Bramble, Norman and Winter from the North American continent. We will also have the Borelli Award lecture by Dr. M.R. Yeadon (Canada). I am sure all will generate new interest, enthusiasm, further participation and collaboration. We thank them sincerely for taking time to join us.

I very much look forward to participating in this three-day conference. The papers are of high quality, and the number of participants is by far the largest for both societies. I look forward to meeting and welcoming you in person during this first North American Congress on Biomechanics.

Sincerely yours,

Savio L-Y. Woo, Ph.D.
President

SOCIÉTÉ CANADIENNE
DE
BIOMÉCANIQUE.

CANADIAN SOCIETY
FOR
BIOMECHANICS

WELCOME

The Canadian Society for Biomechanics is pleased to welcome guests and delegates from overseas and across this continent to the North American Congress on Biomechanics in Montreal, Canada. This beautiful city, first discovered in 1535, is located on the Island of Montreal, an extinct volcano. It is the second largest city in Canada and the largest French-speaking city outside of France. We do hope that you find time to tour the city, sample its cuisine and enjoy its night life.

This is the first combined meeting of the American Society of Biomechanics and the Canadian Society for Biomechanics. We are honoured to share in this meeting with our colleagues from the South. The scientific program reflects the breadth and depth of research in biomechanics. May we all benefit in the interchange of information and from the social interaction that will occur. The program provides the opportunity for the fostering of new ideas, rekindling of old friendships and the development of new ones, all of which should well be the main purpose of this Congress.

The organizing committee has provided the forum and now depends on the individual commitment and participation of the delegates to render the Congress successful.

BIENVENUE

La Société Canadienne de Biomécanique est heureuse de souhaiter la bienvenue aux unités et délégués d'outre-mer et de ce continent pour le Congrès Nord-américain de Biomécanique qui a lieu à Montréal, Canada. Cette belle ville, d'abord découverte en 1535, est située sur l'Ile de Montréal, un volcan éteint. C'est la deuxième plus grande ville du Canada et la plus grande ville francophone à l'extérieur de la France. Nous espérons que vous trouverez le temps de visiter la ville, d'essayer ses styles culinaires et d'apprécier sa vie nocturne.

Il s'agit de la première réunion conjointe de l'American Society of Biomechanics et de la Société Canadienne de Biomécanique. C'est pour nous un honneur de prendre part à cette réunion avec nos collègues du Sud. Le programme scientifique reflète l'ampleur et la profondeur de la recherche en biomécanique. Puissions-nous tous bénéficier des échanges d'information et des interactions sociales qui auront lieu. Le programme donne l'opportunité de stimuler de nouvelles idées, de faire renaître d'anciennes amitiés et d'en développer de nouvelles; tous ces aspects devraient effectivement constituer le but principal de ce Congrès.

Le comité organisateur a fourni un forum et il dépend maintenant de l'engagement individuel et de la participation des délégués d'assurer la réussite du Congrès.

J. Gavin Reid
President
CSB/SCB

CONGRESS SCHEDULE

Le Grand Hôtel, Montréal

Sunday Evening, 24 August 1986

19:00 - 22:00	Registration (Foyer du banquet)
19:00 - 22:00	Welcoming Reception (Cartier A-B)

Monday, 25 August 1986

07:30	Registration and Information (Foyer du banquet)
08:00	Announcements and Welcoming Address (Room A)
08:15	Keynote Lecture 1 • **Dr. Donald B. Chaffin** (Room A), University of Michigan, Ann Arbor, MI, U.S.A.
08:45	SESSION 1 - Joint Mechanics (Room A) SESSION 2 - Human Locomotion IV Walking and Running (Room B)
10:15	Intermission
10:45	Keynote Lecture 2 • **Dr. Denis Bramble** (Room A), University of Utah, Salt Lake City, UT, U.S.A.
11:15	SESSION 3 - Muscle I (Room A) SESSION 4 - Human Locomotion IV Foot Dynamics (Room B)
12:30	Lunch
12:30	ASB Executive Meeting CSB/SCB Executive Meeting
13:30	SESSION 5 - Human Locomotion IV - Poster Session I (Régence A)
14:45	Intermission
15:00	Borelli Lecture • **M.R. Yeadon** (Room A), University of Calgary, Calgary, AB, Canada
15:30	SESSION 6 - Human Locomotion IV Rehabilitation (Room A) SESSION 7 - Sport (Room B)

Tuesday, 26 August 1986

08:00	Keynote Lecture 3 • **Dr. David A. Winter** (Room A), University of Waterloo, Waterloo, ON, Canada.
08:30	SESSION 8 - Occupational Biomechanics (Room A) SESSION 9 - Muscle II (Room B)
10:00	Intermission
10:30	Keynote Lecture 4 • **Dr. R. McNeill Alexander** (Room A), University of Leeds, Leeds, United Kingdom.
11:00	SESSION 10 - Human Locomotion IV Gait (Room A) SESSION 11 - Muscle Control (Room B)
12:15	ASB Presidential Address and Business Meeting (Room B) CSB Business Meeting (Room A)
13:00	Lunch
14:00	Laboratory Tours
19:30	Banquet

Wednesday, 27 August 1986

07:00	ASB Executive Meeting
08:00	Keynote Lecture 5 • **Dr. Rik Huiskes** (Room C), University of Nijmegen, Nijmegen, Netherlands.
08:30	SESSION 12 - Spine (Room C) SESSION 13 - Human Locomotion IV (Room B), Orthopaedic Gait
10:00	Intermission
10:30	Keynote Lecture 6 • **Dr. Robert W. Norman** (Room C), University of Waterloo, Waterloo, ON, Canada.
11:00	SESSION 14 - Poster Session II (Régence A)
12:15	Lunch
13:30	SESSION 15 - Bone Mechanics (Room C) SESSION 16 - Human Locomotion IV (Room B), Sport
15:00	Keynote lecture 7 • **Dr. Aurelio Cappozzo** (Room C), University of Rome, Rome, Italy.
15:30	Intermission
15:45	SESSION 17 - Human Locomotion IV (Room C), Altered Gait SESSION 18 - Orthopaedic Fixation (Room B)

Please note the following locations:
Audio-visual room: (Le Royer)
Secretariat: (Vitré)
Exhibits: (Régence A)

CONGRESS PROGRAM

Monday, August 25

Morning

08:00 - 08:15 Announcements and Welcoming Address (Room A)

08:15 - 08:45 **Keynote 1** (Room A)
Dr. Donald B. Chaffin, University of Michigan, Ann Arbor, MI, USA.
LOW BACK MUSCLE MODELS FOR LIFTING EVALUATION

SESSION 1

- JOINT MECHANICS (Room A)
CHAIRPERSONS:
I.A.F. Stokes & S. Naumann

08:45 - 09:00 DIFFERENTIATION OF COMPONENTS OF RESISTANCE TO PASSIVE MOVEMENT USING VOLUNTARY MANEUVERS
S. Desjardins, C.L. Richards, M. Filion, D. Gravel & V. Piette
Hôpital l'Enfant-Jésus and Laval University, Quebec, PQ.

09:00 - 09:15 IN VIVO MEASUREMENTS OF PASSIVE MOMENTS OF THE HUMAN HIP
M. Vrahas, T. Brown, J. Andrews, R. Brand & D. Pederson
University of Iowa, Iowa City, IA.

09:15 - 09:30 LOAD TRANSMISSION OF THE WRIST JOINT AND PATHOMECHANISM OF KIENBÖCK'S DISEASE
H. Tsumura, S. Himeno, K.N. An & E.Y.S. Chao
Mayo Clinic, Rochester, MN.

09:30 - 09:45 ASYMMETRICAL KNEE LAXITIES: AN OBJECTIVE EVALUATION
T.B. Hoshizaki, H. Sveistrup & G. Vagenas
McGill University, Montreal, PQ.

09:45 - 10:00 ANALYSIS OF SQUEEZE-FILM LUBRICATION IN HUMAN JOINTS BASED ON NON-NEWTONIAN PROPERTIES OF SYNOVIAL FLUID
T.J. Pratt & D.F. James
University of Toronto, Toronto, ON.

10:00 - 10:15 IN-VIVO KINEMATIC PROPERTIES OF THE HUMAN SHOULDER COMPLEX
A.E. Engin & S.M. Chen
Ohio State University, Columbus, OH.

SESSION 2

- HUMAN LOCOMOTION IV
- WALKING AND RUNNING
(Room B)
CHAIRPERSONS:
S. Olney & P.E. Martin

08:45 - 09:00 VISUAL ASSESSMENT OF HUMAN GAIT - A RELIABILITY STUDY
A.E. Patla & S.D. Clouse
University of Waterloo, Waterloo, ON.

09:00 - 09:15 KNEE BRACE INFLUENCES ON THE SUPPORT PHASE OF RUNNING
K. Knutzen, P. Schot & B.T. Bates
Western Washington University, Bellingham, WA and University of Oregon, Eugene, OR.

09:15 - 09:30 BIOMECHANICAL CHARACTERISTICS OF THE SWING LIMB IN MASTERS RUNNERS
E.M. Roberts, T.K. Cheung, A.A.M. Hafex, S.K. Bullard
University of Wisconsin, Madison, WI and Helwan University, Cairo, Egypt.

09:30 - 09:45 COMPARISON OF TWO ELECTROGONIOMETER PLACEMENTS FOR THE MEASUREMENT OF ANKLE MOVEMENTS DURING GAIT
D. Gravel & C.L. Richards
Laval University, Quebec, PQ.

09:45 - 10:00 CHILD AMPUTEE WALKING AND RUNNING GAIT: A COMPARISON BETWEEN THE SACH AND SINGLE-AXIS FOOT COMPONENTS
B. Brouwer, P. Allard & H. Labelle
McGill University, University of Montreal and Hôpital Sainte-Justine, Montreal, PQ.

10:00 - 10:15 QUANTITATIVE THERAPY CONTROL USING GAIT ANALYSIS
S. Luethi, E. Stuessi & B. Segesser
Federal Institute of Technology, Zuerich and Rennbahn Klinik, Muttenz, Switzerland.

10:15 - 10:45 **Intermission**

10:45 - 11:15 **Keynote 2** (Room A)
Dr. Denis Bramble, *University of Utah, Salt Lake City, UT, USA.*
MECHANICAL AND PHYSIOLOGICAL ISSUES UNDERLYING LOCOMOTOR AND RESPIRATORY COUPLING IN MAMMALS.

SESSION 3

- MUSCLE I (Room A)
CHAIRPERSONS:
F.E. Zajac & M. Lamontagne

11:15 - 11:30 PHYSIOLOGICAL AND MECHANICAL FACTORS INFLUENCING THE PREDICTION OF MUSCLE FORCES ABOUT THE KNEE JOINT DURING GAIT
R.P. Mikosz
Rush-Presbyterian - St. Luke's Medical Center, Chicago, FL.

11:30 - 11:45 ELECTRO-MECHANICAL ADAPTATION TO MUSCULAR STRENGTH TRAINING
G.A. Wood, K.P. Singer & A.G. Cresswell
University of Western Australia, Australia.

11:45 - 12:00 PREDICTION OF ANKLE MOMENTS IN GAIT USING CALIBRATED EMG-FORCE-JOINT ANGLE RELATIONSHIPS
S.J. Olney, M.P. Griffin, P.A. Costigan & U.P. Wyss
Queen's University, Kingston, ON.

12:00 - 12:15 THE EFFECT OF THE MUSCLES MOMENT ARM ON ITS EMG-FORCE RELATIONSHIPS
M. Solomonow, R. Chuinard & R. D'Ambrosia
Louisiana State University Medical Center, New Orleans, LA.

12:15 - 12:30 COMPUTER GRAPHICS OF MUSCLE KINEMATICS AND ELECTROMYOGRAPHY IN GAIT
B. McFadyen, D. Winter, B. Day & F. Burkowski
University of Waterloo, Waterloo, ON.

SESSION 4

- HUMAN LOCOMOTION IV
- FOOT DYNAMICS (Room B)
CHAIRPERSONS:
G.A. Valiant & K.R. Williams

11:15 - 11:30 BIOMECHANICAL ASPECTS OF SHOCK ABSORBING DEVICES
A.S. Voloshin
Lehigh University, Bethlehem, PA.

11:30 - 11:45 DISCRETE IN-SHOE PLANTAR STRESS VARIATIONS WITH RUNNING SPEED
T.S. Gross & R.P. Bunch
Converse Biomechanics Laboratory, North Reading, MA.

11:45 - 12:00 THE INFLUENCE OF LATERAL HEEL FLARE ON PRONATION AND IMPACT FORCES
B.M. Nigg, J. Denoth & R. Glover
University of Calgary, Calgary, AB and Federal Institute of Technology, Zurich, Switzerland.

12:00 - 12:15 EVALUATION OF SHOE-ORTHOTIC INTERACTIONS USING AN IN-SHOE PRESSURE SENSOR SYSTEM
J. Hamill, B.T. Bates, M.D. Ricard & M.K. Miller
Southern Illinois University, Carbondale, IL and University of Oregon, Eugene, OR.

12:15 - 12:30 EFFECTS OF FOOT INSERTS ON THE GAIT PARAMETERS OF RHEUMATOID ARTHRITIC PATIENTS
P. Allard, W. Loo & H. Tannenbaum
University of Montreal, Sainte-Justine Hospital and Montreal General Hospital, Montreal, PQ.

Afternoon

SESSION 5

- HUMAN LOCOMOTION IV
- Poster Session I (Régence A)
CHAIRPERSONS:
G. Drouin & T. Brown

13:30 - 14:45

PERFORMANCE CHARACTERISTICS OF THE BIOMECHANICS FORCE PLATE
D.A. Schieb
Kistler Instrument Corporation, Amherst, NY.

A CLINICALLY VIABLE FORCE PLATFORM MEASUREMENT TECHNIQUE FOR THE VISUAL AND NUMERICAL ASSESSMENT OF FORCE DISTRIBUTIONS BENEATH THE FEET
C.D. MacKinnon & C.M. Godfrey
Wellesley Hospital, Toronto, ON.

A TECHNIQUE FOR NORMALIZING CENTER OF PRESSURE PATHS
H.U. Motriuk
University of Calgary, Calgary, AB.

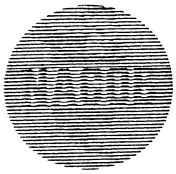

EMG PATTERNS OF THE QUADRICEPS DURING TREADMILL RUNNING: A DESCRIPTION OF PATELLOFEMORAL PAIN SYNDROME
D. MacIntyre & D.G.E. Robertson
University of British Columbia, Vancouver, BC and University of Ottawa, Ottawa, ON.

INTEGRATED BIOMECHANICAL & EMG ANALYSIS OF STAIR WALKING
B. McFadyen & D. Winter
University of Waterloo, Waterloo, ON.

THE USE OF MULTIPLE REGRESSION IN THE DESIGN AND TESTING OF DYNAMIC MUSCLE MODELS
J.J. Dowling & R.W. Norman
University of Waterloo, Waterloo, ON.

A DIMENSIONLESS MUSCULOTENDON ACTUATOR MODEL FOR USE IN COMPUTER SIMULATIONS OF BODY COORDINATION: STATIC PROPERTIES
F.E. Zajac, P.J. Stevenson & E.L. Topp
Standford University, Standford and Veterans Administration Medical Center, Palo Alto, CA.

MUSCULOTENDON ENERGETICS OF HUMAN JUMPS
M.G. Hoy, F.E. Zajac, E.L. Topp, C.T. Cady, M.E. Gordon & W.S. Levine
Veterans Administration Medical Center, Palo Alto, CA; Standford University, Standford, CA and University of Maryland, College Park, MD.

ELASTIC ENERGY STORAGE DURING SIMPLIFIED JUMPING MOVEMENTS IN MAN
M.R. Shorten, R.T. Mueller & L.B. Cooper
Nike Sports Research Laboratory, Beaverton, OR.

IN-VIVO PASSIVE RESISTIVE PROPERTIES BEYOND THE HUMAN SHOULDER COMPLEX SINUS
A.E. Engin & S.M. Chen
Ohio State University, Columbus, OH.

14:45 - 15:00 **Intermission**

15:00 - 15:30 **BORELLI LECTURE (ROOM A)**
Dr. M.R. Yeadon, *University of Calgary, Calgary, AB, Canada.*
THE BIOMECHANICS OF TWISTING SOMERSAULTS

SESSION 6

- HUMAN LOCOMOTION IV
- REHABILITATION (Room A)
CHAIRPERSONS:
J. Sullivan & M.H. Pope

15:30 - 15:45 FINITE ELEMENT MODEL OF ASYMMETRICAL RIB GROWTH IN SCOLIOSIS
J. Dansereau, I.A.F. Stokes, J.P. Laible & M.S. Moreland
University of Vermont, Burlington, VT.

15:45 - 16:00 THE EFFECT OF LIMITED KNEE-FLEXION RANGE ON PEAK HIP JOINT TORQUES IN HUMANS TRANSFERRING FROM SITTING TO STANDING
S.J. Fleckenstein, R.L. Kirby & D.A. MacLeod
Dalhousie University and Nova Scotia Rehabilitation Centre, Halifax, NS.

16:00 - 16:15 RELIABILITY AND APPLICATION OF A COMPUTERIZED TRIAXIAL ELECTROGONIOMETER FOR THE EVALUATION OF HEAD MOVEMENTS
F. Malouin & J. Préfontaine
Laval University, Quebec, PQ.

16:15 - 16:30 BIOMECHANICAL ASPECTS OF PRECLINICAL DESCRIPTORS OF OSTEOARTHRITIS
J. Alexander, A. Bhattacharya, P. Patel & S Brooks
University of Cincinnati Medical Center, Cincinnati, OH.

16:30 - 16:45 USE OF STATIC PRE-LOADING IN ESTIMATION OF DYNAMIC STRENGTH WITH THE KIN-COM DYNAMOMETER
V. Piette, C. Richards & M. Filion
Hôpital l'Enfant-Jésus, Québec, PQ.

16:45 - 17:00 MUSCLE UTILIZATION IN GAIT DETERMINED BY A PHYSIOLOGICAL CALIBRATION OF EMG
M.C. Normand, C.L. Richards & M. Filion
Université du Québec à Trois-Rivières and Hôpital l'Enfant-Jésus, Québec, PQ.

SESSION 7

- SPORT (Room B)
CHAIRPERSONS:
J. Dapena & D.G.E. Robertson

15:30 - 15:45 THREE MODE PRINCIPAL COMPONENT ANALYSIS OF ARM SEGMENT VELOCITIES IN THROWING
R.J. Neal, C.W. Snyder Jr. & B.D. Wilson
University of Queensland, Australia.

15:45 - 16:00 DYNAMICS OF THE SHOULDER AND ELBOW JOINTS OF THE THROWING ARM DURING A BASEBALL PITCH
M.E. Feltner & J. Dapena
Indiana University, Bloomington, IN.

16:00 - 16:15 A MODEL FOR OPTIMIZING THE TIMING OF THE RELATIVE FORCE PATTERNS OF THE ARMS, TORSO, AND LEGS DURING SPRINGBOARD DIVING TAKE-OFFS
E. Sprigings, G. Watson, E. Haseganu & D. Derby
University of Saskatchewan, Saskatoon, SK.

16:15 - 16:30 AN EXAMINATION OF MECHANICAL ENERGY TRANSFERS AMONGST LOWER EXTREMITY SEGMENTS DURING A KICKING MOTION
P.E. Martin & W.L. Siler
Arizona State University, Tempe, AZ.

16:30 - 16:45 KINEMATICS OF A WORLD RECORD IN THE TRIPLE JUMP
J.A. Miller Jr. & J.G. Hay
University of Iowa, Iowa City, IA.

16:45 - 17:00 FACTORS DETERMINING SQUASH BALL VELOCITY AND IMPLICATIONS FOR THE STROKE
A.E. Chapman
Simon Fraser University, Burnaby, BC.

Tuesday, August 26

Morning

08:00 - 08:30 **Keynote 3** (Room A)
Dr. David A. Winter, *University of Waterloo, Waterloo, ON, Canada.*
STRATEGIES AND CONCERNS REGARDING THE ASSESSMENT OF PATHOLOGICAL GAIT

SESSION 8

- OCCUPATIONAL BIOMECHANICS (Room A)
CHAIRPERSONS:
J.A.A. Miller & M. Lortie

08:30 - 08:45 A MATHEMATICAL MODEL FOR NECK TENSION AS RELATED TO SOURCE DOCUMENT POSITION
N. Hamilton
University of Illinois, Urbana, IL.

08:45 - 09:00 PRESSURE DISTRIBUTION IN OFFICE SEATING
S. Reinecke, G. Weisman, A. Stifter & M.H. Pope
Vermont Rehabilitation Engineering Center and University of Vermont, Burlington, VT.

09:00 - 09:15 BIOMECHANICAL BASIS OF MUSCULOSKELETAL DISORDERS AMONG VISUAL ARTISTS
W. Chang., F.J. Bejjani & D. Chyan
Hospital for Joint Diseases Orthopaedic Institute, New York, NY.

09:15 - 09:30 ARM LIFT STRENGTH AT DIFFERENT REACH DISTANCES
S. Kumar & D. Hill
University of Alberta, Edmonton, AB.

09:30 - 09:45 WORK-ENERGY REQUIREMENTS FOR TRANSLATING AND TURNING PATIENTS IN BED AS EXECUTED BY NURSING AIDES
M. Gagnon, F. Akre, M. Lortie, A. Chehade & F. Kemp
University of Montreal and Institut de recherche en santé et sécurité du Québec, Montréal, PQ.

09:45 - 10:00 POSTURAL KINEMATICS OF TRUMPET PLAYING
N. Halpern & F.J. Bejjani
Hospital for Joint Diseases Orthopaedic Institute, New York, NY.

SESSION 9

- MUSCLE II (Room B)
CHAIRPERSONS:
R. Wells & M.R. Shorten

08:30 - 08:45 INFLUENCE OF THE AMOUNT OF INFORMATION ABOUT MUSCLE PROPERTIES IN THE COST FUNCTION ON THE ESTIMATE OF INDIVIDUAL MUSCLE FORCES
W. Herzog *University of Calgary, Calgary, AB.*

08:45 - 09:00 SURFACE ELECTROMYOGRAPHY OF ILIOPSOAS
N. Evans Stüber & R. Wells
University of Waterloo, Waterloo, ON.

09:00 - 09:15 ISOKINETIC AND ISOMETRIC STRENGTH ANALYSIS OF HIP MUSCULATURE
T.D. Cahalan, S.H. Liu & E.Y.S. Chao
Mayo Clinic, Rochester, MN.

09:15 - 09:30 SYNERGISTIC BEHAVIOUR OF THE TRICEPS SURAE UNDER SUSTAINED SUBMAXIMAL ISOMETRIC CONTRACTIONS
A.V. Sirin & A.E. Patla
University of Waterloo, Waterloo, ON.

09:30 - 09:45 THE PREDICTION OF MUSCLE FORCE USING EMG AND A MUSCLE MODEL
S.C. White & D.A. Winter
University of Wisconsin, Madison, WI and University of Waterloo, Waterloo, ON.

09:45 - 10:00 BIARTICULAR MUSCLES IN MULTISEGMENT LIMBS
R.H. Rozendal, G.J. van Ingen Schenau, M. Bobbert & L.H.V. van der Woude
Vrije Universiteit, Amsterdam, Netherlands.

10:00 - 10:30 **Intermission**

10:30 - 11:00 **Keynote 4** (Room A)
Dr. R. McNeill Alexander, *University of Leeds, Leeds, United Kingdom.*
ELASTIC MECHANISMS IN THE MOVEMENT OF MAMMALS

SESSION 10

- HUMAN LOCOMOTION IV
- GAIT (Room A)
CHAIRPERSONS:
C.L. Richards & M.G. Hoy

11:00 - 11:15 BILATERAL ANALYSIS OF THE LOWER LIMBS DURING WALKING IN NORMAL INDIVIDUALS
S. Ounpuu & D.A. Winter
University of Waterloo, Waterloo, ON.

11:15 - 11:30 ASYMMETRY IN LOADING TIMES BETWEEN THE NATURAL AND PROSTHETIC LIMBS IN THE ABOVE-KNEE AMPUTEE
W. O'Connor
Royal Ottawa Regional Rehabilitation Centre, Ottawa, ON.

11:30 - 11:45 SYSTEM FOR LOCOMOTOR REHABILITATION
H. Barbeau, L. Finch & M. Wainberg
McGill University, Montreal, PQ.

11:45 - 12:00 KINEMATIC ANALYSIS OF GAIT PATTERNS IN UNOPERATED CHILDREN WITH SPASTIC DIPLEGIA
O. Huk, H. Labelle, M. Duhaime & P. Allard
Hôpital Sainte-Justine and University of Montreal, Montreal, PQ.

12:00 - 12:15 HIGH-RESOLUTION REAL-TIME MOVEMENT ANALYSIS AT 100 Hz WITH STROBOSCOPIC TV-CAMERA AND VIDEO-DIGITAL COORDINATE CONVERTER
E.H. Furnée
Delft University of Technology, Delft, Netherlands.

SESSION 11

- MUSCLE CONTROL (Room B)
CHAIRPERSONS:
G.A. Wood & H. Debruin

11:00 - 11:15 THE DEPENDENCE OF THE EMG-FORCE RELATIONSHIP ON THE MUSCLES MOTORUNITS RECRUITMENT RANGE
M. Solomonow, B.-H. Zhou, R. Baratta, H. Shoji & R. D'Ambrosia
Louisiana State University Medical Center, New Orleans, LA.

11:15 - 11:30 FEEDFORWARD POSTURAL CONTROL IN CHILDREN
C.L. Riach & K.C. Hayes
McMaster University, Kingston and Parkwood Hospital, London, ON.

11:30 - 11:45 ELECTROMYOGRAPHIC RESPONSES OF THE LOWER LIMB MUSCULATURE IN SIMULATED POSTURAL AND LOCOMOTOR ACTIVITIES
R. Wells & N. Evans Stüber
University of Waterloo, Waterloo, ON.

11:45 - 12:00 MODULATION OF LIMB DYNAMICS DURING THE LEARNING OF RAPID ARM MOVEMENTS
K. Schneider, R.F. Zernicke, R.A. Schmidt & T.J. Hart
University of California, Los Angeles, CA.

12:00 - 12:15 DOES BICEPS FEMORIS RESPONSE ALWAYS PRECEDE VOLUNTARY ARM RAISES DURING LOCOMOTION IN HUMANS? A.E. Patla
University of Waterloo, Waterloo, ON.

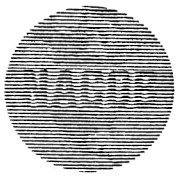

Wednesday, August 27

Morning

08:00 - 08:30 **Keynote 5** (Room C)
Dr. Rik Huiskes, *University of Nijmegen, Nijmegen, Netherlands.*
HUMAN JOINT KINEMATICS: A STRUCTURE BASED APPROACH

SESSION 12

- SPINE (Room C)
CHAIRPERSONS:
J. Dansereau & A.H. Ahmed

08:30 - 08:45 QUANTITATIVE ANATOMY OF TRUNK MUSCLES
G.A. Dumas, M.J. Poulin, B. Roy, M. Gagnon & M. Jovanovic
Queen's University, Kingston; Laval University, Quebec and University of Montreal, Montreal, PQ.

08:45 - 09:00 CORRELATION OF OBJECTIVE MEASURES OF TRUNK MOTION AND MUSCLE FUNCTION WITH LOW BACK DISABILITY RATINGS
J. Triano & A.B. Schultz
National College, Lombard, IL and University of Michigan, Ann Arbor, MI.

09:00 - 09:15 EFFECTS OF CHANGE IN INTRADISCAL FLUID CONTENT ON MECHANICAL RESPONSE OF A LUMBAR MOTION SEGMENT IN COMPRESSION AND EXTENSION
A. Shirazi-Adl & G. Drouin
Ecole Polytechnique de Montréal, Montréal, PQ.

09:15 - 09:30 FAILURE OF INTRA-ABDOMINAL PRESSURIZATION TO REDUCE ERECTOR SPINAE LOADS DURING LIFTING TASKS
M.H. Krag, K.B. Byrne, L.G. Gilbertson & L.D. Haugh
Vermont Rehabilitation Engineering Center, University of Vermont, Burlington, VT.

09:30 - 09:45 VIBRATION AND IMPACT RESPONSE OF THE SEATED HUMAN
M.H. Pope, D.G. Wilder, L. Jorneus, H. Broman, M. Svensson & G. Andersson
University of Vermont, Burlington, VT: Ort. Kir. 1, Sahlgrenska Sjukhuest, Goteborg, Sweden; Chalmers Technical University, Goteborg, Sweden; Rush Presbyterian-St.-Luke's Hospital, Chicago, IL.

09:45 - 10:00 ENERGY TRANSFERS IN THE SPINAL ENGINE
S.A. Gracovetsky & S. Iacono
Concordia University and Diagnospine Research Inc., Montreal, PQ.

SESSION 13

- HUMAN LOCOMOTION IV
- ORTHOPAEDIC GAIT (Room B)
CHAIRPERSONS:
M. Duhaime & B.T. Bates

08:30 - 08:45 FUNCTIONAL ANALYSIS OF HIP RESECTION ARTHROPLASTY
C.M. Tylkowski, J. Chase, R.W. Petty & G. Miller
University of Florida, Gainsville, FL.

08:45 - 09:00 CHANGE IN ADULT ACQUIRED HEMIPLEGIC GAIT PATTERN FOLLOWING SURGICAL CORRECTION OF EQUINUS
R. Sherman, M. Pinzur, P. DiMonte-Levine & J. Trimble
Loyola University Medical Center and Hines VA Hospital.

09:00 - 09:15 ANALYSIS OF CANINE GAIT WITH FORCE PLATFORMS FOLLOWING ANTERIOR CRUCIATE LIGAMENT REPAIR: A PILOT STUDY
B.T. Meller, M.T. Manley, P. Hurley & S. Yoshia
Cleveland Clinic Foundation, Cleveland, OH.

09:15 - 09:30 GAIT OF PATIENTS WITH TOTAL KNEE REPLACEMENTS (TKR)
U.P. Wyss, S.J. Olney, I. McBride & T.D.V. Cooke
Queen's University, Kingston, ON.

09:30 - 09:45 EFFECTS OF PROXIMAL TIBIAL OSTEOTOMY ON KNEE JOINT LOADING
B. Cairns, S. Naumann, P. Tepperman & V. Kekosz
University of Toronto, Toronto, ON.

09:45 - 10:00 BIOMECHANICAL ASSESSMENT OF THE RESULTS OF KNEE SURGERY
M.W. Whittle & R.J. Jefferson
University of Oxford, Headington, Oxford, England.

10:00 - 10:30 **Intermission**

10:30 - 11:00

Keynote 6 (Room C)
Dr. Robert Norman, *University of Waterloo, Waterloo, ON, Canada.*
CAN BIOMECHANICAL SCIENCE BE EFFECTIVE IN AN ELITE ATHLETE DEVELOPMENT PROGRAM?

SESSION 14

- Poster session II (Régence A)
CHAIRPERSONS:
C. Putnam & G. Dumas

11:00 - 12:15

JOINT SURFACE GEOMETRY AND ESTIMATION OF JOINT FORCES
I.A.F. Stokes
University of Vermont, Burlington, VT.

SIMULATION OF KNEE JOINT MECHANICS IN TWO DIMENSIONS
G.T. Yamaguchi, M.G. Hoy & F.E. Zajac
Standford University, Standford and Veterans Administrations Medical Center, Palo Alto, CA.

PRESSURE DISTRIBUTION ON ARTICULAR SURFACE: APPLICATION TO MUSCLE FORCE DETERMINATION AND JOINT STABILITY EVALUATION
S. Himeno, K.N. An, H. Tsumura & E.Y.S. Chao
Mayo Clinic, Rochester, MN.

EMG ENVELOPES FROM NORMAL AND ANTERIOR CRUCIATE LIGAMENT DEFICIENT INDIVIDUALS
R. Shiavi, H. Borra, M. Frazer & T. Limbird
Vanderbilt University, Nashville, TN.

THE EFFECT OF DEGREES OF FREEDOM ON VARUS-VALGUS KNEE LAXITY
J.M. Hollis, M.A. Gomez, M. Inoue, E.M. Burleson & S.L-Y. Woo
University of California, Veterans Administration Medical Center, San Diego, CA.

A TWO DIMENSIONAL ANALYSIS OF THE CONTRIBUTION OF THE ABDOMINAL MUSCLES TO TRUNK FLEXION
D.J. Morton & J.G. Reid
Queen's University, Kingston, ON.

A COMPARISON OF ACTUAL INTERNAL DISPLACEMENTS OF HUMAN SPINAL MOTION SEGMENTS PRODUCED BY IN VITRO LOADING AND FINITE ELEMENT MODEL PREDICTIONS
M.H. Krag, R. Seroussi, D.G. Wilder, K.B. Byrne & I. Trausch
Vermont Rehabilitation Engineering Center and University of Vermont, Burlington, VT.

THE MECHANICAL EFFECT OF SUSTAINED SIMULATED SEATING ON THE LUMBAR MOTION SEGMENT
D.G. Wilder, R.E. Seroussi, J. Dimnet & M.H. Pope
University of Vermont, Burlington, VT and Ecole Centrale de Lyon, Lyon, France.

PARAVERTEBRAL MUSCLE RECRUITMENT IN LATERAL SPINE CURVES
J.A.A. Miller, A.B. Schultz, H. Steen & I. Bjerkreim
University of Michigan, Ann Arbor, MI and Sophies Minde Orthopaedic Hospital, University of Oslo, Norway.

THE ANALYTICAL MEASUREMENT OF VERTEBRAL ROTATION
V.J. Raso, D.L. Hill, J.B. McIvor & G.G. Russell
Glenrose Rehabilitation Hospital and University Hospital, Edmonton, AB.

ESTIMATIONS OF FORCE AND MOMENT GENERATING CAPACITY OF TRUNK MUSCULATURE FROM CT SCAN MEASURES
S.M. McGill, R.W. Norman & N. Patt
University of Waterloo, Waterloo and St. Michael's Hospital, Toronto, ON.

OBJECTIVE DETERMINATION OF TRUNK MUSCLE DIMENSIONS USING ULTRASOUND: IMPLICATIONS FOR LOW BACK PAIN RESEARCH
M.H. Krag, L. Miller, K.B. Byrne, L.G. Gilbertson & G.B. Johnson
Vermont Rehabilitation Engineering Center and University of Vermont, Burlington, VT.

EFFECT OF LOAD HEIGHT, WEIGHT AND DISTANCE FROM THE BODY ON KNEE AND LUMBAR SPINE FORCES DURING LIFTING
M. Parnianpour, L. Pavlidis, F.J. Bejjani & M. Nordin
Hospital for Joint Diseases Orthopaedic Institute, New York University, New York, NY.

THE USE OF TRUNK MUSCLE ELECTROMYOGRAPHY TO HELP VALIDATE A SIMPLE PHYSICAL MODEL FOR LIFTING TASKS
R.E. Seroussi & M.H. Pope
University of Vermont, Burlington, VT.

A 3-D ANALYTICAL MODEL FOR THE CANCELLOUS BONE OF HUMAN LUMBAR VERTEBRAE
H. Vaillancourt, G. Drouin & G. McIntyre
Ecole Polytechnique de Montréal, Montréal, PQ.

THE SOFT TISSUE SYSTEM AT THE HEEL REGION OF THE FOOT: ITS MECHANICAL BEHAVIOR AND FUNCTION
S.E. Robbins & A. Hanna
Concordia University, Montreal, PQ.

A MECHANICAL TEST FOR THE MODULUS OF TRABECULAR BONE TISSUE
J.L. Ku, S.A. Goldstein, K.W. Choi, S. Stein, L. Degnore & L.S. Matthews
University of Michigan, Ann Arbor, MI.

MONITORING SYSTEM FOR HARRINGTON ROD IN VIVO STRESS EVOLUTION
N. Charbonneau, G. Drouin, G. Dumas & C.H. Rivard
Ecole Polytechnique de Montréal and Sainte-Justine Hospital, Montréal, PQ.

BENDING AND TORQUE STIFFNESS OF A NEW NAIL WITH SPREADING MECHANISM FOR FEMORAL FRACTURES
C. Krettek, N. Haas & L. Gotzen
Hannover Medical School, Hannover, Federal Republic of Germany.

MATHEMATICAL MODELS FOR PREDICTING BONE DENSITY FROM STRESS HISTORY
D.R. Carter, D.P. Fyhrie & R.T. Whalen
Standford University, Standford and Veterans Administration Medical Center, Palo Alto, CA.

SCALING OF LONG BONE FRACTURE STRENGTH WITH ANIMAL MASS
F. Selker & D. Carter
Standford University, Standford, CA.

SCALING OF LONG BONE TORSION STRENGTH DURING GROWTH
T.S. Keller, D.R. Carter, J.A. Main, A.M. Strauss & D.M. Spengler
V.A. Medical Center, Nashville, TN; Standford University, Standford, CA and Vanderbilt University, Nashville, TN.

THE ROLE OF COLLAGEN CROSSLINKS IN THE AGE RELATED CHANGES IN MECHANICAL PROPERTIES OF PIG DIGITAL TENDONS
R.E. Shadwick
Agricultural and Food Research Council, Bristol, United Kingdom and University of Calgary, Calgary, AB.

EVALUATING THE DYNAMIC PERFORMANCE OF POSITION MEASUREMENT SYSTEMS
Z. Ladin
Boston University, Boston, MA.

ANTICIPATORY POSTURAL ADJUSTMENTS IN CHILDREN: DEVELOPMENTAL CHARACTERISTICS
L. McCarthy, J. Frank, J. Brown & S. Maki
University of Waterloo, Waterloo, ON.

MOBILITY OF HALO-VEST ON THORAX: COMPARATIVE BIOMECHANICS OF 7 CURRENT AND 1 EXPERIMENTAL VEST DESIGN
M.H. Krag & B.D. Beynnon
Vermont Rehabilitation Engineering Center and University of Vermont, Burlington, VT.

Afternoon

SESSION 15

- BONE MECHANICS (Room C)
CHAIRPERSONS:
M.H. Krag & R. Black

13:30 - 13:45

THE INFLUENCE OF PHYSICAL ACTIVITY ON BONE DENSITY
R.T. Whalen, D.R. Carter & C.R. Steele
Veterans Administration Medical Center, Palo Alto and Standford University, Standford, CA.

13:45 - 14:00 REGIONAL VARIATIONS IN THE COMPRESSIVE PROPERTIES OF HUMAN LUMBAR VERTEBRAL TRABECULAE: INFLUENCE OF TISSUE PHYSICAL CHARACTERISTICS
T.S. Keller, T.H. Hansson, M.M. Panjabi & D.M. Spengler
V.A. Medical Center, Nashville, TN; Sahlgren Hospital, Gothenburg, Sweden; Yale Medical School, New Haven, CT and Vanderbilt University, Nashville, TN.

14:00 - 14:15 MORPHOLOGICAL AND MECHANICAL RESPONSES OF LONG BONE TO WEIGHTLESSNESS
S. Shaw, R. Zernicke, A. Vailas & R. Grindeland
University of California, Los Angeles and NASA-Ames Research Center, Moffett Field, CA.

14:15 - 14:30 MECHANICAL PROPERTIES OF BONE ALLOGRAFTS
K. Cowling, J. Mukherjee, R.W. Soutas-Little, R. Hubbard & J. Forsell
Michigan State University, East Lansing, MI and Edward Sparrow Hospital, Lansing, MI.

14:30 - 14:45 THE VISCOPLASTIC BEHAVIOR OF CORTICAL BONE
M. Fondrk, E. Bahniuk, D.T. Davy, C. Michaels & P. Pallone
Case Western Reserve University, Cleveland, OH.

14:45 - 15:00 ESTIMATION OF MECHANICAL PROPERTIES OF BONE USING COMPUTED TOMOGRAPHY
E. Schneider, P. Weber, B. Gasser & S.M. Perren
University of Bern, Bern, Switzerland.

SESSION 16

- HUMAN LOCOMOTION IV
- SPORT (Room B)
CHAIRPERSONS:
A. Chapman & J. Hamill

13:30 - 13:45 BIOMECHANICAL CORRELATES WITH RUNNING ECONOMY IN ELITE DISTANCE RUNNERS
K.R. Williams & P.R. Cavanagh
University of California, Davis, CA and Pennsylvania State University, University Park, PA.

13:45 - 14:00 MUSCULAR AND "MECHANICAL" MOMENTS OF FORCE IN SWING MOTION
E.M. Roberts, J.L. Lin & R.P. Moorman
University of Wisconsin, Madison, WI.

14:00 - 14:15 AN EMPIRICAL MODEL TO CALCULATE THE EFFECTS OF WIND AND ALTITUDE ON THE TIMES OF 100 METER SPRINT RACES
J. Dapena & M.E. Feltner
Indiana University, Bloomington, IN.

14:15 - 14:30 IDENTIFICATION OF SKATEBOARD RIDER CONTROL STRATEGIES
M. Hubbard & H. Fujikawa
University of California, Davis, CA.

14:30 - 14:45 MEASUREMENTS OF THE ROTATIONAL FRICTION OF COURT SHOES ON AN OAK HARWOOD PLAYING SURFACE
G.A. Valiant, L.B. Cooper & T. MCGuirk
Nike Sports Research Laboratory, Beaverton, OR.

14:45 - 15:00 THE USE OF AUGMENTED FEEDBACK TO MODIFY PEDALLING MECHANICS
D.J. Sanderson & P.R. Cavanagh
Pennsylvania State University, University Park, PA.

15:00 - 15:30 **Keynote 7** (Room A)
Dr. Aurelio Capozzo, *University of Rome, Rome, Italy*
MECHANICAL LOADING OF THE HUMAN SKELETAL SYSTEM

15:30 - 15:45 Intermission

SESSION 17

- HUMAN LOCOMOTION IV
- ALTERED GAIT (Room C)
CHAIRPERSONS:
M. O'Rian & M. Hubbard

15:45 - 16:00 THE KINEMATICS OF UPHILL AND DOWNHILL WLAKING
J.C. Wall & J. Charteris
Dalhousie University, Halifax, NS and Rhodes University, Grahamstown, South Africa.

16:00 - 16:15 ELECTROMYOGRAPHIC PATTERNS DURING VISUALLY PERTURBED GAIT
A.W. Smith & D.A. Winter
University of Waterloo, Waterloo, ON.

16:15 - 16:30 THE GAIT OF PACERS
B.D. Wilson, R.J. Neal & J.S. Groenendyk
University of Queensland, Brisbane, Australia.

16:30 - 16:45 A PRELIMINARY STUDY OF THE TEMPORAL GAIT KINEMATICS OF AFRICAN OCCUPATIONAL HEADLOAD CARRIERS
J. Charteris, P.A. Scott & J.C. Wall
Rhodes University, Grahamstown, South African and Dalhousie University, Halifax, NS.

16:45 - 17:00 A COMPARISON BETWEEN FORWARD AND BACKWARD WALKING
B.T. Bates & S.T. McCaw
University of Oregon, Eugene, OR.

SESSION 18

- ORTHOPAEDIC FIXATION
(Room B)
CHAIRPERSONS:
D.R. Carter & C.H. Rivard

15:45 - 16:00 A BIOMECHANICAL ANALYSIS OF GRAFT FATIGUE FRACTURE IN A RESECTION ARTHRODESIS
N.R. Williamson, C. Tylkowski, G. Piotrowski, G. Miller & D. Springfield
University of Florida, Gainsville, FL.

16:00 - 16:15 ANALYSIS OF BONE MODEL MATERIAL FOR EXTERNAL FRACTURE FIXATION EXPERIMENTS
T.J. Hein, A. Perissinotto, R.N. Hotchkiss & E.Y.S. Chao
Mayo Clinic, Rochester, MN.

16:15 - 16:30 MECHANICAL PERFORMANCE OF PROPHYLACTIC KNEE BRACES
S. Meyer, D. Anderson, M. Jimenez, T. Brown & R. Brand
University of Iowa, Iowa City, IA.

16:30 - 16:45 FRACTURE GAP MOTION IN EXTERNAL FIXATION
B. Fleming, T. Kristiansen, G. Neale, S. Reinecke & M. Pope
Vermont Rehabilitation Engineering Center and University of Vermont, Burlington, VT.

16:45 - 17:00 FATIGUE EVALUATION OF A NEW SPINAL FIXATION DEVICE
M.H. Krag, B.D. Beynnon, M.H. Pope, J.W. Frymoyer & L.D. Haugh
Vermont Rehabilitation Engineering Center and University of Vermont, Burlington, VT.

Keynote Lectures

MECHANICAL AND PHYSIOLOGICAL ISSUES UNDERLYING LOCOMOTOR-RESPIRATORY COUPLING IN MAMMALS

Dennis M. Bramble, Department of Biology, University of Utah
Salt Lake City, Utah, 84112 USA

INTRODUCTION

This paper is intended to present an overview of current problems concerning the biomechanical and physiological basis of locomotor-respiratory coupling (LRC) in running mammals. Of particular interest are the distinctions between quadrupedal species and humans which arise from difference in body design, posture, and locomotor kinematics. Despite these differences, however, it now appears that both quadrupeds and humans closely integrate gait and breathing patterns in order to: (a) avoid mechanical interference; (b) exploit locomotor forces for respiratory purposes; (c) appropriately scale pulmonary ventilation to the metabolic requirements of the locomotor machinery.

REVIEW AND THEORY

LRC has only recently been recognized as a widespread and important mechanism in mammals (1). Precise phase-locking of locomotor and respiratory cycles has now been reported in several divergent species, including horses, hares, dogs, and humans (1,2). Quadrupedal mammals tend to exhibit a constant 1:1 coupling ratio (= strides/breath) when running at faster speeds. Humans, in contrast, may utilize up to 6 ratios (e.g., 4:1, 3:1, 2:1) but normally do not exhibit the 1:1 pattern of quadrupeds (3). The kinematics of quadrupedal running, especially the periodic impulsive loading of the forelimbs and thorax, seems to constrain respiration to a simple 1:1 synchronization with the gait cycle. Bipedalism in humans confers greater flexibility in respiratory patterning during running. The choice of any particular coupling ratio seems to depend upon physiological state including such associated parameters as running speed and metabolic demand. Recent theoretical considerations suggest that rhythmic stimulation of mechanoreceptors in the chestwall and diaphragm are possibly key elements in the neurophysiological integration of the locomotor and respiratory cycles in exercising mammals (4).

METHODOLOGY

Qualitative and quantitative data on LRC have been obtained from freely running subjects (1,3). A small stereophonic tape recording system carried by the subject is used to record breathing sounds on one channel and gait information from limb-mounted accelerometers on the other. High speed cine recordings are used to obtain kinematic detail on limb and trunk motion.

RESULTS AND DISCUSSION

Recent investigations of mammalian LRC have helped to clarify the mechanical and physiological correlates of this phenomenon. Among the more important findings are the following.

I. Locomotor induced displacements of a "visceral piston" probably have a central role in the mechanical coupling of breathing and gait. Due to its mass and direct attachment to the muscular diaphragm, the liver is the principal component of the piston. In galloping mammals, horizontal cranial and caudal inertial displacements of the piston are associated with exhalation and inhalation respectively. Piston motions in running humans are essentially vertical and are more complex than in quadrupeds. Nonetheless, correlated respiratory and locomotor profiles indicate that piston action is important to pulmonary mechanics in human runners. Further, the data suggest that the dynamics of the visceral piston may be partly responsible for the double-peaked ground reaction force so characteristic of footstrike in human subjects (5,6).

II. Preliminary mathematical modeling indicates that piston mechanics may constrain the maximum economical stride frequency of running mammals to those approximately equal to the natural frequency of the piston system itself (4). This could help to explain the empirical fact that stride frequency in quadrupedal mammals remains nearly constant and independent of running speed above the trot-gallop transition (7).

III. The linking of locomotor and respiratory parameters may provide exercising mammals with a simple but effective means of matching lung ventilation to running speed and, hence, metabolic power requirements. Theoretically, this can be accomplished by simply making breath frequency and tidal volume proportional to (respectively) stride frequency and stride length. Recently published data for exercising horses (2) confirm the predictions of this model. More experiments will be required to determine whether a basically similar (but more complex) relationship exists in humans.

IV. Preliminary data indicate that for humans there is an optimal coupling ratio for sustained running at a particular speed (or range of speeds). Suboptimal coupling patterns appear to result in excessive lung ventilation and possibly excessive energy expenditure. The system of alternate coupling ratios seen in human runners may constitute a gearing system whose purpose is to minimize the energetic cost of both respiration and locomotion. Such a strategy would be analogous to the changing of gait (e.g., trot to gallop; Fig. 1) in quadrupedal runners, an act which is known to minimize the cost of transport (8).

V. The scaling of stride frequency and stride length against speed is strikingly different for quadrupedal and human runners of equal body size. As Figure 2 shows, the expected stride frequency of an experienced human runner is approximately 85 min^{-1} at a speed of 5 meters sec^{-1}, whereas that of

North American Congress on Biomechanics
Montréal (Québec) Canada, 25-27 August 1986

a quadruped is nearly 150 min^{-1}. At this speed the respiratory frequency of the quadruped is (with 1:1 coupling) equal to its stride frequency (~ 150 min^{-1}), but the breathing frequency of the human is only 30-45 min^{-1} depending upon the coupling ratio. Hence, at sustainable aerobic running speeds (< 6 m/sec), a human respires much more slowly and with a relatively much larger tidal volume than does a quadruped moving at the same speed.

It also appears that the fundamental differences in locomotor kinematics of quadrupedal and human runners account for the use of multiple coupling ratios in the latter. Figure 2 is a simple working model which illustrates how stride and ventilation frequency as well as tidal volume and minute lung ventilation are expected to change with increasing running speed in a well-conditioned, elite distance runner. The model suggests that abrupt changes from one breathing pattern to another (e.g., 3:1 to 2:1) are triggered by an upper limit (= threshold value) on tidal volume. The model predicts that such switches in coupling ratio are accompanied both by a sudden increase in ventilation frequency and a correlated drop in tidal volume. Preliminary experimental data seem to support the model.

CONCLUSION

Both empirical and experimental data indicate that locomotor and respiratory patterns and mechanics in running mammals are strongly coupled and highly interdependent. Such close integration presumably favors mechanical efficiency and reduces the overall cost of locomotor exercise. Major differences exist in the pattern of locomotor-respiratory coupling exhibited by quadrupedal and human runners. These stem mainly from important differences in the body design and locomotor kinematics of the two groups.

References

1. Bramble, D.M., et al. Science 219:251-256, 1983.
2. Hörnicke, H., et al. Equine Exercise Physiology, D.H. Snow (ed.), Burlington Press, Cambridge (1983), pp. 7-16.
3. Bramble, D.M. Modelling and Control of Breathing, Whipp, B.J. and D.M. Wiberg (eds.), Elsevier, New York (1983), pp. 213-220.
4. Bramble, D.M. Nonlinear Oscillations in Biology and Chemistry, Lect. Notes in Biomath., H.G. Othmer (ed.), Springer-Verlag (in press).
5. Cavanagh, P.R. et al. J. Biomech. 13:397-406, 1980.
6. Dickinson, J.A., et al. J. Biomech. 18:415-422, 1985.
7. Heglund, N.C. et al. Science 186:1112-1113, 1974.
8. Hoyt, D.F. et al. Nature 292:239-240, 1981.

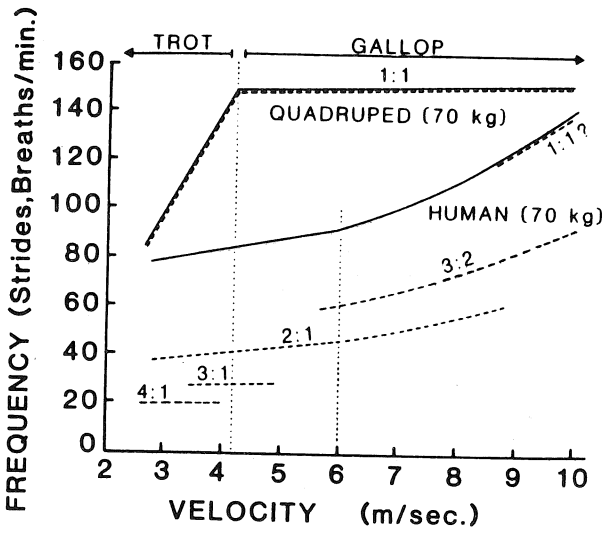

Figure 1. Scaling of coupled stride (solid lines) and respiratory (dashed lines) frequencies against speed in quadrupedal and human runners of equal body mass (70 kg). Speed ranges of various coupling ratios in the human are approximate.

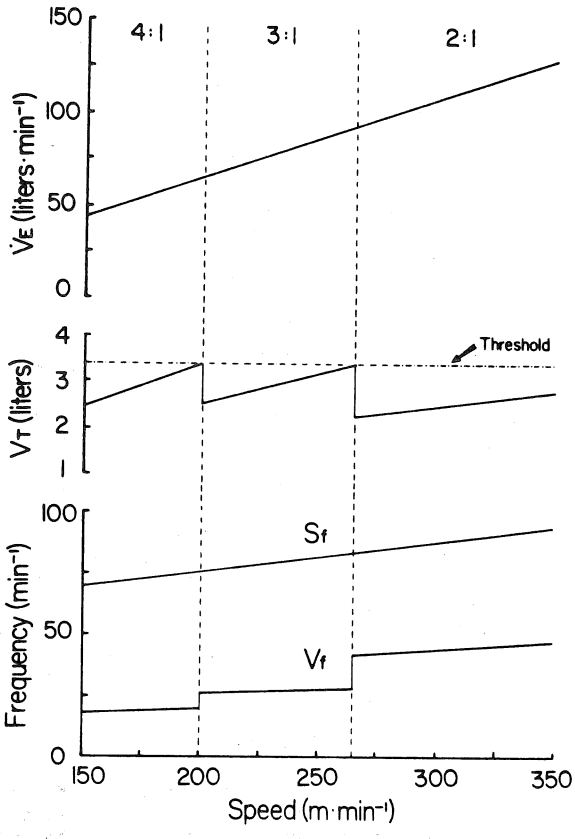

Figure 2. Schematic model of possible interplay of stride (S_f) and ventilation (V_f) frequency with tidal volume (V_T) and minute lung ventilation ($\dot{V}_E$) in a human runner. See text for discussion.

STRATEGIES AND CONCERNS REGARDING THE ASSESSMENT OF PATHOLOGICAL GAIT

D. A. Winter

Department of Kinesiology
University of Waterloo
N2L 3G1

INTRODUCTION

Clinical gait laboratories have proliferated during the past decade and a wide range of assessments of pathological gait are being reported. Some justified criticisms have been levied; many laboratories merely monitor the progress or lack of progress of patients and are not actively providing information critical to surgical or therapy decisions. Most laboratories are not able to quantify the degree of abnormality at both the motor and kinematic level and few are documenting the adaptions that patients are making that may confound planned therapy. Also, this author would question the validity of some therapy which automatically assumes that a patient must be forced to achieve a more normal gait (in spite of evidence that indicates that an abnormal pattern is safer or more optimal).

The purposes of this paper are: (i) to document basic information about normal gait that will influence our diagnostic procedures, (ii) to summarize the scientific steps to arrive at a definitive diagnosis at the motor level, and (iii) to comment on some potentially erroneous rehab strategies.

Diagnosis at the Motor Level

Much of the pessimism regarding clinical gait labs is based on the fact that too much effort has focussed on descriptive measures (velocity, cadence, symmetry, joint angles) which are limited to monitoring changes of global measures of the abnormal movement pattern. They don't diagnose the cause of the pattern they observe. It is only at the kinetic and EMG level (suitably correlated with the abnormal pattern) can we achieve a cause-effect diagnosis.

Because so many muscles are involved in gait, we are faced with a serious indeterminacy problem: there are an infinite number of muscle force patterns that can produce the same moment of force profile. The "bad news" that results from this indeterminacy is that normal subjects will have a wide range of motor patterns, so wide that it may be difficult to define what really is normal. The "good news" is that this variability means flexibility and is indicative of tremendous plasticity in the neural control system to adapt to pathological situations.

Normal Kinematic and Kinetic Patterns

Statistically reliable kinematic and kinetic patterns for normals are required for comparison with our pathological profiles. Figure 1 is a typical set of profiles of moments of force for fast walking adults. Because the kinetic profiles vary considerably with cadence and body mass, we have subdivided our database into three cadence groups and have normalized all of our kinetic curves by dividing by body mass. Further normalization for body height and sex resulted in insignificant improvements to the inter-subject profiles. We now have available normalized profiles of moment of force, joint mechanical power and EMG patterns for 16 muscles against which our patients can be compared.

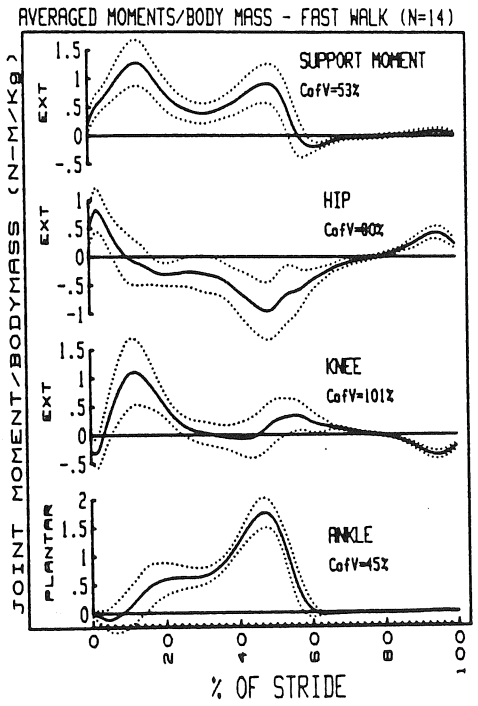

Figure 1: Normalized moment of force profiles for fast walking normals. Mean curve (solid) and ± standard deviation (dotted) for 14 subjects is plotted. The coefficient of variation is a measure of the inter-trial variability expressed as a percent of the amplitude of the signal.

Strategy for Diagnosis

Based on many years experience, we have developed a fairly routine strategy to arrive at a specific diagnosis for each individual patient. The first step is to observe all movement abnormalities; we use TV and summa-

North American Congress on Biomechanics
Montréal (Québec) Canada, 25-27 August 1986

rize the total gait pattern using a computerized gait profile form (Figure 2). Details of the use of this form are presented in another paper in this Congress. It is sufficient to note that the * alerts us as to phases of the gait cycle that are out of normal range.

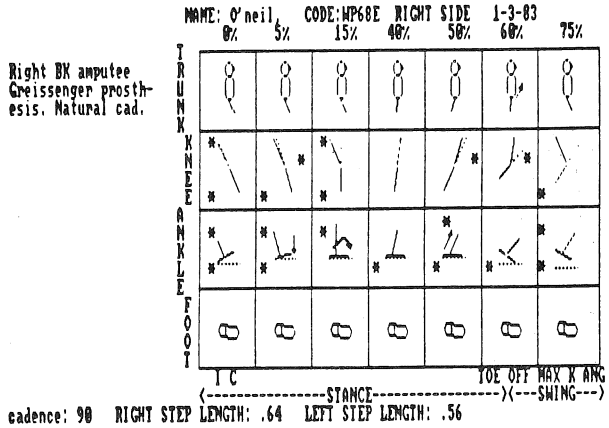

Figure 2: Computerized Gait Profile Form with the profile of the B/K amputee described in the example diagnosis.

TABLE 1

Observed Abnormality	Possible Causes	Biomechanical and Neuromuscular Evidence
Short step-length	Weak push-off prior to swing	Below normal plantarflexor moment or power generation or EMG during push-off
	Weak hip flexors at toe-off and early in swing	Below normal hip flexor moment or power or EMG during late push-off and early swing
	Excessive deceleration of leg in late swing	Above normal hamstring EMG or knee flexor moment or power absorption late in swing
	Above normal contralateral hip extensor activity during stance	Hyperactivity in EMG of contralateral hip extensors
Stiff-legged weight bearing	Above normal ankle, knee or hip extensors early in stance	Above normal EMG activity or moments in hip extensor or plantarflexors early in stance

The second step is to list all possible causes of the observed abnormal movement. Table 1 gives a summarized version of two commonly observed abnormalities: short step length and stiff-legged weight bearing. Then, the final challenge is to examine the patient's biomechanical profiles and, by comparison with those from normals, we should be able to pinpoint the exact cause of the abnormal gait patterns, and also show any compensating patterns.

Example Diagnosis

The Computerize Gait Profile for B/K amputee wearing a Gressinger prosthesis is presented in Figure 2. From this profile, the following information was extracted: (i) entire lower limb was extended more than normal at HC. Flat foot did not occur until 15%; initial knee flexion was reduced, (ii) push-off (50%) was weak, HO was delayed and knee flexion was delayed, and (iii) normal hip extensor pull-off occurred. As this patient was a B/K amputee, his foot could not plantarflex after HC, thus, the delay noted in (i). The fact that he had any observable push-off is somewhat surprising. The biomechanical analyses of joint powers is presented in Figure 3, and which correlates completely with the profile information. Normals are plotted with a solid line and the amputee with a dashed line. A1 power shows the amputee's ankle mechanism (a spring) storing energy, and a small amount is returned during push-off (A2). The amputee had little knee flexion early in stance, therefore did not have a K1 burst. When his knee did break in late stance, he had to use above normal knee extensor power (K3) to control excessive flexion. At the hip, the pull-off power (H3) by the hip flexors was slightly above normal and was the major compensation for the lack of a strong push-off

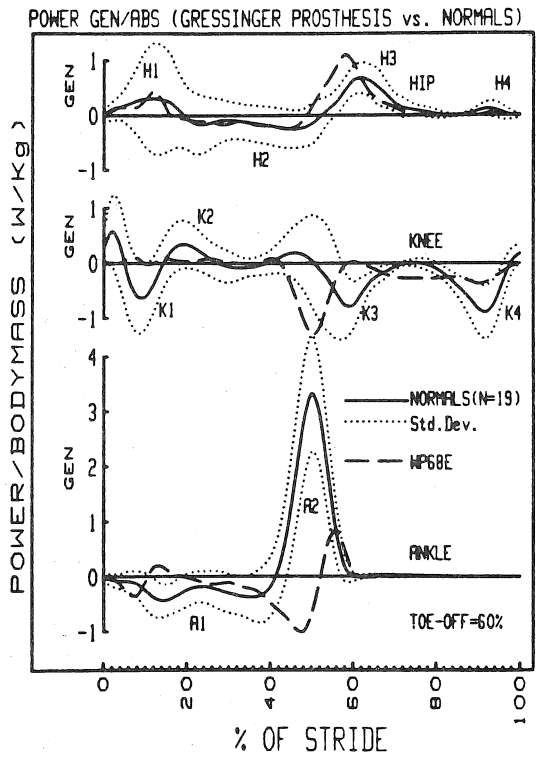

Figure 3: Mechanical power generation and absorption at the ankle, knee and hip for the B/K amputee (dashed line) compared with that for normals (solid line for average, dotted line for s.d.).

Conclusions

A systematic and scientific approach has been presented for the diagnosis of pathological gait at the motor level. The procedure not only pinpoints the abnormal motor or biomechanical patterns but also identifies the compensating motor patterns in the residual muscles. Caution is, therefore, suggested when therapy is prescribed which does not recognize these adaptions. For example, forcing an amputee to walk more symmetrically, may undo a new optimal pattern; or, lack of prescribed exercise for newly-compensating muscles may result in early fatigue.

ELASTIC MECHANISMS IN THE MOVEMENTS OF MA

R. McNeill Alexander
Department of Pure & Applied Zoology
University of Leeds, Leeds LS2 9JT, U.K.

The elastic properties of materials are exploited in mammals, in several distinct ways.

The ligamentum nuchae in the necks of ungulates serves as a muscle antagonist, helping to support and raise the head (1). The paw pads of mammals serve as shock absorbers (2). Elastic structures serve as catapults in jumping insects (3), but no catapults seem to have been identified in mammals.

This paper is concerned mainly with another function of elastic structures, as pogo-sticks. A running man or a hopping kangaroo loses kinetic energy (KE) and potential energy in the first half of each step and regains them in the second half (4). Each leg exerts a braking action and then an accelerating one, both in bipeds and in quadrupeds. Energy is saved by using muscles and tendons like the springs of pogo-sticks, to absorb energy and then return it. The tendons are particularly important (5). Some distal leg muscles of ungulates have vestigial muscle fibres but retain strong tendons which serve as passive springs. Tendon is an excellent material for such functions because it returns, in its elastic recoil, 93% of the work done stretching it (6). Mechanical tests on feet of donkeys, deer and wallabies have supplied data for rough estimates of energy savings (7), and similar tests are being made on human feet.

The KE fluctuations discussed so far are of external KE, that is of KE associated with movement of the centre of mass. As speed increases, internal KE becomes increasingly important: this is KE associated with movements of feet and other parts relative to the centre of mass. Transition from symmetrical gaits to galloping enables mammals to use an aponeurosis in the back as a spring, storing energy as the legs are halted at the end of a swing and returning it in an elastic recoil (8).

There seems to be scope for saving energy by tendon elasticity in the swimming of whales, but a preliminary analysis suggests that the tendons are more compliant than would be optimal.

References

1. Dimery, N.J., et al. J.Zool., Lond. (A) 206: 341-351, 1985.
2. Alexander, R.McN., et al. J.Zool., Lond. (A) 209: in the press, 1986.
3. Bennet-Clark, H.C. J.exp.Biol. 63: 53-83, 1975.
4. Cavagna, G.A., et al. Am.J.Physiol. 233: R243-261, 1977.
5. Alexander, R.McN. Am.Zool. 24: 85-94, 1984.
6. Ker, R.F. J.exp.Biol. 93: 283-302, 1981.
7. Ker, R.F. et al. J.Zool., Lond. (A) 208: 417-428, 1986.
8. Alexander, R.McN. et al. J.Zool., Lond. (A) 207: 467-482, 1985.

North American Congress on Biomechanics
Montréal (Québec) Canada, 25-27 August 1986

Sessions' Papers

VISUAL ASSESSMENT OF HUMAN GAIT - A RELIABILITY STUDY

Aftab E. Patla and Susan D. Clouse
Department of Kinesiology
University of Waterloo
Waterloo, Ontario, N2L 3G1

INTRODUCTION

In numerous clinics and centers, visual assessment of human gait forms an integral part of patient evaluation. For example, at the Worker's Compensation Board Center in Toronto each physiotherapist sees up to twenty patients a day. The battery of tests performed on each subject includes visual assessment of gait. At present only an overall judgement on the quality of gait is made. A more detailed recording of various kinematic aspects of gait would improve the assessment, by suggesting biomechanical causes of the observed abnormalities and help in diagnoses [1,2]. Because physiotherapists often perform many other tests, it is necessary to minimize time and effort required to do simple gait assessment. Visual observation of gait, done in real time or later through the use of a video is appropriate. But before we attempt to extract more information, it is necessary to determine the interrater reliability on these measures.

Despite widespread use of visual assessment of movement, there is a surprising lack of studies examining the reliability. Goodkin & Diller [3] found poor reliability among therapists on major gait deviations across the whole stride but good agreement on other measures. Recently Krebs et al. [4] observed moderate reliability in the stance phase for children's gait. These studies have examined only particular patient population, and assessment was done over the full stride or just the stance phase. Besides the data analyses which has mainly looked at percent agreement between raters can potentially inflate the reliability coefficient [5]. The focus of this study is to examine interrater reliability on a variety of measures for a wide range of patient population over both stance and swing phases.

METHODOLOGY

Patients: Eight patients (Table 1) whose gait was previously analysed in the Kinesiology Gait Laboratory were used in the study. Their gait pattern in the saggital plane consisting of minimum five strides was transferred on to a video recorder.

Table 1: Description of Pathology in Patients Studied.

1. Left Total Hip Arthroplasty
2. Cerebral Palsy, Left Hemiplegic
3. Turner's Syndrome
4. M.V.A. - fractured L1 vertebra
   Paresthesis at levels of L_1, S_1, S_2
5. Left Above Knee Amputee
6. Left Total Knee Arthroplasty
7. Cerebral Palsy - Spastic Diplegia
   Bilateral tendo - achilles lengthening
8. Right below knee amputee

Raters: Five raters who had good background in gait analyses and assessment were used in the study. These students had coursework in biomechanics and a specific course in gait analyses. Two of them had worked in Gait Laboratory.

Kinematic Chart: The kinematic variables that each of the raters were asked to evaluate are shown in Figure 1. A brief patient history is included. The variables and the phases were as described by Winter [1]. The timing variable was included to get some information on the velocity of movement.

Procedure: Each rater went through a training period. They were shown five normal gait patterns, the phases were identified, and the normal range for the variables were explained. Once they felt comfortable with the normal gait, they were shown a patient gait. The experimentor guided the rater through this gait and identified the abnormalities. Following the training session, the raters were required to view the tape at normal speed of a patient's gait. They could view each of the seven phases up to five times. After viewing each phase, they were required to identify any variable that was abnormal on a binary scale. A sample record is shown in Figure 1. The patients were viewed in random order. The actual testing took two sessions of two hours each. Since many centers do not have slow motion or freeze frame capability, viewing was done in real time.

HISTORY: Left above-knee amputee

For the following variables, place an 'X' in the box if you believe it is abnormal. Complete for all phases of gait.

	Initial Contact	Weight Accept.	Mid-stance	Push-off	Toe-off	Early Swing	Late Swing
Foot Placement							
Ankle Angle		X			X		
Knee Angle	X	X	X	X	X		X
Hip Angle				X	X	X	X
Upper Body							
External Support							
Timing							

Pushoff	X
Step length	
Symmetry	X

Problems:

Phase	
Variable	knee angle

Figure 1: Kinematic chart used in the study.

DATA ANALYSIS

A standard way of analyzing the data such as the one in this study is to determine point to point interrater reliability. This value can be high if the two raters agree on large number of variables that are

North American Congress on Biomechanics
Montréal (Québec) Canada, 25-27 August 1986

normal even though they may disagree on variables that were abnormal. Because of this problem with traditional analysis, a new method developed by Dr. E. Roy of our department was used. See Appendix I for sample calculation. A computer program in addition to calculating the normal reliability coefficients, determined the following:

Average % Occurence Frequency for Raters: If the average occurence frequency of the two raters is $\leq$50% then subsequent analysis concentrates on Occurrence Interrater Reliability. If it is >50% then Nonoccurence Interrater Reliability is used. This avoids inflation of reliability scores.

Occurence/Nonoccurence Interrater Reliability: This is similar to traditional point to point interrater reiability except instead of using all the data the analyses concentrates only on either the occurence or nonoccurence of abnormality in a measure.

Chance Occurence/Nonoccurence Interrater Reliability: This allows us to determine whether or not the reliability value calculated is above chance level.

These analyses were carried out for each variable, across all phases in the step cycle, and stance phase and swing phases separately. The patients were analyzed individually. Five raters gave ten combinations for reliability calculations.

RESULTS AND DISCUSSION

The results are summarized in Table 2. A one was included for each pair of raters that showed above chance reliability. Thus the maximum score in each cell would be 10. Zero score can be obtained in two ways. If the reliability value is not above chance level for any combinations of two raters, the score would be zero. Zero score can also be obtained if the average percent occurence for all combination of raters is zero. In tables, the latter possibility is indicated by a "*".

Table 2: Above chance reliability for the raters for each variable and patient across the whole stride.

	Patients							
Variable	P1	P2	P3	P4	P5	P6	P7	P8
Foot Placement	*	10	6	10	*		10	*
Ankle Angle	6	4	4	5	10	6	5	10
Knee Angle	2	6	10	3	8	6	6	6
Hip Angle	10	1	4	5	3	1	10	
Upper Body	2	*	*	*		*		*
External Support	*	*	*	6	*	*	*	*
Timing		4		2	2	*		

When one examines the angular displacement variables in Table 2, it is clear that the raters were more reliable on identifying abnormal pattern in the ankle and knee joint, than the hip joint. They also had problems in determining abnormalities in the upper body movement when it was present. As the numbers in each cell indicate, even for the ankle and knee joint the reliability was moderate. Thus new strategies would have to be developed to observe these body segments. Among other variables, raters were consistent on foot placement, and the use of external support when present. The timing variable which asked the raters to judge the velocity of movement was the least reliable.

To ascertain which phase of the gait cycle was most reliable in terms of assessment of abnormality, the analyses for each variable were carried out over the stance phase and swing phase separately. When these results were examined, it was clear that raters were far more consistent during the stance phase than swing phase. This agrees with the comments made by Krebs et al. *[4]*.

The pathologies studied in this project can be broadly classified into two categories; neuromuscular (patients 2,3,4,7) and musculoskeletal (patients 1,5, 6,8). From the analyses presented, it appears that raters were more consistent in their observation of patients suffering from musculoskeletal disorders. The three parameters: push-off, step length and symmetry which the raters were asked to judge were not included in the previous analyses. When the raters judgements of presence of abnormality in these variables were examined, it was clear that they were very good at judging abnormal push off. In contrast, assessment of step length and symmetry between limbs was poor.

SUMMARY

This study sheds light on visual observation of gait in real time. The variables which were well defined were assessed more reliably than variable such as "timing". The results suggest that assessment during stance phase is more reliable than during swing phase. Assessment on a binary scale is a first step. Subsequent studies will have to incorporate at least an ordinal scale, examine movements in other planes, and determine validity of these measures.

REFERENCES

1. Winter, D.A. (1985). Physio. Canada, 37:245-251.
2. Tracy, K.B. et al. (1979). Physical Therapy, 59: 268-277.
3. Goodkin, R. & Diller, L. (1973). Perceptual & Motor Skills, 37:727-734.
4. Krebs, D.E. et al. (1985). Physical Therapy, 65: 1027-1033.
5. Roy, E. et al. (1985). International Neuropsychological Society Conference.

ACKNOWLEDGEMENT

Supported by a grant from the Worker's Compensation Board, Toronto.

APPENDIX I

Sample Calculation

Variable: Hip Angle (1 - Abnormal)

↓Rater	Phases →						
1	0	0	1	0	0	0	1
2	0	0	1	1	0	0	0

Contingency Table:

		Rater 1	
		1	0
Rater 2	1	1	1
	0	1	4

Calculations:

Point to Point Interrater Reliability = 5/7 x 100 = 71.42%

Average % Occurence Frequency for Raters = 28.57%

Occurence Interrater Reliability = 1/3 x 100 = 33.33%

Chance Occurence Interrater Reliability = 4/49 x 100 = 8.16%

Note high Point to Point Reliability. Because Occurence Reliability is above chance level, a 1 is included for this variable in Table 2.

KNEE BRACE INFLUENCES ON THE SUPPORT PHASE OF RUNNING

K. Knutzen Phil Schot
Department of Physical Education
Western Washington University
Bellingham, Washington 98225

B. T. Bates
Department of Human Development
University of Oregon
Eugene, Oregon 97403

INTRODUCTION

The functional knee brace has been demonstrated to be an effective external force mechanism for the control of excessive knee joint movement parameters. More specifically, brace manufacturers promote designs which are stated to reduce excessive mediolateral and varus/valgus movements while at the same time allowing normal knee joint function necessary in most physical activities. No consideration has been given to the effects of the stabilization on other segments in the lower extremity link. Effectual control of the movement of the tibia on the femur in the sagittal and transverse planes should reflect a concomitant alteration in the movements of the foot-ankle complex and the ground reaction force parameters. The purpose of the present investigation was to evaluate the effects of knee brace application on the kinetic parameters associated with the support phase of running.

REVIEW AND THEORY

The knee joint moves through two planes of movement during the activity of running. These movements consist of ranges of approximately 60 degrees in the sagittal plane for flexion/extension movements and approximately 20 degrees in the transverse plane for movements of external/internal rotation (4,6). The knee also moves in the varus/valgus direction due to mediolateral forces imposed upon the joint during normal knee joint functioning. All of these movements have been demonstrated to affect movements and forces at the foot-ankle complex. The degree of knee extension at contact and the corresponding foot position at contact have been shown to influence both the collision aspects and the braking/propelling aspects of the support phase (3,8). Additionally, the tibial rotation parameters are determined by movements taking place at the knee joint and the subtalar articulation. Therefore, any alteration in knee joint or foot function is hypothesized to be countered by a compensatory reaction in the adjacent joint.

The application of the derotation or functional knee brace has been shown to control knee joint movement parameters by reducing movement parameters as much as 11 percent and 20-30 percent for movements in the sagittal and transverse planes, respectively (6). Preliminary investigations on the influence of knee joint restriction on the ground reaction force parameters have indicated that the limitations imposed by the brace application generated associated reactions in the kinetic parameters during foot support (5).

METHODOLOGY

Twenty-one subjects, 20-42 years of age, were selected from a group of volunteers to participate in the study. Three subject groups were evaluated: normal subjects indicating no history of injury to the lower extremity, an arthroscopic group whose medical records substantiated anterior cruciate ligament (ACL) insufficiency, and a reconstructive group who had undergone extra-articular repair of ACL damage. Four test conditions were instituted: a non-brace condition on the injured or experimental limb, application of the Marquette Knee Stabilizer (MKS) functional brace, application of the Generation II (G-II) functional brace, and a healthy or contralateral limb condition. Subjects were casted for the braces by a qualified orthotist. Upon receipt of the braces, the subjects were fitted with the braces by representatives from the two brace companies.

The kinetic data were collected over a two-hour experimental session using an AMTI force platform system. At the initiation of the session, subjects were fitted with the same running shoe to minimize shoe effects. Following the collection of physical characteristics, subjects were randomly assigned a test order for the four conditions. In the case of the brace conditions, the brace was applied by the same experimenter. Subjects then practiced running through a 20 meter experimental area until they could maintain an uninterrupted running cycle while reporting no major encumbrances. Running speed was monitored over a 5 meter area using a photoelectric timing system and maintained at 3.33 m/s (SD = .11). Ten running trials were collected for each condition and stored for later analysis.

The vertical, fore-aft and mediolateral force components for each trial were scaled and normalized for body weight and analyzed individually using specifically designed curve analysis software (2). Fourteen vertical, 13 fore-aft and 16 mediolateral values were extracted from each curve. Mean values were computed across the ten trials for the four conditions.

The average values were analyzed using a repeated measures multivariate analysis of variance to evaluate the effect of group membership in one of the three groups and the effect of the four different knee joint test conditions. Univariate results and contrasts comparing the four conditions were examined. All statistical tests were scrutinized at the $p<.05$ level of significance.

RESULTS AND DISCUSSION

The results of the multivariate analysis conducted on the vertical, fore-aft and mediolateral force components revealed no significant differences as a result of group membership. There were significant differences across the four conditions for all three force parameters. Mean data for selected vertical, fore-aft and mediolateral force variables representing all subjects for the four conditions are presented in Tables 1, 2, and 3, respectively. Vertically, there were significant univariate differences across the four conditions for the relative time to

North American Congress on Biomechanics
Montréal (Québec) Canada, 25-27 August 1986

first maximum force, first maximum force, relative time to minimum force, minimum force, impulse to first maximum force, impulse to minimum force, and total impulse. Contrasts revealed no significant differences between the two braces for any of the vertical force parameters. Differences were recorded between the two brace conditions and the injured or experimental limb. Brace applications were shown to elicit a delay in the time to the achievement of the initial collision force while concurrently producing greater maximum values in the force. This alteration in force generation has previously been shown to be associated with changes in running speed, different foot types or footwear (1) and the knee angle at contact (3). The knee brace application has been shown to alter the knee angle (6) and may also influence the foot position at contact. These variations may be directly responsible for the changes noted above.

In the fore-aft direction, significant differences were noted in relative time to maximum braking force, maximum braking force, relative time from transition from braking to propulsion, and braking impulse. There were no differences between the two braces. Comparisons between the two brace conditions and the experimental limb demonstrated the brace's influence in delaying transition to maximum braking and additionally producing greater braking values. These changes can be specifically related to the reduction of knee extension produced by the brace at foot contact. The data would indicate that the compensatory movement in response to the knee restriction is an attempt to contact the ground with the foot further away from the center of gravity and would thus explain the increased braking values.

Mediolaterally, significant differences were identified in the total excursions during the first 30 percent, between 30-60 percent, and between 40-75 percent of the support phase. Contrast analyses indicated the difference in the excursions during the early 30 percent of the support period to be a significant difference between the MKS and the G-II braces. The G-II produced a greater amount of excursions during this time period. The two brace conditions demonstrated greater amounts of excursions during the mid-support period of the contact phase when compared to the experimental limb. The incresed cycling of movement in the mediolateral direction may be associated with the reduction in rotation parameters being effected by the brace at the knee joint producing a functional alteration at the foot-ankle complex.

CONCLUSIONS

Functional knee brace application was shown to significantly alter the kinetic parameters associated with the support phase of running. Generally, the braces altered the ground reaction force parameters during the collision phase by delaying the attainment of maximum force values and producing greater impact values in both the vertical and fore-aft directions. Furthermore, brace application increased the mediolateral excursions during the middle portion of the support phase. Additional studies are needed to quantify the relationship between lower extremity kinematic alterations and support phase kinetics following knee brace application.

References

1. Bates, B.T., et al. Biomech. VII-B 226-233, 1981.
2. Bates, B.T., et al. Biomech. VIII-B 635-640, 1983.
3. Frederick, E.C., et al. Int. J. Sp. Biomech. 2:41-49, 1986.
4. Kettlecamp, D.B., et al. J. Bone Jt. Surg. 52-A: 775-790, 1970.
5. Knutzen, K.M., et al. Proc. Hum. Loc. II - Can. Soc. Biomech. 72-73, 1982.
6. Knutzen, K.M., et al. Am. J. Phys. Med. 62: 172-181, 1983.
7. Mann, R.A., Hagy, J. Am. J. Sports Med. 5:345-350, 1980.
8. Mann, R.V. Med. Sci. Sp. Exer. 13:325-328, 1981.

TABLE 1. VERTICAL FORCE PLATFORM VARIABLES

VARIABLES	CONDITIONS			
	NO BRACE	MKS	GEN II	HEALTHY
Relative Time to First Max. Force*	12.32 (1.70)	13.40 (1.31)	13.46 (1.24)	12.32 (1.25)
First Max. Force*	18.34 (2.67)	19.27 (3.01)	19.73 (3.45)	17.82 (2.46)
Relative Time to Minimum Force*	17.67 (1.69)	19.84 (2.00)	19.91 (2.48)	17.46 (1.45)
Minimum Force*	15.27 (2.82)	15.85 (3.04)	16.66 (3.30)	14.69 (2.45)
Relative Time to Second Max. Force	42.37 (3.11)	41.84 (2.70)	42.70 (2.91)	42.26 (2.14)
Second Max. Force	25.06 (1.84)	25.38 (1.66)	25.46 (1.86)	25.36 (1.84)
Impulse to First Max. Force*	.25 (.06)	.28 (.06)	.29 (.07)	.26 (.05)
Impulse to Minimum Force*	.48 (.08)	.58 (.14)	.60 (.16)	.47 (.09)
Total Impulse*	3.61 (.27)	3.65 (.21)	3.68 (.20)	3.74 (.21)
Support Time	.26 (.02)	.26 (.02)	.25 (.06)	.26 (.02)

Relative Time = % Support Phase
Force = N/kg of Body Mass
Impulse = N·Sec.
Support Time = Sec.
* = Significant Univariate Analyses (p<.05)

TABLE 2. FORE-AFT FORCE PLATFORM VARIABLES

VARIABLES	CONDITIONS			
	NO BRACE	MKS	GEN II	HEALTHY
Relative Time to Max. Braking*	24.06 (2.39)	25.44 (2.84)	25.60 (2.97)	23.51 (2.48)
Max. Braking Force*	3.54 (.53)	3.75 (.59)	3.83 (.51)	3.93 (.41)
Relative Time to Transition*	49.43 (3.55)	48.98 (3.87)	49.20 (2.85)	51.02 (3.01)
Relative Time to Max. Propulsion	70.97 (2.26)	70.83 (1.81)	70.97 (2.06)	72.00 (1.58)
Max. Propelling Force	3.05 (.35)	3.09 (.22)	3.14 (.26)	3.11 (.43)
Braking Impulse*	.24 (.05)	.25 (.05)	.27 (.04)	.28 (.06)
Propelling Impulse	.22 (.03)	.22 (.02)	.23 (.02)	.22 (.03)
Average Braking Force	1.89 (.31)	1.96 (.38)	2.13 (.39)	2.11 (.31)
Average Propelling Force	1.69 (.22)	1.70 (.17)	1.75 (.18)	1.75 (.27)

Relative Time = % Support Phase
Force = N/kg Body Mass
Impulse = N·Sec.
* = Significant Univariate Analyses (p<.05)

TABLE 3. MEDIOLATERAL FORCE PLATFORM VARIABLES

VARIABLES	CONDITIONS			
	NO BRACE	MKS	GEN II	HEALTHY
ALGEBRAIC IMPULSE				
0-30% Support	.017 (.008)	.015 (.009)	.015 (.010)	.015 (.011)
30-60% Support	.036 (.025)	.038 (.027)	.035 (.023)	.047 (.031)
60-75% Support	.039 (.027)	.040 (.031)	.035 (.025)	.049 (.034)
0-100% Support	.055 (.030)	.053 (.035)	.045 (.031)	.057 (.045)
TOTAL EXCURSIONS				
0-30% Support*	2.62 (.78)	2.60 (.73)	2.88 (.74)	2.53 (.82)
30-60% Support*	.87 (.20)	1.01 (.23)	1.06 (.31)	.92 (.17)
60-75% Support*	1.19 (.26)	1.34 (.31)	1.39 (.39)	1.29 (.31)
0-100% Support	4.20 (.85)	4.38 (.88)	4.51 (1.22)	4.21 (.96)

Impulse = N·Sec.
Excursions = N.
*Significant Univariate Analyses (p<.05)

BIOMECHANICAL CHARACTERISTICS OF THE SWING LIMB IN MASTERS RUNNERS*

Elizabeth M. Roberts
Physical Ed. & Dance
Univ. of Wisconsin
Madison, WI 53706

Tak K. Cheung
Mechanical Engr.
Univ. of Wisconsin
Madison, WI 53706

Adel A. M. Hafez
Helwan Univ.
Cairo, Egypt

Susan K. Bullard
Physical Ed. & Dance
Univ. of Wisconsin
Madison, WI 53706

Introduction

Although it is generally known that individuals perform many speed dependent motor tasks more slowly as they age, it is not clear whether the speed decriment also includes a change in the pattern of performance. It is also not always clear how much of the loss in speed is related to aging and how much to a sedentary, or disuse factor that frequently accompanies advancing years. This study reports some preliminary findings on the kinematic and kinetic pattern characteristics of male runners over 60 years of age in comparison to those of young adults. Subjects who were in the habit of running regularly were recruited so that the influence of disuse would be minimized.

Review and Theory

Research on the morphological changes in skeletal muscle associated with age indicates that there is loss of muscle mass due both to loss of fiber number and diameter, a tendency toward dedifferentiation of fiber types associated with "functional denervation" at the myoneural junction, differential loss of fast (Type II) versus slow (Type I) fiber types (Fitts) and loss of reflex excitability (Sabbahi). Disruptions of movement associated with these changes include decrease in movement and reaction time (eg. Welford), decrease in isometric and isotonic strength (Murray, 1980) and decrease in movement speed with a relative increase in endurance (Fitts).

While little data are available on the biomechanical characteristics of movement skills as age advances, Murray's (1969) studies on walking in "healthy old men" showed a slowing of walking speed with decrease in stride length and increase in stance time, and general decreases in range of motion at upper and lower limb joints after 60 years. Although all of the changes cited are associated with age they are not necessarily due to age. They could be caused in part by disuse or disease.

Running has become an activity that many older people engage in regularly. Such individuals tend to be free of decrements in performance due to disuse and thus are more likely to show true decrements due to age. Since variability tends to be greater in submaximal than maximal, or near maximal performance the latter was chosen for study. The range and speed of motion are greater in the swing limb than in the stance limb, thus swing limb measurements were considered more likely to discriminate pattern differences. Data on younger runners are available for comparison (eg. Cavanagh) but to our knowledge little is available on Masters runners other than that contained in our own early report.

Methodology

Five Masters runners 60–65 years of age and three middle distance runners 20–22 years were recruited for the study. The Masters subjects ran regularly; the younger subjects were members of the track team. Cinematographic records at 200 fps of the subjects running at, or near maximum speed were taken at an outdoor track. Three of the Masters subjects also ran at a more moderate speed representing their regular running speed. Three to six trials were filmed during two sessions. A 25mm lens was used with a camera distance of 15.24m. Centers of mass (Dempster, 1955) and angles of inclination were calculated for the thigh and combined shank-foot and curve fitted by augmented cubic spline function. Joint forces and moments were subsequently calculated.

Results & Discussion

Actual maximal effort running speeds ranged from 5.2 to 7.2 m/s and 8.8 to 9.6 m/s for Masters and young adults respectively, with stride lengths from 3.08 to 3.58 m and 4.6 to 5.02 m. Figures 1 and 2 show the angular velocity of the shank-foot and thigh respectively for all usable maximum effort trials for all subjects. Although the scatter is considerable the patterns of angular velocity for both the thigh and shank-foot appear quite similar across groups with peak values occuring at approximately the same percent of time. The primary differences are in the magnitudes of peak values, and in the acceleration and deceleration slopes, with all these being least for the Masters runners.

The early flexion (neg.) peak for shank velocity occurs near 10% of swing for both groups but with a separation of peak values of about 5 rad/s. The extension (pos.) peak occurs near 58%, again with a peak value separation of about 5 rad/s. The peak values are lowest for Masters being approximately -12 rad/s for flexion and 15 rad/s for extension. Between 80% and 100% of swing shank angular velocity is again in the flexion direction with values somewhat less in magnitude for the Masters.

Thigh angular velocity (Fig.2) similarly shows lesser values for the Masters than the young adults. The separation between peaks is less than for the shank, however, being on the order of 3-4 rad/s for the flexion of midswing (50%) and the extension prior to touchdown (80% to 100%). The initial portion of thigh motion tends to show zero velocity for Masters but a flexion velocity for the young adults.

Linear kinematic parameters were in keeping with the angular. Horizontal values particularly discriminated magnitudes as could be expected. However, while linear horizontal velocity patterns were generally similar across all subjects individual pattern characteristics were clearly discernable and quite stable over trials and speeds.

Data on the Kinetic characteristics of the swing limb in general substantiated the kinematics, however the separation in peak magnitudes was less clear cut and overlapping of the high values of Masters runners with low values of young adults was present. Fig.3 showing the moment of force at the knee (M_1) for selected trials illustrates the findings. Despite overlapping during the first 25% of swing Masters' values generally are lower than young adults'. Peak flexor (neg.) moments near touchdown are large and clearly separated. At the initiation of swing most trials for younger subjects showed a brief flexor moment (neg.) while most trials for Masters did not. Total moments ($I\ddot{\theta}$) for Masters were flexor even though M_1 was zero or extensor. This resulted

North American Congress on Biomechanics
Montréal (Québec) Canada, 25-27 August 1986

because moments due to joint forces were flexor for Masters as well as young runners.

Within the limitations of the present data it appears that patterns of kinematic and kinetic variables are not clearly different between these Masters runners and young adults. Thus differential losses in fast type II muscle fibers, if they are in fact present in these physically active older males, do not appear to result in pattern changes. Rather, clear magnitude decreases occur which may result in part from overall muscle fiber losses.

References

Cavanagh, P.R. et al. Ann. N.Y. Acad. Sci. 301, 328-345, 1977.

Fitt, R.H. in Smith, E.L. Exercise & Aging. Enslow Pub., 1981, pp. 31-44.

Murray, M.P. et al. J. Gerentol. 24, 169-178, 1969.

Murray, M.P. et al. Phys. Ther. 60, 412-419, 1980.

Sabbahi, M.A. et al. J. Gerentol. 37, 24-32, 1982.

Welford, A.T. in Berren, J.E. Handbk. Psychol. Aging VNR, 1977, pp. 450-496.

*Supported in part by the Research Committee of the Graduate School Grant #101-1527 and by extramural grant #133-G537.

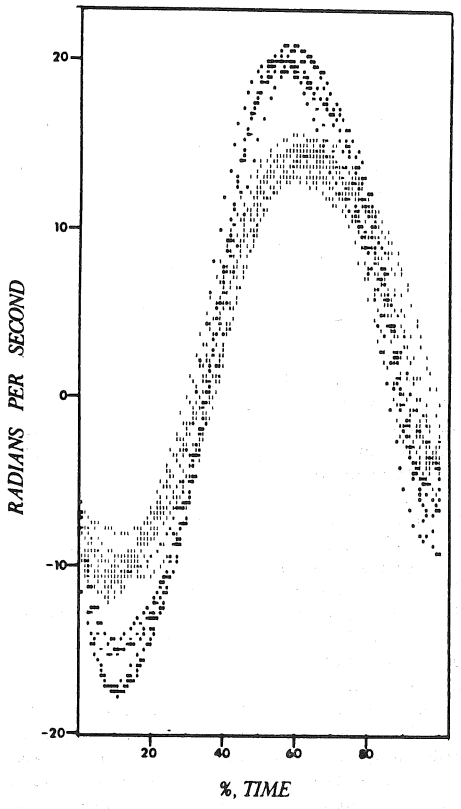

Fig.1 Shank-foot angular velocity. Young adults, O; Masters, I. Positive represents extension.

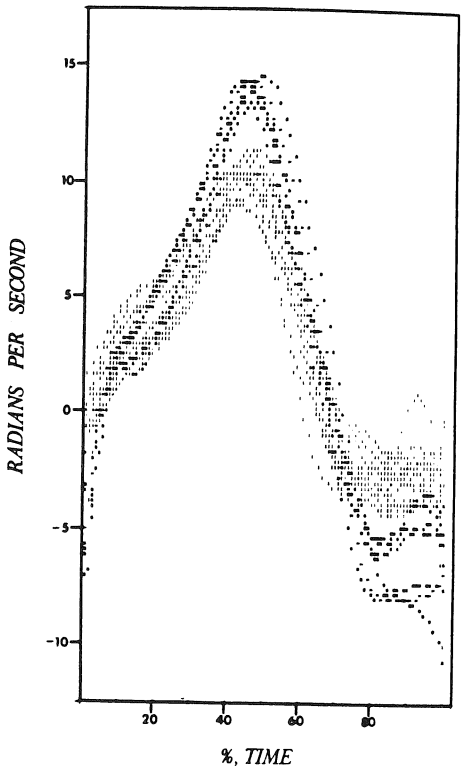

Fig.2 Thigh angular velocity. Young adults, O; Masters, I. Positive represents flexion.

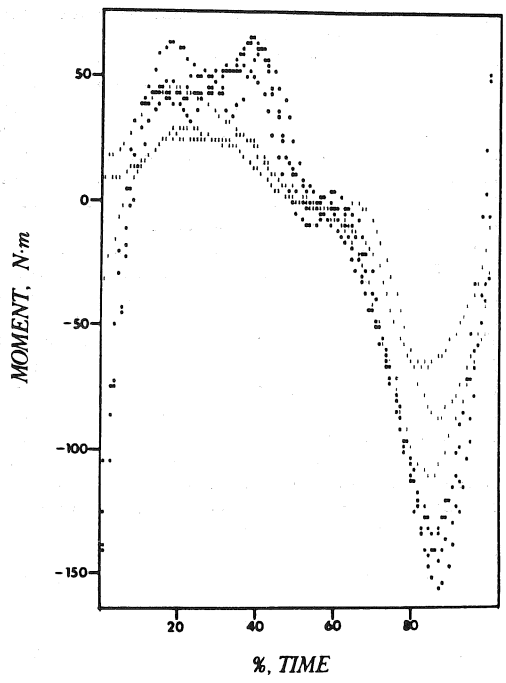

Fig.3 Knee muscular moment. Young adults, O; Masters, I. Positive represents extensor.

COMPARISON OF TWO ELECTROGONIOMETER PLACEMENTS FOR THE MEASUREMENT OF ANKLE MOVEMENTS DURING GAIT

D. GRAVEL and C.L. RICHARDS

Neurobiology Laboratory and Physiotherapy Section
Faculty of Medicine
Laval University
Québec, Québec, G1K 7P4

INTRODUCTION

Electrogoniometers (EGM) combined with on-line computer processing offer many advantages for the measurement of lower extremity movements during gait. The reliability of EGM measurements of hip (1) and knee (2) movements have been reported but information is lacking for ankle movements. EGM measurements of joint motion, however, require careful applications of the device to the limb segments. Since we encountered problems approximating the axis of our EGM to that of the ankle joint for sagittal movements, we tested alternative alignments of the EGM. The purpose of this paper is to describe the difference between measurements taken with two alignments. In one, the ankle EGM sagittal axis is above the ankle axis, while in the other, the EGM and ankle joint axes are approximately co-axial. The distal attachments are altered accordingly for each placement.

METHODOLOGY

Five normal subjects participated in this study. The MERU electrogoniometer, also known as the CARS-UBC electrogoniometer (3) and later modified by Knutsson and Gransberg (Karolinska Sjukhuset, Stockholm) was used in this study. The signals from the potentiometer were processed by Grass amplifiers (model 7P1) and subsequently sent to a LS1-11/03 computer. Profiles of 20 gait cycles (determined from footswitch closures) were averaged. The two alignments were produced by altering the placement of the distal arm (which in this EGM is composed of three interconnected potentiometers and the distal attachment plate). The first placement, (H), was with the distal arm fixed to the lateral side of the heel (Fig. 1a). In the second placement (M), the fixation of the distal arm was on the metatarsal region of the foot (Fig. 1b). For each placement, two series (1 and 2) of 20 cycles separated by removal and then re-application of the EGM were recorded, in order to evaluate the reproducibility of the placement. A common ankle reference position (zero in the figures) for the placements was determined by instructing the subject to stand upright with the feet close to each other. Subjects walked along a 5 meter walkway at natural cadence. The movement profiles obtained with the two placements were compared by Pearson correlation coefficients calculated for angular displacements at each 2% of the mean movement cycle in each subject. Absolute differences between the two placements were also calculated at each 2% of the gait cycle and averaged to give an estimate of the difference (in degrees) for the complete cycle. The total excursions, maximal dorsiflexion minus maximal plantar flexion, during the gait cycle were also compared. Statistical differences were determined with the Student t test for paired values.

RESULTS

Figure 2 illustrates the results obtained in one of the subjects. As seen in the figure, the differences between the two series with each placement (A and B) or between the two different placements (C) are quite small. Table I gives the mean values and the range for the differences between specific placements. As expected, the absolute difference between the two series (1 vs 2) for each placement is lower than the difference between placement H and M. It should be noted, however, that the mean absolute difference (2.59 degrees) between placements H and M is only about one degree greater than the difference between repeated tests with each placement (1.59 and 1.26 degrees). The high correlation coefficients for all the tests also indicate that, in general, the profile of the ankle motion is similar for all placements. Some differences can, however, be noted in a visual comparison of the curves. For example, with placement H, oscillations of the curves between 0 and 10% of the cycle appear larger and the slope of the dorsiflexion movement between 10 and 50% of the cycle is steeper than with placement M. The excursion measured with placement M (30.96 ± 3.11) is significantly higher ($p < .05$) than the excursion obtained with placement H (25.48 ± 3.28).

DISCUSSION

The differences between the measurements obtained with the two different EGM placements are small and not much greater than differences in repeated measures for one placement. Since the order of magnitude of the absolute difference between the two placements was similar to that obtained with the repeated measurements, it is not surprising that the profile differences were small as indicated by the high correlation coefficients. It does appear, however, that with the M placement, oscillations in the angle profile due to impact forces following heel contact are reduced. The significantly greater excursion with the M placement can probably be explained by the contribution of the mid-tarsal joint movements (4), although we cannot completely exclude the effects of mis-alignment of the EGM to the joint axis. These findings suggest that other methods of ankle joint measurements during gait which consider the foot as a rigid segment give representative profiles of sagittal ankle movement (5,6,7). Movements measured in the other two planes will, however, be differentially affected by the placements. Furthermore, the reproducibility of the ankle measurements obtained with each placement is comparable to that described for electrogoniometric hip and knee measurements (1,3).

REFERENCES

1. Johnston, R.C. et al. J. Bone Joint Surg. 51-A: 1083-1094, 1969.
2. Kettelkamp, D.B. et al. J. Bone Joint Surg. 52-A: 775-790, 1970.
3. Hannah, R.E. et al. Arch. Phys. Med. Rehabil. 65: 155-158, 1984.
4. Tardieu, G. et al. J. Biophys. Med. Nucl. 6: 27-29, 1982.
5. Sutherland, D.H. et al. J. Bone Joint Surg. 54-A: 787-797, 1972.
6. Richards, C. et al. Scand. J. Rehabil. Med. Suppl. 3: 61-68, 1974.
7. Winter, D.A. et al. J. Biomech. 7: 479-486, 1974.

TABLE I

Values obtained in the comparison of the electrogoniometer placements.

Placement comparison	Absolute difference (degrees)	Correlation coefficient (r)
H1 vs H2	1.59[a] (1.08-2.36)	0.980 (0.962-0.994)
M1 vs M2	1.26 (0.51-2.69)	0.993 (0.986-0.998)
H vs M	2.59 (1.46-3.98)	0.971 (0.959-0.980)

a Values given as mean with the range in brackets

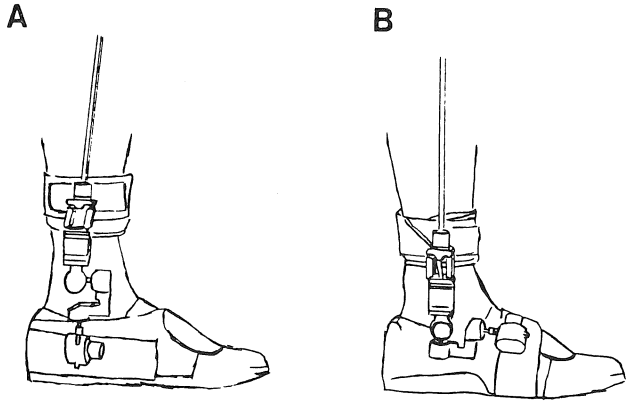

Figure 1. Illustration of placements tested: In A, the distal arm of the electrogoniometer is attached to the lateral side of the heel (placement H) and B, the distal arm is attached to the metatarsal region (placement M). Note: although 3 potentiometers are shown in the figure, only sagittal movements (proximal potentiometer) were recorded.

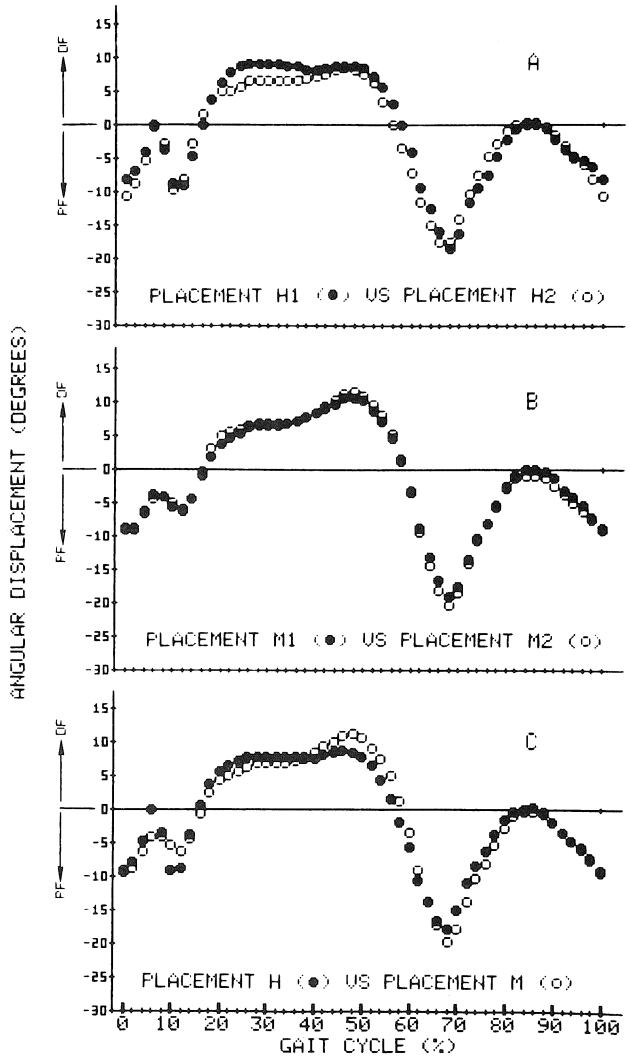

Figure 2. Ankle movement profiles obtained with the different placements of the electrogoniometer in one subject. In A, placement H is repeated, in B, placement M is repeated, and in C placement H is compared with placement M. In A and B, each profile is the average of 20 gait cycles; in C, each profile represents the mean (40 gait cycle) of the two series of movements shown in A and B. Cadence (N=40) was 118.9 steps/min for H placement and 116.4 steps/min for M placement.

ACKNOWLEDGMENTS

The authors thank Daniel Tardif, Gérard Guano and Lise Laroche for technical assistance. This work was supported by a grant from l'Institut de Recherche en Santé et en Sécurité du Travail du Québec (IRSST).

CHILD AMPUTEE WALKING AND RUNNING GAIT: A COMPARISON BETWEEN THE SACH AND SINGLE-AXIS FOOT COMPONENTS

B.Brouwer P.Allard H.Labelle

School of Physical & Occupational Therapy, McGill University Montreal, Quebec.

Dept.of Physical Education University of Montreal, Montreal, Quebec.

Dept. of Orthopaedics Sainte-Justine's Hospital Montreal, Quebec.

INTRODUCTION

Temporal parameters, angular displacement patterns and joint moments have been analyzed to describe the walking and running gait of below-knee (BK) child amputees with respect to a given foot prosthesis worn. The solid ankle cushion heel (SACH) and single-axis (SA) prostheses are substitutes for the weight-bearing foot and the ankle joint permitting simulated plantarflexion through heel compression and limited dorsi and plantarflexion from a hinged axis joint respectively. Scaled down versions of the adult models of the foot components are provided for children, however their appropriateness in view of the child's ongoing developmental growth and diverse activities remains in question. The findings implicate inadequacies for both components, although lessened for the SA in walking.

REVIEW AND THEORY

Prolonged inter-limb asymmetries have been linked with degenerative changes in the lumbar spine and the prevalence of osteoporosis and osteoarthritis on the affected and unaffected limbs respectively of lower limb amputees (1). The extent of which may be related to the degree of asymmetry and the force magnitudes involved, often exceeding twice body weight in running. An appropriate substitution for the lost limb may reduce any undesirable gait patterns and improve the amputee's stability in various activities (2). Whether the SACH and SA components meet such criteria is examined herein.

METHODOLOGY

Cinematographic and forceplate data were collected on two occasions from six unilateral BK child amputees. During the first session all subjects wore their SACH components and were each filmed bilaterally in the sagittal plane walking at their natural cadence along an instrumented walkway and again while running. The SACH foot was then replaced with a SA and following two weeks accomodation the children were retested. The digitized body markers and external references were processed yielding kinematic information. Link segment analysis (3) using combined kinematic and forceplate data provided the moments about the ankle, knee and hip. Using NEXUS, a computer language for signal and system analysis (4), angular displacements were normalized to a 60/40 percent stance/swing ratio in walking and a 34/66 ratio in running; the moments were normalized to the stance phase only. Residual angle and moment curves were calculated by subtracting each subject's specific SACH limb parameter from their intact limb's counterpart, SA from intact, and the SACH from the SA. Each of the three residuals were then averaged across subjects, hence providing a measure of asymmetry and prosthetic performance relative to the gait cycle (GC).

RESULTS AND DISCUSSION

In walking, less time was spent on the amputated side largely due to an early push-off from the affected limb as indicated by the shorter late double support (DS) duration compared to the early DS (SACH:$p < .02$, SA:$p < .05$). This is attributed to the inability to generate a downward thrust via active plantarflexion as confirmed by a smaller than normal second vertical ground reaction force (VGRF) peak for both components ($p < .05$), as well as the large asymmetry revealing the incapacity of the SACH and SA feet to plantarflex to the extent of the natural limb at toe-off (arrow, fig.1a). Figure 1a illustrates the ability of the SA foot to dorsiflex during midstance, a movement not permitted by the SACH foot. The forceplate data exaggerates this limitation as the characteristic dip centered in the VGRF curve is markedly less than the SA and intact limbs ($p < .05$) indicating a diminished capacity for the SACH limb to accelerate upwards following heelstrike. The SA restoring moment from the dorsiflexion allows greater extensor contribution than the SACH and less discrepancy from the natural limb (fig.1b). The remaining limb's compensation is most evident at the knee particularly at heelstrike and toe-off (fig.2a and b). The affected knee yields less initial flexion corresponding to a below normal extensor moment and more flexion at toe-off, preceded by an above normal extensor moment to enhance stability and compensate for the lack of extension provided by the ankle. The compensations at the hip (not shown) were not as evident.

For the running condition, the amputees spent more time on their prostheses (SACH:37.2%; SA:36.0%) than their natural limb (31.0%) which effectively limited stride length and velocity, both of which may enhance feelings of safety and stability. The reduced VGRF on the prosthesis side, 210% and 206% body weight (BW) for the SACH and SA respectively, as compared to the unaffected side, 245% BW ($p<.01$) was probably secondary to the slower prosthetic running speed and reduced acceleration. Relative to walking, the inter-limb asymmetry magnitudes were larger and the difference between the SACH and SA limbs were smaller. The foot components themselves displayed less than $\pm 2^{o}$ difference at the ankle throughout the GC, yet they were unable to generate the desired movement outcome. At initial contact, the intact foot dorsiflexes whereas the prostheses respond by plantarflexion due to their structure. This promotes a peak asymmetry in addition to that noted, as in walking, at toe-off due to the absence of plantarflexion. It follows that the ankle's extensor ability was diminished to an extent irrespective of the component worn (not shown). The flexion excursion of the knee at initial contact was reduced exposing it to higher force loads than normal, requiring strong extensor activity at that time (fig.3a and b). Throughout the remainder of stance, substantially lower extensor moments were generated despite more similar joint patterns, intimating a secondary effect of reduced speed, increased stance and possibly a loss in the knee's

mechanical advantage. This appears to be compensated by an above normal hip extensor moment, although, saving initial contact, the extension was less on the amputated side which may increase stability (fig.4a and b). At all joints, the characteristics of the SACH and SA limbs were similar, yielding a maximum residual amplitude representing less than 12% of the respective joint or moment range. Also, the prosthetic limb's muscle moments did not exceed the range determined for the intact limb.

CONCLUSIONS

It is evident that symmetries exist between the amputated and intact limbs, however, in walking they are less when the SA foot is worn, due mainly to its ability to dorsiflex. In running, the inter-limb asymmetries are augmented and are not influenced by the prosthesis worn suggesting that neither component is designed for such activity. Finally, although the forces may not in themselves be excessive, the continued imbalance of their application on a developing skeletal system may have adverse long term effects (5).

ACKNOWLEDGEMENTS

This work was supported by the War Amputations of Canada, FCAR and a McGill Major Fellowship. The authors gratefully acknowledge the programming assistance of Serge Lafontaine and the availability of McGill's Biomedical Engineering Unit's Computing facilities.

References

1. Burke,M.J. et al. Annals of Rheum.Dis.,37:252-254, 1978.
2. Burgess,E.M. et al. Orth. and Pros.,37:26-31, 1983.
3. Bresler,B., et al. Trans. ASME, 72:27-36, 1950.
4. Hunter,I.W. et al. Comput.Biol.Med.,14:385-401, 1984.
5. Perry,J. A.A.O.S.(eds). Atlas of Orthotics, pp.144-168, 1975.

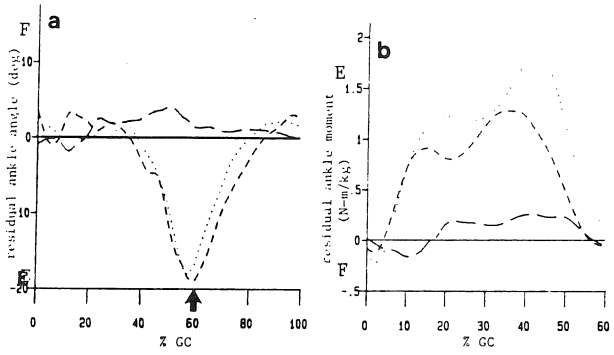

Figure 1 The mean residual ankle angle (a) and moment (b) curves representing the difference(asymmetry)between the SACH limb and the intact limb (...), the SA limb and the intact limb (---) and the SACH limb and the SA limb (— —). Moments are normalized to body weight.
F=net flexion (dorsiflexion),
E=net extension (plantarflexion)

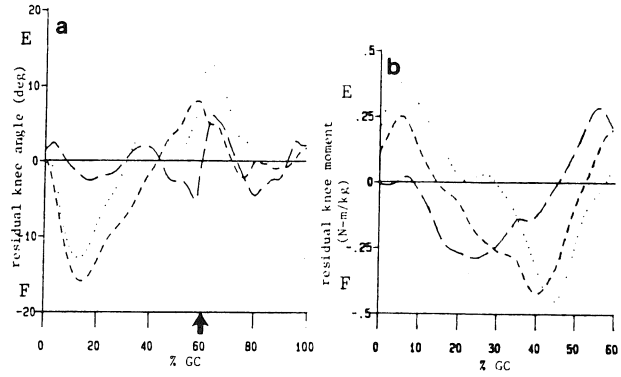

Figure 2 The mean residual angle (a) and moment (b) curves for the knee joint in walking.

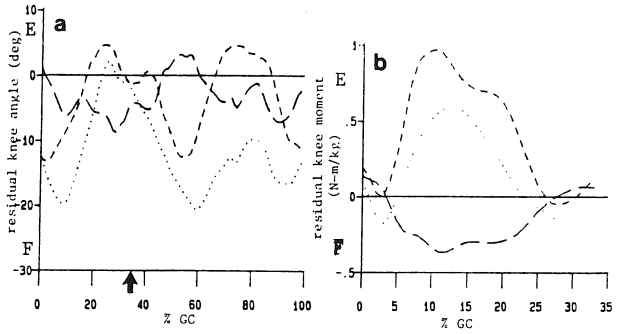

Figure 3 The mean residual angle (a) and moment (b) curves for the knee joint in running.

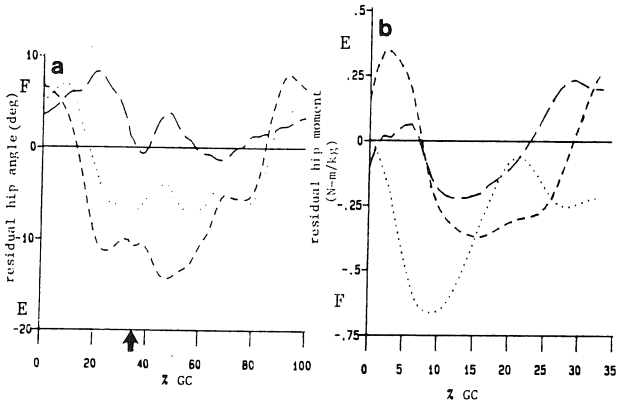

Figure 4 The mean residual angle (a) and moment (b) curves for the hip joint in running.

QUANTITATIVE THERAPY CONTROL USING GAIT ANALYSIS

S. Luethi
Biomechanics Laboratory
Fed. Institute of Techn.
Zuerich, Switzerland

E. Stuessi
Biomechanics Laboratory
Fed. Institute of Techn.
Zuerich, Switzerland

B. Segesser
Rennbahn Klinik
Muttenz
Switzerland

INTRODUCTION

The purpose of the present study was to apply gait analysis as a clinical tool for quantitative control during rehabilitation of an elite gymnast after achilles tendon rupture. The analysis was started five weeks postoperative and stopped six weeks later when gait symmetry was recovered. The analysis proved to be a useful help for the clinician in order to get quantitative information about the load carried in the achilles tendon during gait over the different stages of rehabilitation.

REVIEW AND THEORY

Rupture of the achilles tendon is a typical sports injury. About 80% of the cases occurr during sports activity (1). The injury is crucial since it affects a whole muscle group, the m. triceps surae, which is a main functional structure in order to maintain human locomotion. Late complications may result in a reruptur of the tendon, usually occurring before 4 months after the operation (1,3) with a frequency between two and six percent.

Clinician as well as athlete are faced with the problem on how to progress during rehabilitation with respect to the increase in loading of the tendon. Since no quantitative information is available the recommendations given in literature are mostly cautious in nature. Immobilization up to eight weeks are suggested, followed by careful therapeutical treatment. On the other hand the negative influence of total immobilization on the properties of biological materials are well known (2). The present pilot study was to investigate the possibility of a quantitative control of early therapy during different stages of rehabilitation.

METHODOLOGY

The subject was analyzed while walking 5, 7, 9 and 11 weeks after operative treatment. External kinetic measurements were carried out using a KISTLER force plate and data were stored on-line on a LSI 11/23 minicomputer. The external force data were combined with a quasistatic analytical model developed by Stuessi (4). Subsequently, the actual load carried by the achilles tendon during stance phase was calculated. Graphical and numeric results were available immediately after the measurements so that the following therapeutical treatment could be based on it.

RESULTS

The results of the calculated internal forces are summarized in figures 1 and 2. Figure 1 shows the development of force in the achilles tendon during walking over the six weeks of analysis. The recovery in gait symmetry with respect to the function of the triceps surae muscles is indicated in figure 2.

DISCUSSION

Within the limitations of a case study the results show the effect of early postoperative therapy on the load in the achilles tendon during walking. The greatest increase in absolute maximum force is seen between the seventh and the ninth week after operative treatment (1.2 BW up to 2.7 BW) which is in agreement with the results of Arndt (1). During this period the maximum force was more than doubled. The same relative increase is demonstrated for the period between the fifth and the seventh week, wheras the increase in maximum

North American Congress on Biomechanics
Montréal (Québec) Canada, 25-27 August 1986

force over the last period (ninth - eleventh week) is comparatively moderate. Gait symmetry with respect to the function of the calf muscles was practically recovered after 11 weeks (see figure 2). When comparing the results between the affected and the non-affected leg then the greatest improvement towards gait symmetry was again made during the period from the seventh to the ninth week. According to these results physical therapy was stopped after this period and the athlete started with a continously progressing training program which is considerably earlier than suggested in literature.

The findings of this pilot study suggest that an objective and quantitative control of therapy may be a useful tool for the rehabilitation process. It leads to the hypothesis that such a biofeedback system would have significant consequences on the optimization of quality and time of postoperative therapy. The encouraging results of the present study will therefore lead to a larger investigation in the near future.

References

1. Arndt, K.H., Med. u. Sport, 26:31-32, 1986.
2. Noyes, F.R., et al., Clin. Orthop. 123:210-242, 1977.
3. Thiel, A., Z. Orthop. 110:796-798, 1972.
4. Stuessi, E., et al., 2. Nuernb. Gelenks. 27-40, 1985.

Acknowledgment

This project is supported by the SWISS NATIONAL FOUNDATION

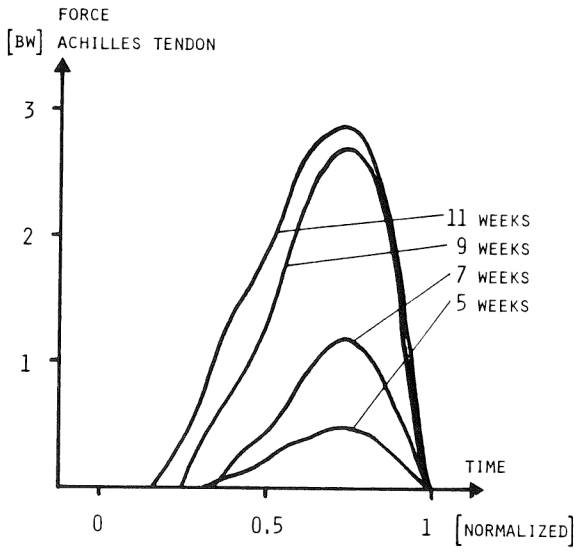

Figure 1. Calculated force in the achilles tendon during stance phase over six weeks of rehabilitation.

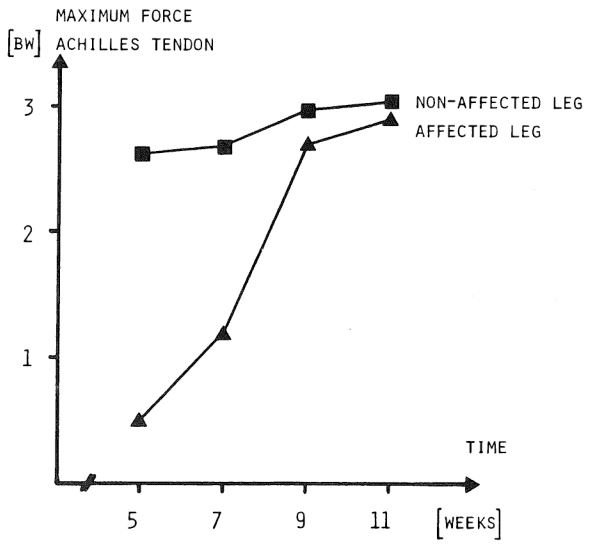

Figure 2. Calculated maximum force in the achilles tendon.

Biomechanical Aspects of Shock Absorbing Devices

Arkady S. Voloshin

Department of Mechanical Engineering and Mechanics
and Division of Bioengineering, Center for Health Sciences

Lehigh University
Bethlehem, PA 18015

INTRODUCTION

One of the negative results of man's development was the altering of his environment which removed him from resilient, grassy grounds to the concrete reality of the city. This transition resulted in much higher physical loads on the human musculoskeletal system. The natural shock absorber which is built into every one's heel pad became an insufficient one. The energy which invades the body during each heel strike can no longer be any more sufficiently attenuated, modified and dissipated by only the heel pad which leads to an overloading of the natural shock absorbers of the musculoskeletal system.

Mechanically induced shock waves (walking on a hard surface, standing on a vibrating surface or near vibrating machinery, etc.) not only cause excessive fatigue, but are also suspected to be a main cause of low back pain (LBP) (1), occupationally induced headaches and some degenerative joint disorders in humans (2).

Significant reduction or even elimination of the injurious effects of the shock waves are contingent upon development of the accurate methods to quantify these waves and the effect of various shock absorbing devices on the human body.

METHODOLOGY

A variety of methods were suggested for evaluation of the shock absorbing capacity of footware. Usually performance of the footwear by itself is studied, without taking into account actual foot-footwear interaction. In this investigation a novel approach, by which a small low-mass accelerometer is strapped externally to the selected point on the human body, was utilized (3). The signal, which represents shock waves actually induced into the human musculoskeletal system during walking, was acquired by a digital oscilloscope and its maximum amplitude was recorded for each heel strike. A 20 year old female served as a test subject. She was allowed 20 minutes to get used to instrumentation. During data acquisition, her average speed was adjusted to 1.2 sec/walking cycle.

RESULTS

The maximum amplitude of the signal (in g-units) was recorded during walking in the shoe only, shoe with device A, B and C, each representing a different, commercially available insole. The combined results are presented in Table 1.

Table 1. Maximum values of acceleration.

Type of test	Number of trials	Average acceleration	Standard deviation
Shoe only	32	2.097	0.161
Shoe + A	32	1.612	0.100
Shoe + B	32	1.592	0.096
Shoe + C	31	0.911	0.053

The shock absorption of the investigated insoles was defined with respect to a base-line, which was established as walking in the shoe without any insole in it. Relative attenuation was defined as a ratio of mean difference between measured acceleration in the shoe only and in the shoe with the insole over the base-line value. Calculated average reduction in the measured acceleration level for each insole is presented in a graphical form in the Figure 1.

The implication of the above results are that the use of viscoelastic insoles during normal walking will decrease the amplitude of the shock wave propagating through the body and therefore, protect the joints from overloading their capacity to sustain intermittent loading.

The statistical "two sample t-test" was used to evaluate the significance of the obtained differences. If one sets a goal of at least 15% reduction in the amplitude of the incoming shock wave, the probability of an error is less than 0.0005 for all insoles tested. The overall performance of the insoles is summarized in Table 2.

Table 2. Performance of the insoles.

Type of insole	% of shock wave dissipated	Probability of error
A	20.	0.0500
B	20.	0.0250
C	50.	0.0005

DISCUSSION

As one can see from the Table 2, the investigated insoles are capable of attenuating the heel strike-induced shock wave with a high degree of confidence. However, the usefullness of any insole depends on a particular application. For example, the insole A, which is thin and relatively light and on average provides only 22.7% reduction of the amplitude can be of importance for people who spend their day in thin-soled shoes, which by themselves provide very little shock absorption. The insole B provides a little bit better protection (23.7%);

North American Congress on Biomechanics
Montréal (Québec) Canada, 25-27 August 1986

however, it is much heavier than insole A. On the other hand, insole B will provide better protection in the metatarsal area, thus making it very attractive for court game players. The insole C provides maximum reduction of the amplitude of the shock wave, but its construction is relatively large; thus it can not be used in regular everyday footwear, but may be exellent in heavy boot applications.

It is therefore probably difficult to expect an insole that can be good for all occasions, but special purpose insoles can be built to satisfy a variety of requirements.

CONCLUSIONS

The methodology presented here can be used for non-invasive, in-vivo evaluation of the shock absorbing capacity of a variety of insoles during actual use, i.e. walking, running, jumping, working in a vibrating environment, etc. The main advantage of the presented technique is the use of actual foot-insole interaction during evaluation. The same approach can be used during development of new insoles for specific applications.

ACKNOWLEDGMENT

The author thanks Ms. Andrea Oehlke, Ms. Carla Burd and Mr. Edgardo Queirolo, Lehigh University students for their interest, help and engagement of this method.

References

1. Wosk, J., et al. Archives of Physical Medicine and Rehabilitation 66:145-148, 1985.
2. Radin, E.L., et al. Ann. Rheum. Dis. 34:132-133, 1975.
3. Voloshin, A.S., et al. J. of Biomedical Engineering 5:157-160, 1983.

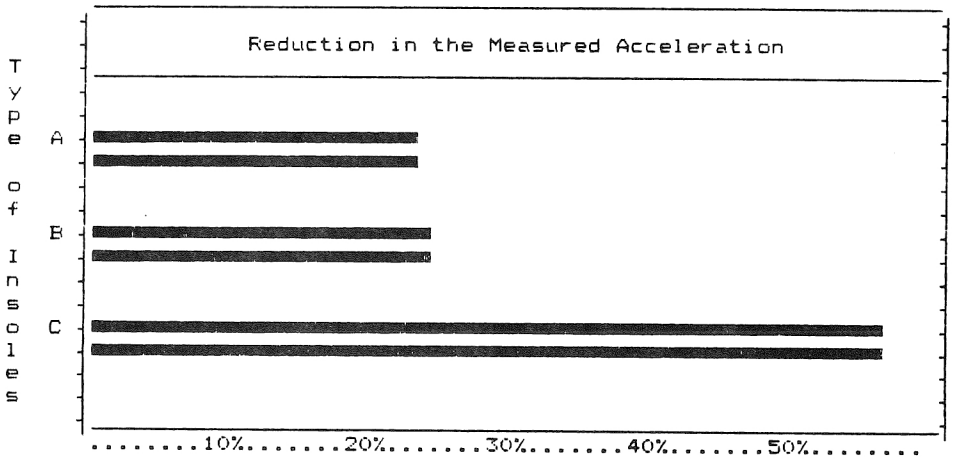

Figure 1. Shock Absorption of the Insoles.

Discrete In-shoe Plantar Stress Variations with Running Speed

Ted S. Gross and Richard P. Bunch

Converse Biomechanics Laboratory
1 Fordham Rd.
North Reading, MA 01864 U.S.A.

INTRODUCTION

Eight discrete piezoelectric transducers were constructed to record in-shoe plantar stresses as subjects ran on a treadmill. The sensors were placed beneath anatomical points of interest on the underside of running shoe insoles. Plantar stress variations with running speed were examined to assess a hypothesized causal relationship between increased symmetric metatarsal loading and increased running speed. In addition, loading patterns gave insight to discrete foot function during distance running.

REVIEW AND THEORY

A majority of investigations examining the foot/ground interaction have involved force plates. Resultant force and center of pressure plots have been used to indicate the magnitude and approximate orientation of loads in relationship to the foot. However, detailed investigation of loading with respect to foot anatomy is not possible with force plates. Instead, investigators (Stott et al.; 1973, and Cavanagh and Rodgers; 1985) have developed equipment to record the distribution of plantar loads. While possessing a higher dimensional resolution than force plates, these studies were limited by the effects of targeting a small area and an inability to include the shoe as a component of the foot/ground interaction. As a result, plantar stress investigations have focused on barefoot walking.

The equipment developed for this investigation allowed measurement of localized stress inside running shoes during distance running while freeing subjects from targeting concerns. Although placement beneath the insole prevented direct discrete stress measurement, this attachment method was necessary to preserve element integrity throughout the experiment.

METHODOLOGY

The ten competitive distance runners participating in this study were rearfoot strikers across the protocol running speeds (2.98, 3.57, 4.50m/s). Subjects trained an average of 80km per week and were selected based on a training pace within 0.2m/s of the median test speed.

The transducers were characterized in a manner similar to Hennig et al. (1982). Average nonlinearity and hysteresis were less than 1% when measured with the elements between the insole and midsole of the running shoe utilized in the study.

Transducers were located by palpation under the following anatomical points of interest (see Fig. 1.): 1) calcaneal midline, 2) inferior to the medial navicular prominence, 3) base of fifth metatarsal, 4) head of fifth metatarsal, 5) head of third metatarsal, 6) head of second metatarsal, 7) head of first metatarsal, and 8) centered plantar surface of the hallux.

A potential criticism of discrete transducer use is the variability associated with element placement. To assess this variability, one subject performed the test protocol six times over a three week period. Variability of the within day means for each element were assessed over the six test sessions. The average coefficient of variation across running speeds and elements was 7.6% of the mean. Included within this error estimate were trial, day to day, and placement variability.

The elements were secured inside the left shoe after a fifteen minute treadmill warmup. Running speed was sequenced randomly across subjects. Participants ran at each test speed for approximately six minutes. The first minute was used to allow the subject to reach a steady and comfortable running form. Five left footstrikes were recorded at one minute intervals at each speed.

The instrumentation gain conditioned the analog output to a plus/minus 10V. Voltages were sampled at 333Hz per channel and were stored in a PDP 11/44. Data analyzed included peak stress and impulse (stress output multplied by transducer surface area, integrated over time). Running speed effects were assessed with repeated measure analysis of variance at the $p=0.05$ level of significance. The Tukey WSD was used for post hoc comparisons.

RESULTS

Peak stresses under the foot were influenced by running speed (see Table 1.). The medial midfoot region displayed constant stress across speeds. The trend of the lateral midfoot, and first and fifth metatarsal heads was to slightly increase stress as running speed increased. The second and third metatarsal heads, along with the hallux and calcaneus produced significantly increased peak stresses at each speed.

Two impulse analyses were performed. Absolute impulse was designated as the individual transducer force/time integral. However, this measurement was misleading when used to examine stress variations as a result of running speed. Decreased foot contact time experienced at increased speeds were confounded by increased peak stresses. The general trend for all elements was a slight decrease in absolute impulse as

North American Congress on Biomechanics
Montréal (Québec) Canada, 25-27 August 1986

running speed increased. Relative impulse proved to be a more useful descriptor of discrete foot function. This measurement normalized the contribution of each element to the total impulse recorded during foot contact. The only statistically significant changes in respective contribution across running speeds were found between the high and low speeds at the calcaneus, medial midfoot, and first metatarsal head. The actual differences were less than 0.7%.

DISCUSSION

Peak stress data, resulting from functional loading of the foot, suggested kinetic variations as subjects increased running speed. Within the range of a slow jog and a 10k race pace, two regions of function were evident in the rearfoot striking runners; the rearfoot, or heel region, and the forefoot, which included the metatarsal heads and the toes.

Higher peak stresses under the calcaneus were found as running speed increased, indicating more severe landings. Similar results were noted by Nigg (1986), who examined bimodal vertical force plate data produced by runners at different speeds. Data from the current investigation indicated that, across running speeds, peak calcaneal stresses occurred at approximately 14% of foot contact time. Loading for the first, second, and third metatarsal heads did not begin until 11% of foot contact time. This finding suggests a delineation between rearfoot braking and forefoot propulsion in rearfoot striking runners.

Peak stresses did not increase systematically under the forefoot as running speed increased. A distinctive facet of fifth metatarsal function was the onset of loading prior to medial midfoot loading. The small fifth metatarsal peak stress variations, coupled with early loading, suggested an important role in stabilizing the foot and minimal use as a propulsive mechanism. In addition, loading under the first metatarsal head increased slightly with speed and was approximately 55% the magnitude of stresses recorded under the second metatarsal and hallux. Low first metatarsal loading was surprising. Apparently, as the hallux forcibly plantarflexed, a bridge was formed by the first metatarsophalangeal joint which prevented increased application of stress under the first metatarsal head. The propulsive rigid lever idealized in foot function literature appeared to be formed by the second and third metatarsal heads and the hallux rather than the whole forefoot.

Decreased contact time as speed increased confounded absolute impulse calculations. Hypothesized increases in forefoot propulsion with increased speed were evident only in peak stress analyses. However, relative impulse was used to describe individual contributions of structural foot components. The three principal load bearing structures were the second and third metatarsal heads and the hallux. The summed impulse of these elements was greater than 57% of the total recorded impulse. One implication of the findings is that changes in running speed were accomplished by a synchronous, simultaneous increase in forefoot loading, rather than by "pushing" off harder with either the hallux or metatarsal heads individually.

REFERENCES

Cavanagh, P., Rodgers, M. (1985). Pressure distribution underneath the human foot. In S. Perren and E. Schneider (Eds.), Biomechanics: Current Interdisciplinary Research (pp. 85-95).

Hennig, E. et al. (1982). A piezoelectric method of measuring the vertical contact stress beneath the human foot. J. Biom. Engr., 4:213-222.

Nigg, B. (1986). Experimental techniques used in running shoe research. In B. Nigg (Ed.), Biomechanics of Running Shoes (pp. 27-61).

Stott, J., et al. (1973). Forces under the foot. J. Bone Joint Surg., 55B:335-344.

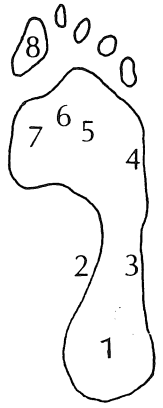

Figure 1. Plantar Surface of Left Foot Showing Discrete Element Placement.

Table 1. Mean (s. dev.) peak plantar stress variations with running speed.

Element	Running Speed (m/s) 4.50	3.57	2.98
Calcaneus	426.6 (84.5)	361.8 (79.8)	303.9 (62.7)
Lateral Midfoot	463.5 (102.1)	423.6 (89.7)	405.2 (82.4)
Medial Midfoot	164.8 (45.1)	165.7 (36.9)	167.0 (35.2)
Fifth Met.	378.1 (141.2)	366.1 (146.8)	346.8 (130.5)
Third Met.	515.5 (127.9)	481.1 (100.9)	446.4 (93.1)
Second Met.	730.5 (155.4)	676.8 (122.7)	633.5 (102.6)
First Met.	386.7 (110.3)	373.4 (91.0)	357.9 (83.7)
Hallux	712.4 (349.4)	642.1 (321.0)	575.1 (297.9)

All stresses in Kpa. Underlined values are not significantly different at p=0.05.

THE INFLUENCE OF LATERAL HEEL FLARE ON PRONATION AND IMPACT FORCES

B.M. Nigg
Biomechanics Laboratory
University of Calgary
Calgary, Canada

J. Denoth
Biomechanics Laboratory
ETH Zurich
Switzerland

R. Glover
Biomechanics Laboratory
University of Calgary
Calgary, Canada

INTRODUCTION

In the last ten years, running shoe research yielded three general findings: (a) The running shoe should absorb and/or reduce impact forces in the first 50 milliseconds of ground contact (Nigg et al., 1978; Cavanagh, 1978; Frederick et al., 1981; Clarke et al, 1984; Nigg et al., 1986) since these impact forces are assumed to be associated with injuries such as fatigue fractures, tendinitis and cartilage damage (Segesser et al., 1980; Radin et al., 1982; Voloshin et al., 1982). (b) The running shoe should provide lateral stability and/or control which sometimes is referred to as rearfoot control (Nigg et al., 1977; Bates et al., 1979; Cavanagh, 1980; Stacoff et al., 1983; Clarke et al., 1984) since lateral instability is assumed to be connected with overuse injuries such as anterior medial compartment syndrome (James et al., 1978; Segesser et al., 1980; Clement et al., 1981) or iliotibial band syndrome. (c) The running shoe should provide direction at take-off avoiding an oversupination of the foot during the take-off phase (Nigg et al., 1980; Stacoff et al., 1983; Nigg et al., 1986). Oversupination at take-off is speculated to be connected with achilles tendon problems.

These three main criteria are widely accepted. However, there is considerable discussion about the strategies to choose on how to reach the goal described in these three aspects. One of the main discussion points is the aspect of rearfoot control. Various constructional aids (such as heel stabilizers, wedges, double density soles, various heel flares and heel caps) are offered as possible solutions to reduce pronation and to increase "rearfoot stability."

The purpose of this paper is to study the influence of sole geometry (flare at the lateral side of the heel of running shoes) on initial and total pronation and impact forces in heel-toe running.

MATERIAL AND METHODS

Rearfoot movement was quantified by using markers on the heel of the shoe or the heel of the subject and the posterior side of the lower leg (Nigg et al., 1977; Bates et al., 1978; Nigg and Luethi, 1980; Cavanagh, 1980; Clarke et al., 1984). The projection of these markers in a plane perpendicular to the running direction was used to define the rearfoot angle γ between the markers on the heel and the horizontal on the medial side, and the achilles tendon angle β between the markers on the lower leg and the heel on the medial side. The method which is explained in detail elsewhere (Nigg, 1986) describes the motion of the shoe with its rearfoot angle γ, and the motion in the joints (subtalar and ankle joint) with its achilles tendon angle β. Because of the two dimensional approach, rotation around the ankle and/or subtalar joint could not be determined in this investigation.

The ground reaction forces recorded during the first 50 ms after touchdown of the heel were chosen as the measure of the impact forces. These measurements provide the initial ground reaction forces which are external forces describing the impact phase. They are not identical with the internal impact forces in ankle or knee joint.

The experimental part of the study was performed with fourteen male runners with a mean mass of 69.8 kg (S.D. 5.3 kg) who ran a minimal weekly distance of 15 km. Three pairs of running shoes (size 9) were used in the study. They were identical in construction except in the geometrical shape of the lateral posterior part of the shoe sole. Shoe A had a flare of 16 degrees on the lateral side. Shoe B had a flare of 0 degrees, and Shoe C had the lateral posterior part of the sole rounded (radius about 3 cm) so that it had a negative flare with a changing value. The runway was about 16 m long with a force platform located in the middle of the runway. The running velocity was 4 m/s ± 0.2 m/s, controlled by photocells. Simultaneous film measurements were taken from a posterior and a lateral view of the runner with a film frequency of 100 frames per second. The variables discussed in this context are defined and discussed in detail by Nigg (1986).

RESULTS

The mean values of initial pronation decrease from shoe A to shoe B to shoe C which means from positive to negative flare for both the initial joint pronation and the initial shoe pronation. The reduction from shoe A to shoe C is 40% for the initial joint pronation and 45% for the initial shoe pronation. The contact time did not change significantly for the three shoe types.

The mean values of total pronation do not differ for the three shoe types and are between 14.1 and 15.1 degrees for the total joint pronation and between 11.4 and 12.7 degrees for the total shoe pronation. A change of the shape of the lateral heel flare construction reduces therefore the initial pronation for joint and shoe but does not influence the total pronation for both joint and shoe.

The mean values of the vertical impact force peaks and the maximal loading rate do not change significantly due to the different heel flares. However, the time of occurrence of the impact peak changes from 37.8 ms for shoe A with the conventional positive flare to 29.4 ms (29%) for shoe C with the rounded heel (negative flare).

DISCUSSION

The results for the reduction of initial pronation were expected. They are connected with a change in lever arm. An illustration of the influence of lever arm on initial pronation for running with a conventional running shoe with positive flare compared to barefoot running is explained by Stacoff and Luethi (1986, p.136). The result of reduced initial pronation is also consistent with results of another experiment where shoes with different midsole hardnesses were compared (Nigg et al., 1986, p.154). Mechanical consideration and experimental results for initial pronation are therefore in agreement.

North American Congress on Biomechanics
Montréal (Québec) Canada, 25-27 August 1986

The result that total pronation is not influenced by the geometrical construction of the lateral heel flare may seem surprising. It certainly was not expected based on previous experiments (Nigg et al., 1986, p.157) where total pronation was different for a standard shoe with positive flare compared to a special shoe with slightly negative flare. A possible explanation for our result may be found in the midsole construction of the medial part of the shoe sole. The shoe used in our experiment had a relatively stable medial midsole construction (Shore 45). In the experiment with two different shoes, the medial midsole was, in both cases, harder for the shoe with a negative flare. In addition, the rounded heel shoe had a leather upper and the other shoes had nylon uppers. This suggests that total pronation is associated with the midsole hardness on the medial side beneath the arch or generally on medial stability of a shoe.

If these assumptions and conclusions are correct, one would speculate that:
(1) the geometrical construction of the lateral heel flare has little influence on total pronation of the running shoe if the medial side is stable and firm, and that
(2) the geometrical construction of the lateral heel flare may have influence on total pronation if the running shoe at the medial side provides little support. However, these speculations have yet to be supported by further experimental and/or theoretical evidence before they can be accepted or rejected.

One would expect the impact force peaks to increase for the rounded heel shoe C compared to the conventional shoe A. However, the experimental results do not show such an increase and contradict the expectations and the "common sense." Denoth's (1986, pp.80-81) simple spring mass model for ideal heel landing can be used to explain the results of this experiment for the impact force peaks:

$$F_{zi} = v \cdot \sqrt{f \cdot m^*}$$

where v = touch-down velocity
f = spring constant of the shoe-heel system
m^* = effective mass (mass primarily involved in the deceleration process) (Denoth, 1986, p.82).
F_{zi} = maximal vertical impact force

The change of impact force depends (a) on the change of the vertical touch-down velocity, (b) the change in the spring stiffness of the heel-shoe system, and (c) the change in the effective mass. It is known (Nigg et al., 1981; Denoth, 1986) that the effective mass depends on the knee angle at touch down and on the time characteristics of the impact force.

Substituting all the discussed effects, the relative change of external impact forces in this experiment is predicted to be -4.9%. In other words, the experimental result of the impact force peaks can be understood by using a simple effective mass-spring model in which the experimental results for initial and boundary conditions as well as the first part of the movement are included.

The experimental analysis of the influence of the sole geometry (flare) on the lateral side of the heel of running shoes on the initial and total pronation in heel-toe running can be summarized as follows:
(a) The initial pronation and the initial pronation velocity are significantly influenced by the sole flare at the lateral heel. Negative flare has less initial pronation than positive flare.
(b) The total pronation was not influenced in this experiment by changed heel flare. It is speculated that the geometrical construction of the lateral heel flare has only an influence on total pronation if the running shoe provides little support on the medial side.
(c) The impact force peaks did not change as a consequence of changed lateral heel flare in this experiment. It is not clear whether this is a general finding or whether this is a specific finding for this particular type of shoe.

ACKNOWLEDGEMENT

This research was supported by grants from Natural Sciences and Engineering Research Council of Canada, Alberta Heritage Foundation for Medical Research and ADIDAS. The assistance of V. Fisher is also acknowledged.

References

Bates, B.T., et al. Biomechanics VI-A, 31-39, 1978.
Bates, B.J., et al. Med. Sci. in Sports, 11:328-331, 1979.
Cavanagh, P.R. Runner's World, 10:70-80, 1978.
Cavanagh, P.R. The Running Shoe Book, 1980.
Clarke, T.E., et al. Sport shoes and playing surfaces, 166-189, 1984.
Clement, D.B., et al. Phys. Sports Med., 9:47-58, 1981.
Denoth, J. Biomechanics of running shoes, 63-117, 1986.
Frederick, E.C., et al. J. Biomech., 14:498, 1981.
James, S., et al. Am. J. Sports Med., 6:40-50, 1978.
Nigg, B.M. Biomechanics of running shoes, 27-61, 1986.
Nigg, B.M., et al. Biomechanics of running shoes, 139-159, 1986.
Nigg, B.M., et al. Biomechanics VII, 88-99, 1981.
Nigg, B.M., et al. Biomechanics VI-A, 303-309, 1978.
Nigg, B.M., et al. Medizinisch-Orthopaedische Technik, 97, 178-180, 1977.
Nigg, B.M., et al. Medita, 9a:160-163, 1977.
Nigg, B.M., et al. Sportwissenschaft, 3:309-320, 1980.
Radin, E.L., et al. J. Biomechanics, 15:487-492, 1982.
Segesser, B., et al. Orthopaede, 9: 207-214, 1980.
Stacoff, A., et al. Biomechanical aspects of sport shoes and playing surfaces, 143-151, 1983.
Stacoff, A., et al. Biomechanics of running shoes, 117-137, 1986.
Voloshin, A., et al. J. Biomechanics, 15:21-27, 1982.

EVALUATION OF SHOE-ORTHOTIC INTERACTIONS USING AN IN-SHOE PRESSURE SENSOR SYSTEM

J. Hamill, Ph.D.
Biomechanics Laboratory
Southern IL University
Carbondale, IL 62901

B.T. Bates, Ph.D.
Biomechanics Laboratory
University of Oregon
Eugene, OR 97403

M.D. Ricard, M.S.
Biomechanics Laboratory
Southern IL University
Carbondale, IL 62901

M.K. Miller, M.S.
Biomechanics Laboratory
Southern IL University
Carbondale, IL 62901

INTRODUCTION

It has been suggested that many lower extremity problems encountered by runners are related to foot structure and function during the support phase of the running stride (Bates, et. al., 1975; James et. al., 1978; Schuster, 1974). In a clinical study, James et. al., (1978) reported that many common lower extremity problems experienced by runners could be alleviated by the use of orthotic appliances. Forty-six percent of the injured runners were prescribed orthotic appliances as a treatment and 78% of these runners were able to return to their previous running schedule.

Orthotic appliances have been found to primarily affect the medio-lateral function of the foot and to significantly change lower extremity mechanics when the foot is in contact with the ground (Bates et. al., 1979). Podiatrists, therefore, generally prescribe orthotic appliances to reduce excessive pronation during running. However, it has also been determined that running shoes, with a wide variety of mid-sole constructions and durometers, may also reduce pronation and significantly change lower extremity mechanics.

The evaluation of the effectiveness of orthotic appliances and shoes in altering lower extremity mechanics has previously been carried out using either high speed cinematograhy (Bates et. al., 1979) or ground reaction force platform systems (Hamill et. al., 1982). Bates et. al., (1984) reported that an in-shoe pressure sensor system (Electrodynogram™) developed by the Langer Biomechanics Group was an effective recording system providing valuable information concerning the internal shoe environment.

The purpose of this study was, therefore, to evaluate the interaction between orthotic appliances and two types of running shoes with different mid-sole constructions using the Langer Electrodynogram™ System.

METHODS AND PROCEDURES

Four young, healthy females, all of whom were regular runners and who regularly wore semi-rigid orthotic appliances when running, served as subjects. The orthotic appliances were prescribed by a podiatrist in all cases because of severe pronation problems. The subjects ranged in height from 1.68 m to 1.72 m ($\bar{X}$ = 1.68 m, S.D. = 0.05 m) and in weight from 542.7 N to 629.9 N ($\bar{X}$ = 595.2 N, SD = 38.8 N). All subjects were running in excess of 50 km per week and, according to University policy, signed informed consent forms prior to participation in the study.

The experimental set-up consisted of a Langer Electrodynogram™ System (EDG) and a photoelectric timing system. Data sampling for the EDG system was 200 Hz and was not under control of the investigator. The EDG system sampled for 2.5s during which approximately 3 right footfalls occurred.

The seven EDG sensors were applied to the right foot of the subject in accordance with the instructions provided. The sensors were applied to the lateral (l) and medial aspects (m) of the heel, the lateral arch area (x), the leads of the first (1), second (2) and fifth (5) metatarsals and the hallux (H).

The subject then jogged about in order to become accustomed to the equipment. They practiced in the test area at the required pace (14.3 km/hr ± 5%) which was monitored over a 4m interval by two photo-cells attached to a digital clock. Following the preparation and practice period, each subject performed ten successful trials in each of four conditions. The four conditions were: 1) C1-running shoe (injected PU, durometer 55); 2) C2-previous shoe + semi-rigid orthotic appliance; 3) C3-running shoe (compression molded EVA, durometer 25); and 4) C1-previous shoe + semi-rigid orthotic appliance. A randomized order of conditions was used for each subject.

The EDG data was input into a micro-computer after each trial and stored for later evaluation. Variables describing peak pressure values for each sensor were generated for each footfall. The footfall values were then averaged to generate representative values for each trial. Ten trial mean values and standard deviations were then calculated. Three comparisons (C1-C3, C1-C2 and C3-C4) were evaluated statistically using a single subject design developed by Bates et al., (1983).

RESULTS AND DISCUSSION

A summary of the statistical results and the percentage differences between the compared means for each sensor location and each subject is presented in Table 1. It should be pointed out that the 10 trial standard deviations for all sensors, conditions and subjects were relatively small save the lateral and medial heel sensors of Subject 1. It appeared, therefore, that the footfalls were consistent within a subject/condition. However, as indicated in Table 1, the subjects reacted markedly different to each other and thus no overall trend was obvious.

In comparing the different shoes without orthotic appliances (C1-C3), all subjects demonstrated significant differences at the lateral and medial heel sensors with the higher pressures always exhibited by the 25 durometer shoe. Since all runners were heel-toe foot strikers and thus the initial impact of the foot would be on the lateral aspect of the heel, the higher pressure values seemed to indicate that the subjects were compressing the mid-sole of the 25 durometer shoe to its limit. The larger pressure values on the medial aspect of the heel also reflected the mid-sole conforming to the shape of the heel. Further, the two relatively heavy subjects (629.9 N and 618.3 N) generally had high forefoot pressures in the softer mid-sole shoe while this

North American Congress on Biomechanics
Montréal (Québec) Canada, 25-27 August 1986

TABLE 1 - Comparisons between shoes and shoe-orthotic conditions by Subject and Variables[a]

	S1			S2			S3			S4		
	C1-C3	C1-C2	C3-C4	C1-C3	C1-C2	C3-C4	C1-C3	C1-C2	C3-C4	C1-C3	C1-C2	C3-C4
l	17.1*	11.2*	7.9	7.5*	2.0*	1.2*	1.3*	-3.8*	1.0*	2.0*	2.5*	< 1
m	12.8*	21.1*	-1.6*	4.0*	6.9*	3.9*	1.8*	-2.2*	-5.7*	1.8*	1.0*	-1.0*
x	-4.9	-14.2*	1.6	0	5.9*	2.9*	< 1	-4.3*	-1.6*	-14.7*	-1.4	11.2*
5	3.9*	2.3*	8.7*	-29.7*	< 1	< 1	12.9*	3.6*	2.5*	-15.7*	3.1*	22.0*
2	2.6*	< 1	-1.8*	-21.38*	-1.6*	11.8*	16.6*	20.1*	5.45*	-3.5*	-1.0*	2.2*
1	10.6*	10.0*	-1.8*	-2.2	-8.8*	-4.3*	-13.3*	-18.9*	-24.9*	5.1*	13.0*	13.7*
H	-4.7*	< 1	1.3	< 1	-4.2*	3.3*	5.4*	1.0*	-3.66*	-4.1*	-1.8*	-1.1*

*Significant differences.

[a]All values presented as percent differences (sign implies directionality of difference).

trend was reversed for the other two subjects (542.7 N and 589.9 N). These data are in agreement with those of Bates et. al. (1984) who noted marked differences between rigid and soft mid-sole shoes during walking.

The internal shoe environment changed in each case with the removal of the sock liner and the addition of the prescribed semi-rigid orthotic appliance. In comparing the firm mid-sole shoe and that shoe with an orthotic appliance (C1-C2), three of the four subjects demonstrated statistically significant increased pressure values on the sensors of the lateral and medial aspects of the heel. The 55 durometer mid-sole shoe with the addition of a semi-rigid orthotic device produced an internal shoe environment which was less forgiving than that of the shoe by itself. Thus, higher pressure values at impact. A significant increase in the medial heel sensor implied a resistance to pronation and thus more medio-lateral control with the addition of the orthotic appliance then with the shoe itself.

Changing the internal environment of the 25 durometer mid-sole shoe (C3-C4) resulted in a less consistent pattern than the 55 durometer mid-sole shoe. At impact, the difference in pressure values at the lateral heel sensor revealed significant results between the shoe and shoe-orthotic condition for two subjects and no change in the other subjects. The significant results indicated that the insertion of a semi-rigid orthotic appliance increased pressure values at impact. The medial heel pressures (for three of the four subjects) were significantly less in the orthotic condition. It would appear that the interaction of the orthotic and soft mid-sole shoe did not control the foot medio-laterally as the orthotic appliance was intended. The orthotic appliance did not appear to increase the rigidity of the shoe during pronation.

In the forefoot area, there were many significant differences in all comparisons of all subjects but no pattern was evident. The small standard deviations of the forefoot sensors implied consistent footfall patterns which might reflect the uniqueness of the indidivual running styles.

In conclusion, the addition of a semi-rigid orthotic appliance appeared to control the foot at impact better in a rigid mid-sole shoe than in a soft mid-sole shoe. The 25 durometer mid-sole appeared to be too soft to effectively control the shoe medio-laterally even with the addition of an orthotic appliance.

References

1. Bates, B.T., Osternig, L.R., Mason, B.R. and James, S.L. Lower Extremity Function During the Support Phase of Running. Biomechanics VI, pp. 30-39, E. Anussen and K. Jorgensan (Eds.) Baltimore: University Park Press, 1978.

2. Bates, B.T., James, S.L. and Osternig, L.R. Foot Orthotic Devices To Modify Lower Extremity Mechanics. American Journal of Sports Medicine, 7(6), 1979.

3. Bates, B.T., DeVita, P. and Kinoshita, H. Effect of Intra-Individual Variability On Sample Size. Biomechanical Aspects of Sport Shoes And Playing Surfaces, pp. 191-198, B.M. Nigg and B.A. Kerr (eds.). Calagary: University Printing, 1983.

4. Bates, B.T., DeVita, P. and Lander, J.E. Evaluation of Foot Function Using Two Measurement Systems. Proceedings of Human Locomotion III, Winnipeg, Manitoba, 1984.

5. Hamill, J., Bates, B.T. and White, C.A. Evaluation of Foot Orthotic Appliances Using Ground Reaction Force Data. Proceedings of Human Locomotion II, pp. 74-76, Kingston, Ontario, 1982.

6. James, S.L. and Osternig, L.R. Foot Orthotic Injuries To Runners, American Journal of Sports Medicine, 6(2), 1978.

7. Schuster, R. New York RRC Newsletter, 1974.

EFFECTS OF FOOT INSERTS ON THE GAIT PARAMETERS OF RHEUMATOID ARTHRITIC PATIENTS

Paul Allard
Sainte-Justine Hospital and
Department of Physical Education,
University of Montreal,
Montreal, Quebec, H3T 3J7

Winnie Loo
Sainte-Justine Hospital
Pediatric Research Center
Montreal, Quebec, H3T 1C5

Hyman Tannenbaum
Head, Division of Rheumatology,
Montreal General Hospital
Montreal, Quebec, H3H 1G1

INTRODUCTION

Rheumatoid arthritis is a systemic disease whose essential lesion is synovitis. In time, the continued inflammation of connective tissue leads to the damage of joints. This is often associated with much pain, limited range of motion and muscle weakness which reduce the patients independence. Though rheumatoid arthritis can occur in any joint, those of the feet are some of the most often affected (1).

There have been several studies describing the pathology and treatment of the rheumatoid foot (1,2). Orthotic management for those with metatarsalgia is usually in the form of metatarsal pads and arch supports which aim at redistributing the loads under the feet and thereby, reducing pain.

These measures, although pain relieving to many patients are "miss and hit" approach and do not address the basic problem of what is wrong with the rheumatoid foot or how normal gait influence the evolution of the foot abnormalities found in arthritis patients.

The objectives of this study was to assess the gait parameters of patients having painfull rheumatoid arthritis in the feet and to determine which biomechanical parameters are affected by the use of a metatarsal pad inserted into the patients' shoes.

METHODOLOGY

In this pilot study, four rheumatoid arthritic patients (3 females and 1 male) diagnosed by a rheumatologist as having principally painfull metatarsalgia participated in this study. The average age was 51 years (± 8 years) and the onset of the disease was 8.8 years (± 3 years).

There were two test conditions. Subjects walked consecutively with a pair of their most comfortable shoes and with these same shoes fitted with metatarsal pads. The orthoses were custom built and fitted by the same orthotist.

Kinematic data was obtained by means of foot switches and a high speed camera while kinetic information was collected by means of an AMTI forceplate linked to a PDP 11/23 computer. Subjects were initially fitted with foot switches connected to a portable microprocessor. Then, adhesive markers were placed on the subject to identify the joints of the upper and lower limbs and the trunk. Afterwards, the subject was instructed to walk at his natural cadence along a 10 m long elevated walkway and take step on the forceplate.

The data acquisition from the foot switches was initiated by the use of an ultrasonic switch which was activated after the subject had walked approximately 3 m. Data was collected over a distance of about four strides. Simultaneously the subject was filmed with a HYCAM II camera at 100 frames per second and forceplate data was sampled at 200 Hz. After a run, the data stored in the microprocessor of the foot switch system was then transferred to another microprocessor which in turn immediately calculated the temporal-distance parameters of gait. This procedure was repeated five times for the right and left sides of the subject. Once developed, the films were digitized and the data processed for kinematic and kinetic analysis.

RESULTS

Generally, the reported values for the temporal-distance parameters are relatively close are not significantly different from those for normal adult female and male respectively. These are for speed 80 m/min, cadence 110 steps/min, stride length 1.50 m. Stance and swing phase were also normal at 60% and 40% of the gait cycle respectively. The orthoses seem not to have influence these gait parameters.

Figure 1 illustrates for the right and left limb of a patient the hip, knee and ankle motion reported as a function of the gait cycle expressed in percentage. Results with and without the orthoses and for all the trials are shown. For all patients no significant differences were observed between the two test conditions and that for the hip, knee and ankle motion. These values represents the largest variations observed in all four patients. Furthermore, subjects showed what appeared to be normal succession of heel-strike, flat-foot and toe-off.

Figure 2 presents for the same subject as above the vertical ground reaction force expressed as a percentage of the gait cycle. Results with and without the orthoses and for each trial are shown and are expressed as percent of body weight. Again all the curves are very close together. The first peak in the vertical force was at 110% ± 6.2% of body weight and the second peak was at 107% ± 4.6% of body weight. The minimum value during the levitation period was at 79% ± 10% of body weight. There were no significant differences between the values measured when the subjects were using the orthosis or not.

Subjectively, by means of a questionnaire, all subjects found the orthoses very helpful. In a follow-up telephone conversation conducted four months after the study, three of the subjects were wearing the orthoses constantly. The fourth subject wore them at least 3-4 hours a day, and the reason for not wearing them all the time was because the orthoses fit in only one pair of shoes which were not always worn. One subject reported a dramatic relief of lower-back and hip pain after wearing the orthoses. Another subject claimed that the orthoses relieved all soreness in the feet.

North American Congress on Biomechanics
Montréal (Québec) Canada, 25-27 August 1986

CONCLUSIONS

Murray (3) found slower walking speeds to be typical of many pathological gaits. This finding was not observed in the present study. Minns and Craxford (4) found that rheumatoid arthritic patients walk by placing their feet flat on the floor and using them as platforms. In this study though, subjects demonstrated the normal succession of heel-strike, flat-foot and toe-off. All subjects appear to walk quite normally. A possible explanation for this is that these subjects are a biased and non-randomly selected sample of mild cases of rheumatoid arthritic patients.

Objective analysis of the data showed that the orthoses had no significant effect on the gait parameters measured on the sagittal plane. Subjectively though, subjects claim the orthoses to be highly beneficial. From this pilot study it seems that other biomechanical parameters are involved in the relief of painfull metatarsalgia when special shoes are worn.

ACKNOWLEDGEMENTS

This was funded by CAFIR, University of Montreal, and by J. Slawners Ltd of Montreal, Canada.

References

1. Coughlin, M.J. Postgrad. Med. 75:207, 1984.
2. Calabro, J.J. Arthritis Rheum. 5:19, 1962.
3. Murray, M.P. Am. J. Phys. Med. 46:290, 1967.
4. Minns, R.J., Craxford, A.D. Clin. Orthop. 187:235, 1984.

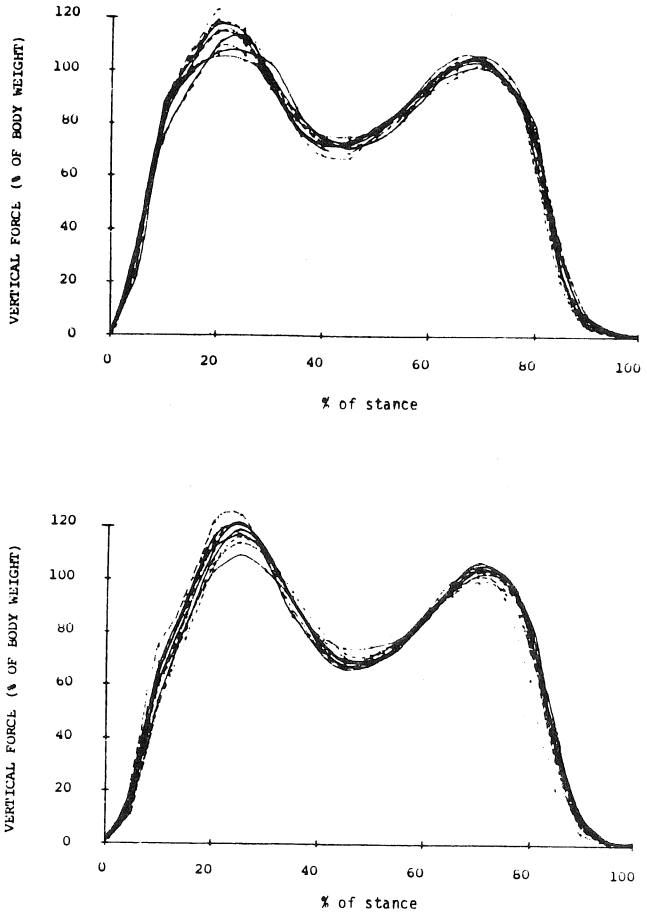

Figure 2. Vertical ground reaction force for the right (below) and left (above) limb.

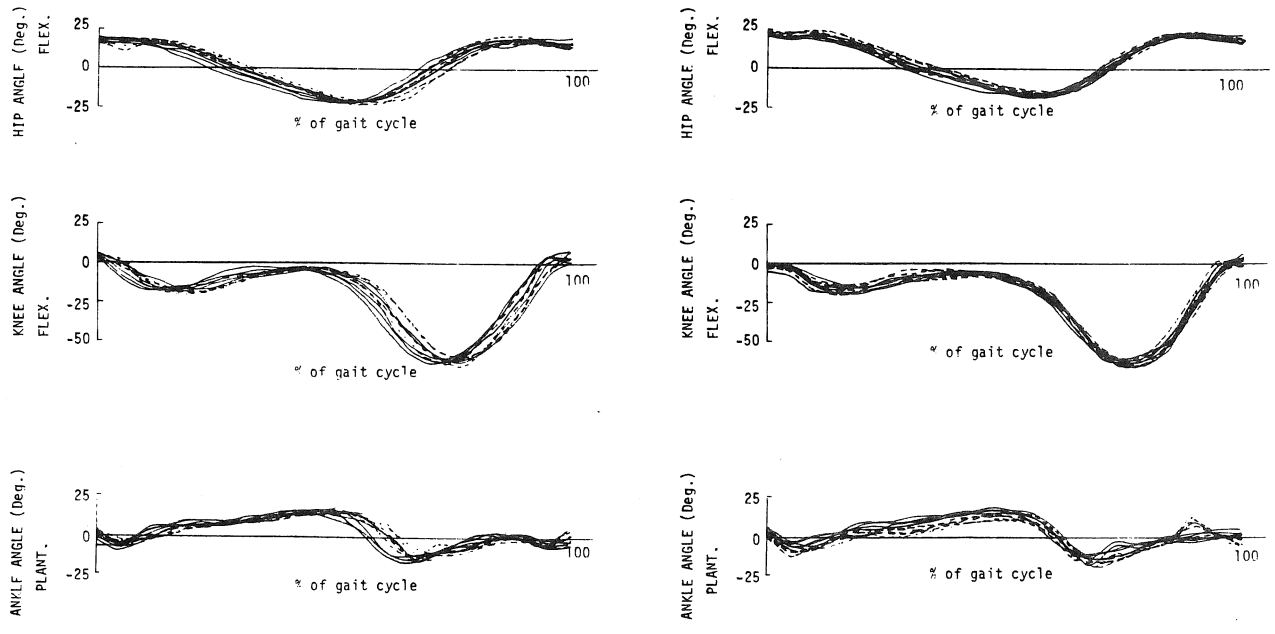

Figure 1. Hip, knee and ankle movement for the right and left limb.

PERFORMANCE CHARACTERISTICS OF THE BIOMECHANICS FORCE PLATE

David A. Schieb
Kistler Instrument Corporation
75 John Glenn Dr., Amherst, NY 14120

The evolution of the force plate has led to the inception and development of the multicomponent piezo-electric force plate (MPFP) which has been used successfully in over 80 North American institutions performing biomechanics research. Two problems of the early strain guage platforms, low resonant frequency and limited stiffness, have been virtually eliminated by the MPFP, using quartz crystals as sensing transducers. From a review of the force plate literature, and a returned questionnaire from Kistler force plate users, this presentation describes the performance characteristics of the multicomponent quartz piezo-electric force plate.

Certain advantages and disadvantages are reported in using a force plate compared to other types of kinetic and kinematic instrumentations. Advantages of the MPFP include 1) the direct measure of actual body data, 2) the recording of both quasi-static and dynamic ground reaction force (GRF), 3) accurate and reliable data, and 4) interpretation of data with little expertise required.

MPFP disadvantages that were reported include 1) the force plate size of 40cm x 60cm (can order other sizes), might be confining in certain studies, thereby affecting a representative sample, 2) the testing environment and/or MPFP surface may be unnatural, 3) limited portability, 4) the inability to measure statically absolute values over unlimited time. In addition, some researchers have noted a relationship between plate mounting and signal noise. Solutions to these apparent shortcomings are described in many articles.

In general, basic performance characteristics of the force plate (e.g. calibration stability, or natural frequency of Kistler 9281B11 is 850 hz) should not vary. However, owing to differences in the laboratory, plate mounting, research protocol, amplification and recording equipment, A/D interface, sampling rate, and ultimately signal noise, these characteristics have been shown to differ. For example, a force plate mounted into the common building foundation may be recording floor vibrations as a running subject approaches the plate. Other sources of signal noise include luminescense, electromagnetic interface, frequency aliasing, and analog noise.

In any motion analysis laboratory one must achieve a reasonable trade-off between noise rejection and signal corruption. Low frequency noise and signals are difficult to differentiate (Antonsson & Mann, 1985). High frequency noise can be removed by using appropriate electrical, mechanical or mathematical filtering schemes. Filtering methods include fast fourier transformation, low and high pass filters, and double differentiation. There is some favoring of numerical differentiation by polynomial methods, which seem to give better results than those obtained by fourier methods. From a review of the literature, studies integrating kinetic and kinematic data provide the most complete information regarding force production. To coordinate this data, it is important that the time bases are similar for EMG, film/video and force plate instrumentation and that an appropriate method of synchronization, data acquisition, sampling rate, and data display be incorporated.

With regard to sampling frequency, Berme (1980) suggests establishing an appropriate range of interest before data collection. If the sample frequency is too high, computer time and space is wasted. If too low, important information can be lost between samples. GRF sampling rates range from 2 hz for postural sway over a 4 min period, to 30 hz for 60 sec of standing rifle shooting, to 10,000 hz in a study of running shoe impact.

If a filtering technique is used to limit noise, two conditions must be met: 1) noise frequencies must not overlap signal frequencies, and 2) the data must be sampled at more than twice the highest frequency in the composite signal and noise (Antonsson & Mann, p. 40).

Synchronization of kinetic and kinematic parameters is accomplished using various timing devices. Several groups have developed fully automated and synchronized data acquisition and reduction systems.

Data display is a function of software and hardware. While the earliest GRF platforms quantified and displayed only the vertical component, several unique procedures are currently utilized to display some 15 GRF parameters.

CONCLUSIONS

1) Force plate measurements are of greater value to the researcher if other parameters are measured simultaneously.

2) Few measurement problems regarding performance of the multicomponent

North American Congress on Biomechanics
Montréal (Québec) Canada, 25-27 August 1986

piezo-electric force plate have been noted by biomechanics researchers using a properly mounted plate.

3) Data display using graphical CRT and hard copy is a powerful conceptual tool for both layman and practioner. Data acquisition and display techniques of instantaneous 3-D integrated kinetic and kinematic parameters are being perfected.

4) Utilization of the multicomponent piezo-electric force plate has contributed significantly to our understanding of sport, rehabilitation, industry, neuromuscular control, and most recently, areas of human factors and robotics.

Antonsson, E.K. & Mann, R.W. The frequency content of gait. J. Biomech. 18(1):39-47, 1985.

Berme, N. Control and movement of lower limbs. Biomechanics of Motion (ed. E. Morecki) pp. 185-217. Springer-Verlag, NY, 1980.

A CLINICALLY VIABLE FORCE PLATFORM MEASUREMENT TECHNIQUE FOR THE VISUAL AND NUMERICAL ASSESSMENT OF FORCE DISTRIBUTIONS BENEATH THE FEET

MacKinnon, C.D., Godfrey, C.M.,M.D. The Wellesley Hospital, Department of Rehabilitation Medicine.
Toronto, Ont., Canada
M4Y 1J3

INTRODUCTION

A technique has not been developed which can provide both a quantitative and visual assessment of ground reaction force patterns beneath the feet during locomotion within a clinically viable time frame. Without a positional reference of force application relative to the foot clinically significant information is lost. This paper documents a simple, quick and low cost technique for the acquisition of a dynamic foot imprint which can be superimposed on force-position data, thereby providing an accurate reference of the placement of the centre of pressure path. The information can then be used by physicians in the assessment of patient's weight bearing dynamics and aid in the prescription of treatment regimes for persons with foot pain.

REVIEW

The potential clinical use of data acquired with the use of force plates has been elucidated by many researchers investigating the resultant ground reaction forces or pressure patterns developed during the stance phase of gait (1,2,7,9,10). The clinical value and interpretation of force or pressure data is made tenuous by the absence of a positional reference frame for the distribution of forces relative to the foot. Techniques utilizing cinematography have been developed which provide both numerical data and a visual reference (1,4,5,6,8,10) but require expensive, labour intensive and time consuming data analysis. For example, Cavanagh et al (4) have outlined a technique which provides a numerical and visual assessment of foot-to-ground pressure distributions beneath the foot which requires the digitization of x,y coordinates for each pressure cell over time. Although such a technique provides valuable insight into the effects of dynamic weight bearing, the technique required for data acquisition is "unacceptably laborious".

It is the purpose of this paper to outline a simple, fast and low cost technique which can provide an accurate quantitative and visual assessment of the magnitude and placement of ground reaction forces exerted beneath the feet during locomotion.

METHODOLOGY

The gait laboratory at The Wellesley Hospital consists of two principle components: a standard six-channel, computerized force platform system and a dynamic foot imprint mat.

(i) Force Platform System

An A.M.T.I. (Advanced Mechanical Technology Inc. r) force platform is used to measure three orthogonal forces (Fx, Fy, Fz) and three moments (Mx, My and Mz) using four metal foil strain gauges arranged in a four-arm full wheatstone bridge. Calibration of the six-channel dynamometer is completed by the placement of known loads in known positions and the creation of a 6X6 sensitivity matrix. The platform has a resolution of 2% and resonant frequency of 200Hz. Analog signals are sampled at 100 samples/s, filtered (2nd order low-pass) at a cut-off frequency of 10.5 Hz, amplified, and A/D converted for storage on diskette.

(ii) Dynamic Foot Imprint Mat

During walking trials a unique 1mm thick mat encased in a 3mm high metal frame is placed on top of the force platform The mat lies flush with the walkway and is thin enough to prevent attenuation of force measurements. The underside of the mat is thinly coated with oilless pelican ink and a sheet of bond paper is placed over the force platform beneath the mat.

The dyanmic foot imprint technique allows for a permanent and accurate recording of the subject's foot imprint. The foot imprint can then be used to pinpoint pressure points and relative weight bearing discrepancies beneath the feet during locomotion. A separate data acquisition phase is now possible using the dynamic foot imprint and a 5 lb constant force roller. The roller is used to exert a constant force above the trigger threshold of the force platform while tracing an accurate outline of the foot imprint. Forces exerted by the roller are sampled at 10hz and stored on diskette. The imprint centre of pressure path can then be superimposed over the centre of pressure path plotted on a force-position graph from data generated during the actual walking trial. The centre of pressure, foot outline, force-position and force-time information provides a direct visual reference of the magnitude and placement of the centre of pressure beneath the foot. Typically, a total of 5 trials are collected and averaged for each leg. Centre of pressure paths are averaged using the technique described by Cavanagh (3). The total time for data acquisition and analysis is one hour for each condition studied.

DATA COLLECTED:

Force-time, Force-position
Centre of pressure
Dynamic Foot imprint
Impulse data for X,Y, and Z
Stance time
Average walking velocity in m/s and statures/s

North American Congress on Biomechanics
Montréal (Québec) Canada, 25-27 August 1986

DISCUSSION

The use of ground rection force data alone in the analysis of human movement is of little value when applied to the analysis of movements generated at specific joints. It must be kept in mind at all times that ground reaction force data represents the sum of all body segment mass-acceleration products. The patterns generated by foot to ground contact can therefore be the result of an infinite combination of movements in all planes of motion. The clinical application of ground reaction force data is based upon the fact that the patterns produced are mathematically representative of the support moments (11) generated in the sagittal and frontal planes. Although the actual summative components of the support moment are unknown, the pattern is indicative of the person's ability to generate moments about a series of joints sufficient to support their body weight, provide medial/lateral stability, and generate forward propulsion.

The problem with existing laboratories has been the absence of a quick and reliable method for providing a visual reference of the average points of application of these forces beneath the feet. The integration of quantitative force-time data, positional reference and pressure point information provided by this technique is of value in the assessment of weight bearing kinetics and the identification of pressure bearing irregularities. For health care centres which cannot afford the expense of three dimensional image processing systems this technique provides clinical viability to force platform information. In summary the benefits of the technique are threefold:

1. The technique allows for the simultaneous collection of ground reaction force data and a dynamic foot imprint so that both a quantitative and visual reference of foot-to-ground contact is possible.
2. Data can be collected and analyzed within a clinically viable time frame. The data is available to the physician within the day of examination. In addition, a large number of trials can be sampled and averaged in order to improve the statistical power of the measurements taken.
3. The technique is easy to implement and of sufficiently low cost that gait laboratories using a force platform can adopt the technique with little difficulty.

REFERENCES

1. Arcan, M., et al. J. Biomech. 9:453-7. 1976.
2. Betts, R.P., et al. Med. Biol. Eng. Comp. 18: 674-684. 1980.
3. Cavanagh, P.R., et al. J. Biomech. 11:487-491. 1978.
4. Cavanagh, P.R., et al. J. Biomech. 13:69-75. 1980.
5. Duckworth, T., et al. Foot and Ankle. 3(3): 130-141. 1982.
6. Hutton, W.C., et al. Rheum. Phys. Med. 11: 313-317. 1972.
7. Hutton, W.C., et al. Int. Orthop. 3:153-157. 1979.
8. Scranton, P.E., et al. J. Biomech. 9(1):45-48. 1976.
9. Sharma, M., et al. Annals Rheum. Dis. 38:549-552. 1979.
10. Simkin, A. Rheum.& Rehab. 20:88-97. 1981.
11. Winter, D.A. J. Biomech. 13:923-927. 1980.

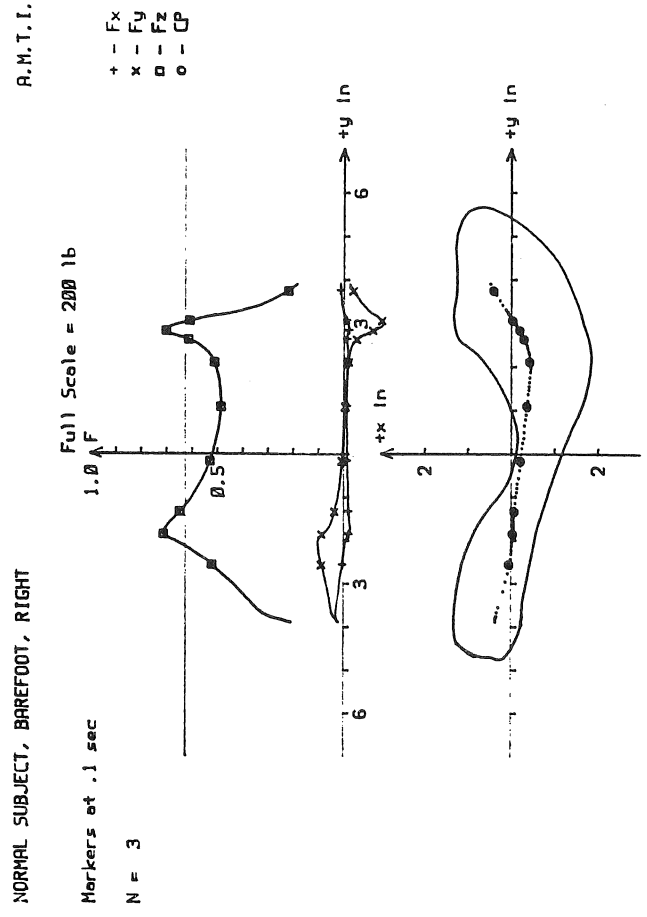

The Wellesley Hospital
Department of Rehabilitation Medicine
Clinical Gait Laboratory

Force Data for :NORMAL SUBJECT, BAREFOOT, RIGHT N = 5
AVERAGED OVER FIVE TRIALS

Force Data (% body weight)		Time Data (% stance)	
Vertical Data:	(S.D.)		(S.D.)
F1 = 113.4	(3.8)	T1 = 19.9 *	(1.2)
F2 = 77	(2)	T2 = 49.9	(2.5)
F3 = 111.5	(1.8)	T3 = 78.5	(1.4)
Fore/Aft Data:			
F4 = 16.5	(.5)	T4 = 12.5 **	(.6)
F5 = -24.4 *	(1.4)	T5 = 85.2	(1.4)
Medial/Lateral Data:			
F6 = 4.4	(.7)	T6 = 2	(.6)
F7 = -4.8	(.8)	T7 = 22.9	(1.5)
F8 = -4	(.6)	T8 = 67.5	(18.1)

Average Velocity (m/s)	: 1.29	(.04)
Standardized Velocity (statures/s)	: .77	(.03)
Stance Time (s)	: .59	(.01)

Impulses (lb-sec):

X = 0	(1)
Y = -1.2	(.7)
Z = 68	(1.9)

(*) one std. dev. from norm
(**) two std. dev. from norm

A TECHNIQUE FOR NORMALIZING CENTER OF PRESSURE PATHS

H.U. Motriuk
Biomechanics Laboratory
University of Calgary
Calgary, Alberta, T2N 1N4

INTRODUCTION

It has been suggested [1,5] that center of pressure (COP) paths might be useful for evaluating gait abnormalities. Not only do they produce a characteristic pattern which could indicate normal or pathologic gait [5], but also, in conjunction with film data, they provide information as to where the resultant ground reaction force acts in relation to the joints. To determine the normal COP distribution, it is necessary to examine normal gait and to apply repeatable and valid normalizing and averaging techniques. Such a technique is presented below. It utilizes force platform data (F_x, F_y, F_z) together with information about the placement of the foot on the force platform.

REVIEW AND THEORY

1. Defining the dimensions of the foot and its placement on the force plate.

The COP location can be related to the sole of the foot only if the placement of the foot on the force platform is known. The placement of the foot can be uniquely described by specifying (i) the position of the "center" of the foot (C), and (ii) the angle of abduction (ϕ), which may be defined as the angle between the "midline" of the foot and the line of progression. To determine these, one can record a complete footprint [1,4,5,6] for each trial. However, two marks whose positions on the sole of the foot are known would be enough information to describe the placement of the foot on the force platform. Cavanagh [2,3], who first proposed this method, drilled two holes into the midline of the shoe sole , and made the subject walk through powdered chalk before stepping on the force platform. Then, he measured the coordinates of the marks left on the platform surface. A similar method is used for barefoot subjects. Markers filled with ink are attached to the sole of the foot at two points. Any points which make contact with the floor can be chosen. The points are then uniquely related to the midline and center of the foot, using a separate footprint.

The midline position is determined from the footprint by drawing lines tangent to the most prominent points on the medial and lateral sides of the foot outline [6]. For an anatomically normal foot, they form an angle. The bisector of this angle is defined as the midline. The lines parallel and perpendicular to the midline and enclosing the footprint form a rectangle whose dimensions are referred to as the length and the width of the foot. The line perpendicular to the midline and dividing the footprint into two equal parts: anterior and posterior, crosses the midline at a point which is referred to as the centre of the foot. The coordinate system associated with the footprint is then established, as shown in Figure 1.

2. Position of the center of pressure with respect to the midline.

The location of the center of pressure P with respect to the $(xyz)^1_C$ coordinate system is derived (see Figure 2) from the following moment equations:

$$\bar{M}_C = \bar{R}_{CP} * \bar{F}\ , \quad \begin{vmatrix} M^1_{Cx} \\ M^1_{Cy} \\ M^1_{Cz} \end{vmatrix} = \begin{vmatrix} i^1 & j^1 & k^1 \\ x^1_{CP} & y^1_{CP} & z^1_{CP} \\ F^1_x & F^1_y & F^1_z \end{vmatrix} \qquad (1)$$

Thus, for $z^1_{CP} = 0$,

$$x^1_{CP} = -M^1_{Cy}/F^1_z \qquad (2)$$

$$y^1_{CP} = M^1_{Cx}/F^1_z \qquad (3)$$

F^1_z is equal to F^0_z which is obtained from the force platform measurements. M^1_{Cx} and M^1_{Cy} also must be expressed in terms of measured quantities. Since $\bar{R}_{0P} = \bar{R}_{0C} + \bar{R}_{CP}$,

$$\begin{vmatrix} {}^0x_{0P} \\ {}^0y_{0P} \\ {}^0z_{0P} \end{vmatrix} = \begin{vmatrix} {}^0x_{0C} \\ {}^0y_{0C} \\ {}^0z_{0C} \end{vmatrix} + T^{01} \begin{vmatrix} {}^1x_{CP} \\ {}^1y_{CP} \\ {}^1z_{CP} \end{vmatrix} \qquad (4)$$

where T^{01} is the rotation matrix:

$$T^{01} = \begin{vmatrix} \cos\phi & -\sin\phi & 0 \\ \sin\phi & \cos\phi & 0 \\ 0 & 0 & 1 \end{vmatrix} \qquad (5)$$

x^1_{CP} and y^1_{CP} can be expressed as functions of x^0_{0C}, x^0_{0P}, y^0_{0C}, y^0_{0P} and ϕ. Substituting these into (1) gives:

$$M^1_{Cx} = (M^0_{0x}\cos\phi + M^0_{0y}\sin\phi) + a_z(-F^0_x\sin\phi + F^0_y\cos\phi) + F^0_z(x^0_{0C}\sin\phi - y^0_{0C}\cos\phi) \qquad (6)$$

$$M^1_{Cy} = (-M^0_{0x}\sin\phi + M^0_{0y}\cos\phi) - a_z(F^0_x\cos\phi + F^0_y\sin\phi) + F^0_z(x^0_{0C}\cos\phi - y^0_{0C}\sin\phi) \qquad (7)$$

The moments M^0_{0x} and M^0_{0y} are obtained from:

$$M^0_{0x} = y^0_{0P}F^0_z - a_zF^0_y \qquad (8)$$

$$M^0_{0y} = -x^0_{0P}F^0_z + a_zF^0_x \qquad (9)$$

North American Congress on Biomechanics
Montréal (Québec) Canada, 25-27 August 1986

It can be seen that in order to determine x^1_{CP} and y^1_{CP}, the following are needed: F_x, F_y and F_z from force platform measurements, as well as x^0_{0C}, y^0_{0C} and ϕ all describing the foot placement on the force platform.

METHODOLOGY

Normalizing and Averaging

It is desirable to preserve the individual features of a trial until the final averaging since otherwise information is lost. Also, the inclusion of unnecessary normalizations increases the final error. The following procedure is proposed:

a) Calculate the location of the midline (x^0_{0C}, y^0_{0C}, ϕ) for trial "i".

b) Normalize with respect to time: $(F^0_x)_i$, $(F^0_y)_i$ and $(F^0_z)_i$; i.e. take the stance period as the unit of time and divide it into K equal intervals. The calculation can then be done for each time $t_j = (j-1)/K$, where j changes from 1 to K+1.

c) Calculate moments $(M^1_{Cx})_i$ and $(M^1_{Cy})_i$ for t_j.

d) Calculate position of the center of pressure with respect to $(xyz)^1_C$ and normalize it with respect to width and length of the foot, correspondingly. For time t_j:

$$(x^1_{CP})_i = -(M^1_{Cy})_i/(F^0_z)_i * \frac{1}{2w_i} \qquad (10)$$

$$(y^1_{Cp})_i = (M^1_{Cx})_i/(F^0_z)_i * \frac{1}{2l_i} \qquad (11)$$

e) Calculate the average position at time t_j, for N trials:

$$(x^1_{CP})_{ave} = \frac{1}{N}\sum_{i=1}^{i=N}(x^1_{CP})_i \qquad (12)$$

$$(y^1_{CP})_{ave} = \frac{1}{N}\sum_{i=1}^{i=N}(y^1_{CP})_i \qquad (13)$$

f) Determine standard deviations for the two COP coordinates to determine variability of data.

DISCUSSION

COP paths might provide information in clinical gait analysis. However, if they are to be of any use in identifying pathologies, their normal values and variabilities have to be established. Thus, averages for certain groups of people are of interest (although some investigators are satisfied with inspecting individual trials only [1,5]). There is a consequent need to relate COP locations to a standard coordinate system for all trials and subjects, for example, to the system associated with the footprint.

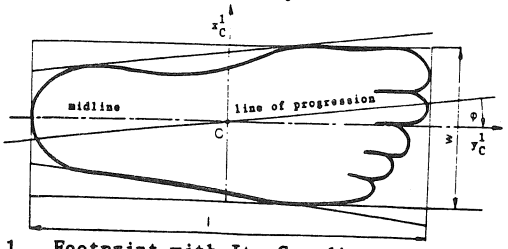

Figure 1. Footprint with Its Coordinate System

It is important to avoid loss of information in the averaging process. For example (i) The speed of COP is determined from the change in its coordinates between specific time samples. This information is lost if the final paths are averaged, as in ref. [6]. (ii) Averaging of the components of the variable of interest rather then the variable itself introduces the need for additional normalizing, as normalizing to body weight in ref. [2]. This is not desirable because normalizing any variable is associated with creating a fictitious value which is not necessarily a proper one. For example, the F_z forces exerted by a person's foot may not change in proportion to this person's body weight. (iii) Associated with the previous point, the separate averaging of forces (from force platform input) and abduction angles is even more questionable [2].

REFERENCES

1. Grundy, M., et al., J. Bone Jnt. Surg. 57-B, 1, 98-103, 1975.
2. Cavanagh, P.R., J. Biomechanics, 11, 487-491, 1978.
3. Cavanagh, P.R., and Lafortune, M.A., J. Biomechanics, 13, 397-406, 1980.
4. Draganich, L.F., et al., J. Biomechanics, 13, 875-880, 1980.
5. Brand, R.A., et al., Clin. Orthop., 160, 43-47, 1981.
6. Katoh, Y., et al., Clin. Orthop., 177, 23-33, 1983.

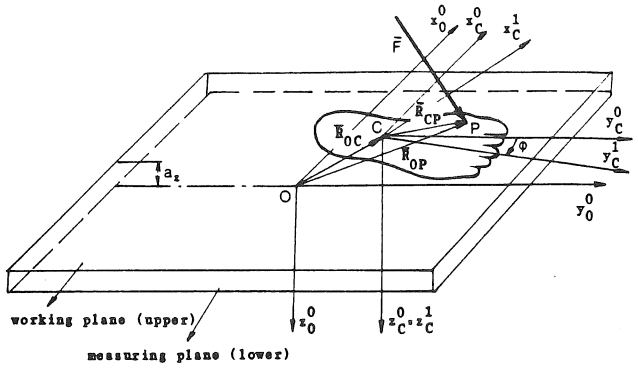

Figure 2. Coordinate Systems Used in Calculations

$(xyz)^0_0$ inertial coordinate system associated with the force platform

$(xyz)^0_C$ above system translated so that the origin is at C

$(xyz)^1_C$ coordinate system associated with the footprint (superscript - angular position, subscript - origin)

C centre of the foot

P centre of pressure

ϕ abduction angle

A DEVICE FOR THE MEASUREMENT OF FIRST RAY MOBILITY

M.M. Rodgers
Orthopedic Surgery Research Laboratory
West Virginia University Medical Center
Morgantown, West Virginia 26505

P.R. Cavanagh
Biomechanics Laboratory
The Pennsylvania State University
University Park, Pennsylvania 16802

INTRODUCTION

First ray mobility has been discussed by many authors as an important indicator of foot structure and function. The first ray is defined as a functional unit of the foot consisting of the first metatarsal bone and the first cuneiform bone. Many different foot problems have been attributed to either a lack of first ray movement (rigid first ray) or a first ray which allows too much movement (hypermobile first ray). Investigation of these assertions has been limited by the inability to objectively measure first ray range of motion in vivo. The purpose of this investigation was to determine the reliability of a prototype first ray mobility measuring device.

REVIEW AND THEORY

The first metatarsal bone and first cuneiform bone function together as a unit called the first ray (1). The movement occurring between the first ray and the cuboid bone is called first ray mobility, and was first identified as a factor in foot pathomechanics by Morton in 1930 (2). Morton believed that when the first ray is hypermobile, the second metatarsal head carries most of the load, and the foot rolls inward because the first metatarsal is ineffective until ligamentous slack is taken up. This is said to result in pronation causing an increase in functional stresses on the medial ankle muscles, and eventually, strain in the muscle, ligament and tendons.

Although Morton wrote extensively about foot function and dysfunction, he did not present data to support his theories. His assessment of first ray hypermobility was based on combined results from physical and X-ray exams. His criteria for hypermobility included:

1) a pronated posture of the foot in stance,
2) a kinetographic (ink) print showing more pressure concentrated under the second and third metatarsal heads than under the first,
3) enlargement of the second metatarsal bone shaft as viewed on x-ray, and
4) distinct separation between the inner two cuneiform bones as viewed on x-ray.

Harris and Beath (3) disputed the use of x-ray for delineating the hypermobile first ray since the results are dependent on the angle of the x-ray. In their study of short first metatarsals, they found even distributions under the metatarsal heads using the Harris mat. These prints were made in standing as opposed to Morton's suggestion of using walking prints. Although Morton's theories have been challenged, the difficulty of measuring first metatarsocuneiform hypermobility has prevented a resolution of the controversy.

Quantitative information is available describing the anatomical movement of the first ray (5,6), but these studies were done on cadavers and therefore have limited application to clinical evaluation of first ray mobility. Despite the fact that the normal range of first ray motion in the living foot has not been quantified, most articles on clinical evaluation of the foot discuss the need to evaluate first ray mobility subjectively and include this assessment in treatment design.

METHODOLOGY

Seven males and five females (mean weight 720 N $\pm$ 126.4, height 1.73 m $\pm$ .10) were subjects in the study. The mobility of each subject's right first ray was subjectively assessed by the investigator. The subject was then installed into the device (shown in Figure 1) which enabled measurement of first ray displacement in a dorsal direction. The foot was placed in the device so that the lateral metatarsals were securely immobilized by a clamp. The first metatarsal head was contacted with a manually operated plunger composed of a force transducer (Kistler 9322) and a Linear Variable Differential Transformer (LVDT). The amount of force exerted on the first ray and the displacement of the first metatarsal head were simultaneously recorded. Two measurements of first ray mobility were obtained for each subject on each of two separate days for a total of four trials. Each subject was positioned in the apparatus so that the hip, knee and ankle joint angles were maintained at 90 degrees of flexion. The lateral four metatarsal heads were clamped securely to ensure stabilization. Each trial consisted of five consecutive cyclic loadings and unloadings with a maximum force of approximately 80 N which resulted in a 20 mm maximum displacement of the head of the first metatarsal. These ranges were found to be within the pain tolerance of all subjects.

Force-displacement hysteresis plots of each trial were collected online by an SMS 1000 minicomputer. An example of the resulting force-displacement hysteresis diagram is shown in Figure 2. The diagrams exhibited two distinct phases; stiffness values for the initial phase (k1) and the second phase (k2) of the rising part of the diagram were calculated in kN/m. Within day reliability was determined by correlating the results from the two trials on the second day, while between day reliability was expressed as the correlation between the mean of all trials on day 1 and all trials on day 2.

RESULTS AND DISCUSSION

Mean values for stiffness were 18.4 and 72.6 kN/m for phases 1 and 2 respectively. The ranges were 13.4 - 24.2 kN/m for k1 and 62.3 - 101.7 kN/m for k2, indicating a considerable range in this symptom free sample. The measures also appeared to be reliable, exhibiting within day and between day

North American Congress on Biomechanics
Montréal (Québec) Canada, 25-27 August 1986

correlations of 0.87 for k1 and similar values of 0.91 and 0.95 for k2.

The validity of the device is somewhat more difficult to assess since the subjective examination of the foot can reveal little more than a 3 point scale - stiff, normal or mobile. The 3 individuals who were rated by the examiner as being "stiff" were ranked 1,2 and 5 on the stiffness value k2. The three individuals who were rated subjectively as "mobile" were ranked 3, 8 and 9 on the value of k2. Despite the anomalous findings for the single "mobile" subject who exhibited high measured values of the constant k2, the values for k2 appeared to show better agreement with subjective findings than those for k1.

It is likely that some clinicians factor in such variables as body weight and foot length into their subjective assessment. Such considerations can be addressed quantitatively by the formulation of a dimensionless index to represent the 1st ray stiffness. One suitable measure may be the following:

$$\text{Stiffness Index, } Sn = kn * \frac{\text{(Foot Length in m)}}{\text{(Body Weight in kN)}}$$

where n= 1 or 2

When the present results were expressed as a dimensionless stiffness index, the values for S2 ranked the individuals with subjectively rated "stiff" first rays 1,2, and 6 while those rated as "mobile" were ranked 3, 11, and 12 in stiffness. Again, except for the single anomalous subject, the normalized values appeared to agree well with the extremes identified by subjective assessment.

CONCLUSIONS

A device has been developed for the measurement of first ray mobility. Based on the results from repeated trials of 12 subjects, the device demonstrated repeatable findings. Comparison of the results to subjective assessment shows, in general, a good separation of the extreme feet - particularly when normalized values are considered. However, a true validation of the device would require simultaneous x-ray and force-displacement measures to be made. It is likely that the present device may enable the clinician to objectively assess the contribution of first ray movement to various foot deformities and symptoms, and provide a more discriminating measure of first ray mobility than is available using present subjective techniques.

References

1. Hicks, J.H. J Anat 87:345, 1953.
2. Morton, D. Am. J. Surg. 9(2):315-328, 1930.
3. Harris,R.I., et al.JBJS 31-A(1):116-140,1948.
4. D'Amico, J.C., et al. JAPA 69(1):17-23, 1979.
5. Kelso, S.F., et al. JAPA 72(12):600-605, 1982.

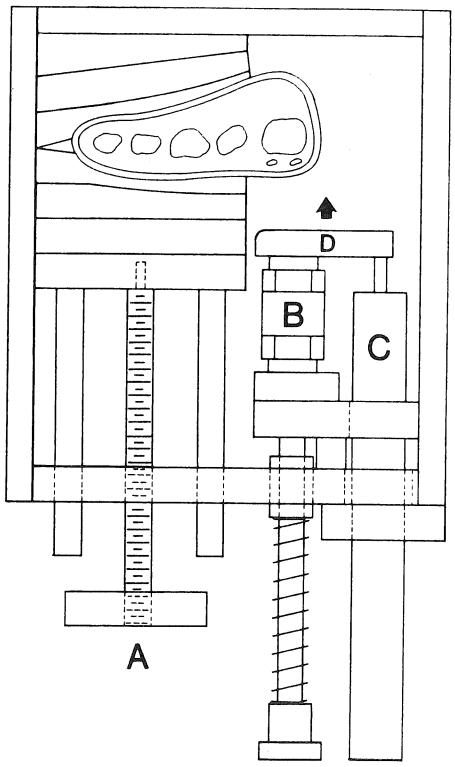

Figure 1. Schematic diagram of the first ray mobility measuring device. The foot is restrained by the clamp, A, and the plunger, D, is advanced against the foot. As the 1st metatarsal head moves dorsally, the force and displacement are measured by the transducers B and C respectively.

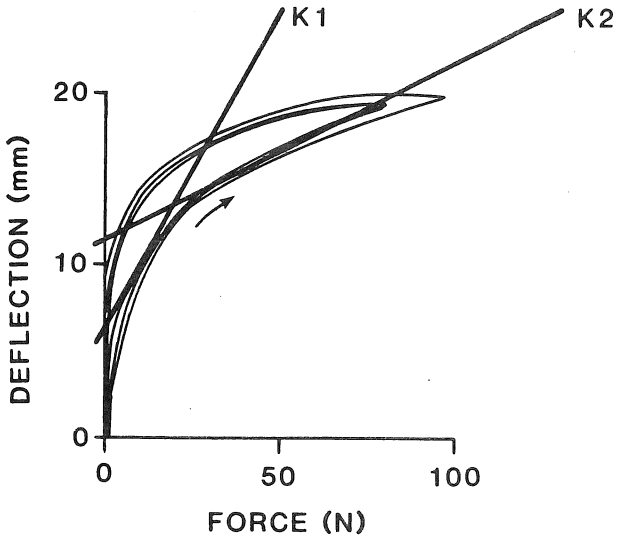

Figure 2. An example of a set of force-displacement hysteresis curves from 3 successive trials. The lower set of curves reflect the initial push of the plunger against the first metatarsal head, while the upper set show the return portions. The tangents to the two phases of the rising part of the curves were used to calculate the two stiffness values K1 and K2 in kN/m.

A KINEMATIC ANALYSIS OF SHANK MOTION RELATIVE TO THE CALCANEUS DURING THE SUPPORT PHASE OF RUNNING

Jack R. Engsberg
Department of Sport Sciences and Physical Education
University of Denver
Denver, CO 80208-0200

James G. Andrews
Department of Exercise Science and Physical Education
The University of Iowa
Iowa City, IA 52242

INTRODUCTION

In recent years, the number of people participating in recreational activities has increased tremendously. Many recreational activities require support from the lower extremities. Missuse and/or overuse of the lower extremity joints and their interconnecting muscular and ligamentous structures can lead to pain, injury and/or dysfunction. The shank and calcaneus are two components of the lower extremity. Relative motion between the shank and calcaneus has been studied by many investigators. Some investigators considered a simplified motion between the two segments (1,2,4). These investigators used 2-D cinematography to record the frontal plane projection of the angle formed by lines placed on the posterior aspects of the calcaneus and shank. Thus the motion being examined during the support phase of running was a form of eversion-inversion (EI), and did not necessarily represent total relative motion between the shank and calcaneus (i.e., the combined talocalcaneal (TC)/talocrural joint). The purpose of this investigation was to obtain a complete description of the kinematic behavior of the relative motion between the shank and calcaneus during the support phase of running.

METHODOLOGY

Surface markers were applied to the skin superficial to standardized locations on the shank and calcaneus of five subjects. Three markers were placed on each segment to allow for a six degree of freedom analysis. Kinematic data were collected from four Locam cameras operating at a nominal rate of 400 frames per second as a subject ran barefoot on a tartan covered runway. The direct linear transformation method was used to obtain 3-D coordinates of each surface marker during the run. A computer program reduced the raw data to yield equivalent screw displacement (ESD) parameter information for selected pairs of TC/talocrural joint configurations.

RESULTS

Table 1 presents the ESD parameters for consecutive pairs of characteristic foot positions. This table is divided into three sections. Each section presents the ESD parameters calculated for all subjects for position changes from one characteristic foot position to the next. The mean and standard deviation (SD) for that interval are also indicated .

DISCUSSION

Table 1 presents joint displacement information allowing for comparison of the ESD parameters between and within subjects. Large variations existed between direction cosine vector (DCV) components (i.e., PF/DF, EV/IN, AB/AD) orienting the ESD axis and other ESD parameters during corresponding time intervals for all five subjects. Despite this between-subject variation, trends in the results did exist.

Touchdown (TD) to Footflat (FF) Trends

When considering the DCV components from TD to FF (Table 1a), the predominant rotation was plantarflexion (PF) in three of the five cases (Subjects 1,3,5). However, observations indicated that Subjects 2 and 4 had a more rapid PF than the other three subjects, and this large PF motion occurred before the entire foot was flat on the ground.

If subjects were being placed into categories based on similar ESD parameter characteristics, the early PF component of Subject 4 could place her in the same category as Subject 2. However, based on the EI and abduction-adduction (AA) components for Subject 4, she would be placed in a separate category from Subject 2. Subject 4 was chosen because of the extreme 'pronation' that could be observed qualitatively when she ran. This 'overpronation' was quantified when examining the 2-D EI results as recorded by Camera 1. These frontal plane results indicated 19.1 degrees of eversion (EV) at 3.9% of the total support time, and 10.7 degrees at the time of the FF position. However, this EV component for Subject 4 was only the second largest DCV component during the TD to FF interval; the abduction (AB) component for this subject was the largest of the three DCV components. All other subjects except one (Subject 5) had this AB/AD component as the smallest DCV value during this interval, and all exhibited adduction (AD) instead of AB. This AB/AD component of TC/talocrural joint motion has not been considered previously in analyzing the behavior of these 'overpronators'.

The presence of AD components for the remaining four subjects during the TD to FF phase seemed to contradict results reported by previous investigators for the support phase of walking (5). These investigators reported that internal rotation of the shank occurred relative to a laboratory coordinate system during this phase of walking. Depending upon the motion of the calcaneus, however, internal rotation of the shank relative to a laboratory based coordinate system corresponded to either AB or AD of the combined TC/talocrural joint in the present investigation.

Another discrepancy that appeared when relating the results of this study with previous investigations concerns the mitered or oblique hinge hypothesis (5). This hypothesis implies that internal rotation of the shank (AB) will cause a concomitant EV of the calcaneus relative to a laboratory reference frame. However, the present investigation showed four of five subjects to be simultaneously adducting and everting the shank with respect to the calcaneus. This would not be possible if the ankle joint complex were equivalent to an oblique fixed hinge as this hypothesis suggests.

FF to Maximum Pronation (MP) Trends

The present investigation indicated EV was the major component of the DCV for all subjects but one (Subject 2) during the FF to MP time interval (Table 1b). These results are consistent with one of the

North American Congress on Biomechanics
Montréal (Québec) Canada, 25-27 August 1986

results reported by previous investigators, namely that EV was the major component during the FF to MP time interval (5,10,27). However, the previous 2-D investigations only examined EV/IN, and neglected the other two rotational components, PF/DF and AB/AD. Results from the present investigation indicate that both PF/DF and AB/AD occur during the FF to MP time period, and that the magnitudes of these components differ between subjects. Thus, while the EV component predominates in this time interval, the other components should be considered when examining total combined joint motion and addressing such issues as injury prevention and rehabilitation. In addition, subject variability, exemplified by the large SD's, would seem to indicate a need for grouping subjects, with this grouping based on characteristic joint motions occurring during support.

When examining these FF to MP results in terms of the combinations of the DCV components, it becomes clear that the term pronation, as currently defined (i.e., a combination of dorsiflexion (DF), EV and AB), may not be appropriate to describe combined TC/talocrural joint motion during this interval. Although three of the five subjects studied in this investigation exhibited this combination, two subjects exhibited something other than pronation, and no single term exists for these other combinations of rotational components.

MP to Takeoff (TO) Trends

The major component of the DCV during the MP to TO support interval (Table 1c) was PF in all but one case (Subject 4). The PF result for the four subjects was not surprising since the foot terminated ground contact with the ankle in a PF configuration. The results for Subject 4 show that the MP to TO time interval was not a good indicator of the amount of PF rotation occurring during the latter stages of support, since a substantial amount of IN was occurring during the initial portion of the interval.

Upon considering the EV/IN and AB/AD rotations during the interval, it was noted that Subjects 1,2 and 3 displayed an EV component in the motion. Other investigators have stated that supination occurred during the latter stages of support in walking (3,5). Supination has been defined as consisting of a combination of PF, inversion (IN) and AD (3,5). Some 2-D investigations have also supported this supination hypothesis during running by indicating that IN of the shank relative to the calcaneus occurred during the latter portion of support (1,4). Although the small number of subjects tested in this investigation limits the generality of the interpretations that can be drawn from these results, it does call into question the currently accepted hypothesis that inversion occurs during the latter stages of support. In addition, these results indicate that the term supination, as currently defined (i.e., a combination of PF, IN, AD), may not be appropriate for describing the combinations of rotations that exist during the late stages of running support.

CONCLUSIONS

This investigation has brought new information to the current body of knowledge concerning motion of the combined TC/talocrural joint during the support phase of running. The following conclusions seem warranted.

1. For all subjects, pronation (DF, EV, AB) and supination (PF, IN, AD), as defined in this investigation and in others, may not be adequate to realistically describe what is actually occurring during the support phase of running.

2. The monitoring of TC/talocrural joint motion in the frontal plane (2-D eversion-inversion) does not accurately describe the motion at this joint. The other rotational components of this motion (i.e., DP and AA) should also be considered. Injury prevention measures and treatment modalities might thereby be significantly improved.

3. Locations and orientations of ESD axes for the combined TC/talocrural joint have been identified during the support phase of running. Variation in the orientation of this axis was great within and between subjects. These results indicate that a method of categorizing subjects may be necessary to obtain further information about these joints, diagnose joint pathology, and prescribe effective prevention and rehabilitation modalities.

REFERENCES

1. BATES, B.T., et al. Functional Variability of the Lower Extremity During the Support Phase of Running. **Med Sci Sports Exerc.** 11:328-331, 1979.
2. CLARKE, T.E., et al. The Effects of a Soft Orthotic Upon Rearfoot Movement in Running. **J Am Acad Podiatric Sports Med.** in press. 1982.
3. CLOSE, J.R. Some Axes and Centers of Rotation of the Skeletal System. **Motor Function in the Lower Extremity.** Institute of Engineering Research, University of California at Berkley. Series II, Issue 24, 1953.
4. NIGG, B.M., et al. Gait Analysis and Sport-shoe Construction. In: E. Asmussen and K. Jorgensen (eds.), **Biomechanics VI-A**, University Park Press, Baltimore. 303-309, 1978.
5. WRIGHT, D.G., et al. Action of Subtalar and Ankle-Joint Complex During the Stance Phase of Walking. **J Bone Joint Surg.** 46A:361-464, 1964.

Table 1

ESD Parameters for the Motion of the Shank Relative to the Calcaneus during the Three Characteristic Time Intervals

a. TD-FF

Subj. No.	Time of PCP* (%)	σ (degrees)	s (cm)	PF/DF (+/-)	EV/IN (+/-)	AB/AD (+/-)
1	0-10.2	19.9	0.3	0.906	0.328	-0.268
2	0-12.1	18.5	0.3	0.616	0.694	-0.373
3	0-10.8	14.2	0.0	0.838	0.031	-0.545
4	0-10.4	8.5	-0.2	0.469	0.584	0.662
5	0- 9.3	29.2	0.7	0.969	0.172	-0.179
Mean (SD)	0-10.6 (1.0)	18.1 (7.6)	0.2 (0.3)	0.760 (0.210)	0.362 (0.277)	-0.141 (0.469)

b. FF-MP

1	10.2-39.8	18.8	0.0	-0.383	0.787	0.483
2	12.1-58.1	24.3	0.1	-0.685	0.331	0.649
3	10.8-48.9	34.9	-0.3	-0.084	0.939	0.333
4	10.4-55.8	44.1	0.3	0.546	0.779	0.309
5	9.3-34.4	18.4	-0.7	0.351	0.932	-0.093
Mean (SD)	10.6-47.4 (1.0)(10.2)	28.1 (11.1)	-0.1 (0.4)	-0.051 (0.508)	0.754 (0.248)	0.336 (0.276)

c. MP-TO

1	39.8-100	43.0	-0.4	0.863	0.350	-0.363
2	58.1-100	54.1	0.4	0.838	0.472	-0.273
3	48.9-100	84.2	0.5	0.736	0.562	-0.377
4	55.8-100	67.0	0.3	-0.093	-0.995	0.036
5	34.4-100	26.0	-0.6	0.918	-0.306	0.252
Mean (SD)	47.4 (10.2)	54.9 (22.3)	0.0 (0.5)	0.647 (0.419)	0.017 (0.660)	-0.145 (0.278)

TD=touchdown, FF=footflat, MP=maximum pronation, TO=takeoff, σ=rotation about the ESD axis, s=translation along the ESD axis, PF=plantarflexion (+), DF=dorsiflexion (-), EV=eversion (+), IN=inversion (-), AB=abduction, and AD=adduction (-).
*PCP=paired characteristic positions

THE FREE MOMENT OF GROUND REACTION IN DISTANCE RUNNING AND ITS CHANGES WITH PRONATION

J.P. Holden
Knee Technologies, Inc.
One Lytle Place
Cincinnati, Ohio 45202

P.R. Cavanagh
Biomechanics Laboratory
The Pennsylvania State University
University Park, Pennsylvania 16802

INTRODUCTION

It has been suggested that a ground reaction moment about a vertical axis develops during the support phase of gait as a direct response to the tibial rotation that is occurring (1,2). The magnitude and direction of the moment is also assumed to be related to subtalar joint pronation and supination, which permit relative transverse rotations to occur between the leg and foot. This paper reports the effects of changes in pronation on the free moment (Mz') of ground reaction during distance running. The results, which are the first Mz' measurements reported for more than one subject during running, draw into question some earlier assumptions about the relationship between Mz' and leg rotations.

REVIEW AND THEORY

Frictional forces at the foot/ground interface cause rotational moments to exist about axes normal to the surface. A moment can develop due to friction even if the net shear force is zero, as with the case of a force couple. Mz' is equivalent to a force couple acting in the plane of the ground, and it can exist in either the presence or absence of any net shear forces. The value of Mz' is determined by calculating the net moment about a vertical axis through the center of pressure (COP), where any resultant shear force would have a zero moment arm and would not contribute to the moment.

METHODOLOGY

Ten male runners who did not use foot orthoses and who demonstrated heelstriking running styles were selected as subjects for this study. Normal foot types were also sought, and arch indices ranging from 0.20 to 0.28 were measured for the 20 feet. The mean height and weight for all subjects were 177.5 cm and 697 N, respectively. The subjects ran at 4.5 m/s over a Kistler force platform mounted in the middle of a 30 meter runway. Each subject completed five trials for both right and left foot contacts in each of three pairs of running shoes provided by the investigator. The shoes differed only in their midsole constructions, which incorporated mediolateral differences in height that forced the feet into varus, neutral, or valgus positions during standing. The neutral shoes represented a conventional running shoe condition, while the varus and valgus shoes were designed to cause decreased and increased pronation, respectively. All trials in the neutral shoes were completed first, and the order for the varus and valgus shoe conditions was varied systematically between subjects.

The eight analog outputs of the platform were each sampled at 1250 Hz by a 12-bit A/D converter. Data reduction and analysis included statistical comparisons using analysis of variance for seven measures taken from the normalized Mz' (divided by body weight x height). These measures were: maximum and minimum Mz' and their times of occurrence during the first half of support phase; percent of total contact time with Mz' positive; net angular impulse; and rectified angular impulse (using absolute values of Mz'). The sign convention specified that a positive Mz' acted on the foot in the direction tending to resist foot abduction (Figure 1). All trials were time normalized to the mean contact duration of 192 ms, using a two-phase normalization procedure. A two-phase process was employed to minimize the attenuation and cancellation effects of averaging across the five trials within each foot/shoe combination; the effects of averaging over all subjects to obtain the mean curve for each shoe type could not be avoided.

RESULTS

The Mz'-vs-time patterns were consistent from trial to trial for a given foot/shoe combination, but there was considerable variation between individual feet. Figure 2 shows the mean curves for each of the three shoe conditions, and Table 1 lists the mean values for the seven Mz' variables.

Mz' acted on the foot in the positive direction, tending to resist abduction, during a majority of the foot contact periods for all shoe types. The periods of positive Mz' in the neutral and valgus shoes included nearly all of the early contact phase, when subtalar joint pronation is known to occur. In the varus shoe, which was intended to severely limit pronation, the mean Mz' was near zero for the 20 ms immediately following footstrike. Throughout the entire period where Mz' was positive, the trend in Mz' from varus to neutral to valgus shoes was for an increased moment tending to resist abduction. Mz' changed direction and tended to resist foot adduction during the late support phase in all shoe conditions.

DISCUSSION

When considering the components of joint axis rotations, one should recall that subtalar joint pronation includes dorsiflexion, eversion, and abduction, and that rotation about the ankle joint in the direction of dorsiflexion also has a small abduction component (3). Therefore, both joints can contribute in varying degrees to relative transverse rotations between the foot and tibia. Concerning the components of the net moments tending to cause or to resist rotations about these axes, it is important to remember that other factors, such as the ground reaction forces (GRFs), can also make a significant contribution. The net shear GRF can contribute to foot ab/adduction moments about a vertical axis (e.g., through the ankle joint), and all three GRF components, including the relatively large vertical force, can contribute to moments about the subtalar and ankle joint axes.

Several authors have stated that a "torque" (i.e., moment about a vertical axis at the ankle) is applied to the foot to resist foot adduction during the first half of the support phase in walking(1,2).

North American Congress on Biomechanics
Montréal (Québec) Canada, 25-27 August 1986

Their assumption is that the foot tends to want to follow the internal tibial rotation known to occur at that time. This assumption neglects the effects of other factors contributing to the tendency for foot ab/adduction during support. For example, the line of action of the GRF may tend to cause pronation and dorsiflexion about the subtalar and ankle joint axes, respectively. These rotations include components of foot abduction, and may be responsible for the Mz' that, in running, tends to resist foot abduction. In the present study of running and in a report by Nigg (4) for running trials by one subject, Mz' resisted abduction during the first 60-70% of support, when pronation is known to occur. Mz' resisted adduction later in the support phase, when supination is occurring.

CONCLUSIONS

The rationale used previously to explain ground reaction moments measured for walking cannot be applied to running. The Mz' component of ground reaction in normal running acts to resist foot abduction during a majority of the support phase. Footwear-induced changes in pronation affect Mz' such that increases in pronation produce increases in Mz' acting to resist foot abduction during the first two-thirds of support.

References

1. Mann, R.A. In D'Ambrosia, et al., Prevention and Treatment of Running Injuries, pp. 1-13, 1982.
2. Root, M.L., et al. Clinical biomechanics: Vol. II., 1977.
3. Inman, V.T., et al. Human Walking, 1981.
4. Nigg, B.M. Biomechanics of running shoes, 1986.

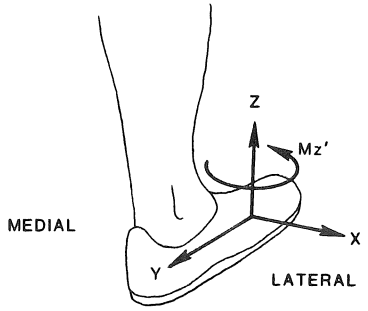

Figure 1. Sign convention for positive ground reaction forces and Mz', shown here for a right foot. Mz' acts on the foot (right or left) in a direction tending to resist foot abduction.

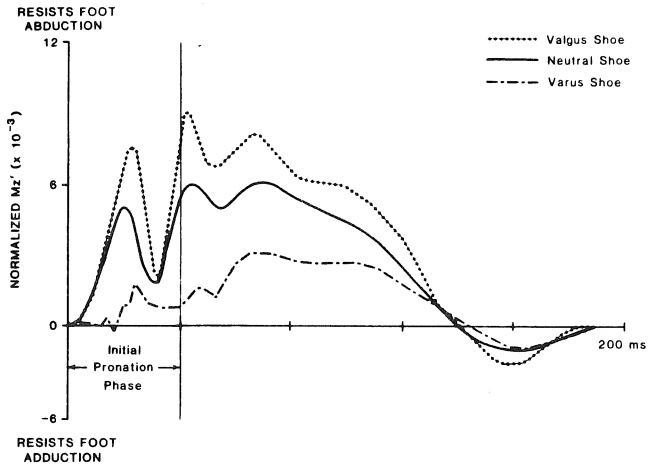

Figure 2. Mean curves of Mz'-vs-time for each of the three shoe conditions. The first 40 ms of foot contact is indicated as the initial pronation phase.

Table 1. Mean values of the Mz' variables.*

Variable	Varus	Neutral	Valgus
Maximum Mz'	6.5	9.7	12.4
Minimum Mz'	3.5	1.8	1.8
Time to max Mz'	21.8	20.1	20.7
Time to min Mz'	15.2	11.2	11.3
Time Mz' positive	53.3	70.9	74.1
Net Impulse	1.9	4.7	6.8
Rectified Impulse	4.7	6.1	8.1

* Dimensionless Mz' values are * 10E-3.
Times are expressed as % of contact duration.
Normalized impulse units are seconds, and values are * 10E-4.
Underlining connects means that are not significantly different ($p < .05$).

THE INFLUENCE OF LOAD ON MOVEMENT FREQUENCY

Robert J. Neal and Barry D. Wilson

Department of Human Movement Studies
University of Queensland. AUSTRALIA

INTRODUCTION

Early studies of the influence of load on movement frequency (1,8) found that movement frequency in bicycling was much higher (5.6 - 6.1 Hz) than that in sprinting and concluded that the rate of leg movement in sprinting is determined by the inertial load. The influence of unexpected loads on the trajectories of various body segments and of the speech articulators has also been investigated (1,2,6). The results tended to show that action by structures remote to the perturbation compensated for the disturbance so that the desired outcome was still achieved. A number of studies (5,3,4) by Kelso and coworkers have demonstrated that movement kinematics can be simulated by simple mass-spring models. These models predict stable and unstable states of movement as well as the discontinuous transitions between stable states which are indicative of mechanisms of human motor control. Transition between stable states is believed to be brought about by changes in driving frequency, rate of movement and load. It seems imperative, as a first step to investigating the nature of control strategies, to systematically investigate factors which effect transformations. Further study of the influence of load on movement patterns then seems warranted.

The purpose of this study was to investigate the influence of additional load, placed at the distal end of the throwing arm, on subjects' movement patterns when throwing a softball for maximum distance.

METHOD

Twelve male subjects were filmed while performing six throws for maximum distance. A high speed cine camera located with its film plane parallel to the assumed plane of motion and operating at 50 fps was used to film all trials. Subjects were instructed to throw a ball for maximum distance using a preferred style. No run up was allowed but a step and rotation motion was permitted. Three softballs of masses 180g, 802g and 1316g were used to provide three different load conditions. To distribute the possibility of fatigue effects in the design, the order of throwing the differently weighted balls was varied across subjects by using a Latin square design.

Film was digitally analyzed, data were smoothed and the angles describing a body posture were calculated for every film frame analyzed. Cluster analysis was used as a basis for determining whether the movement pattern was different for the two trials of each of the three load conditions and if the technique of the subjects changed across the conditions. Sequences of modal postures (MPs) for every trial were clustered to form movement patterns indicative of various styles of throwing.

RESULTS AND DISCUSSION

The movement pattern adopted by each subject on every trial was represented as a sequence of these 22 modal postures. This number of MPs indicates large intersubject variability. To identify common subject styles a second level of cluster analysis on transition matrices, representing the transition from any one MP to another within a trial, was conducted. Two groups, indicative of two different styles of throwing were extracted by this procedure. The essential difference between these styles is shown in figure 1 by stick figures of the mean positions adopted by the subjects. A chi square analysis, which was conducted to determine if there was any difference in the way in which subjects used the two techniques identified in the cluster analysis over the load conditions, revealed no significant difference ($X^2 = 0.5$, df = 2, p = 0.7780). That is, although some individuals may have adopted a different technique to throw the differently weighted balls there was no consistent pattern of change under the three load conditions. Comparison of the stick figures of the two styles at the same times highlights a number of interesting phenomena. Firstly, between frames 35 and 48, the position of the forearm and hand segments of style 2 throwers lagged the position of the same segments of style 1 throwers. At release

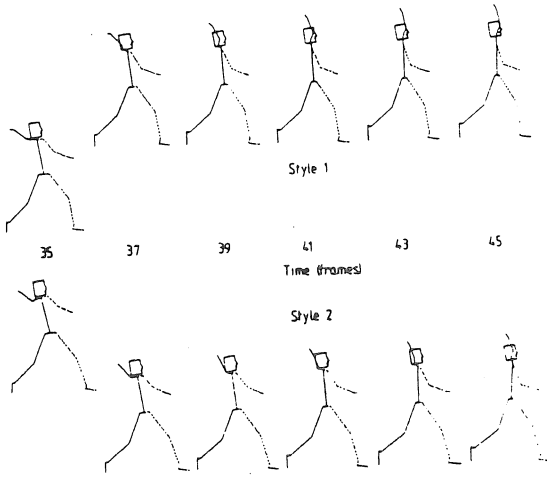

Fig. 1. Stick figures showing the differences between style 1 and style 2.

North American Congress on Biomechanics
Montréal (Québec) Canada, 25-27 August 1986

however, identical positions, regardless of style were evident. It appears that style 2 throwers really whipped the forearm and hand forward and upward during the final stages of the throw. By comparison, style 1 throwers used a technique that did not demanded less whip action than style 2, used the large segments of the body (trunk and legs): a style more akin to an "over the shoulder" type motion. ANOVA indicated that there was no relationship between group membership and the distance thrown ($F(1,22) = 0.549$, $p = 0.527$) highlighting that neither technique is any more effective than the other, for these subjects, in achieving maximum distance of the throw.

CONCLUSIONS

Advocates of a homeokinetic based theory of motor control may argue that since no consistent change was observed across the three conditions, the applied load was not large enough to cause instabilities in the dynamics of the system and thus no uniform bifurcation of modes was evidenced. The irregular change may indicate that the system is unstable and would need only be loaded slightly more to cause a new mode or style of throwing to emerge. For example, S5, who was one of the smallest of the subjects, changed from style 2 to style 1. This change may have occurred because the heaviest load was large enough to push this subject past the unstable region and into the next stable area. It was concluded that subjects were not altering their technique to compensate for the additional loading at the distal end of the arm and that most subjects used the same technique for the two trials of each condition.

References

1. Bizzi, E., Accornero, N., Chapple, W. and Hogan, N. (1982) Arm trajectory formation in monkeys. *Exp. Brain Res.* 46:139-143.

2. Folkins, J.W. and Abbs, J.H. (1975) Lip and jaw motor control during speech: Responses to resistive loading of the jaw. *J. Speech Hearing Res.* 18:207-220.

3. Haken, H., Kelso, J.A.S. and Bunz, H. (1985) A theoretical model of phase transitions in human hand movements. *Biol. Cybern.* 51:347-356.

4. Kelso, J.A.S., V-Bateson, E., Saltzman, E. and Kay, B. (1985) A qualitative dynamic analysis of reiterant speech production: Phase portraits, kinematics and dynamic modeling *J. Acoust. Soc. Am.* 77:266-280.

5. Kelso, J.A.S. and Scholz, J.P. (1986) Cooperative phenomena in biological motion. In Haken, H. (ed.) *Synergetics of Complex Systems in Physics, Chemistry and Biology* Heidelberg: Springer-Verlag, in press.

6. Marsden, C.D., Merton, D.A. and Merton, H.B. (1983) Rapid postural reactions to mechanical displacement of the hand in man. In Desmedt, J.E. (ed.) *Motor Control Mechanism in Health and Disease* New York: Raven, pp. 645-659.

7. Slater-Hammel, A. (1941) Possible neuromuscular mechanism as limiting factor for rate of leg movement in sprinting. *Res. Quart.* 12:745-756.

8. Sperry, R. (1939) Action current study in movement coordination. *J. Gen. Psych.* 20:295-313.

THE WOBBLING MASS - A RELEVANT VARIABLE IN GAIT AND LOAD ANALYSIS

J. Denoth
Biomechanics Laboratory
Swiss Federal Institute of Technology (ETH), ETH-Centre
CH-8092 ZUERICH, Switzerland (Director: Dr. E. Stuessi)

INTRODUCTION

In gait analysis ground reaction force or kinematic variables such as angular velocity or acceleration are usually used to describe the movements of interest. Often the shape of the ground reaction force or the shape of movement patterns are discussed in connection with pain, injury, progress in rehabilitation or anatomical abnormalities. The conclusions drawn are often due to the results of statistical analysis with 'some model of the human body in mind'.

Fundamental statements concerning the load on the locomotor system is possible only with the help of an idealization --a model-- of the human body [1]. Usually such models consist of a number of rigid segments, movably connected to each other to simulate the corresponding movement. However, the locomtor system itself is a system of many 'more-rigid' (bones) and 'less-rigid' (e.g. muscle tissue, fat) bodies. Therefore, the restriction of the human body to rigid bodies may create problems. One problem, for instance, is the mass of the rigid bodies 'foot', 'shank' 'thigh' and so on. In movements like walking the mass of the rigid body 'shank' is often assumed to be equal to the mass of the leg. For the impact phase, however, this is not correct. During this phase, in order to satisfy the mechanics of rigid bodies, the mass of the rigid body 'shank' has to be in the order of 50% of the mass of the leg (for an impact phase shorter than 15 ms). The reason is, that a leg is not a rigid body, parts of it may oscillate or in other words parts of it are wobbling.

The aim of this investigation is:

a) to show theoretically the consequencies of the wobbling mass on the grond reaction force and the acceleration of the 'ankle' in impact situations and
b) to discuss the influence of the wobbling mass onto the active phase.

REVIEW AND THEORY

In order to increase the understanding of the variable wobblig mass the behaviour of a very simple model, a one-segment planar model during impact is discussed. The one-segment represents the leg. This situation is similar to the impact phase in walking or jogging. The one-segment consists of a rigid body representing the skeletal part and the wobblig mass consisting of muscles, connective tissue, fat and skin. There are several posibilities to model the wobbling mass, as a particle, a rigid body or a 'continuum'. In the following the second possibility is taken into account [2]. As an example the equations of motions in the vertical direction are listed below.

```
MS*ZS2DOT = -MS*G + FGZ - FWZ
MW*ZW2DOT = -MW*G + FWZ
```

where:

```
MS      -mass of the rigid body 'skeletal part'
MW      -mass of the rigid body 'wobbling mass'
ZS2DOT  -acceleration of the 'skeletal part'
ZW2DOT  -acceleration of the 'wobbling mass'
G       -gravitational acceleration
FGZ     -ground reaction force
FWZ     -couplig between bone and wobbling mass
```

```
FWZ = FWL*SIN(PHIS) + FWT*COS(PHIS)
```

where:

```
FWL     -coupling in longitudunal direction
FWT     -coupling in transversal direction
PHIS    -angle of the 'skeletal part'
```

```
FWL = DL*(FWL3*DL**2 + RWL*DLDOT)
FWT = DT*(FWT3*DT**2 + RWT*DTDOT)
```

with:

```
DL     -displacement of MS and MW (long.)
DT     -displacement of MS and MW (trans.)
DLDOT  -time derivative of DL
DTDOT  -time derivative of DT
FWL3   -material constant (long. dir.)
FWT3   -material constant (trans. dir.)
RWL    -material constant (long. dir.)
RWT    -material constant (trans. dir.)
```

```
FGZ = NOT(ZSA)*FGZ1*ZSA
```

with:

```
FGZ1   -spring constant repres. the 'ground'
ZSA    -coordinate of the 'ankle'
```

METHODOLOGY

The impact of the one-segment-model onto different hard materials is simulated by numerical integration of the differential equations. For the simulations presented here the constants are evaluated from different experiments with one subject. The constants of the equations listed above are set to:

```
MS = 1.4kg, MW = 3.6kg
FWL3 = FWT3 = 4.20E+09, RWL = RWT = 2.48E+05
FGZ1 = 0.5E+05, 1.0E+05, 2.0E+05, 5.0E+05
```

The initial conditions were:

```
ZSA = 0.02 m
ZSDOT = ZWDOT = -1.0 m/s
PHI = 100 degrees
PHIDOT = 0.0 degrees/s
```

RESULTS

The oscillation of the wobbling mass is illustrated in Fig. 1 by the vertical component of the ground reaction force-time curve and the force-time curve of the product of mass (of the skeletal part of the leg) times the acceleration (vertical component) of the 'ankle' (MS*ZSA2DOT).

North American Congress on Biomechanics
Montréal (Québec) Canada, 25-27 August 1986

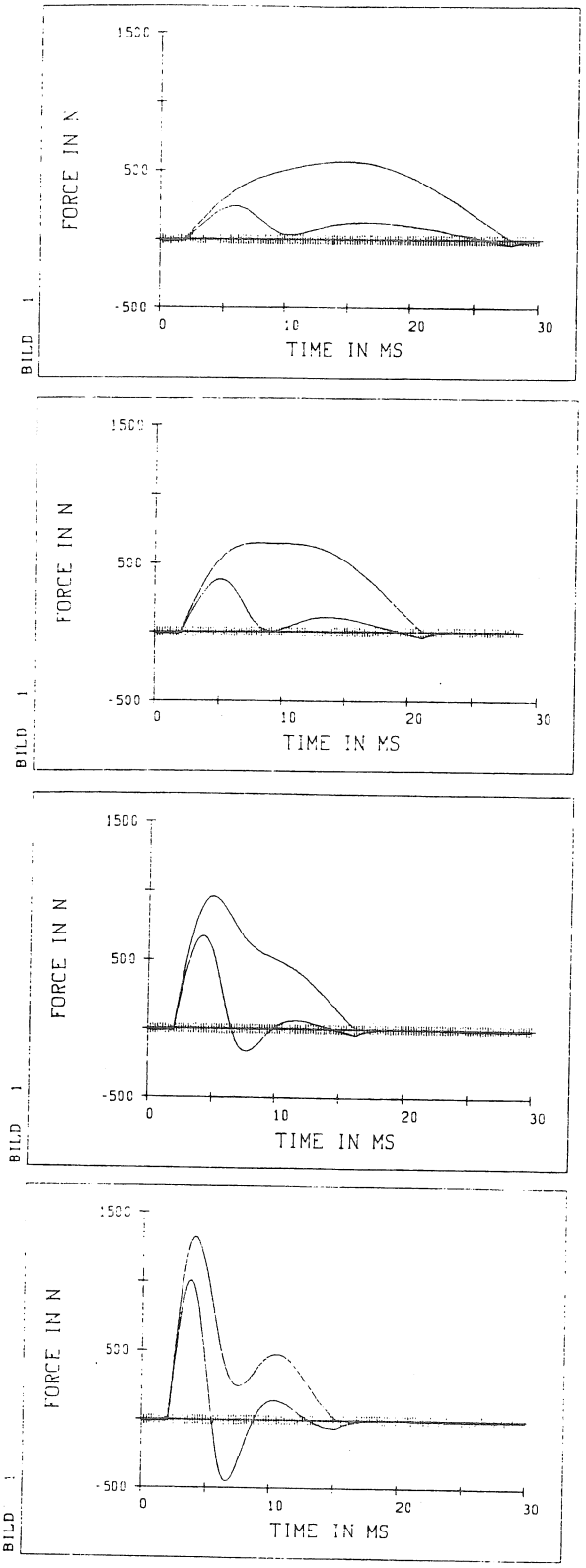

Figure 1. Ground reaction forces ([N]) and the acceleration of the ankle ([(m/s**2)*(1.4 kg)]) obtained from model simulations for different values of the hardness of the 'ground' (see text). Very soft (FGZ1=0.5E+05, top) very hard (FGZ1=5.0E+05, bottom).

DISCUSSION

The ground reaction force as well as the acceleration at the 'ankle' changes the shape when landing barefoot on a soft or on a hard floor. Such types of force-time curves are often observed e.g. in running shoe analysis. Without the wobblig mass, both the force and the acceleration, show a sinusoidal shape. This illustrates that, for instance, an interpretation of the ground reaction force can bee wrong if a wobbling mass is not included in the considerations. The problem lies in the fact that a change of the shape of the ground reaction force may be due to either the wobbling mass or the movement in the ankle joint with different muscle activities or due to changes of the foot-ground contact area.

The maximum ground reaction force increases with increasing hardness of the floor. But landing on the hard floor produces a maximum force which is about 35% smaller than one would expect without the wobbling mass. The reason for this discrepancy is that in fast movements (high frequency) less wobbling mass is connected to the bone than in slow movements. Normally one would not need hard and soft floors to get similar effects. The shoe or the type of jogging (heelstrike or forefoot strike e.g.) may have the same effect.

The wobbling mass has also consequences on the active phase if the reflexe-mechanisms are taken into account. When including the wobbling mass the skeletal part "moves" faster compared to a model without wobbling mass. Firstly there are higher angular velocities which occur. Secondly the sign of the angular velocity may change several times during the impact. This results in a higher reflexe activity and therefore the wobbling mass has an influence on the ground reaction force during the active phase, too.

Other interesting aspects are the stress on the wobbling mass itself and the reflexes produced by such an inhomogenously stressed muscle.

CONCLUSIONS

1. The wobbling mass has a relevant influence on the force-time curve in impact situations. Therefore the description and the interpretation of "peaks" of the ground reaction forces should bee done very carefully.
2. Quantitative comparison and the interpretation of impact peaks on soft and hard floors or with soft and hard shoes without the variable 'wobbling mass' may be wrong by about 30%.
3. Some extra peaks in the active phase of the ground reaction force e.g. may be a consequence of a greater activity induced by the stretch-reflexe during the impact phase.

References

1. Denoth, J. Load on the Locomotor System and Modelling. In: B. M. Nigg (Ed.), Biomechanics of Running Shoes, Human Kinetics Publishers Champain, Illinois. 63-116, 1986.
2. Denoth, J., Gruber, K., Keppler, M., Ruder, H. Forces and torques during sport activities with high accelerations. In: S. Perren and E. Schneider (Eds.), Biomechanics: Principles and Applications, Vol. 2. Martinus Nijhoff Publishers, 1985.

Acknowledgement

This research was supported by the SWISS NATIONAL FOUNDATION

THE EFFECTS OF ADDITIONAL LOAD ON IMPACT FORCE

B.T. Bates and P. DeVita
Biomechanics/Sports Medicine Laboratory
University of Oregon
Eugene, OR 97403, USA

J. Hamill
Biomechanics Laboratory
Southern Illinois University
Carbondale, IL 62901, USA

INTRODUCTION

A protective mechanism within the body to control the level of the impact force during running has been postulated as a result of observing no differences in these forces when weights up to 600g were attached to the tibia (1). The runners studied accommodated to the additional weight with changes in running style. The purpose of this study was to further examine this hypothesis by investigating the strategies used by runners to accommodate to additional loading of the leg. All subjects exhibited some effects due to additional loading although no consistent strategy was observed.

REVIEW AND THEORY

The ground reaction forces (GRF) generated during running typically consist of two components: 1. An impact or passive force and 2. A loading or active force. The impact force reaches maximum values of 1 to 3 times body weight within the first 30-35 ms of the support period. This force initiates a shock wave that propogates through the musculoskeletal system and must be attenuated by the various components of the system often resulting in injury to the runner. The force occurs in too brief a time period to be influenced by neuromuscular intervention and therefore its characteristics are determined by preprogrammed muscular activity which control lower extremity kinematics and stiffness characteristics, prior movements and the material properties of the contact elements.

METHODOLOGY

The experimental set up consisted of a force platform (515 Hz) interfaced to a computer and a photoelectric timing system to monitor running speed ($4.29+/-0.15ms^{-1}$) over a 4m interval. In addition, two high speed cameras (150 Hz) were positioned to record the contact phase from the posterior and lateral views. Four males volunteered as subjects (S). S1 was an occasional runner and the other 3 were regular runners. Each S performed seven blocks (C1-C7) of 10 valid trials requiring approximately 90 minutes. All subjects ran in the same shoes for all conditions. C1, C2, and C7 were performed with no leg weights. C3 thru C6 were performed with additional load masses of 300 and 600g securely attached around each leg above the tibio-talar joint. The initial load condition was randomly selected. Following a brief accommodating period (several practice trials) data were collected. This was followed by an accommodating run of approximately 1500 m and the acquisition of a second block of 10 trials. The procedure was then repeated for the other load condition.

The analytical method used to assess the affects of each condition consisted of an individual within subject design. Mean values were computed for each condition and compared serially by load magnitude and order of performance. Significant differences were determined using the 95% confidence limit values of the mean absolute differences of the seven conditions (0.604 times the mean standard deviation) for each subject (2). The preliminary data presented in this paper are those related to the impact force only.

RESULTS AND DISCUSSION

A summary of the 10 trial mean values for all subject-conditions is presented in Table 1. Significant within subject differences of 57.1% were observed for S1, S3, and S4 and 71.4% for S2. Previously reported, intraday reliability results for force parameters of 10.4% (3) and 18.7% (4) suggest that the observed differences were at least in part due to the affect of the added loads.

Examination of the first two no-load conditions (C1, C2) showed significant differences for three of the subjects (S2, S3, S4). These results could have been the result of normal variability or could indicate a learning affect. Since it was not possible to determine the cause, the second no-load condition (C2) was considered the more reliable and used for the remaining comparisons.

Within load condition analyses resulted in significant differences between the two 300g load conditions for three of the subjects (S1, S2, S3). S2 and S3 exhibited increases of 0.63 and 1.49 N/kg body mass, respectively while S1 showed a decrease of 1.75 N/kg. No significant differences resulted from the accommodating run for the 600g loads.

Figure 1 shows the relationship between conditions 2(no-load), 4(300g, post), 6(600g, post) and 7 (no-load) for all subjects. S1's performance was very consistant with no significant differences between the four conditions. Examination of S1's total performance, however, showed a pronounced increase in the impact force value following the initial load application. The accommodating run lowered the

North American Congress on Biomechanics
Montréal (Québec) Canada, 25-27 August 1986

Table 1. Ten Trial Mean Impact Force Values For All Subject-Conditions

	S1		S2		S3		S4	
Condition	$\bar{X}$	SD	$\bar{X}$	SD	$\bar{X}$	SD	$\bar{X}$	SD
1. No-load	15.58	1.25	19.17	0.73	20.13	2.37	19.27	1.36
2. No-load	15.25	1.22	18.54	0.22	18.48	1.70	20.07	1.25
3. 300g (Pre)	16.56	1.39	18.13	0.87	19.21	2.10	18.96	0.94
4. 300g (Post)	14.81	1.44	18.76	0.66	20.70	1.11	18.99	1.01
5. 600g (Pre)	14.02	0.85	19.42	1.11	20.76	1.56	19.85	1.09
6. 600g (Post)	14.65	1.08	19.65	0.89	21.74	2.27	19.70	0.64
7. No-load	14.58	1.48	17.78	0.75	19.17	2.20	18.31	1.36
Mean	15.06	1.24	18.79	0.75	20.02	1.90	19.31	1.09

All values are given in N/kg body mass. Pre and Post refer to the values obtained before and after the 1500m accommodating run. S1 and S3 were exposed to the 300g load first while S2 and S4 experienced the 600g load first.

value to slightly less than the no-load value (C2) where it remained for the remainder of the conditions. This strategy suggests the use of a "protective mechanism" as postulated by Bahlsen et al. (1).

The other three subjects performed quite differently. S2 and S3 exhibited increased values with the addition of 300g of weight while S4 showed a decreased value. All three subjects showed increased values for 600g compared to 300g averaging 0.88 N/kg or 4.5%. Following the removal of the weights, the average impact force value decreased 1.94 N/kg or 9.5%. The impact force model (1) predicts increased force values of 3.0 and 6.0% for loads of 300 and 600g, respectively. S2 and S3 performed in approximate agreement with the model when given the opportunity to accommodate to each new condition. S4's initial performance (C2 to C4) was not consistant but his latter performances were.

Evaluation of the data by order of weight presentation as opposed to weight magnitude provided no additional insights.

SUMMARY

All subjects exhibited some effects due to additional loading of the leg. The occasional runner (S1) appeared to use a different strategy than the regular runners in accommodating to the increased loads. Although the responses to the initial load condition differed, all subjects exhibited increased impact forces with load increments from 300 to 600g and reduced force values when the weights were removed.

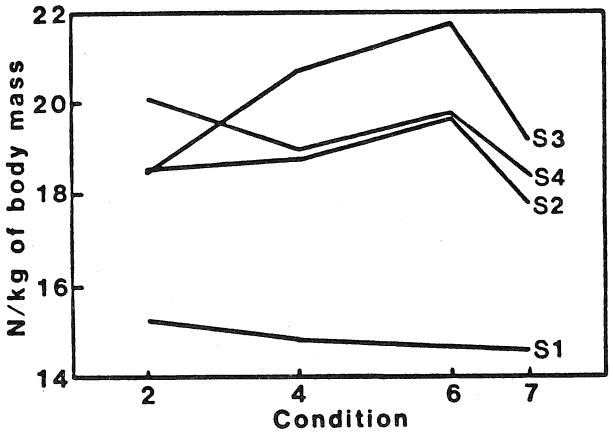

Figure 1. Impact force values for all subjects for four conditions: C2 = no-load, C4 = 300g Post, C6 = 600g (Post), and C7 = no-load.

REFERENCES

1. Bahlsen, H.A., et al. Kinetic and Kinematic Analysis of the Effective Mass in Heel-Toe Running. Human Locomotion III, 3:63-64, 1984.
2. Bates, B.T. et al. The Effect of Intra-Individual Variability on Sample Size. Biomechanical Aspects of Sport Shoes and Playing Surfaces, 191-198, 1983.
3. DeVita, P., et al. Reliability of Ground Reaction Force Data. Human Locomotion III, 3:77-78, 1984.
4. DeVita, P., et al. The Effects of Time on Selected Ground Reaction Force Parameters. Biomehanics X (In Press).

PREDICTION OF OPTIMAL STEP LENGTH USING THREE SIMPLE DYNAMIC MODELS OF WALKING

M. Huboard, E. G. Paterson, A. E. Orcutt
Department of Mechanical Engineering
University of California
Davis, CA 95616 USA

REVIEW AND THEORY

Energy expenditure in biped locomotion depends on step length λ and velocity u. It has often been observed [1-3] that as speed increases, λ increases in a regular fashion, and suggested that the preferred step length is chosen because it results in least energy cost. There have been no purely theoretical investigations, however, which predict that the observed λ-u patterns are indeed optimal. This study examined progressively more complicated mathematical models of biped locomotion in an attempt to predict energetic optimality of experimentally observed λ-u patterns. All models investigated were similar to that of Mochon and McMahon [4], with plane motion of four rigid bodies pinned at the hips, knees, and ankles. Energy costs as a function of λ and u were determined by: 1) Integrating the equations of motion through swing. This used a shooting procedure similar to [4] to calculate the pre-swing angular velocities which produce the desired step length and time, assuming a ballistic swing phase, i.e. energy conservative. 2) Calculation of energy losses at knee lock and heel and toe strike. 3) Replacement of these energy losses by work done only in stance phase. Three variations of the above dynamic model were: I) A 2 DOF model with straight rigid legs, II) A 4 DOF model with straight legs but separate feet, and III) A 4 DOF model with knees similar to [4]. These models are shown schematically in Figure 1.

RESULTS AND DISCUSSIONS

The major conclusions of the investigation were: 1) The energy costs of low speed walking can be reasonably well predicted using simple models with ballistic swing phases and ideal inelastic collisions with the ground. Much of the energy cost is in losses in collisions with the ground. 2) "Natural step lengths" appear to result from a tradeoff between frequency and severity of these collisions. 3) Model I predicts the correct magnitude for λ but not the trend of increasing λ with u. In Fig. 2 the results of Model I (heavy line) are presented together with experimental data from [1]-[3] and others. 4) Figure 3 shows similar results for Model II against the same experimental data. The trend of "Natural step length" dependence on velocity can be predicted for low speeds using Model II with only ankle flexion. The cushioning effect of heel strike and subsequent foot rotation to toe strike is an important energy conserving feature of Model II. 5) Knee motion must be included to predict λ vs. u at higher speeds, but the more complex model must maintain ankle motion and the cushioning of heel strike by foot motion described above. Model III was not successful because it contained knee motion but deleted ankle motion.

References

1. Alexander, R. M., in Scale Effects in Animal Locomotion, (T. J. Pedley, Ed.), Academic Press, London, pp. 93-110, 1977.

2. Cotes, J. E. and Meade, F., Ergonomics, 3, pp. 97-119, 1960.

3. Grieve, D. W. and Gear, R. J., Ergonomics, 9, pp. 379-399, 1966.

4. Mochon, S. and McMahon, T. A., J. Biomechanics, 13(1), pp. 49-57, 1980.

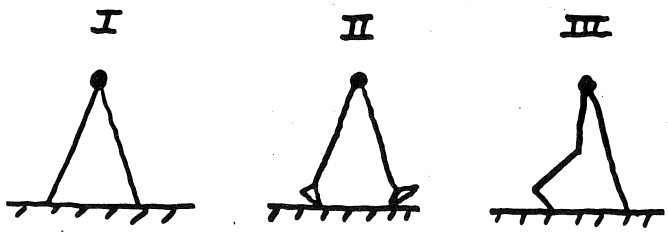

Figure 1.

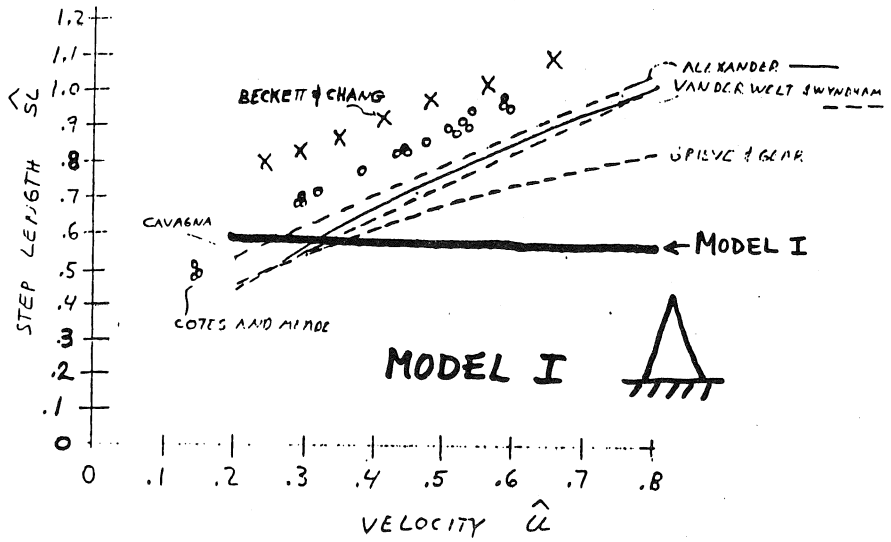

Figure 2.

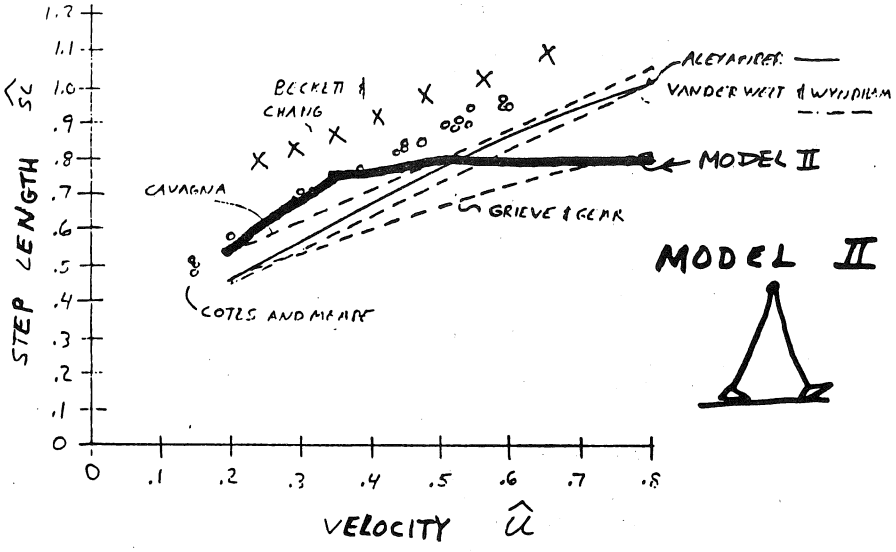

Figure 3.

A COMPUTERIZED GAIT PROFILE SYSTEM

James P. Dickey
David A. Winter

Department of Kinesiology
University of Waterloo
Waterloo, Ontario
N2L 3G1

INTRODUCTION

A broad range of techniques for gait evaluation are available, providing various types of information at different levels of sophistication. The purpose of the Computerized Gait Profile System (CGPS) is to provide an easy and inexpensive method for objectively summarizing gait patterns, including segment and joint angles as well as cadence and step length data. Such recording systems are critical for monitoring the progress of rehabilitation patients during therapy or post surgery, and are a prerequisite for the detailed diagnosis of gait abnormalities.

CGPS is based on an IBM PC with a high resolution graphics card and uses information obtained from sagittal plane stop motion video recordings of gait to create stick figures for critical phases of the cycle. The CGPS is computerized in order to overcome several of the shortcomings of previous systems. The sequence of data entry is rigorous, ensuring that all information is entered which results in efficient use of time, because pertinent variables are cued sequentially. The gait profile charts are easily created, interpreted, corrected, stored, and retrieved. The profiles are automatically compared with normal patterns, and deviations are flagged to indicate the specific features which fall outside of the normal range.

REVIEW AND THEORY

Previous attempts at gait description techniques can be classified as either indices or profile forms. Typical indices stress individual parameters, and produce single scores intended to adequately describe the gait. While this approach has been shown to have some assessment value(1), it has limited value for evaluation or detailed diagnosis. Previous ambulation profiles(2) have had problems of redundant measures or measures that lack adequate information for detailed evaluation and diagnosis(3).

METHODOLOGY

The development of the CGPS occured in two phases. Phase one consisted of developing a simple gait profile form. The form consisted of normal and various abnormal stick figures describing the lower limb position at seven critical phases of the gait cycle; with space for step length, cadence and related comments. The most appropriate figures were circled based on comparison with stop motion video recordings. This system was estimated to be ninety percent effective as indicated by the range of abnormal gait patterns observed at the University of Waterloo Gait Laboratory. Shortcomings of the system included an inability of the symbols to describe all possible gait profiles, and an inability to represent the characteristic range of normal profiles. The sequence of filling out the form was at the discretion of the observer and, therefore, important features of the gait cycle might pass unnoticed. The CGPS was developed to overcome these shortcomings.

RESULTS AND DISCUSSION

The CGPS is composed of a flexible, user-friendly, menu-driven computer program that produces gait profiles. All the required data can be obtained from a stop-motion video recording of the subject's gait in the sagittal plane. The stick figures are produced by overlaying stored symbols (lines, arrows, etc.) which are selected based on the gait trial data.

Figure 1 shows the resulting gait profile of a normal subject. Creation of a profile begins by inputting the trial related data as it is prompted (refer to numbers 1 to 4 in Figure 1). After the cadence (area 5) and step length in meters (area 6 and 7) are entered, a blank chart showing the entered trial information is displayed. Figures are added to the chart working down the columns, moving from initial contact (0% of stride) through mid swing (75% of stride). Required information is prompted for each square. The video is paused at initial contact of the limb, and the appropriate trunk position figure (see label 8) selected from the menu of possible choices. The knee and ankle figures are created through angle data entered. The absolute angle of the leg, and relative angle of the knee are prompted to create the knee symbol (label 9). The absolute angle of the foot is entered, and used along with the previous information about the leg to create the ankle symbol (label 10). Foot symbols, reflecting the amount of internal or external rotation, are selected from the menu of possibilities (label 11) similar to selection of the trunk position figure. The video is advanced and paused at the next phase of the gait cycle, allowing the next column to be completed as described. Arrows at appropriate joints and phases of the gait cycle represent the "vigour" of the motion. Normally, controlled foot lowering and rotation of the leg over the foot are seen in early stance, while active plantarflexion and some hip

North American Congress on Biomechanics
Montréal (Québec) Canada, 25-27 August 1986

pull-off are seen at toe off (refer to figure 1 for corresponding arrows). Clearly written prompts at the appropriate phases permit the selection of appropriate movement arrows; for example, normal foot lowering versus foot slapping.

Completed charts can be easily stored on disk for future retrieval, updating or comparison. Comments regarding the head, upper extremities, external support and balance accompanying the trial can also be stored. This text can be displayed to the left of the chart.

Figure 2 shows the gait profile of a patient with unilateral right below-knee amputation. The asterisks displayed beside the individual figures indicate deviations beyond the range of normal patterns. The location of asterisks indicates specific joints or phases of the gait cycle where deviations may be clustered. The location of the asterisk(s) beside the figure indicates which aspect of the figure is abnormal. The asterisk labelled 1 in Figure 2 indicates that the absolute angle of the thigh segment at initial contact falls outside of the normal range of plus or minus one standard deviation about the mean. Asterisks 2, 3, and 4 indicate that the absolute angle of the leg and the foot respectively, are abnormal at initial contact. The absence of an asterisk on the right side of the knee figure indicates that the knee angle is within range in spite of the abnormal values for absolute segment angles. The asterisks in the ankle row (4, 5, etc.) indicate that the ankle angle is consistently abnormal across the entire gait cycle. This is not unexpected as no movement is possible at the prosthetic "ankle". Asterisk 6 denotes weak or negligible plantarflexion at this phase. The arrow marked by 7 indicates strong hip pull-off. Circumduction, if present, would be represented by an additional arrow at this location. The asterisk coding system is, thus, a powerful method for indicating specific deviations from normal. The location and extent of the abnormalities is quickly and easily assessed.

The chart in Figure 2 shows that the gait of the patient WP91E is characterized by abnormalities at initial contact and during swing. At initial contact, the lower limb is fully extended to increase the step length. The negligible plantarflexion and compensation with strong hip pull-off are to be expected as a result of the amputation. The knee angles are completely normal throughout the entire gait cycle, although the absolute angle of the thigh and leg are abnormal at initial contact and during swing. The right and left step lengths are quite consistent, and the cadence is normal.

CONCLUSIONS

The CGPS is a powerful gait description system that yields detailed data required for monitoring and detailed diagnosis purposes. The aim of the CGPS is to undergo further testing in clinical settings.

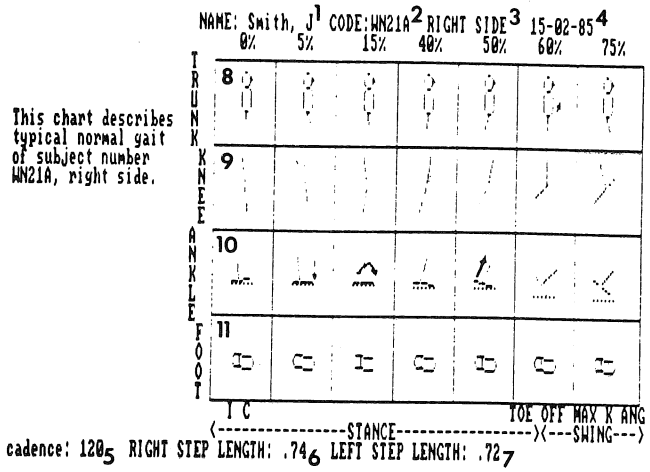

Figure 1. A completed gait profile form of a normal subject. Time is represented across the page as percent of stride; the figures represent segment and joint angles for the particular phases.

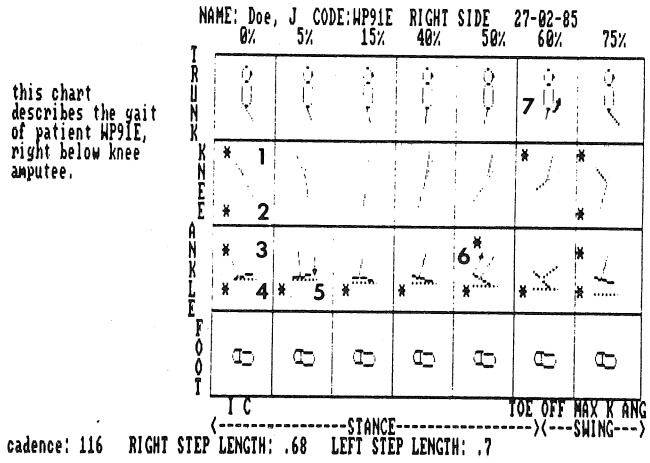

Figure 2. A completed gait profile form of a right leg B/K amputee. Asterisks beside the figures indicate specific deviations from normal.

REFERENCES

1. Andriacchi et al. J. Biomech., 10: 261-268, 1977.
2. Olney et al, Physiother. Can., 31: 85-90, 1979.
3. Winter, Physiother. Can., 37: 245-252, 1985.

ACKNOWLEDGEMENTS

The authors wish to acknowledge the support of the Medical Research council (Grant MT4343) and of NRC summer studentship support of Mr. Dickey.

GAIT PATTERNS AND ENERGY EXPENDITURE OF PATIENTS AFTER RESECTION ARTHRODESIS OF THE KNEE

Tylkowski, C., Miller, G., Springfield, D., Williamson, N., Enneking, W., Gait Analysis Laboratory,

University of Florida, Department of Orthopaedic Surgery, Box J-246 JHMHC, Gainesville, FL 32610.

Introduction

Resection arthrodesis for resectable malignant tumors about the knee is an alternative to amputation or custom joint replacement (1). The functional limitations imposed by knee arthrodesis on gait have not been thoroughly delineated. Thus in the past there has been no data to compare the kinematic, kinetic or oxygen utilization patterns of fused knee gait with that of the amputated limb or limb with a custom joint implant. Kinematic, kinetic and oxygen use is reported in this study to document the characteristics of fused knee gait.

Methods

Nine patients, average age 32.1y (range 15-51y), an average of 3.6 years (range 2-5 yrs) after knee resection arthrodesis, were evaluated in the Gait Analysis Laboratory at the University of Florida. The tumors resected included 2 periosteal osteosarcomas, 1 liposarcoma, 4 osteosarcomas, 1 malignant fibrous histiocytoma, and 1 giant cell tumor. All patients were tumor free and not on chemotherapy for at least one year prior to gait analysis. Each patient had fasted prior to the morning study. Joint range of motion and manual muscle testing was performed on each patient.

Kinematic data was collected by filming each walk with three Redlake synchronized movie cameras operating at 50 frames per second. After processing the patient landmarks were digitized by a Graf-pen digitizer to the minicomputer. Kinetic data was collected using an AMTI (Cambridge, MA) force plate. Dynamic electromyographic data was collected by surface electrodes to skin mounted preamplifiers and sent to the final amplifiers by a light trailing cable. All data was collected on, synchronized by, and processed by a Dec PDP11/34A minicomputer. Kinematic, kinetic, and dynamic electromyographic data were synchronized (5,7) and collected simultaneously with oxygen consumption. Oxygen use was monitored and averaged over one minute intervals using a Water's Oxygen Analyzer (Rochester, Minnesota) (8).

The free walking speed, two slower and two faster speeds were recorded for each patient. Two representative walks were recorded at each speed. Steady state oxygen consumption was documented at each speed prior to recording the walk. Aerobic functioning was monitored by pulse and respiratory rate. Computer processing yielded gait parameters of velocity, cadence, step lengths, stride, and time spent in single and double limb stance. Simultaneous EMG, medial/lateral, fore/aft, and vertical ground reaction forces were plotted. The joint and segment motions were calculated and displayed graphically and by three view stick figure representations.

Results

The calculated gait parameter are listed in Table 1.

Table 1

Parameter	pt. average(S.D.)	Normal	p
Velocity(m/sec)	0.93 (0.16)	1.51	0.01
Cadence(steps/min)	91.9 (8.6)	116	0.01
Stride(m)	1.15 (0.18)	1.56	0.01
Step(fused limb)	0.61 (0.1)	0.78	0.01
Step(opposite limb)	0.51 (0.08)	0.78	0.01
%SLS*(fused limb)	32.11 (1.81)	39	0.01
%SLS*(opposite limb)	41.51 (2.61)	39	0.02
%SLS*(fused-opp limb)	9.15 (2.16)	0	0.01

*SLS = single limb stance

There was no statistically significant correlation between age and either velocity or single limb stance. The compensatory body motions were identified. Pelvic tilt was normal. The pattern of pelvic obliquity was normal but with an increased degree of motion in fused limb SLS and swing. Pelvic and hip transverse rotation were affected by the surgically determined rotatory position of the leg and foot. Any position other than the normal 10 to 15 degrees of anatomic external rotation, that is internal or excessive external, caused a disruption in the normal cyclical motion of the pelvis through the gait cycle, and as a consequence affected hip rotation. There was less hip adduction primarily on the fused limb side. Fused limb hip extension was delayed into weight release. Knee flexion on the normal limb was increased in the weight acceptance portion of stance. Fused limb ankle motion was in the dorsiflexion range during stance and swing. Kinetic data showed decreased fused limb loading by the vertical ground reaction force. The vertical ground reaction force of the normal limb was not significantly different from normal.

Oxygen consumption was increased by more than 12% at a free walking speed which was 20% less than normal (9). A polynomial regression was used to plot the oxygen vs. velocity curves for laboratory normals and knee fusion patients. These were then compared to literature normals. (fig. 1)

Discussion

Normal limb single limb stance was increased to allow more time for the fused limb to swing. The increased ankle dorsiflexion and delayed hip extension were due to the lack of the knee flexion wave in stance. Increased pelvic obliquity during fused limb swing as well as increased hip abduction and ankle plantar flexion was used to clear the limb. The opposite knee flexion and pelvic drop during opposite single limb stance was used to minimize the excursions of the bodies' center of gravity. If the surg-

ically determined rotation of the foot was greater or less than the normal external rotation, there were disruptions in the pattern and amplitude of transverse plane pelvic rotation.

There was decreased loading of the fused knee limb during single limb stance with no significant changes in medial/lateral or fore/aft ground reaction forces. The opposite limb was loaded in a normal manner.

There was a 20% decrease in free walking speed. All speeds showed a marked increase in oxygen consumption (12% at free walking speed) for the fused limb gait when compared to laboratory and literature normals as in fig. 1.

The study suggests that attention to normal limb rotational position at the time of the surgical procedure will minimize abnormalities of pelvic and consequent hip rotation. Most important, objective data on the basic parameters of knee fusion gait, and its obligatory increase of oxygen consumption is provided. This will serve for comparison with data generated on the gait and energy requirements of above knee amputees or those patients with a custom total joint replacement after knee joint resection (6,2,3,4).

Funded by the Orthopaedic Research and Education Foundation.

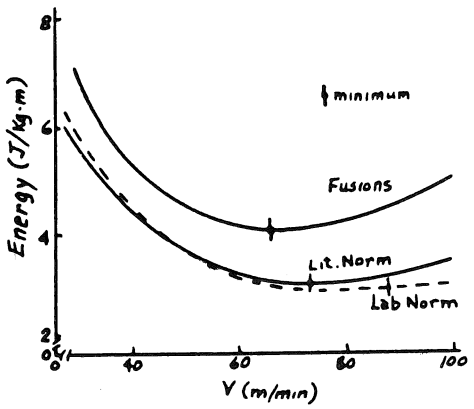

Figure 1 - Energy vs. Velocity

BIBLIOGRAPHY

1. Enneking, W.F., and Shirley P.D.: Resection-Arthrodesis for Malignant and Potentially Malignant Lesions about the Knee Using an Intramedullary Rod and Local Bone Grafts. J. Bone Joint Surg., 59-A(2): 223-236, 1977.

2. Fisher, S.V., and Gullickson, G.: Energy Cost of Ambulation in Health and Disability: A Literature Review. Arch. Phys. Med. Rehab., 59:121-133, 1978.

3. James U: Oxygen Uptake and Heart Rate during Prosthetic Walking in Healthy Male Unilateral Above-Knee Amputees. Scand. J. Rehab. Med., 5:71-80, 1973.

4. Mansour, J.M., Lesh, M.D., Nowak, M.D., and Simon, S.R.: A Three-Dimensional Multi-Segmental Analysis of the Energetics of Normal and Pathological Human Gait. J. Biomech. Vol 15, No 1:51-59, 1982.

5. Simon, S.R., Nuzzo, R.M. and Koskinen, M.F.: A Comprehensive Clinical System for Four Dimensional Motion Analysis. Bull. Hosp. Joint Dis., 38(1):41-44, 1977.

6. Takahashi, K., Laughman, R.K., Chao, E.Y. and Sim, F.H.: Functional Performance of Patients with Custom Bone and Joint Prostheses at the Hip and Knee. Trans. Orthop. Res. Soc., 7:130, 1982.

7. Tylkowski, C.M., Simon, S.R., Mansour, J.M.: Internal Rotation Gait in Spastic Cerebral Palsy. In the Hip Society: The Hip: Proceedings of the Tenth Open Scientific Meeting of the Hip Society, 1982, CV Mosby, 1982

8. Webb, P., and Troutman, S.: An Instrument for Continuous Measurement of Oxygen Consumption. Journal of Applied Physiology, Vol. 28:867-871, June, 1970.

9. Zarrugh, M.Y., Todd, F.N., and Ralston, H.J.: Optimization of Energy Expenditure during Level Walking. Europ. J. Appl. Physiol. 33:293-306, 1974.

O_2 CONSUMPTION IN A GAIT LABORATORY SETTING

D.L. Wheeler, G.J. Miller, C.M. Tylkowski, Gait Analysis Laboratory

University of Florida, Department of Orthopaedic Surgery, Box J-246 JHMHC, Gainesville, FL 32610.

INTRODUCTION: The oxygen consumption of 16 normal females walking at five speeds varying between 0.5 and 1.8 m/sec was determined by continuous monitoring with a Water's Oxygen Analyzer (4). Data was collected on a straight (13m) reversing path within the University of Florida Gait Analysis Laboratory. The values of velocity dependent rates of oxygen consumption were compared to the Douglas Bag using a 60.5m circular track (2) and Beckman method using a treadmill (1). Results in this study were comparable to the data previously reported (1-3). This study validates the use of the Water's Oxygen Analyzer and highlights its advantages in the simultaneous recording of metabolic activity and gait parameters.

REVIEW AND THEORY: A standard method of evaluating the energy cost of walking is to record oxygen consumption. Research to date has centered on the Douglas Bag or Beckman oxygen analyzer evaluation methods conducted either on a treadmill or large radius track. These methods are not easily applied in a gait analysis laboratory setting using a straight line path.

There is a direct relationship between walking speed and metabolic energy consumption (3). The energy is more accurately represented if oxygen use is normalized to velocity. A free walking speed of 80.0 m/sec has been shown by Zarrugh (3) to correspond to a minimal energy expenditure of 3.35 J/kg*m and Burdett obtained values of 78 m/s and 3.5 J/kg*m respectively (1). The purpose of this study was to compare the results previously reported to those generated at several velocities in a gait laboratory setting.

METHODOLOGY: Sixteen healthy females between the ages of 18 and 30 years were studied at five different gait velocities. The course was a straight path with 180 degree turns at each end. The free speed walk was monitored and measured by recording the time required to traverse a premeasured distance along the straight central portion of the course. The subject was then encouraged to assume a fast speed, a faster speed, a speed slower than normal and finally a much slower speed. Consistency at each speed was carefully monitored. At each of the five velocities the oxygen consumption was monitored by the Water's unit until steady state was achieved. Heart and respiratory rates were continuously monitored to ensure aerobic performance.

(The analyzer utilizes a servo-controlled blower which draws room air through a loose fitting face mask. The volume flow is adjusted by the servo so that pO_2 at the belt worn polarographic O_2 sensor is maintained.)

RESULTS AND DISCUSSION: As can be seen in figure 1, the minimum in the energy consumption curve appears at approximately the average composite normal velocity as predicted by Zarrugh (3) and Burdett (1). Thus it appears that the use of the Water's Oxygen Analyzer is useful for aerobic metabolic data acquisition in the gait lab. The systems portability, ease of use for experimenter and subject, and continuous, instantaneous output of oxygen consumption data to assist in steady state status determination allows for the simultaneous collection of metabolic, kinematic, kinetic and dynamic electromyographic data.

CONCLUSION: The above results validate the current system for use in evaluating oxygen consumption. The close correlation of our results to those of the literature allows for comparison with previously reported data. The future implication to these findings are substantial. The efficiency of pathological gait can now be determined at the same time compensatory mechanisms are evaluated by kinetic, kinematic and dynamic electromyographic methods. The mechanical energy determined by means of segmental energy analysis or joint moments can be compared to that of metabolic energy consumed during the same monitored cycle.

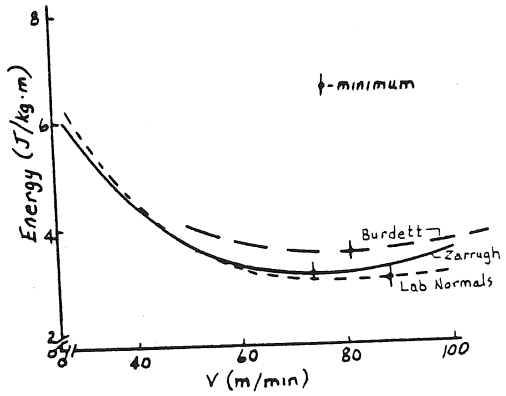

Figure 1 - Energy vs. Velocity

REFERENCES:
1. Burdett, R.G., Skrinar, G.S., Simon, S.R.: Comparison of Mechanical Work and Metabolic Energy Consumption During Normal Gait. J Ortho. Res., 1:63-72, 1983.
2. Waters, R.L., Hislop, H.J., et al: Comparative Cost of Walking in Young and Old Adults. J Ortho. Res., 1:73-76, 1983.
3. Farrugh, M.Y., Todd, F.N., Ralston, H.J.: Optimization of Energy Expenditure During Level Walking. Europ. J. Appl. Phys., 33:293-306, 1974.
4. Webb, P., Troutman, S.J.: An Instrument for Continuous Measurement of Oxygen Consumption. J. Appl. Phys., 28:6:867-871, 1970).

THE DIVERSITY OF NORMAL GAIT

J.C. Wall

School of Physiotherapy,
Dalhousie University, Halifax,
Nova Scotia, B3H 3J5

J. Charteris*

*Department of Human Movement Studies,
Rhodes University, Grahamstown,
South Africa

G.I. Turnbull

INTRODUCTION

One approach used in the clinical assessment of the gait cycle requires that any such evaluation be made with reference to normative data. This is in contrast to the use of the performance of the patient on a previous occassion or to the typical walking pattern adopted by patients with the same condition as bases for comparison. This "normal" approach to gait assessment implies that clinicians not only know the normal ranges of gait data but also appreciate inter-individual differences. Implicit in this approach is a clear understanding, by the clinician, of the effect on these data of other parameters, such as walking speed. It also implies an understanding of the concepts of the terms normal and pathological. It is a discussion of this final point, as it relates to human locomotion, which is the focus of this paper.

DISCUSSION

The fundamental question to be considered in this paper is: what criteria is applied in order to determine whether a gait pattern is "normal"? In medical jargon, pathological means pertaining to or caused by disease. In certain instances, determination of a pathological condition is unequivocal. The disease is either present or it is absent. However, when it comes to function, particularly movement, "abnormal" may be more difficult to ascertain. Perhaps the most common method of deciding what is normal is that used in anthropological studies. Measurements are taken on as large a population as possible and from these data are obtained the mean and standard deviation. Normal is then defined as being within two standard deviations on either side of the mean. This accounts for 95% of the population thereby arbitrarily designating the remaining 5% as abnormal. However, it is a method that has found widespread acceptance and has been used to define the normal ranges of certain gait parameters[1].

There is a spectrum of values possible, the central region of which is regarded as normal, with values below this range being classified as subnormal and above, as supranormal, as shown in Figure 1. These terms simply state that the values are outside the normal range and that they are less than, or greater than, the normal. They do not imply pathology per se. Indeed the term supranormal could refer to a pathological or an elite performance depending upon the parameter being measured. For instance, if speed of walking were considered then supranormal might be regarded as elite. However, if the time taken to cover a given distance was being measured, then the subnormal values would be regarded as elite. In other instances, anything outside of the normal range, whether smaller or greater than normal, might be regarded as pathological. For example, regarding the degree of knee flexion during the swing phase, too little range will result in a functionally longer leg requiring the patient to adopt compensatory strategies to prevent toe-scuff, while too much range of motion would lead to an inefficient walking pattern such as that observed in a steppage gait.

One of the major deficiencies in the true understanding of gait is that a sufficiently broad data base for normal walking has not yet been generated. One of the major reasons for this situation stems from the fact that the majority of gait studies have focussed on clinical problems where, very commonly, a few normal subjects may be included as a basis for comparison. It is, however, fundamentally important to realise that biological systems, of which man is but one example, are characterised by the ability to adapt, which in turn leads to variability. When considering normal gait therefore, one must take into account the ranges of variability that span normality. Human gait, for example, is affected by the mean overground velocity of its performance, the age, sex, gross somatotype, clothing, mental status, neuromotor control and mood of the individual. Similarly, the socio-cultural mileau with which the subject identifies, his morphological and physiological distance from a valid population mean, and the motivation of the subject may also contribute to normal variability.

To highlight the ramification of inter-individual differences on the normal-abnormal spectrum, Figure 2 shows patterns of knee flexion through a stride cycle. The subjects all walked at a speed equivalent to 75% of stature in overground distance per second. Trace A represents the pattern of a group of normal adults. Traces B and C follow virtually identical paths, B being the pattern of a group of normal one-year olds walking alone, while C is the pattern of an adult exhibiting unilateral quadriceps paralysis. The differences between A and B show that normal distributions in gait parameters vary ontogenetically while the similarities between B and C demonstrate that normality at one ontogenic stage is, in this example, pathological at another.

It should be noted, with respect to Figure 2, that the "Normal Adult" trace is based on a sample, not a population. That sample is drawn, intentionally, from a population of adults adjudged clinically, to be asymptomatic and without relevant (locomotor) medical history. Furthermore, such samples are seldom, if ever, randomly selected. If trace A indeed reflected the entire human population of "healthy young adults" then it would be permissable, on statistical grounds, to compute Standard Error ($S_{\bar{x}}$) bars, rather than Standard Deviation (S) bars as has been done in Figure 3. Given that $S_{\bar{x}} = S/\sqrt{N-1}$, the resulting bars would be considerably smaller and the "distance" of the trace reflecting quadriceps deficiency would be dramatised in graphical presentation. However, the

problem of determining what constitutes a "pathological" discrete value or pattern is in essence a logical, not a statistical issue. Not all parameters reflect interval data which are normally distributed, for in many instances the determination is made, not on a graded scale, but simply on an all-or-none basis. In short, not all parameters of concern to the student of gait abnormalities are normally distributed.

In highlighting the lack of normative gait data one point becomes clear. There is considerable literature on normal human locomotion if by "normal" it is meant that the characteristics of several subjects classified as normal on the basis that they exhibit or fail to exhibit certain characteristics, and analysed in terms of one or several parameters. This is not the same as saying that the normal ranges of variability under a wide range of walking conditions have been widely identified. For any subject the act of walking is affected by the speed of walking. Thus normative ranges of variability are required for all reasonable increments of speed through the normal range of walking speeds. Clearly normal ranges of variability in human gait are not possible in the absence of a reference to the whole spectrum of "normal" speeds. It is for this reason that studies such as those that develop regression equations relating various gait parameters to walking velocity [2,3] are so fundamental to an understanding of normal gait. Our knowledge of normal gait is expanding daily with the publication of papers on the walking patterns of elderly men and women, and on young adults and children, for example. Even though some of these studies have involved large samples, it is still true to say that neither the bio-scientist nor the practical clinician can state (except in the vaguest terms) the range expected of normal groups. Exactly what the parameters of gait are for healthy 85 year old walkers in comparison to sedentary as distinct from very active 35 year olds (if there are any distinctions), or of obese versus lean young adult females in the third trimester of pregnancy are examples of this point.

CONCLUSION

In concluding, the discussion in this paper has been restricted primarily to walking which is but one movement or series of movements of which man is capable. The underlying thesis developed in the paper is however applicable to other movements as well as the components of functional movement. The same philosophy could be applied to such assessments as postural characterisitics or muscle strength. If the approach to clinical gait assessment, suggested at the outset of this paper, is to be truly effective, then it requires that clinicians become more familiar with normal patterns of human movement and appreciative of inter-individual differences. It also requires that gait analysts provide a more extensive data base upon which to build a more complete understanding of normal human locomotion. Such a data base would make the "normal" approach to gait assessment much more powerful.

REFERENCES

1. Murray, M.P. In Black, J. and Dumbleton, J.H. (eds) Clinical Biomechanics. Churchill Livingstone, New York. 1981 pp173-200

2. Grieve, D.W. and Gear, R.J. Ergon. 5: 379-399, 1966

3. Rosenrot, P. et al. J. of Hum. Mov. Stud. 6: 323-334, 1980

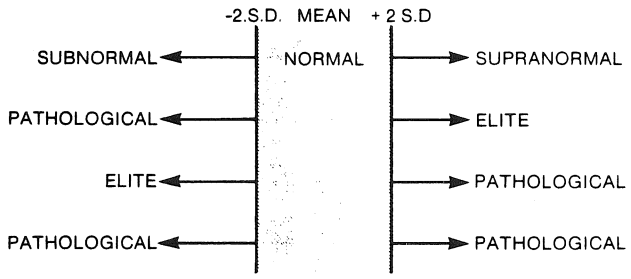

Figure 1. Terms for the consideration of data outside the normal range.

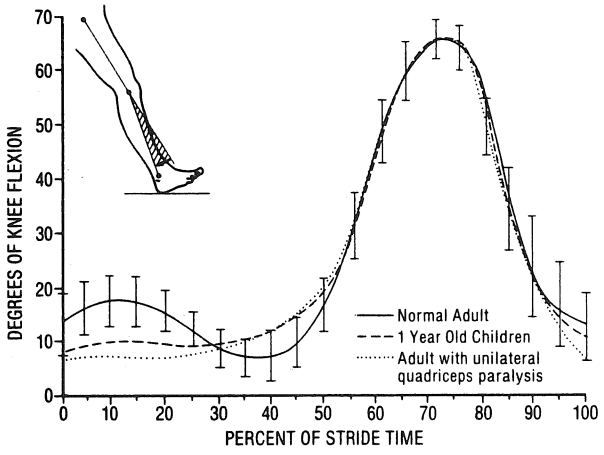

Figure 2. Angular displacements of the knee during walking.

A NEW TECHNIQUE FOR THE DETERMINATION OF BODY SEGMENT PARAMETERS UTILIZING CAT AND CAD PROCEDURES

M. H. Moeinzadeh, S. A. Burns, R. J. Borre
Department of General Engineering
University of Illinois at Urbana-Champaign
Urbana, Illinois 61801

G. J. Pijanowski
Department of Veterinary Biosciences
University of Illinois at Urbana-Champaign
Urbana, Illinois 61801

The accurate determination of body segment parameters (segment mass, location of center of mass, moment of inertia, surface area, volume) are essential components of the mathematical modeling of the kinematics and kinetics of the body.

Presently used databases are based on cadaver studies. The cadaver studies have lacked sufficient data to instill complete confidence in the models developed. The reasons for sparsity of cadaver data are: the lack of available material and the difficulty of complete assessment of the inertial properties even when cadavers are available. Furthermore, the extrapolation from cadaver data to live subjects is known to contain large errors due to the fact that the cadaver subjects were of unknown body type. Representative cadaver studies are Braune and Fischer (1889), Dempster (1955), Clauser (1969), and Chandler (1975).

A few attempts have been made to determine body segment parameters on live subjects employing geometric modeling (Hanavan, 1964), reaction board studies (Bernstein, 1967), vibration techniques (Hatze, 1975), and optimization techniques (Vaughan, 1982). All of these methods have practical and technical problems which limit their use in the generation of a large database.

It is the purpose of this study to present and examine a new practical and accurate in vivo technique for determining body segment parameters on a wide variety of human subjects. The technique utilizes the capabilities of computerized axial tomography (CAT scan) and computer-aided design (CAD) to account for the geometry and distribution of tissues within a body region.

Each body segment is divided into a series of CAT scan cross-sections. From each cross-section, the outline of the major tissue type (bone, muscle, fat) are input into the solids modeler of the CAEDS computer-aided design system. The skinning procedure within CAEDS reconstructs the three-dimensional geometry of the body segment by stretching a "skin" across the series of cross-sections. Given the tissue densities for bone, muscle, fat, the system can calculate the body segment parameters for each cross-section and then for the complete body segment.

Validation of the procedure was accomplished through testing objects of known geometry and parameters following a modified version of the moment table and oscillation techniques described by Lephart (1984). Further validation of the procedure was accomplished by determining the body segment parameters of canine limb segments by both methods.

References

Bernstein, N., The Coordination and Regulation of Movements, Pergamon Press, London, pp. 9-14, 1967.

Braune, W., et al., "Uber den Schwerpunkt des Menschlichen Korpers," Abhandlungen der Mathematisch-physiche Klasse der Konigl. Sachsichen Gesellschaft der Wissenschaften, S. Hirzel, Leipzig, 1889.

Chandler, R.F., et al., "Investigation of Inertial Properties of the Human Body," AMRL Technical Report 74-137, Wright-Patterson Air Force Base, Ohio, 1975.

Clauser, C.E., et al., "Weight, Volume and Center of Mass of Segments of the Human Body," AMRL Technical Report 69-70, Wright-Patterson Air Force Base, Ohio, 1969.

Dempster, W.T., "Space Requirements of the Seated Operator," WADC Technical Report 55-159, Wright-Patterson Air Force Base, Ohio, 1955.

Hanavan, E.P., "A Mathematical Model of the Human Body," AMRL Technical Report 64-102, Wright-Patterson Air Force Base, Ohio, 1964.

Hatze, H., "A New Method for the Simultaneous Measurement of the Moment of Inertia, the Damping Coefficient and the Location of the Centre of Mass of a Body Segment in Situ," European Journal of Applied Physiology, Vol. 34, pp. 217-226, 1975.

Lephart, S.A., "Measuring the Inertial Properties of Cadaver Segments," Journal of Biomechanics, Vol. 17, pp. 537-543, 1984.

Vaughan, C.L., et al., "Selection of Body Segment Parameters by Optimization Methods," Journal of Biomedical Engineering, Vol. 104, pp. 38-44, 1982.

CHANGES IN SEGMENT MASS, RADIUS AND RADIUS OF GYRATION, FOUR YEARS TO ADULTHOOD

Robert K. Jensen
Child and Development Studies and School of Human Movement
Laurentian University, Sudbury, Ontario, Canada, P3E 2C6

INTRODUCTION

Body segment inertial parameters are needed for investigations which progress beyond segment kinematics. These parameters are the mass, location of mass controid and the moments and products of inertia of the segment represented as a rigid body. Although considerable work has been devoted to adult males little is known of the subpopulation parameters for females, children and adolescents and even less is known of parameter development. The purpose of this paper is to report on changes in body segment mass and mass centroid radius and radius of gyration proportions for the transverse axis between four and nineteen years of males. A fifteen segment model of the body based on two cm wide elliptical zones (Jensen, 1978) was used in a mixed longitudial investigation over nine years. The estimated parameters were related to age and polynomial regressions fitted to the inter-individual data. Most of the parameters change with age and these developments need to be considered when segment parameters are needed.

REVIEW

For adult males, the cadaver studies of Dempster (1955), Clauser et al (1969) and Chandler et al (1975) have been used as direct proportions or predicted from associated anthropometry (Hinrichs, 1985) or scaled (Forwood et al, 1985). Zatsiorski and Seluyanov (1985) prepared mean values and prediction equations for young athletic males using gamma mass scanning. Mathematical models have progressed from the representation of a segment by a single geometric form (Hanavan, 1964) to sectioning using elliptical zones (Jensen, 1978) and defined shapes (Hatze, 1981). Subpopulations other than adult males have been identified but subjected to comparatively little investigation. Herron et al (1974), and Chandler et al (1978) applied biostereometric methods to estimations for children. Huang (1981) used computerized tomography for infants. However, the elliptical zone method (Jensen, 1978) has been applied extensively with cross sectional results for Japanese children (Yokoi, 1985) and mixed longitudial results over four successive years for children and adolescents (Jensen, 1986).

METHODOLOGY

The elliptical zone method (Jensen, 1978) was used with mean segment densities from Clauser et al (1969). The estimated parameters were for fifteen segments with the head and neck considered one (Fig. 1). Parameters were also estimated for four frequently used combinations of segments (Table 1). The mixed longitudial design used for the study was initiated in 1977 with twelve children of different ages (Jensen, 1986). The results covering nine years and 82 annual observations were evaluated using polynomial regression and the inter-individual data with respect to chronological age.

RESULTS

The accuracy of the method has been checked against body mass (error -0.82%, sd 2.63%) and segment parameters compared with the results of similar studies (Jensen, 1986). Polynomial regression coefficients and common variance are given in Table 1. A probability of 0.05 was used to select the degree of polynomial using program P5R from BMDP (Dixon, 1983).

DISCUSSION

The parameters given (Table 1) are sufficient for the analysis or simulation of most saggital movements of the body. Figure 1 can be used to relate shape and size and transverse axes of the body in the reference configuration to the parameters. Segment mass proportions curves were noticably curvilinear for the head, thigh and shank (Table 1). Head mass proportion decreased from 20% at 4 years to 6.5% at 19 years. Thigh mass increased from 7.5% to 11%. Relationships were positive for lower trunk, upper arm and forearm mass and negative for upper trunk mass. The curves also show that overall the foot and hand proportions decrease slightly. The curves for the extremities are consistent with the concept of distal to proximal development proposed by Tanner (1962) and head and trunk segment changes are consistent with cephalo-caudad development. It is evident from the common variance that there is a low relationship between mass proportion and age for some segments. These segments have a relationship which is only slightly better than that given by the mean for the mass proportion, indicating that within the distribution of the data, there is little change. The changes in mass proportion during growth describe then a substantial, non-linear redistribution of mass. The radius to the mass center is given as a proportion of link length from the specified axis. These relationships are either linear or there is no significant change. The highest common variance, for head/arm/trunk, indicates that the position of the mass center relative to shoulder axis changes with age. The relationships for the radius of gyration also indicate that there is little change with age. (Table 1). The proportion decreased slightly for head, upper arm, forearm, thigh and shank and was otherwise stable for the primary segment. This is consistent with the radius squared component of the moment of inertia.

This research was supported in part by Grant #A3693 from the National Sciences and Engineering Research Council of Canada.

REFERENCES

Dixon, W.J., 1983. BMDP statistical software, Berkley:California Press.

Forwood, M.R., et al, 1985. J. Biomech., 18:10:755-761.

Hatze, H., 1980. J. Biomech., 13:833-843.

Hinrich, R.N., 1985. J. Biomech., 18:8: 621-624.

Jensen, R.K., 1978. J. Biomech., 11:349-358.

Jensen, R.K., 1986. J. Biomech., (in press).

Tanner, J.M., 1962. Growth at adolescence, 2nd Edition, Oxford:Blackwell.

FIGURE 1
BODY MODEL

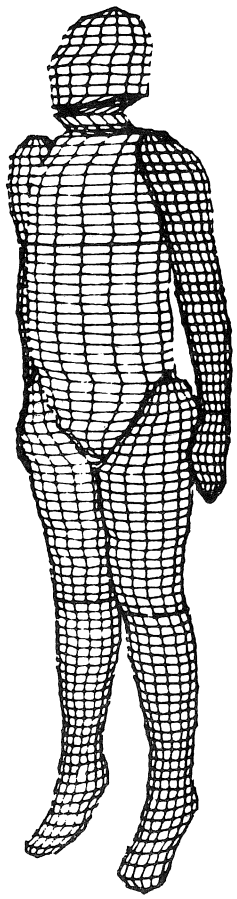

TABLE 1
SEGMENT PROPORTIONS

Mass Proportions

Segment	x^0	x^1	x^2	R^2
Head	0.27482	-0.020228	0.48427E-3	0.75844
Upper Trunk	0.15994	-0.14408E-2		0.10401
Lower Trunk	0.32597	-0.12116E-1		0.14664
Upper Arm	0.023179	0.72703E-3		0.54057
Forearm	0.13555E-1	0.29930E-3		0.37229
Hand	0.67681E-2	0.44736E-3	-0.20961E-4	0.10613
Thigh	0.042993	0.89620E-2	-0.28013E-3	0.66893
Shank	0.0207819	0.50568E-2	-0.19813E-3	0.32828
Foot	0.011975	0.17534E-2	-0.84131E-4	0.22754
Forearm/Hand	0.022913	0.25479E-3		0.16768
Shank/Foot	0.032757	0.68126E-2	-0.28243E-3	0.32970
Trunk	0.48610	-0.014163	0.67832E-3	0.17200
Head/Arm/Trunk	0.84850	-0.031545	0.11248E-2	0.61001

Center of Mass Radius Proportions

Segment	x^0	x^1	x^2	R^2	Axis
Head	0.5061				Prox
Upper Trunk	0.5554				Prox
Lower Trunk	0.46699	0.10027E-1	-0.38495E-3	0.12073	Prox
Upper Arm	0.57647	-0.16937E-2		0.06976	Dist
Forearm	0.56827	0.83450E-3		0.10301	Dist
Hand	0.5913				Dist
Thigh	0.4619				Prox
Shank	0.44479	-0.21424E-2		0.47126	Prox
Foot	0.47223	-0.94514E-2	0.35325E-3	0.11280	Prox
Forearm/Hand	0.61515	-0.69597E-2	0.38259E-3	0.28931	Dist
Shank/Foot	0.44181	-0.23038E-2		0.24219	Prox
Trunk	0.50519	0.64579E-2	-0.23952E-3	0.10822	Prox
Head/Arm/Trunk	0.11104	0.030823	-0.76273E-3	0.65586	Shdr

Radius of Gyration Proportions

Segment	x^0	x^1	x^2	R^2
Head	0.33156	-0.38029E-2	0.14203E-3	0.05106
Upper Trunk	0.3467			
Lower Trunk	0.3466			
Upper Arm	0.32090	-0.12878E-2		0.18553
Forearm	0.29297	-0.74037E-3		0.14105
Hand	0.2384			
Thigh	0.30760	-0.31507E-2	0.13435E-3	0.04247
Shank	0.29226	-0.62498E-3		0.20173
Foot	0.2442			
Forearm/Hand	0.25841	0.38727E-2	-0.17166E-3	0.17880
Shank/Foot	0.2839			
Trunk	0.2995			
Head/Arm/Trunk	0.53319	-0.75462E-2		0.42385

ESTIMATING SEGMENTAL INERTIAL PROPERTIES: MAGNETIC RESONANCE IMAGING VERSUS EXISTING METHODS

Michael Mungiole and Philip E. Martin
Exercise and Sport Research Institute
Arizona State University
Tempe, Arizona 85287

INTRODUCTION

One of the major problems faced by biomechanics researchers is the inability to obtain accurate, personalized estimates of the inertial properties of the body segments. Ideally, these inertial properties would be measured directly on each individual subject. The purpose of this study was to consider the value of using Magnetic Resonance Imaging (MRI) for estimating segmental inertial properties and to compare MRI based measures for segment mass, center of mass location, and transverse moment of inertia with values obtained using more traditional methods. The results of the study showed that there was reasonably good agreement between MRI estimates and those for other methods although MRI seemed to overestimate mass and moment of inertia values.

REVIEW

The accurate determination of the segmental inertial properties is necessary to obtain the internal forces acting on the body during movement. In the past, most of the existing data used for estimating segmental inertial properties has been obtained from elderly male cadavers. Thus, these data are not representative of the subjects often under investigation in many exercise and sport biomechanics studies. More recently, gamma mass scanning (1) and computerized axial tomography (2) have been applied in the analysis of these properties. Although these methods have shown promise in determining segmental inertial properties, both expose the individual to potentially harmful radiation. A medical tool which does not involve radiation but which has the potential for use in estimating segment inertia characteristics through tissue imaging is MRI.

METHODOLOGY

Initially, a series of anthropometric measurements were taken on 12 elite male runners. From these measurements, segmental inertial properties were estimated using the results and procedures of Dempster (3), Chandler et al. (4), and Drillis and Contini (5). These inertial properties were also obtained using the mathematical model given by Hanavan (6) and the regression equations given by Clauser et al. (7) and Hinrichs (8). Results for each of these methods were then compared to MRI-based estimates.

To obtain these MRI-based measures, the lower legs of the 12 subjects were imaged at a local hospital. A series of transverse plane images, spaced 2.5 cm apart, were taken along the length of each segment Using procedures similar to those of Rodrigue and Gagnon (2), the individual tissue areas for each image were determined using a computerized digitizing system. The tissue areas and individual densities along with the known 2.5 cm image spacing were then used to calculate the tissue volumes and segmental inertial properties. For this process, the segments were treated as a series of 2.5 cm long sections which were modeled as frusta of a right circular cone. The density values used for each tissue were obtained from Clauser et al. (7).

RESULTS

Sample means and standard deviations for mass, center of mass, and transverse moment of inertia about the center of mass are given in Tables 1, 2, and 3, respectively, for each method. Also included in each of these tables are the absolute and percent differences between MRI and each of the other methods.

Table 1 indicates that the mean value for mass obtained with MRI was higher than all of the other estimated methods except for Clauser's method. This latter method is also the one with which MRI agreed most closely.

When comparing center of mass locations (Table 2), Clauser's method is the only one which does not agree closely with the MRI results. Clauser's method resulted in a mean center of mass estimation that was considerably more proximal than the value obtained using the other methods.

The transverse moment of inertia mean values given in Table 3 indicate that MRI results in a higher value than every other method except for Hinrichs' mean value, the method most closely in agreement with MRI for this parameter. For the lower leg, Hinrichs derived three distinct moment of inertia regression equations from Chandler's data that utilized various anthropometric measurements. The results in this table represent the mean of these three values.

DISCUSSION

As is evident from each of the tables, there is a large range in the values of the parameters obtained using the various methods. For example, the mean mass values ranged from 2.696 g (Chandler) to 3.732 g (Clauser). Since mass estimates using MRI resulted in a mean value towards the high end of this range, it is suspected that this parameter could have been overestimated with the MRI-based method. These large mass values for MRI would at least partially explain the large moment of inertia values

North American Congress on Biomechanics
Montréal (Québec) Canada, 25-27 August 1986

obtained when compared to Dempster, Hanavan, Chandler, and Drillis and Contini.

The center of mass locations (Table 2) for each method are represented as a percentage of segment length from the proximal end. The reason for this is because the comparison methods used different anthropometric landmarks in determining the length of the lower leg. This resulted in slightly different leg lengths depending on the method used. By measuring the center of mass location as a percent from the proximal end, this discrepancy tended to be reduced.

The use of 2.5 cm spacing between images was adequate for the lower leg central regions but a spacing less than 2.5 cm near the endpoints would improve the analysis process. This is because the moment of inertia about the center of mass is more heavily influenced by the mass near the endpoints. Also, the images obtained near the endpoints are not as well defined due to the increased amount of cancellous bones.

Since the magnetic surface coil used for imaging was shorter than the length of the segment, approximately six images would be taken before the segment was shifted with respect to the coil. Occasionally, the images taken near the extremes of the coil were of marginal clarity making it somewhat difficult to accurately distinguish the different tissues. In most cases, however, the images obtained were quite clear and the different tissues were easily distinguished.

SUMMARY AND CONCLUSIONS

The results of the study indicates that the MRI-based estimates of segmental inertial properties fell within the range of values for the more traditional methods. Even though MRI-based estimates of the inertial properties appear to be valid ones, it must be concluded that the limited availability of MRI facilities, the cost of using such facilities, and the time consuming nature of the analysis do not make this method particularly feasible at the present time. Nevertheless, as facilities become more readily available and as hardware and software are enhanced, MRI may prove to be a useful tool for providing personalized estimates of segment inertial properties. Unlike many other in vivo techniques, an advantage of the MRI method is that it can be used on any portion of the body without exposing the individual to harmful side effects.

MRI also shows great promise in being used for other important aspects of biomechanics research such as the determination of the locations of the origins and insertions of major muscles, of joint axes of rotation, and of muscle moment arms. It is believed that the applicability of MRI for these and other biomechanics research applications will improve as hardware and software are continuously enhanced for this medical tool.

Acknowledgements

This study was supported by a University Research Fund grant, Arizona State University.

References

1. Brooks, C.B., et al. Med. Sci. Sport Exer. 7:290-294, 1975.
2. Rodrigue, D., et al. J. Biomech. 16:907-913, 1983.
3. Dempster, W.T. WADC Tech. Rep. 55-159, 1955.
4. Chandler, R.F., et al. DOT HS-801 430, 1975.
5. Drillis, R., et al. DHEW Rep. 1166-03, 1966.
6. Hanavan, E.P. AMRL-TR-64-102, 1964.
7. Clauser, C.E., et al. AMRL-TR-69-70, 1969.
8. Hinrichs, R.N. J. Biomech. 18:621-624, 1985.

Table 1. Sample means and standard deviations for mass (g) along with the absolute and percent differences between MRI and the other methods.

Method	Mean	S.D.	Abs Δ^1	% Δ^2
MRI	3.56	0.340	-----	-----
Dempster	3.05	0.171	-0.51	-14.5
Clauser	3.73	0.189	0.17	4.7
Hanavan	3.21	0.205	-0.35	-9.8
Chandler	2.70	0.141	-0.86	-24.3
Drillis & Contini	2.78	0.156	-0.78	-21.9

Table 2. Sample means and standard deviations for center of mass (% from proximal end) along with absolute and percent differences between MRI and the other methods.

Method	Mean	S.D.	Abs Δ^1	% Δ^2
MRI	41.37	0.870	-----	-----
Dempster	43.30	0.0	1.93	4.7
Clauser	36.11	0.735	-5.26	-12.7
Hanavan	42.39	0.558	1.02	2.5
Drillis & Contini	39.30	0.0	-2.07	-5.0

Table 3. Sample means and standard deviations for transverse moment of inertia (10^{-2} kg·m^2) along with absolute and % differences between MRI and the other methods.

Method	Mean	S.D.	Abs Δ^1	% Δ^2
MRI	5.30	0.823	-----	-----
Dempster	4.69	0.618	-0.61	-11.5
Hanavan	4.40	0.537	-0.90	-17.0
Chandler	3.99	0.199	-1.31	-24.7
Hinrichs	5.53	0.914	0.23	4.3
Drillis & Contini	3.42	0.450	-1.88	-35.5

[1] absolute difference = other method - MRI
[2] % difference = (other - MRI)*100/MRI

REGRESSION EQUATIONS FOR SEGMENTAL INERTIA PARAMETERS

M. Morlock and M.R. Yeadon
Biomechanics Laboratory
University of Calgary
Calgary, Alberta, T2N 1N4

INTRODUCTION

Attempts have been made to express segmental inertia parameter values in terms of anthropometric measurements using linear regression equations based upon data obtained from cadaver studies (Clauser et al., 1969; Hinrichs, 1985). The use of linear rather than curvilinear equations to express mass and moments of inertia in terms of length and circumference is questionable since the theoretical relationships are not linear. This paper presents an approach based upon the theoretical relationships between moments of inertia and linear dimensions. The two approaches are compared using the cadaver data of Chandler et al.(1975).

REVIEW AND THEORY

For simplicity consider a circular cylinder of radius R, length L and uniform density d. If the mass is m and the moments of inertia about longitudinal and transverse axes through the mass centre are I_L and I_T then:

$$m = \pi * d * R^2 L$$

$$I_L = 1/2 * m * R^2$$

$$I_T = 1/12 * m * L^2 + 1/4 * m * R^2$$

If P is the Perimeter ($2*\pi*R$), I_L and I_T may be expressed in the form:

(1) $I_L = k_1 * P^4 * L$

(2) $I_T = k_2 * P^2 * L^3 + 1/2 * k_1 * P^4 * L$

where k_1 and k_2 are constants.

It should be noted that circular cylinders of uniform density comprise only one class of solids whose moments of inertia are of the form given by equations (1) and (2). More general classes include solids of revolution and prisms where the density of cross-section is a function of the relative level of the cross-section.

For each class of solids k_1 and k_2 will have characteristic values. Figure 1 shows the relationship between I_L, P and L. The corresponding figure for the linear relationship $I_L = k_1 * P + k_2 * L + k_3$ would be a plane. When either P or L is zero, the curvilinear relationship gives a zero value for I_L whereas this is not the case for a linear relationship.

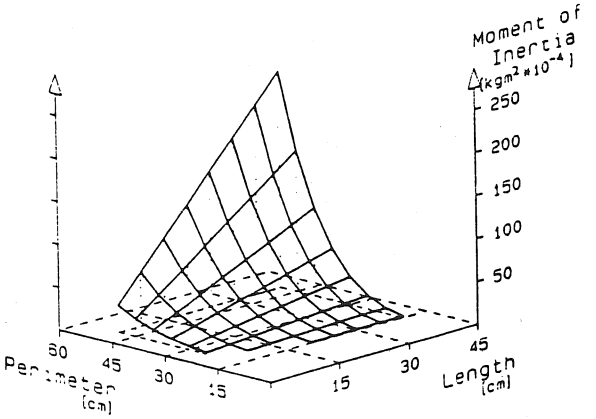

Figure 1: Moment of inertia of a cylinder about the longitudinal axis (Equation (1)).

METHODOLOGY

Values for the following variables were taken from the thigh data of the six cadavers in Chandler et al. (1975):

L : thigh length

P_1: upper thigh perimeter

P_2: mid-thigh perimeter

P_3: knee perimeter

I_L: principal moment of inertia about longitudinal axis

$I_{x,y}$: principal moments of inertia about transverse axes

In addition the following average values were calculated:

$$I_T = 1/2 * (I_x + I_y)$$

$$P = 1/4 * (P_1 + 2*P_2 + P_3)$$

If the thigh is modelled by two cylinders of equal length, the average perimeter is given by the weighted mean P. I_x and I_y are principal moments of inertia about transverse axes. The directions of the principal axes as calculated by Chandler et al. do not appear to be related to any anatomical directions and the values of I_x and I_y are generally close. I_T is therefore taken to be the average of I_x and I_y. Stepwise linear regression equations were obtained, using the statistical software SPSS, for I_L and I_T in terms of L, P_1, P_2 and P_3 for the six left thighs. The same statistical program was used to obtain curvilinear fits of the form given by equation (1) and (2) using P and L for the six left thighs.

In each case (I_L and I_T) the closest single variable and multi-variable linear fit was selected. The accuracies of the two linear fits and the curvilinear fit were then evaluated using the experimentally determined values for the right thighs as criteria. Only the values of five right thighs were used, since Chandler mentioned that the data of one of the thighs was erroneous.

EQUATIONS OF FIT AND STANDARD ERRORS			
Method	Equations for Moment of Inertia	Standard error of fit	
	Perimeter [m], Length [m], $I_{L,T}$ [kgm^2*10^{-4}]	dependent data [%]	independent data [%]
linear multi-variable	$I_L = -2.9 + 12.4*(P2) - 3.2*(P3) + 0.02*(L)$	16	32
	$I_T = -48.9 + 20.4*(P2) + 23.6*(P1) + 0.9*(L)$	14	12
linear one variable	$I_L = -2.8 + 11.6*(P2)$	12	31
	$I_T = -4.0 + 37.3*(P2)$	22	14
curvi-linear	$I_L = 126.0*(P)^4*(L)$	16	22
	$I_T = 626.9*(P)^2*(L)^3 + 0.5*I_L$	14	13

Table 1: Equations calculated from left thigh data (dependent). Right thigh data (independent) used as cross-validation sample.

RESULTS

Table 1 presents the equations for the closest linear fits to the left thigh data (using one variable and several variables) together with the equations for the curvilinear fits. The standard errors of fit are shown for the left thighs, on which the equations are based, and the right thighs, which are used as a cross-validation sample.

For the moment of inertia I_L about the longitudinal axis the curvilinear equation gives the smallest standard error on the cross-validation sample whereas for the transverse inertia axis all three equations give approximately the same error. For the small sample used there are no significant differences ($p>0.10$) in the standard errors of the different fits.

DISCUSSION

The results indicate that the use of linear regression equations in the anthropometric ranges of the sample is not so inappropriate as theoretical considerations suggest. Figure 2 shows the linear and the curvilinear fits to I_L using only the mid-thigh perimeter P_2 as independent variable. It can be seen that the two fits give similar estimates in the sample range but give quite different estimates outside this range. The magnitude of all standard errors of fit are quite large (12%-32%). This is probably a result of poor accuracy of the experimental data used as criteria.

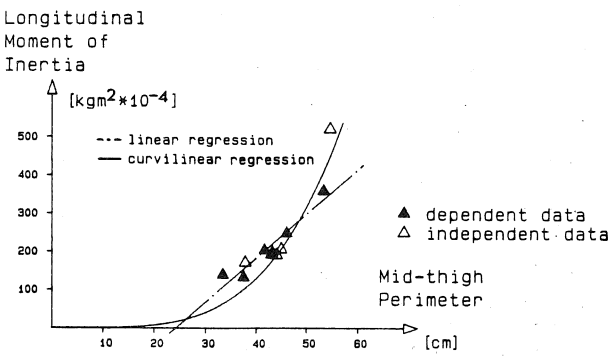

Figure 2: Linear and curved regression lines for longitudinal moment of inertia.

For example, if the mid-thigh perimeter P_2 is less than 23 cm (an appropriate value for a small child), the linear one variable fit would produce a negative value for I_L, whereas the curvilinear fit produces a small positive value. Since moments of inertia ($I = m*d^2$, m = mass, d = radius of gyration) are always positive, the negative value produced by the linear fit is obviously wrong. Thus the small positive value provided by the curvilinear equation is clearly better. For large mid-thigh perimeters outside the sample range(e.g. bodybuilders) it is to be expected that the linear fit will underestimate the moment of inertia.
In general any linear fit to experimental data will exhibit the same kind of behaviour outside the sample range, whereas the curvilinear fits will provide more reasonable values. If data from a larger anthroprometric range were available so that the problem of extrapolation would not arise, the curvilinear fit may be expected to be significantly better than any of the linear fits.

CONCLUSION

In view of the poor levels of accuracy of all the fits even when the cross-validation sample is taken from the same group of cadavers, the use of equations based upon such data is questionable. However, it is recommended that curvilinear fits to such data should be used since there is a theoretical basis for doing so and these equations may be used outside the sample range.

REFERENCES

1.) Clauser, C.E., et al. Weight, volume, and center of mass of segments of the human body. AMRL Technical Report 69-70. 1969.
2.) Hinrichs, R.N. Regression equations to predict segmental moments of inertia. J.Biomech. 18; 621-624. 1985.
3.) Chandler, R.F., et al. Investigation of inertial properties of the human body. AMRL Technical Report 74-137. 1975.

AN EXPLANATION OF THE UPWARD DRIFT IN OXYGEN UPTAKE (UDO) DURING PROLONGED SUBMAXIMAL ECCENTRIC EXERCISE.

Randall W. Dick and Peter R. Cavanagh
Biomechanics Laboratory
The Pennsylvania State University
University Park PA 16802

INTRODUCTION

Upward drift in oxygen uptake (UDO) during prolonged submaximal eccentric activity has received only scant attention in the literature. Klausen et al. first reported the phenomena in 1971 using eccentric bicycling as the exercise (4). The present study was designed to examine the magnitude and mechanism of UDO during downhill running. Oxygen uptake ($\dot{V}O2$), quadriceps muscle EMG, and stride length (SL) were collected from 10 runners during two 40 minute submaximal runs at 3.83 m/s. The first run was performed on a level grade while the second run was performed on a 10% downhill grade. Results of the level run showed non-significant changes in $\dot{V}O2$, IEMG, and SL. Significant ($p < 0.05$) increases in $\dot{V}O2$ and IEMG occurred during the downhill run. No significant changes in downhill SL were observed. Delayed-onset quadriceps muscle soreness, presumably an indication of muscle damage, occurred only following the downhill run. It is hypothesized that the UDO and increasing IEMG during downhill running reflect increased quadriceps motor unit recruitment caused by an ongoing combination of muscle damage, connective tissue damage, and local muscle fatigue.

REVIEW AND THEORY

Submaximal exercise has been characterized by a steady state $\dot{V}O2$. Exercise involving prolonged eccentric muscle action, however, has been shown to exhibit UDO of as much as 25% at a power output that elicited less than 50% of VO2max (4).

Eccentric exercise involves the lengthening of active muscles. A frequently reported sequel to extended submaximal eccentric exercise is delayed onset muscle soreness (DOMS) (1,3). This soreness appears to be related to muscle tissue damage which has been shown to occur during some eccentric exercises (3,7). Increasing muscle activity (IEMG) during an eccentric activity has also been reported (7).

It is evident that tissue damage and DOMS are associated with eccentric muscle action but it is less clear why this metabolically less demanding activity fails to show the distinct steady state $\dot{V}O2$ and IEMG characteristic of submaximal concentric work. This study was conducted to provide insight into the mechanism of UDO and increasing IEMG during an exercise involving eccentric muscle activity.

METHODOLOGY

$\dot{V}O2$, quadriceps muscle EMG, and stride length were collected from 10 experienced male runners (mean VO2max = 65.0 $\pm$ 5.2 ml/kg.min) during two 40 minute submaximal runs at 3.83 m/s. The first run was on a level grade while the second run, completed 1-2 days later, was performed on a 10% downhill grade. Each measure was sampled eight times over the 40 minutes at five minute intervals.

Treadmill speed and stride length were measured using the arrangement described by Kram and Cavanagh (5). Expired air was collected through a Daniels two-way breathing valve connected to a DEEC Metabolic Monitor. Surface EMG was collected from the vastus lateralis and vastus medialis muscles of the left leg using three Beckman silver-silver chloride electrodes. The signal was amplified with a pass band of 10 to 70 Hz and a CMMR of 70 dB. at 60 Hz. A 60 Hz notch filter was also employed. The conditioned signal was monitored on an oscilloscope, sampled at 400 Hz by an analog to digital converter, and stored on a PDP 11/34 minicomputer. Footstrike was monitored by a normally open inertia switch mounted in plexiglass and attached to the heel of the left shoe. The recorded EMG signal was full wave rectified and integrated for each complete running cycle defined by the footswitch pulse (left footstrike to left footstrike).

Perceived muscle soreness was evaluated with a questionnaire similar to that used by Byrnes et al. (1). Written questionnaires were completed 0, 24, 48, and 72 hours following the downhill run.

RESULTS

No significant differences in $\dot{V}O2$, IEMG, and stride length were shown between minute 10 and minute 40 of the level run. Mean $\dot{V}O2$ (43.3 ml/kg.min) during the level run was approximately 66% of the mean VO2max. Mean stride length during the level condition was 2.73 m.

The downhill run elicited significant ($p < 0.05$) changes in $\dot{V}O2$ (10%) and IEMG (23%) over the same exercise interval (Figures 1,2). Mean $\dot{V}O2$ after 10 minutes of downhill running was 44% of the mean VO2max. Mean stride length (2.75 m) did not change significantly over the downhill run.

No subjects reported muscle soreness prior to or following the level run. Peak perceived quadriceps muscle soreness (a mean rating of 7 out of a possible 10) occurred 48 hours following the downhill run.

DISCUSSION

Results from this experiment showed that steady state conditions did not exist for $\dot{V}O2$ and IEMG during a 40 minute downhill run at -10% grade and 3.83 m/s. DOMS, which showed peak intensity at 48 hours post-exercise, also resulted from the downhill run. These findings contrast with the more metabolically demanding level run where steady state $\dot{V}O2$ and IEMG were achieved and no muscle soreness followed the exercise.

UDO and increasing IEMG could be elicited by stride length variation. However, no significant changes in stride length occurred during either the level or downhill conditions. Therefore, the increases in $\dot{V}O2$ and IEMG during the downhill run were not caused by alterations in stride length.

UDO and IEMG changes may also be a response to an unfamiliar motor recruitment pattern associated with downhill running. However, there is limited

evidence which suggests that selected leg muscle motor unit recruitment patterns are similar during level and downhill running at the same speed (7) or intensity (2). In addition, downhill running was not an entirely novel task for the runners in this study. As part of their daily training routine, most of the subjects ran, at least part of the time, downhill. Pilot work conducted in our own laboratory has also shown steady $\dot{V}O2$ and quadriceps IEMG during the novel task of walking backwards at 1.4 m/s (3 MPH) on a level treadmill. These observations would suggest that increases in $\dot{V}O2$ and IEMG during downhill running are not a result of unfamiliar motor unit recruitment patterns.

The muscle soreness reported in this study was similar in time to peak soreness with that reported by other investigators who also showed indications of muscle damage following downhill running (1,8). Although biopsies were not performed in the present experiment, we must assume, because of the muscle soreness, that our subjects experienced muscle damage similar to those reported above.

From the evidence in the literature and the results of the present study, we suggest that a portion of the UDO and increasing IEMG exhibited during a downhill run, as well as the DOMS, may result directly from the ongoing tissue damage caused by eccentric quadriceps muscle action. In the case of damaged muscle fibers, the injured fibers may still utilize energy while producing little or no force. Because the force output falls, additional fibers must be recruited to maintain the net moment required at the knee joint during support. Additional muscle fiber recruitment and the associated increased energy requirements are reflected in the UDO and IEMG increases seen during the downhill run. Damage to the connective tissue, through which muscle fibers transmit their forces to the skeleton, could also cause increasing motor unit recruitment for similar reasons outlined above in the case of muscle damage. It is also likely that a component of the increased $\dot{V}O2$ and IEMG is a reflection of local muscle fatigue.

CONCLUSION

Exercise involving prolonged eccentric muscle action has been shown to exhibit UDO when performed at submaximal intensities. In this study, it does not appear plausible to suggest that changes in stride length or unique motor recruitment patterns are responsible for the non-steady state conditions reported during the downhill run. Instead, a combination of ongoing damage of muscle fibers and/or connective tissue, and local muscular fatigue may cause additional and progressive motor unit recruitment within the eccentrically acting muscles, resulting in upward drifting $\dot{V}O2$ and increasing IEMG. The same mechanism is suggested to occur in other exercises involving eccentric muscle activity.

REFERENCES

1. Byrnes, W., et al. J. Appl. Physiol. 59:710-715, 1985.
2. Costill, D.L., et al. Acta Physiol. Scand. 91:475-481, 1974.
3. Friden, J., et al. Int. J. Sports Med. 4:170-176, 1983.
4. Klausen, K., et al. Acta Physiol. Scand. 83:319-323, 1971.
5. Kram, R., et al. submitted to Med. Sci. Sports Exerc. March 1986.
6. Newham, D.J., et al. Clin. Sci. 64:55-62, 1983.
7. Schwane, J.A., et al. J. Appl. Physiol. 55:969-975, 1983.
8. Schwane, J.A., et al. Med. Sci. Sport 15:124-131, 1983.

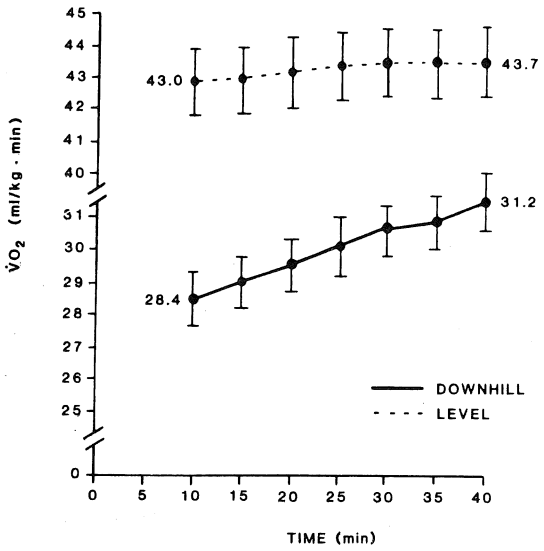

Figure 1

Mean $\dot{V}O2$ in ml/(kg.min) plotted between 10 and 40 minutes for both level (dashed line) and 10% downhill (solid line) runs at 3.83 m/s. Note the gradual and statistically significant 10% increase in $\dot{V}O2$ during the downhill run compared to the non-significant increase in the level run.

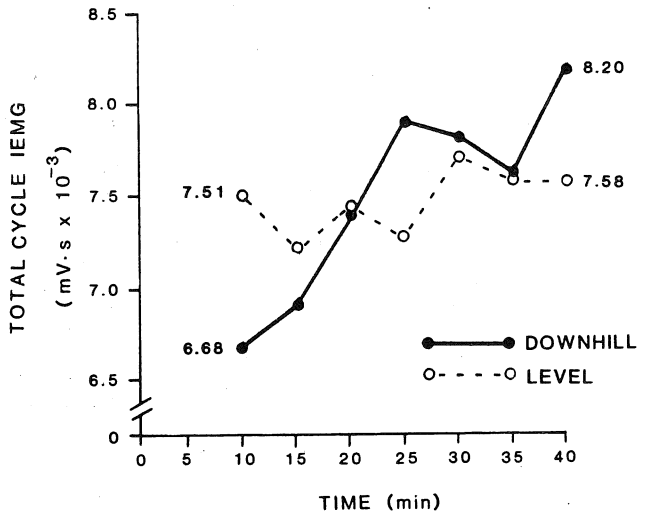

Figure 2

Mean IEMG in mV.s plotted between 10 and 40 minutes for both level (dashed line) and 10% downhill (solid line) runs at 3.83 m/s. The downhill IEMG increased 23% over the exercise interval.

CONTRIBUTIONS OF THE ANKLE AND KNEE MUSCLES TO SPRINT STARTING

D. Gordon E. Robertson
Kinanthropology Department
University of Ottawa
Ottawa, Ontario K1N 6N5

INTRODUCTION

Starting is an important component of the sprint race, especially the 100 m dash, since any errors made will affect a significant proportion of the race. The sprint start has been extensively analyzed (e.g., Dickinson, 1934; Henry, 1952; Baumann, 1976, Gagnon, 1976; Desipres, 1973) yet there is little information available as to which muscle groups contribute to the motion, how much and how does each contribute, and in what order. It was the purpose of this research to investigate these aspects of sprint starting using link segment indirect dynamics.

REVIEW AND THEORY

Link-segment indirect dynamics is a method for computing net forces and moments of force at the joints from body segment parameters and kinematics derived from filmed human motions. It is assumed that the computed moments of force are primarily caused by muscular contractions and, thus, inverse dynamics offers an excellent tool for evaluating muscle functioning. In actuality moments of force represent the summed moments of force of all the structures that act across a joint, whether or not they cross more than one joint.

Unfortunately, solving for actual muscle functions is usually impossible because in human motion analyses most systems of equations are mathematically indeterminant. Thus, the concept of the "single equivalent muscle" is used to simplify the real situation. This concept assumes that there is a pair of "muscles" at each joint--one extensor and one flexor. It is also assumed that pairs of muscles act in reciprocal inhibition, that is, only one of the pair can be active at any given instant.

A single equivalent muscle can be said to contract concentrically when its action (i.e., moment of force) assists the joint's angular motion (i.e., directions are the same). Conversely, the muscle can act eccentrically when its moment resists the joint's motion. These characteristics may be determined by computing the powers produced by the moments of force. These powers are calculated by taking the product of moment of force times joint angular velocity. When the power is positive then the moment is said to be concentric. When the power is negative the moment is an eccentric one. Integration of the power over time yields the work done by the moment or the energy dissipated (Elftman, 1939; Winter, 1979; Robertson and Winter, 1980).

METHODOLOGY

Two subjects who compete nationally in the sprints or sprint hurdles were filmed at 50 fps in a laboratory while starting from a Kistler force platform. Each subject was filmed starting with only one foot on the force plate. Three starts of each foot were filmed with the best trials of each subject being selected for linked-segment analysis.

The subjects ran with their regular running attire and spiked footwear on a material that is used for indoor running tracks. A cutout piece of the material was affixed to the force platform in such a way as to be isolated from the rest of the indoor track. This was necessary to obtain accurate horizontal forces. Previous tests have shown that as much as 50% of the horizontal force can be lost if the indoor track extends in one piece across the force platform.

The subjects used special indoor starting blocks that were separate for each foot. During the filming the athletes were allowed to prepare as is usual in a sprint race. The athletes were instructed to sprint as fast as possible for the first seven metres. As incentive their times over this distance were recorded and reported to them. The athletes, who regularly trained on the same track surface, were allowed sufficient practice trials to accommodate to the laboratory setting.

The film data after processing was projected onto a table equipped with a Numonics digitizer interfaced to a microNova computer. Markers at the approximate joint centres of the shank and foot segments were digitized to an accuracy of 0.3 mm. These data were subsequently transferred along with the synchronized force recordings to a mainframe computer for processing by the computer software, BIOMECH (Kinesiology Dept., Univ. of Waterloo). This package performed the aforementioned inverse dynamics to yield the powers, work , moments of force, and joint angular velocity histories of the ankles and knees.

RESULTS AND DISCUSSION

Angular kinematics. The two athletes exhibited similar kinematic patterns at both joints and for both legs. Both athletes exhibited slowly increasing plantar flexion and knee extension, peaking just prior to toe-off. The peak velocities of these joints occurred almost simultaneously in contrast with the notion that the sequence of joint movements should be knee first then ankle.

These movements were followed immediately by rapidly rising dorsiflexion and knee flexion. The most dramatic pattern being the knee flexion which reached velocities exceeding 15 rad/s.

Ankle kinetics. The two athletes exhibited different patterns at the ankle. One athlete had a single weak plantar flexor concentric contraction which produced only 12 J of work and a peak moment of 70 N.m. The other athlete produced a much larger plantar flexor moment which peaked at 125 N.m. and yielded three work periods. An initial concentric period followed by an eccentric period and then another concentric period. The final concentric period had a peak power output of over 400W compared with a peak of only 200 W by the other athlete.

The front leg of the two athletes begins with a much larger moment of force (100 N.m. vs 0 for the back leg) since this leg is in a better position to carry the body's weight. As with the back leg a plantar flexor moment dominates throughout the thrust period. The peak moment for both athletes was nearly 200 N.m. The functions of this moment were similar for both athletes. Initially, the moment is isometric, that is, its power output is nearly zero yet is moment of force is not zero. After about 0.3 s the moment becomes eccentric allowing the ankle to dorsiflex slightly before plantar flexing. This brief dorsiflexion may act as a counter-movement enabling a more power plantar contraction. The final plantar flexor concentric contractions prior to toe-off reached powers of between 500 and 700 W and produced between 50 and 100 J of work.

After toe-off the work and power output of the ankle muscles drops very low since the muscles are no longer acting to propel the body but are only needed to dorsiflex or plantar flex the foot.

Knee kinetics. The muscles of the back legs of the two athletes had quite different functions. In one athlete the knee extensors predominated acting eccentrically to prevent excessive knee flexion. In the other, the knee extensors acted concentrically causing extension and forward motion of the upper body. Finally, prior to toe-off the knee flexors dominated with an eccentric contraction preventing hyper-extension of the knee similar to the role that they play during the push-off phase of running (Robertson, in press).

The knee muscles of the front leg of both athletes had concentric periods of contraction of the knee extensors prior to toe-off as might be expected. These contractions had peak powers of 400 and 800 W and peak moments of, approximately, 100 N.m. The athlete that had the highest power also had a preceding knee flexor concentric contraction. This contraction caused the knee to flex and perhaps enabled a more forceful knee extensor contraction, however, the additional time required could be disadvantageous.

Additional time spent in the blocks means the athlete will be behind at the start and unless the athlete's velocity is greater he/she will not be able to make up for the loss if other factors are equal. At this stage of the research the author is uncertain as to whether more time spent creating thrust and consequent velocity is more important than getting away earlier. Previous studies compering the "bunch" and "elongated" starts showed that even though the bunch start gets the athlete out of the blocks earlier an elongated start gets the athlete out faster, however, over 5, 10, and 50 yd. the elongated start produced faster times (Henry, 1952).

References

1. Baumann, W. Biomech. V-B, 194-199, 1976.
2. Desipres, M. Biomech III, 364-369, 1973.
3. Dickinson, A.D. Res. Quart. 5(supp): 12-19, 1934.
4. Elftman, H. Amer. J. Physiol. 125: 339-356, 1939.
5. Gagon, M. Biomech, V.-B, 46-50, 1976.
6. Henry, F.M. Res. Quart. 23: 301-318, 1952.
7. Robertson, D.G.E. Biomech. X, in press.
8. Robertson, D.G.E. and Winter, D.A. J. Biomech, 13: 845-854, 1980.
9. Winter, D.A. Biomechanics of Human Motion, Wiley: Toronto, 1979.

Supported by NSERC Grant #A8226

VALIDATION OF PLANAR LINK SEGMENT MODELS FOR THE STUDY OF UPRIGHT BALANCE IN WALKING

Jaynie F. Yang
David A. Winter

Department of Kinesiology
University of Waterloo
Waterloo Ontario

INTRODUCTION

Mechanical models composed of multiple rigid linkages have long been employed to study the biomechanics of human walking. In spite of their popularity, the validity of link segment models, with few exceptions (2,3), has not been challenged. Inherent in these models are many simplifying assumptions, the primary ones being: (a) human body segments can be modeled as rigid segments, (b) the joints can be modeled as pin joints, (c) the geometric and inertial properties of segments can be estimated with reasonable accuracy, and often (d) a planar analysis is adequate. Furthermore, there is no agreement among researchers on the complexity of model necessary to adequately represent human walking; models vary from one segment inverted pendulums to seventeen segment models.

The purpose of this study was to determine the validity of planar link segment models in human walking. Subproblems included the determination of: (A) the influence of kinematic data smoothing, (B) the influence of anthropometric estimates on the model validity, and (C) the complexity of model necessary.

METHODOLOGY

It was assumed that if the model is valid, the sum of the mass acceleration products of the system should equal the total external forces applied. The only substantial external forces acting on the system during walking are the ground reaction forces, which can be measured with force platforms. The mass acceleration products of segments can be estimated with cinematography and anthropometric estimates. The validation was based on the match between the sum of the mass acceleration products and the total ground reaction force in the x (horizontal) and y (vertical) directions. Direct ground reaction forces measured from the force platforms are independent of the model and assumed to be the criteria for validation. The goodness of fit was determined from the root mean square (RMS) difference between the estimates and the R square values over a section of the stride time.

Two healthy subjects participated in the study. They were instrumented with 27 reflective skin markers, to allow a number of model configurations to be studied. The subjects were filmed with a tracking camera as they walked across two force platforms. The camera and force platform systems were synchronized in time, and the force platform data were A/D converted on-line and stored. A number of repeat trials were performed.

The trajectory data from digitized film and the force platform data served as input to the model validation. The iterative validation procedures are shown graphically in Figure 1. Two methods of choosing the filter cutoff were studied: (a) all markers were filtered at the 6th harmonic, (b) markers were filtered at different cutoff frequencies depending on their residual error. Low-pass filtering was performed using a digital Butterworth 2nd order filter, double pass. Two methods to determine anthropometric parameters were studied: (a) the use of fixed fractions based primarily on Dempster (1), and (b) the use of "customized" estimates based on Zatsiorsky's regression equations (4). Four main model types were studied: (a) a fourteen segment model including feet, legs, thighs, forearms, upper arms, head, thorax, mid-trunk and pelvis, (b) a twelve segment model similar to the fourteen segment one but with a single trunk segment, (c) an eight segment model which considered the arms as part of the trunk segment, and (d) a seven segment model which considered the head, arms and trunk as one H.A.T. segment.

RESULTS AND DISCUSSION

The data from one subject on one trial are presented here. The trends were basically the same across trials and subjects. Figures 2 and 3 show the best match in the x and y directions.

The effect of the filter cutoff is shown in Table 1, iterations 1 & 2. The selection of the filter cutoff is critical to the model validity, particularly in the x-direction. The use of a common filter cutoff frequency at the 6th harmonic results in rather poor fits. The best fits were obtained by filtering head, trunk, arms and thigh markers at the 3rd to 4th harmonic, and the leg and feet markers at the 4th to 5th harmonic. The best filter cutoff was not always the same in the x and y directions for a given a marker; generally the y direction required a slightly higher cutoff frequency.

The effect of the different anthropometric estimates is shown in Table 1, iterations 2 & 3. In this trial, the use of Zatsiorsky's regression equations improved the fit by 5% in the x-direction and had no effect in the y-direction. This trend was not consistent across trials and subjects. In some cases,

North American Congress on Biomechanics
Montréal (Québec) Canada, 25-27 August 1986

Zatsiorsky's regression estimates worsened the fit. The change in fit as a result of changes is anthropometric estimates was never greater than 5%. The differences were primarily a result of changes in the mass proportions; changes in the location of the centre of mass had a minor effect on the final outcome.

The model structure is critical to the model validity (Table 1, iterations 4 to 8). Simple trunk models performed as well as the more complicated models, provided that the definition of the trunk segment was appropriate. Any use of hip markers to define the distal trunk resulted in poor matches, suggesting that the trunk segment should be defined by midline markers on the trunk. The arms and head could be lumped with the trunk segment without much loss in validity. This was primarily because the head acceleration was similar to that of the trunk, and the arms were completely out of phase. This may not be the case for movements where the arms are not out of phase. In general, the trunk and thigh segments were critical to the model validity because of their large mass. The markers used to define these segments and their filter cutoffs must be carefully chosen.

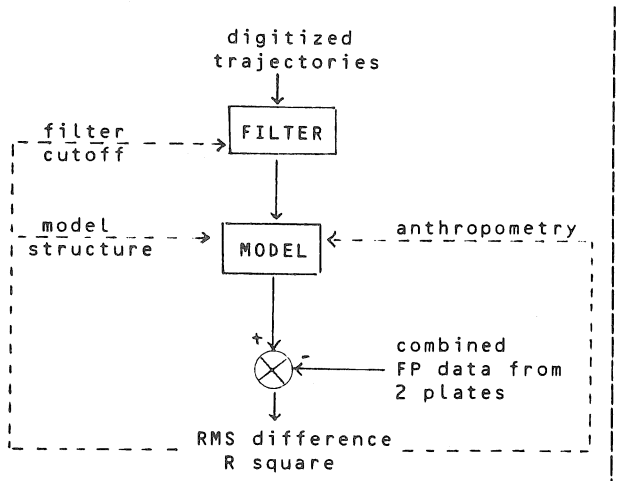

Figure 1: Validation procedures. The dotted lines show the iterative procedures to determine the influence of filter cutoff, model structure and anthropometry on the model validity.

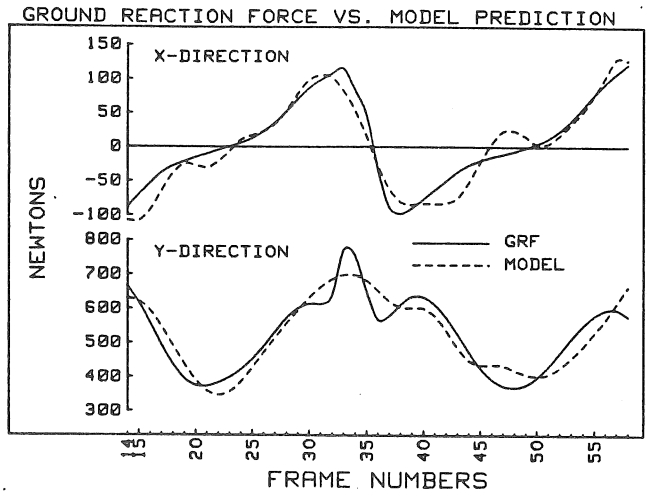

Figure 2: Validation in the x & y directions. Best fit using tailored cutoffs and Zatsiorsky's anthropometric estimates. The validation is from left toe-off (fr.14) to right heel-strike (fr.58).

REFERENCES

1. Dempster, W.T. (1955) Space requirements of the seated operator. USAF, WADC Tech. Rept. 55-159, Wright Air Development Center, Ohio.

2. Pezzack, J.C. and R.W. Norman (1981) Biomechanics VII-A, pp.260-266.

3. Robertson, D.G.E. (1980) Ph.D. Thesis, University of Waterloo.

4. Zatsiorsky, V. and V. Seluyanov (1985) Biomechanics IX,-B, pp.233-239.

Table 1: RMS and R square values showing the results of the iterations.

	x - direction		y - direction	
	Δ RMS (N)	R sq.	Δ RMS (N)	R sq.
1.	46.2	.68	51.4	.81
2.	22.7	.87	44.5	.84
3.	20.1	.91	43.9	.84
4.	19.0	.91	43.8	.84
5.	29.0	.89	46.6	.81
6.	30.2	.87	48.2	.80
7.	19.8	.91	45.2	.84

1. All markers filtered at the 6th harmonic.
2. Tailored filter cutoff for each marker.
3. Zatsiorsky's anthropometric estimates.
4. 12 segment model (trunk: neck to pelvis).
5. 12 segment model (trunk: neck to mid-hip).
6. 12 segment model (trunk: neck to R.hip).
7. 7 segment model (H.A.T. segment used).

Acknowledgements

The authors gratefully acknowledge the financial support of NSERC grant #A2917, MRC grant #MT4343, the fellowship granted to J.F. Yang by the Ontario Ministry of Health, and the technical assistance of Paul Guy.

EMG PATTERNS OF THE QUADRICEPS DURING TREADMILL RUNNING: A DESCRIPTION OF PATELLOFEMORAL PAIN SYNDROME

D. MacIntyre
School of Rehabilitation Medicine
University of British Columbia
Vancouver, B.C. V6T 1W5

D.G.E. Robertson
Human Kinetics
University of Ottawa
Ottawa, Ontario K1N 6N5

INTRODUCTION

Our society's increased attention to physical fitness, which for many people includes running, has resulted in an associated increase in overuse injuries. Clement et al. (1) reported in 1981 that the most common site of injury for the runner is the knee, with patellofemoral pain syndrome the most common clinical finding. The role of the muscles of the knee, in particular the quadriceps, have been studied electromyographically in many ways but most relevant to this study are those that have analyzed the EMG activity of the quadriceps during running (2,3). It was our purpose to establish a baseline of normal quadriceps activity in female runners and then to determine if there was a difference in the EMG patterns of the quadriceps in runners with patellofemoral pain syndrome (PFPS).

REVIEW AND THEORY

Patellofemoral pain syndrome is described as a diffuse, poorly located pain around the patella which arises from abnormal tracking of the patella (4). Compression of the patella against the femoral condyles may elicit pain. Measurement of the Q-angle, which is the angle between the line of pull of the quadriceps and the patellar tendon, is often above 15^{0} (5). By itself, the Q-angle is not diagnostic of PFPS, but it is often associated with other deficiencies of the extensor mechanism (i.e., quadriceps weakness). Structural abnormalities of the lower extremity, such as overpronation of the foot, increased rearfoot and forefoot motion, leg length discrepancy, and increased genu valgum or varum, or the presence of genu recurvatum, must also be assessed for their influence on patellar tracking.

Muscle activity may be monitored by the use of electromyography (EMG). Once the EMG signal has been collected from an active muscle, and amplified, it must be processed in a way that it can be compared to other signals. Linear envelope EMG is one method of processing that follows the trend of the EMG and bears some relationship to the biomechanics of movement (6). To improve the reliability of the EMG in gait analysis, each stride is normalized to 100%, and the linear envelope is averaged from a number of strides to obtain a grand ensemble average for each muscle (7,8).

METHODOLOGY

Twenty female recreational runners, aged 15-36 years, were assessed for their lower extremity alignment. The control group consisted of 12 subjects who had normal alignment, which was considered to be Q-angle 15^{0} or less, rearfoot and forefoot varus alignment four degrees or less, no overpronation, leg length discrepancy less than one centimeter and no genu recurvatum. They had no complaints of knee pain and ran at least 16 km/week (ten miles per week).

The experimental group consisted of eight subjects who had also been running prior to developing knee pain. They were diagnosed as having PFPS by the physicians at the UBC Sports Medicine Clinic. Their lower extremity alignment measures were Q-angle 15^{0} or more, rearfoot and forefoot varus greater than four degrees, and overpronation when weight-bearing. They were also assessed for leg length and genu valgum, varum and recurvatum.

Muscle strength for quadriceps and hamstrings for both groups was tested on an isokinetic dynamometer at 200^{0}/second.

The subjects ran on a treadmill at a speed of 12 km/h (7.5 mph) until ten strides were collected by the computer. Linear envelope EMG signals from the right vastus medialis, vastus lateralis and rectus femoris, together with a footswitch signal, were digitally recorded at a sampling rate of 100 Hz each. Surface electrodes were placed over the motor points of each muscle with an inter-electrode spacing of one centimeter.

Each stride period was normalized to 100%, and then ensemble averaged over the ten strides for each muscle and for each subject. Standard deviations for each interval were also calculated. Subsequently grand ensemble averages for each muscle for all of the subjects in each group were computed.

RESULTS

Figure 1 shows the grand ensemble average from each muscle of the experimental group superimposed on the grand ensemble averages of the control group.

Comparisons of the muscle patterns of each subject in the experimental group were also made to the grand ensemble averages of the quadriceps from the control group. Figure 2 is an example of the quadriceps activity of a subject with PFPS.

DISCUSSION

A comparison of the mean EMG activity of the quadriceps from runners with PFPS, to the mean quadriceps activity of runners free of knee pain and with normal lower extremity alignment (figure 1), showed no statistical difference.

This comparison does reveal, however, that the largest amount of quadriceps activity takes place immediately after foot-strike. Vastus medialis and vastus lateralis have similar curves, differing only in their amplitude. This occurrence of peak muscle activity after heel-strike, to foot-flat, agrees with Elliott and Blanksby (2), and also confirms the suggestion that the knee extensors are working as shock absorbers by working eccentrically to control knee flexion.

During swing phase, there is essentially no other vasti activity, until the end of swing when the knee is preparing for heel-strike.

Rectus femoris also shows activity after heel-strike, verifying that it works with the vasti as a shock absorber, but to a lesser extent. This muscle has a second burst of activity in early swing phase which may be indicative of the fact that rectus femoris is a two-joint muscle, and at this point in the gait cycle it is working as a hip flexor (2).

Individual analysis of the quadriceps activity from a single subject with PFPS, compared to the control group (figure 2), showed that the amplitude of vastus medialis was less than one standard deviation after heel-contact to foot-flat. The amplitude of rectus femoris during stance and swing was also less than one standard deviation. This subject's muscle test revealed values within ± one standard deviation of the control group mean for concentric quadriceps, and eccentric and concentric hamstrings, but her peak torque for eccentric quadriceps was 84 N.m compared to the control group mean of 170 N.m (±50.33). It may be that the decreased EMG amplitude in vastus medialis and rectus femoris during stance, when one is expecting the quadriceps to be working eccentrically as a shock absorber, is reflected in the low peak torque value for eccentric quadriceps during the muscle test.

CONCLUSION

Our results have described the EMG activity of the quadriceps during one stride of running. A comparison of the mean ensemble averages of the quadriceps between a group of runners with patellofemoral pain syndrome and another group of runners free of knee pain showed no statistical differences. However, when single subjects with PFPS were compared to the control group, there were periods in the gait cycle when the amplitude of their muscle activity was outside of ± one standard deviation of the control group's mean. Whether this level of divergence from normal activity is diagnostically significant is not yet known.

REFERENCES

1. Clement, D.G., et al. Phs. and Sports Med. 9:47-58, 1981
2. Elliott, B.C., et al. Med. Sci. Sport. 11:322-327, 1979.
3. Schwab, G.H., et al. Clin. Orthop. 176:166-170, 1983.
4. Grana, W.A., et al. Clin. Orthop. 186:122-128, 1984.
5. Schamberger, W. Can. Fam. Phys. 29:1670-80, 1983.
6. Winter, D.A. Biomechanics of Human Movement, 1979.
7. MacIntyre, D., et al. Biomechanics $\overline{X}$ in press.
8. Winter, D.A. Arch. Phys. Med. Rehab. 65:393-398, 1984

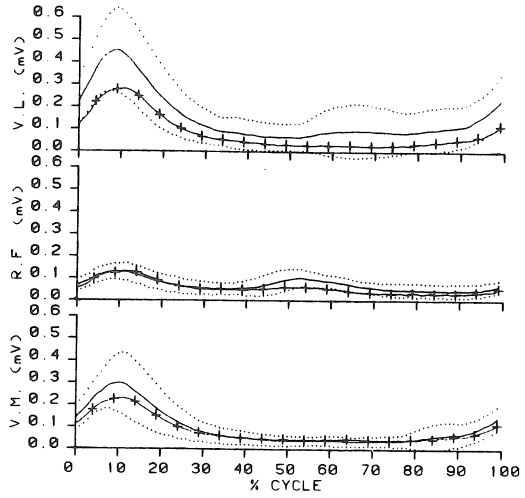

Figure 1. Grand ensemble average of the experimental group (crossed line) superimposed on the grand ensemble average of the control group (solid line). The dotted line represents ±1 standard deviation of the control group's mean. The three muscles are vastus medialis (V.M.), rectus femoris (R.F.) and vastus lateralis (V.L.). The linear envelope amplitude is measured in millivolts (mV).

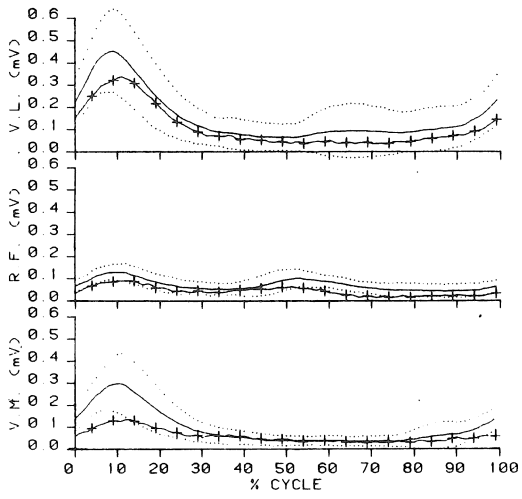

Figure 2. The grand ensemble average of vastus medialis (V.M.), rectus femoris (R.F.) and vastus lateralis (V.L.) for subject HB (crossed line) compared to the grand ensemble average of the control group (solid line), ±1 standard deviation (dotted line). The amplitude is measured in millivolts (mV).

INTEGRATED BIOMECHANICAL & EMG ANALYSIS OF STAIR WALKING

Bradford McFadyen
David Winter
Department of Kinesiology
University of Waterloo
Waterloo, Ontario
N2L 3G1

INTRODUCTION

Stairs are frequently encountered during normal daily activities, but there has been little biomechanical analysis of this type of gait. This paper integrates EMG, kinematic and kinetic analysis to investigate normal stair walking. It is shown that the knee extensor muscles play a major role in both ascent and descent and that the stance and swing phases of the stair gait stride can be further broken down into subphases of progression. As well, the support moments for both modes of stair walking are quite similar to level walking.

REVIEW AND THEORY

There have been a number of EMG related papers on stair walking (1,3,4,6) which have mostly looked at on/off muscular activity. Some of these (1) have also considered the kinematics involved. However, only a few kinetic analyses (1,2,5) exist; the best report is by Cappozzo and Leo (1974) who looked at ascent, but had limited their power analysis to single maximum or minimum values. Yet, the need for an integrated analysis for both ascent and descent still exists.

METHODOLOGY

A five step staircase (21 x 28 cm) was built with a force plate inserted as the second step. Cameras (16mm; 50 f/s) were placed at the side and front of the stairs and simultaneous EMG recordings were made of the rectus femoris, vastus lateralis, semitendinosus, medial gastrocnemius, soleus, tibialis anterior, glutius maximus and gluteus medius. Only sagittal plane motion was analysed.

Three normal male subjects of similar height and weight performed eight trials each of ascent and descent at a fixed cadence matched to their normal ascent gait. Two of the subjects had previous files for level gait in the laboratory data base. Only one stride per trial was collected and the data were synchronized, interpolated to fifty points and appropriate kinematics and moments of force and mechanical power were calculated. Single values of coefficient of variation (CV) were calculated (8) to document the trial-to-trial variability.

RESULTS

Because of the vast amount of data, only one subject will be presented and not all results will be shown. Even though minor differences occured between subjects, the data described here is representative of all three subjects. Figure 1 presents the EMG for ascent. Figures 2 and 4 present the joint and support moments for ascent and descent respectively. Figure 3 and 5 present the muscle powers for ascent and descent respectively. New findings from the present study are discussed below.

DISCUSSION

Each stride was divided according to specific objectives for progression from one step to the next. Ascent involved weight acceptance (WA), pull-up (PU), forward continuance (FCN), foot clearance (FCL) and foot placement (FP). As shown in Figure 3 (K1), and from Figure 2, the knee extensors generated the majority of the energy required during ascent in the pull-up phase. The latter part of the ascent stance phase involved mostly forward translation with slight lift just prior to toe off. The triphasic swing pattern seen in Figure 1 between the RF and ST and represented in Figure 3 by the power bursts K3 and K4 were evident in all trials during ascent without exception. This activity was important to both foot clearance and positioning of the foot for foot contact.

The descent stride was divided according to weight acceptance (WA), forward continuance (FCN), controlled lowering (CL), leg pull-through (LP) and foot placement (FP). The initial acceptance of body weight at the beginning of the descent stride was characterized by the absorption of energy at the ankle. This absorption served to cushion the impact and was assisted soon after by a state of absorption at the knee. The next period in stance to approximately 68% of stride as shown (32% of stance) resulted in a continuation of forward motion with little vertical displacement. The major contribution to descent progression took place during latter stance and was characterized by a predominence of negative power at the knee (K5) as shown in Figure 5. This involved eccentric contractions by the knee extensors (Figure 4). This latter stance phase has been called the controlled lowering phase. The hip played much less of a role in descent as in ascent.

The support moments of Figures 2 and 4 are of similar two peaked pattern. These patterns are also seen in the stance phase during level walking (8). This shape similarity infers a common system output for biped locomotion. Naturally, the support moments for both modes of stair walking were higher on average; the greater need for anti-gravity activity would necessitate such a result.

References

1. Andriacchi, T. et al. J. Bone and Joint Surgery, 62A:749-757, 1980.
2. Cappozzo, A. and Leo, T. First CISM-IFToMM Symposium on Theory and Practice of Robots and Manipulators, 1:115-132, 1974.
3. Joseph, J and Watson, R. J. Bone and Joint Surgery, 49B:774-780, 1967.
4. Mann, R. and Inman, V. J. Bone and Joint Surgery, 46A:469-481, 1964.
5. Morrison, J. Bio-Med. Eng., 4:573-580, 1969.
6. Shinno, N. Medicine and Sport, 6:202-207, 1971.
7. Townsend, M. et al. J. Biomech. 9:227-239, 1976.
8. Winter, D. Human Movement Science, 3:51-76, 1984.

ACKNOWLEDGEMENTS: We acknowledge the support of the Medical Research Council (MT 4343) and partial support through a National Health Fellowship to B.J. McFadyen.

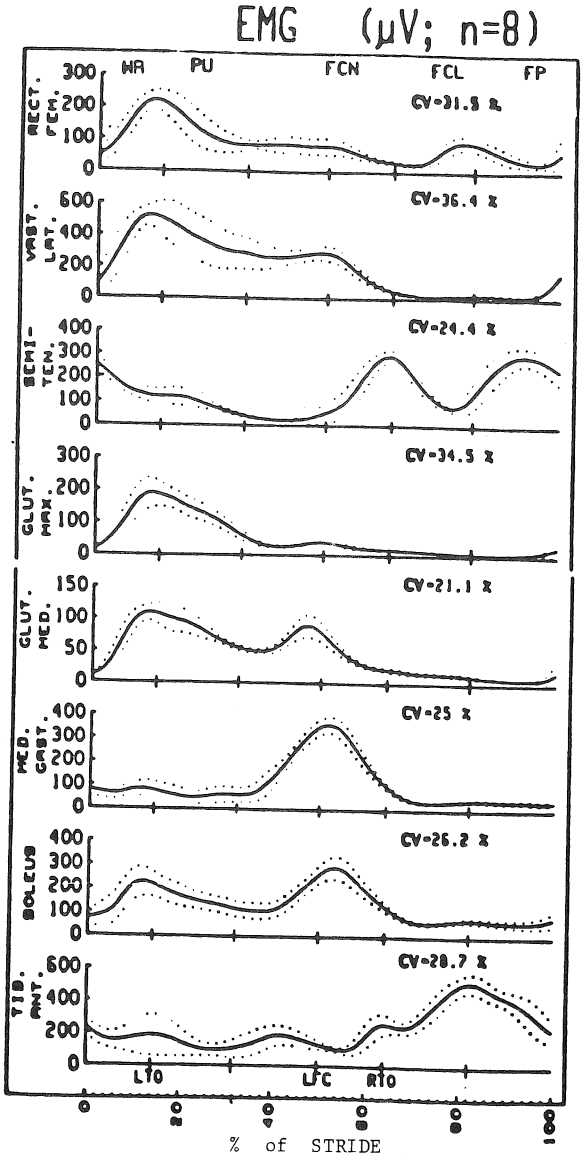

Figure 1: Ascent EMG

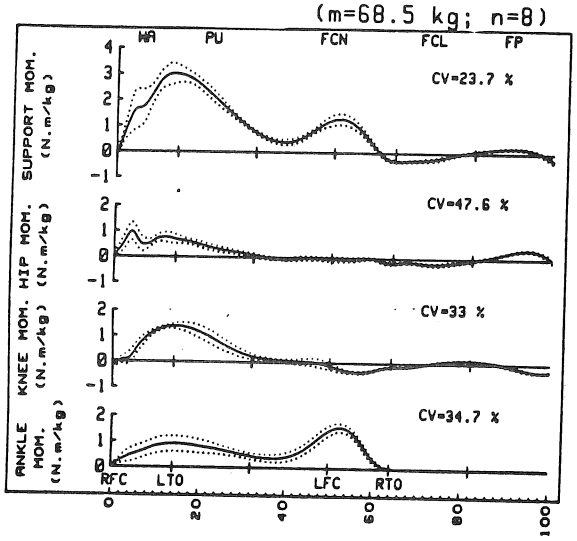

Figure 2: Ascent Joint Moments

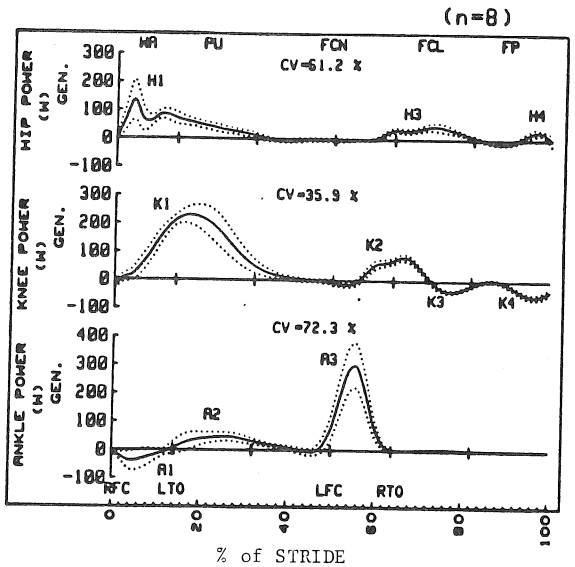

Figure 3 : Ascent Muscle Powers

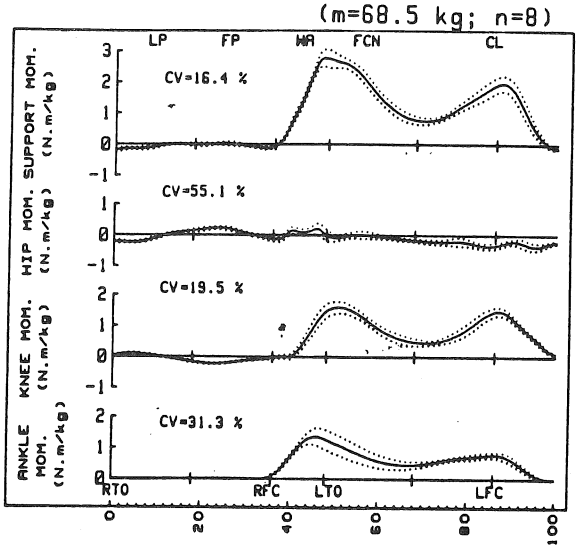

Figure 4 : Descent Joint Moments

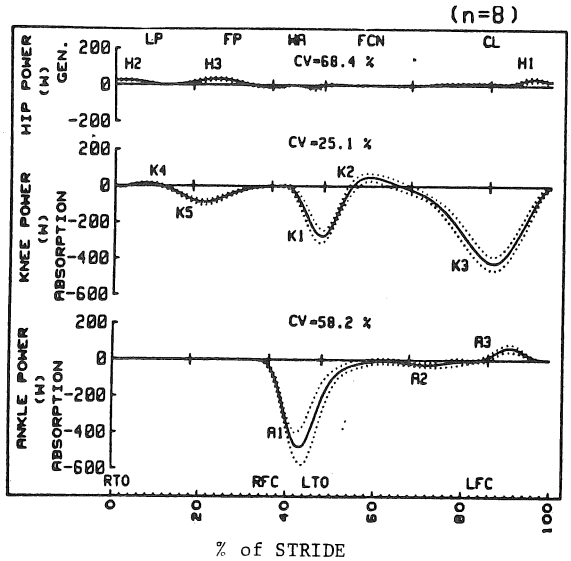

Figure 5 : Descent Muscle Powers

THE USE OF MULTIPLE REGRESSION IN THE DESIGN AND TESTING OF DYNAMIC MUSCLE MODELS

J. J. Dowling and R. W. Norman

Department of Kinesiology
University of Waterloo
Waterloo, Ontario, Canada

Introduction

Several researchers have attempted to extend linked segment models, which predict net joint moments, to predict the individual muscle moments of which the net moments are comprised. A common strategy has been to combine the neural excitation of individual muscles (as reflected by EMG) with anatomical parameters (i.e. cross-sectional area, moment arm length) and mechanical parameters (i.e. muscle length, velocity and passive elements) in order to predict the individual muscle moments acting at a joint (Hatze, 1976; Hof and Van Den Berg, 1981). The algebraic summation of these moments (if modelled correctly) should equal the net joint moment. Numerous models have been constructed that contain different components, different processes and different interactions. They all have weaknesses whose significance and cause is usually left to a qualitative discussion. To our knowledge there has been no method proposed which allows quantitative systematic study of the effects of interacting model features on its output. A consistent strategy of model construction and testing is needed that clearly defines the weaknesses in each model.

Method

A typical muscle model scheme is shown in Figure 1 in which the neural, mechanical, and anatomcal parameters are combined to predict individual muscle moments which, when summed over n muscles with the passive elements, yield the predicted net joint moment. Figure 2 compares the measured joint moment with the predicted moment for a dynamic elbow extension/flexion task. Improvement of the prediction in Figure 2 can be achieved by changing the nature of one or more of the model components or their interactions. It is not clear which component should be changed first or in what way it should be changed. Overall model improvement does not tell the researcher much about what is happening in the intact system if the improvement is gained at the expense of one or more contractile conditions. For example, little is learned about the force-velocity relationship of in vivo muscle if changes are made that improve the overall fit by improving the fit at low velocity at the expense of the fit at high velocity. Several different movement tasks should be performed that encompass the full range of contractile conditions possible for a given joint.

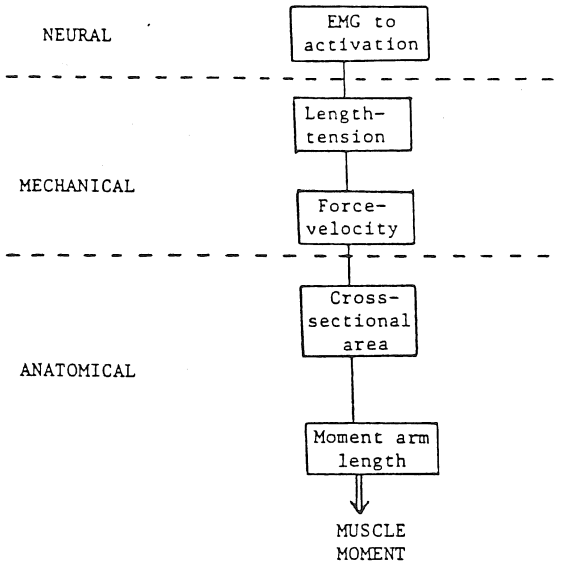

$$\text{Predicted Moment} = \text{Passive Moment} + \sum_{i=1}^{n} \text{Muscle Moment}$$

Figure 1. Scheme of a typical neuro-musculoskeletal model and predicted moment calculation.

Multiple linear regression is a good method to use when comparing the output of a model constructed of several variables with a reference output. The R-square statistic informs the researcher of the percent variance in the reference output that can be accounted for by one or any combination of the variables included in the muscle model. The dependent variable will be the time series of the measured moment values for all of the experimental trials. Different statistical models can then be created using the different muscles and components as independent variables. It is also possible to identify variables that are more likely to be causing errors than others by creating a second dependent variable comprising the errors between the predicted and the measured net joint moment.

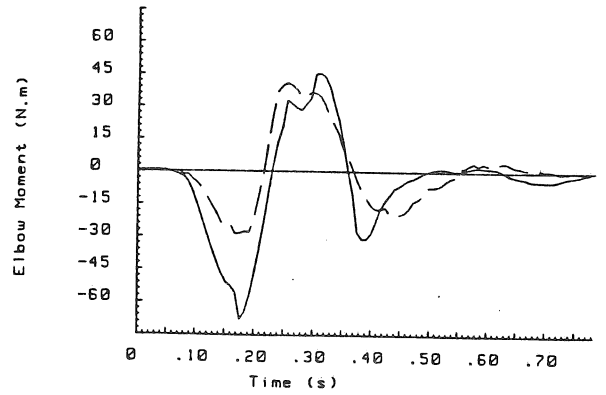

Figure 2. Predicted (——) and measured (- - -) elbow moments during a rapid extension/ flexion movement.

Results

Table 1 shows the effectiveness of 6 statistical models in explaining the variance of measured elbow net joint moments over a series of wide ranging elbow motions. The muscle model contained four major parameters (activation, force-velocity, length-tension, and moment arm) of three muscles (Biceps, Brachioradialis, and Triceps). The full model explains 61% of the variance in the measured moment. By dropping the effect of changing moment arm, the muscle model explains over 75% of the variance. The further dropping of components makes the fit worse. This indicates that the component most responsible for the errors is that of the moment arm calculation.

Table 1. Comparison of six statistical models with measured moment as the dependent variable.

1) Model	R-square = .61
2) Model minus MA	R-square = .754
3) Model minus MA & L-T	R-square = .749
4) Model minus MA & F-V	R-square = .743
5) Model minus F-V & L-T	R-square = .548
6) Model minus MA & F-V & L-T	R-square = .738

By creating new statistical models containing the moment arms of each individual muscle, or by comparing these independent variables with a dependent variable consisting of the error values, the exact source of the poor moment arm values can be located. Depending on the complexity of the model components and their interactions, scores of statistical models may have to be investigated. Once a change has been made, however, the effect of the change and its interaction with the other model components can be monitored.

Discussion

With this method, weak variables or interactions of variables can be identified and individual processes and functions can be evaluated. Model changes can be performed and assessed without the need to recollect raw data. Model building and/or modification in this way is really little more than curve fitting with the sole justification that it predicts better. The model must therefore be tested under a wide range of contractile conditions and parameter changes must be literature supported or at least not in direct violation of reported empirical evidence. Any change must improve the prediction in every contractile condition or at least not weaken the fit of one contraction type in order to improve the overall fit.

References

1) Hatze, H. Math. Biosci. 28:99-135, 1976.

2) Hof, A.L. et al. J. Biomech. 14:747-787, 1981.

A DIMENSIONLESS MUSCULOTENDON ACTUATOR MODEL FOR USE IN COMPUTER SIMULATIONS OF BODY COORDINATION: STATIC PROPERTIES

F.E. Zajac, P.J. Stevenson, E.L. Topp

Design Division, Mechanical Engineering Department, Stanford University, Stanford, CA 94305
and Rehabilitation R & D Center, Palo Alto Veterans Administration Medical Center

INTRODUCTION

Computer simulations of the neuromusculoskeletal system can complement experimental studies of human movement and coordination. Ideally, computer models should include the properties of each of the muscles and tendons deemed important to the motor task under study. We present a dimensionless, 1st-order model of musculotendon contraction dynamics that captures the fundamental properties of muscle and tendon. Three actuator-specific parameters (muscle strength, optimal muscle fiber length, and tendon slack length) are used to scale the generic representation to a specific actuator. We show that the ratio of tendon slack length to muscle fiber length $\tilde{l}_r^T$ distorts muscle's force-length (f-l) curve so that the musculotendon f-l curve has a wider ascending and a narrower descending region. Muscle strength only affects the amplitude of the curve.

REVIEW AND THEORY

For the model of muscle and tendon used (Fig. 1), we assume that active muscle can be represented by a contractile element CE, described by an activation a(t) and length l^M dependent velocity-force (v-f) relationship [1], and a series elastic element SE to account for muscle's short-range stiffness [2].

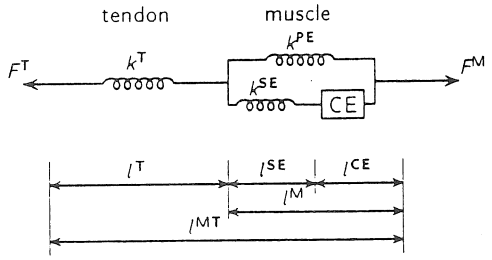

Figure 1.

The normalization parameters used in the dimensionless model are:

$$
\begin{aligned}
F_o^{CE} &= \textit{maximum isometric active muscle force} \\
l_o^M &= \textit{length of muscle at which } F_o^{CE} \textit{ is developed} \\
\tilde{v}_m^{CE} &= \textit{normalized maximum shortening velocity of the contractile element } (10 \cdot s^{-1})
\end{aligned} \tag{1}
$$

Definitions needed are:

$$
\begin{aligned}
F^i &= \textit{force in ith element} \\
\tilde{F}^i &= F^i / F_o^{CE} = \textit{normalized force in ith element} \\
l^i &= \textit{length of ith element} \\
\tilde{l}^i &= l^i / l_o^M = \textit{normalized ith element length} \\
v^i &= \frac{dl^i}{dt} = \textit{velocity of ith element} \\
\tilde{v}^i &= \frac{d\tilde{l}^i}{dt} = \textit{normalized ith element velocity} \\
\tau &= \tilde{v}_m^{CE}\ t = \textit{dimensionless time} \\
\tilde{v}_\tau^i &= \frac{d\tilde{l}^i}{d\tau} = \textit{dimensionless ith element velocity} \\
k^i &= \frac{dF^i}{dl^i} = \textit{stiffness of ith element } (i = T, PE, SE) \\
\tilde{k}^i &= \frac{d\tilde{F}^i}{d\tilde{l}^i} = \textit{normalized ith element stiffness } (i = T, PE, SE) \\
\tilde{k}^M &= \tilde{k}^{PE} + \tilde{k}^{SE} = \textit{muscle stiffness} \\
\tilde{k}^{MT} &= (\tilde{k}^T \ \tilde{k}^M) / (\tilde{k}^T + \tilde{k}^M) = \textit{musculotendon stiffness} \\
l_r^T &= \textit{tendon slack length} \\
\tilde{l}_r^T &= l_r^T / l_o^M = \textit{normalized tendon slack length} \\
\epsilon^T &= (l^T - l_r^T) / l_r^T = (\tilde{l}^T - \tilde{l}_r^T) / \tilde{l}_r^T = \textit{tendon strain.} \\
&\textit{where } i = T, M, PE, SE, \textit{or } CE, \textit{except as noted.}
\end{aligned} \tag{2}
$$

We assume that normalized passive muscle force $\tilde{F}^{PE}(\tilde{l}^M)$ depends on muscle length $\tilde{l}^M$ (Fig. 2;[3]), that tendon's normalized force (or stress)-strain curve ($\tilde{F}^T$ vs. ϵ^T) is given by Fig.3 [4], and that the CE, in steady-state, develops isometric force $\tilde{F}_{iso}^{CE}$ according to

$$
\tilde{F}_{iso}^{CE}(\tilde{l}^M, a(t)) = F_o^{CE}(\tilde{l}^M)\ a(t), \tag{3}
$$

$$
\begin{aligned}
&\textit{where } \tilde{F}_{iso}^{CE} = \textit{normalized isometric force of active muscle at length } \tilde{l}^M \textit{ and activation } a(t) \\
&\tilde{F}_o^{CE}(\tilde{l}^M) = \textit{normalized isometric force of fully activated muscle (Fig. 2)} \\
&a(t) = \textit{normalized muscle activation } (0 < a(t) \leq 1)
\end{aligned}
$$

are actuator non-specific. Defining the v-f curve of the CE by a modified version of Hill's equation [5]

$$
\tilde{v}_\tau^{CE} = f_1(\tilde{F}^{CE} / \tilde{F}_{iso}^{CE}) \tag{4}
$$

then the dimensionless musculotendon contraction dynamics only depends on $\tilde{l}_r^T$ and can be written either as

$$
\begin{aligned}
\frac{d\tilde{F}^T}{d\tau} &= \left(\frac{\tilde{k}^T \ \tilde{k}^M}{\tilde{k}^T - \tilde{k}^M}\right) \left[\tilde{v}_\tau^{MT} - \left(\frac{\tilde{k}^{SE}}{\tilde{k}^M}\right) \tilde{v}_\tau^{CE}\right] \\
&= \tilde{k}^{MT} \cdot \left[\tilde{v}_\tau^{MT} - \left(\frac{\tilde{k}^{SE}}{\tilde{k}^M}\right) \tilde{v}_\tau^{CE}\right]
\end{aligned} \tag{5}
$$

or as

$$
\frac{d\tilde{F}^T}{d\tau} = f_2(\tilde{F}^T, \tilde{l}^{MT}, \tilde{v}_\tau^{MT}, a(t)). \tag{6}
$$

By coupling contraction dynamics (eq. 6) with activation dynamics, given by

$$
\frac{da(\tau)}{d\tau} = f_3(a(\tau), u(\tau)) \tag{7}
$$

where $u(\tau)$ = neural control to muscle ($0 \leq u(\tau) \leq 1$) we have the overall dimensionless dynamics of the musculotendon actuator that is used in our computer models of body coordination. The dynamics of a specific actuator is found by applying four scaling parameters to eqs. 6 and 7 three of which are specific (F_o^{CE}, l_o^M, l_r^T) and one $\tilde{v}_m^{CE}$ non-specific to the actuator being modeled.

METHODOLOGY

Recognizing that

$$\tilde{l}^{MT} = \tilde{l}^{M} + \tilde{l}^{T} \qquad \text{and } \tilde{F}^{T}(\epsilon^{T}) = \tilde{F}^{T}(\tilde{l}^{T} - \tilde{l}_r^{T}, \tilde{l}_r^{T})$$
$$\tilde{F}^{T} = \tilde{F}^{M} \qquad (8)$$

it can be shown that

$$\tilde{F}^{T}(\tilde{l}^{MT} - \tilde{l}_r^{T} - \tilde{l}^{M}, \tilde{l}_r^{T}) = \tilde{F}_o^{CE}(\tilde{l}^{M}) + \tilde{F}^{PE}(\tilde{l}^{M}) \qquad (9)$$

for an isometric musculotendon actuator when $a(t) = 1$. For a given $\tilde{l}_r^{T}$, we solved computationally eq. 9 by varying iteratively $\tilde{l}^{M}$ for each value of $\tilde{l}^{MT} - \tilde{l}_r^{T}$ until equality was found; *i.e.*, until an equal force occurred in tendon and muscle at a specific $\tilde{l}^{MT}$.

RESULTS AND DISCUSSION

For muscle that develops no passive force, and for muscle that does, the musculotendon isometric f-l curves for actuators having tendon with either no compliance ($\tilde{l}_r^{T} = 0$) or much compliance ($\tilde{l}_r^{T} = 16$) are shown in Figs. 4 & 5. Notice that actuators with long normalized tendon slack lengths $\tilde{l}_r^{T}$ distort muscle's f-l curve. This distortion broadens the musculotendon range of motion associated with forces ascending on the active muscle f-l curve, by an amount β (Fig. 4). Notice that this range approaches the full active muscle force range (1.2 l_o^{M} in our model) as $\tilde{l}_r^{T} \rightarrow 16$. Fig. 5 shows that compliant actuators with muscles developing passive force have a wide length range of actuator force generation. Based on reported values of l_o^{M} of human lower extremity muscles [6] our studies of lower limb musculoskeletal geometry [7] suggest that $0.02 \leq \tilde{l}_r^{T} \leq 11$.

CONCLUSION

Compliance of tendon relative to muscle varies much from one musculotendon actuator to another. Tendon of some dramatically affects musculotendon mechanics.

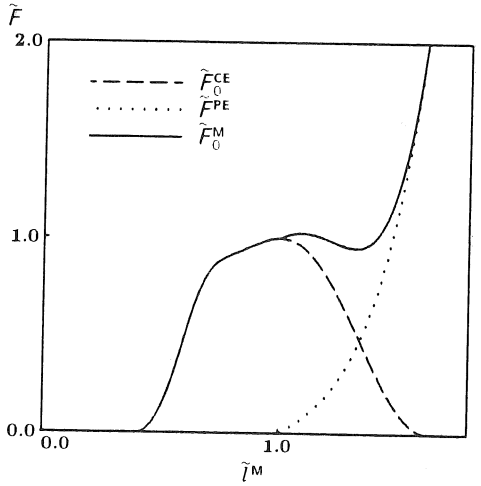

Figure 2. Normalized force-length curve of passive muscle $\tilde{F}^{PE}(\tilde{l}^{M})$, fully activated muscle without any passive force $\tilde{F}_o^{CE}(\tilde{l}^{M})$ and active muscle with passive force $\tilde{F}_o^{M}(\tilde{l}^{M}) = \tilde{F}_o^{CE}(\tilde{l}^{M}) + \tilde{F}^{PE}(\tilde{l}^{M})$.

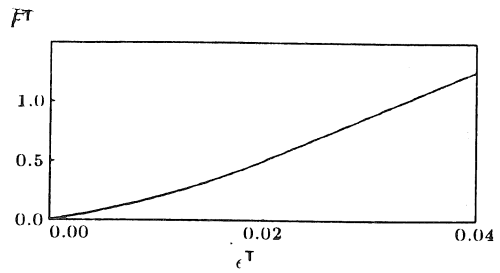

Figure 3. Normalized force-strain curve $\tilde{F}^{T} - \epsilon^{T}$ of tendon. When $\tilde{F}^{T} = 1$, tendon force $F^{T} = F_o^{CE}$.

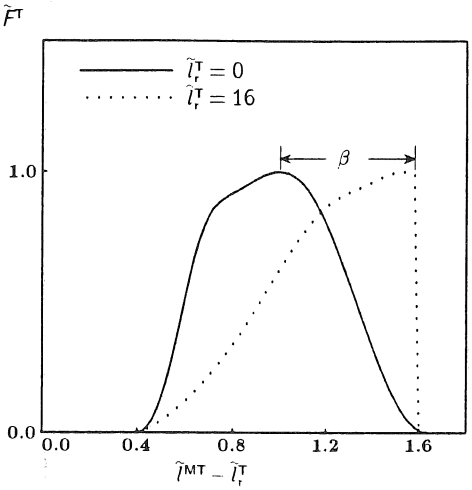

Figure 4. Normalized force-length curves of two musculotendon actuators. Both actuators have muscles that develop no passive force, but one has a compliant tendon ($\tilde{l}_r^{T} = 16$) and the other a stiff tendon ($\tilde{l}_r^{T} = 0$). $\beta \equiv \tilde{l}^{T} - \tilde{l}_r^{T}$ when $\tilde{F}^{T} = 1$.

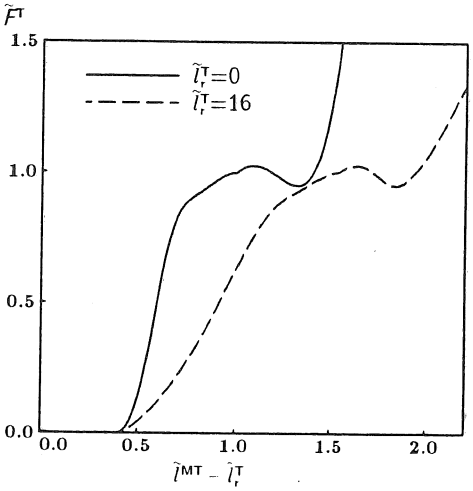

Figure 5. Normalized force-length curves of two musculotendon actuators. This is same as Figure 4 except muscles develop passive force.

References

1. Abbott, B.C., *et al.* J. Physiol. Lond. 120: 214-223, 1953.
2. Huxley, A.F., *et al.* Nature 233: 533-538, 1971.
3. Stephenson, D.G., *et al.* J. Physiol. Lond. 333: 637-653, 1982.
4. Woo, S.L-Y., *et al.* Biorheol. 19: 397-408, 1982.
5. Audu, M.L., *et al.* ASME J. Biomech. Eng. 107: 147-157, 1985.
6. Wickiewicz, T.L., *et al.* Clin. Orthop. Rel. Res. 179: 275-283, 1983.
7. Gordon, M.E., *et al.* Proc. 9th Ann. Conf. Rehabil. Eng. Soc. (in press), 1986.

This work was supported by NIH grant NS 17662 and the Veterans Administration.

MUSCULOTENDON ENERGETICS OF HUMAN JUMPS

M.G. Hoy, F.E. Zajac, E.L. Topp, C.T. Cady, M.E. Gordon and W.S. Levine*

Rehabilitation R & D Center, Veterans Administration Medical Center, Palo Alto, CA 94304 and
Design Division, Mechanical Engineering Department, Stanford University, Stanford, CA 94305
*Electrical Engineering Department, University of Maryland, College Park, MD 20742

INTRODUCTION

Utilization of stored elastic energy has been described as an important determinant of vertical jump height in humans (1,3,5). Although performance has been observed to improve when propulsion is preceded by a downward movement, little is known about the mechanism for enhanced performance. For example, it is not understood how musculotendon dynamics interact with skeletal dynamics during the jump, what the individual capacity of different musculoskeletal actuators is to generate work and store elastic energy, or whether elastic energy is stored in muscle or in tendon. To explore these issues, we developed a computer model of the human neuromusculoskeletal system which incorporates all of the fundamental dynamic properties of muscle and tendon. The musculoskeletal geometry and muscle specific parameters were defined for seventeen lower extremity muscles. Using the model to simulate counter movement jumps, we show that musculotendon energetics depend on the unique properties of each musculotendon actuator.

REVIEW AND THEORY

A neuromusculoskeletal model of the human body was developed to study coordination and energetics of jumping. The body was modeled as four planar, rigid-body segments: trunk, thigh, shank, and foot. Segments were joined by single degree-of-freedom, frictionless joints at the hip, knee and ankle. Skeletal dynamics were formulated using Lagrangian equations of motion.

Seventeen lower extremity muscles were modeled: gluteus maximus, gluteus medius, gluteus minimus, hamstrings, adductor magnus, adductor longus and brevis, iliopsoas, sartorius, gracilis, tensor fascia lata, rectus femoris, vasti, biceps femoris (short head), gastrocnemius, soleus, other plantarflexors, and dorsiflexors. Requisite origin and insertion coordinate data were provided primarily by Brand *et al.* (2). Calculation of musculotendon length and moment arm was based on straight-line models of each muscle, and has been described in detail elsewhere (4). For knee extensors (vasti, rectus femoris) and knee flexors (hamstrings), we used moment arm data reported by Smidt (6).

The dynamics of each musculotendon actuator are described by a single, dimensionless musculotendon model (8). The dimensionless model is scaled to individual musculotendon actuators by three parameters: the maximum isometric strength (F_o^{CE}), the optimal muscle fiber length (l_o^M), and the tendon slack length (l_r^T). Also, the pinnation angle (ff_o) at l_o^M is needed. We used data for l_o^M, A^M (physiological cross-sectional area), and ff_o reported by others (7). Since maximum isometric muscle strength (F_o^{CE}) is proportional to A^M (7), we multiplied A^M by a factor so that the peak isometric knee extensor torque matched experimental data. No experimental data exist for tendon slack lengths (l_r^T) in human muscles. However, published data were used to select tendon slack length according to the following criteria: (1) since passive force is developed in muscle fibers only at lengths greater than l_o^M (8), l_r^T was adjusted so that the joint angles at which l_o^M occurred coincided with the onset of passive joint torque, and (2) since l_r^T determines the joint angle at which F_o^{CE} occurs, l_r^T was further adjusted so that the sum of the individual maximum isometric torque curves for either flexors or extensors coincided with the *in vivo* maximum isometric flexor and extensor joint torque data, respectively.

METHODOLOGY

Counter movement jumps were simulated under two different conditions: (1) freefall from standing position, and (2) initial flexor muscle activation from standing to accelerate the body downward. Coordination was investigated by activating musculotendon actuators at different times during each jump. Jump performance was defined as the airborne height of the body center of mass relative to standing height. For each jump, joint kinematics and kinetics, muscle torques, ground reaction forces, and segmental energetics were assessed. In addition, the energetics of the contractile element, series elastic element, and tendon components of each musculotendon actuator were calculated.

RESULTS AND DISCUSSION

Jump height and skeletal dynamics were very sensitive to the activation pattern of musculotendon actuators. Generally, jump heights were greater when flexors were activated initially. Results of one jump are illustrated in Figs. 1-4. In this jump, rectus femoris was activated initially for 0.025 s, followed by activation of other extensors (gluteus maximus, vasti, rectus femoris, gastrocnemius, soleus, other plantarflexors) at 0.225 s until takeoff. Body positions during the jump are shown in Fig. 1. Minimum knee angle (1.8 rad) occurred at 0.290 s. Jump performance was 0.20 m.

Although uniarticular extensors lengthened during the counter movement phase of the jump, contractile force was not always enhanced. For vasti (Fig. 2), during musculotendon lengthening at the start of the jump, the contractile element (CE) initially produced less than isometric force while the CE shortened, and only produced greater than isometric force during its subsequent brief lengthening which occurred just before the fast vasti shortening during propulsion. For soleus, musculotendon lengthening coincided with a decrease in CE force since the muscle fiber length was greater than l_o^M.

In accordance with experimental data (1,5), work done by vasti was initially negative during the downward phase of the jump, and was positive during propulsion at the end of the jump (Fig. 3). The negative work was produced by the elastic elements absorbing energy from both the downward moving body mass (89.4%) and the actively shortening CE (10.6%). Positive work during propulsion was generated by the CE; however, most of the energy generated by the CE was dissipated (97%). In this jump, 48% of the total energy of the body mass at takeoff was recovered from energy stored in the elastic elements.

The relative role of tendon and series elastic element in storing elastic energy depended on normalized tendon compliance. Normalized tendon compliance is proportional to normalized tendon slack length (l_r^T/l_o^M)(8). With normalized tendon slack length values of 8.9 and 2.9 for gastrocnemius and vasti, respectively, gastrocnemius has a relatively more compliant tendon than vasti. Therefore, although the absolute magnitude of elastic energy stored was greater for vasti (Fig.

North American Congress on Biomechanics
Montréal (Québec) Canada, 25-27 August 1986

4A) than for gastrocnemius (Fig. 4B), the percentage of elastic energy stored in the tendon was greater for gastrocnemius than for vasti.

CONCLUSIONS

This neuromusculoskeletal model of the human body allows us to study the energetics of simulated jumping. In the counter movement jump, musculotendon energetics are determined by the unique properties of each musculotendon actuator and their interaction with the skeletal dynamics accompanying jumping. Potentially, musculotendon actuators that generate large forces and have compliant tendons will facilitate storage of elastic energy, generation of positive work during propulsion, and will increase jump height.

References

1. Asmussen, E., *et al.* Acta physiol. scand. 91: 385-392, 1974.
2. Brand, R.A., *et al.* J. Biomech. Eng. 104: 304-310, 1982.
3. Cavagna, .A., *et al.* J. Appl. Physiol. 24: 21-32, 1968.
4. Gordon, M.E., *et al.* Proc. 9th Ann. Conf. Rehabil. Eng. Soc. (in press), 1986.
5. Komi, P.V., *et al.* Med. Sci. Sports 10: 261-265, 1978.
6. Smidt, G.L. J. Biomech. 6: 79-92, 1973.
7. Wickiewicz, T.L., *et al.* Clin. Orthop. Rel. Res. 179: 275-283, 1983.
8. Zajac, F.E., *et al.* Proc. 9th Ann. Conf. Rehabil. Eng. Soc. (in press), 1986.

This work was supported by NIH grant NS 17662 and the Veterans Administration.

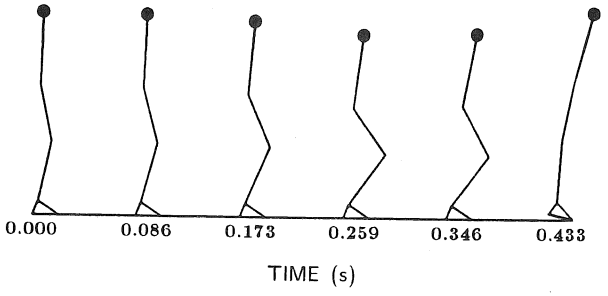

Figure 1. Body positions during the simulated jump. Rectus femoris was activated from 0.000-0.025 s. Other extensors were activated from 0.225 s to take off (0.433 s).

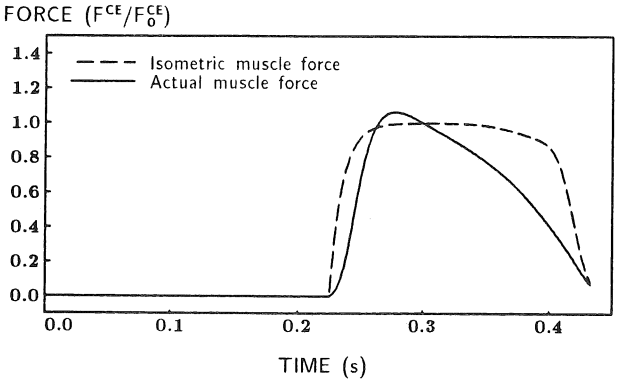

Figure 2. Force produced by the vasti contractile element (CE) during the jump. The actual force is compared with the isometric force that would be produced at the same length and activation. CE lengthening is indicated when the actual force exceeds the corresponding isometric force. Forces are normalized by the maximum isometric force.

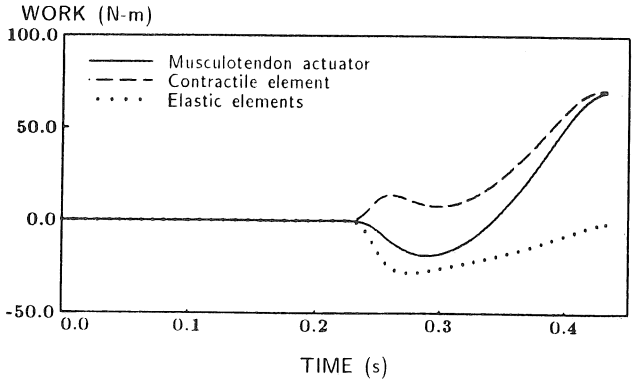

Figure 3. Work done by the vasti during the jump. Work done by the contractile element and elastic elements (tendon and series elastic element) sum to the vasti musculotendon work. Negative values indicate that energy is absorbed.

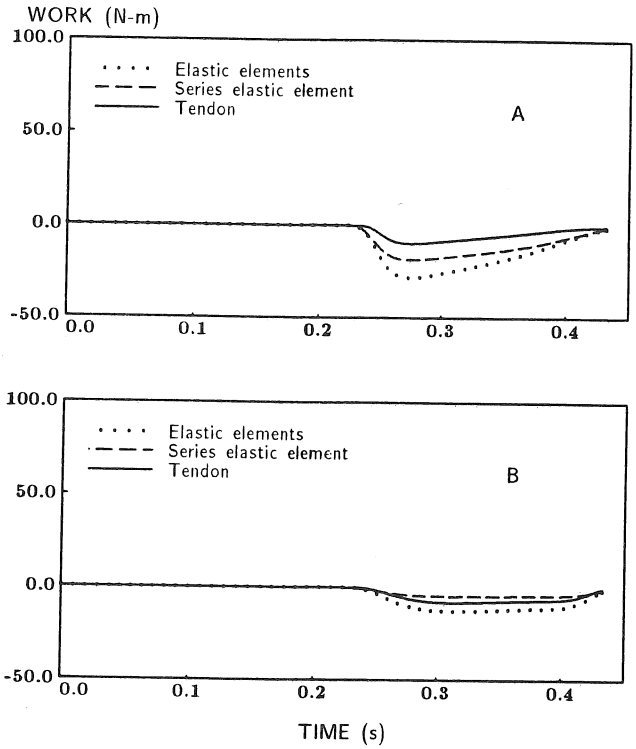

Figure 4. Elastic element work in vasti (A) and gastrocnemius (B) during the jump. Series elastic element work and tendon work sum to total elastic element work.

ELASTIC ENERGY STORAGE DURING SIMPLIFIED JUMPING MOVEMENTS IN MAN

M.R. Shorten, R.T. Mueller and L.B. Cooper
Nike Sports Research Laboratory
9000 S.W. Nimbus Drive, Beaverton, OR 97005

INTRODUCTION

When active muscle is stretched before a concentric contraction, the force, power and work produced can be greater than for a contraction without stretch (Cavagna et al, 1968). Performance enhancement after a stretch is the result of a combination of factors, including reduction in electro-mechanical delay time (Norman & Komi, 1979), favourable shift in the force velocity relationship (Cavagna and Citterio,1974; Komi,1979), activation of stretch reflexes (Melville Jones & Watt, 1971) and strain energy storage in the stretched elastic components of muscle and tendon (Alexander and Bennet-Clark, 1977).

Bosco and coworkers (e.g. Bosco et al, 1982) have made extensive comparisons of static jumps, countermovement jumps and drop jumps from a range of heights. The enhanced jumping performance observed in counter-movement jumps and drop jumps can be attributed to a combination of elastic energy storage and myoelectric potentiation.

The purpose of this paper is to report preliminary findings from a study of simplified jumping movements in which the relative contribution of elastic energy storage to enhanced jumping performance can be quantitatively determined.

THEORY

Strain energy storage in the ankle extensor muscle-tendon system was calculated by assuming that a single angular equivalent muscle acts to extend the ankle joint. During a small time interval, dt the change in the strain energy of stretched muscle and tendon can be calculated by

$$dE = M.dM/K(M)$$

where dE is the change in strain energy, M is the extensor muscle moment at the ankle and K is the angular equivalent stiffness of the ankle extensor muscles, a function of the extensor moment.

METHODOLOGY

A male subject weighing 843.4N performed simplified jumping movements on a Kistler force plate. The subject was trained to jump using only ankle extension (plantar flexion), while keeping the knees locked and the hands resting on the hips.

Three different jumps, with varying potential for pre-jump stretch of the ankle extensors were compared:

1: Static jump (SJ). A vertical jump starting from a static position with feet flat on the force plate.
2: Countermovement jump (CMJ). A vertical jump starting from a balanced position with the heels lifted from the force plate. The subject was allowed to perform a downward countermovement prior to jumping.
3: Drop jump (DJ). A vertical jump performed immediately on landing from a counter-movement jump.

Ground reaction forces and moments were sampled at 200 Hz. Movements of the lower leg in the sagittal plane were recorded at 200 frames/sec using an high speed video system (Motion Analysis Corporation). Force data and kinematic data were combined and applied to a two-segment, planar, linked rigid body model of the lower legs for calculation of the net extension moment about the ankles. Jumping performance was determined by calculating take-off velocity from the time integral of the vertical component of the ground reaction force.

In a separate experiment, an elastic stiffness function for the ankle extensor muscles was calculated using a modification of the method described by Cavagna (1970). The subject supported a loaded frame on the shoulders while the forefeet rested on an aluminium block mounted on the force plate. The elastic stiffness of the ankle extensor muscles was calculated from the natural frequency of damped oscillations in the ground reaction force, initiated by brief pressure to the shoulders. The measurements were repeated five times at each of six different loads in the range 1 to 2 bodyweights.

RESULTS

The stiffness-moment function of the subject's ankle extensor muscles is shown in Figure 1. The angular stiffness increases in an approximately linear manner over the range of moments studied. During most of each jump, the moment about the ankle was in the range 150 to 350Nm, and a linear extrapolation of the stiffness function was considered acceptable for moments outside the measured range.

Relative to take-off position, the subject raised his centre of mass by 4.1 cm, 5.0 cm and 6.6cm in the SJ, CMJ and DJ conditions respectively. Other comparisons between the three jumps are recorded in Table 1.

Figure 2 shows the relationship between ankle extension moment and angular extension velocity for each jump. During SJ, the ankle extension was purely concentric. The

North American Congress on Biomechanics
Montréal (Québec) Canada, 25-27 August 1986

countermovement in CMJ resulted in a brief eccentric contraction phase at the beginning of the jump. The DJ condition is distinguished by the pronounced eccentric phase during the first part of the jump.

Figure 3 compares strain energy storage in the series elastic component (SEC) of the single angular equivalent ankle extensor muscle. During the purely concentric SJ takeoff, 18.2J of strain energy were stored in the stretched SEC. Pre-jump eccentric contraction resulted in greater strain energy levels. The additional energy storage amounted to 2.6J in CMJ and 9.0J in DJ.

Table 1: Comparison of jump performances

PARAMETER		SJ	CMJ	DJ
Peak vertical force	N	1697	2075	2844
Peak extension moment	Nm	282.1	319.6	408.7
Peak angular velocity	s	3.63	3.70	4.44
Jump height	c	4.1	5.0	6.6
Strain energy stored	J	18.2	20.8	27.2
Potential energy gain	J	-	7.6	21.1
Strain energy gain	J	-	2.6	9.0

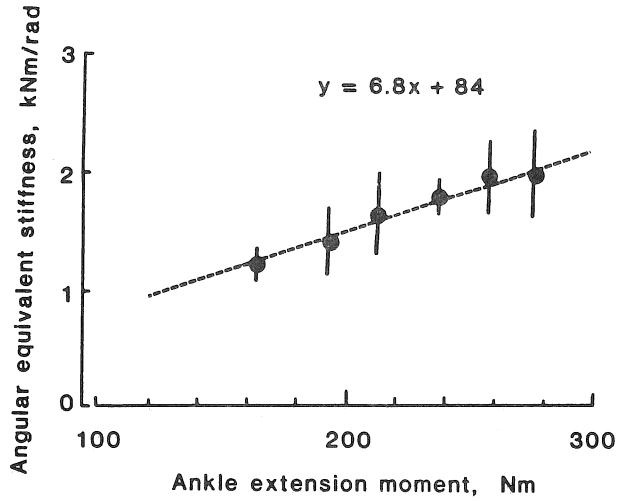

Figure 1. Angular equivalent stiffness of the ankle extensor muscles as a function of ankle extension moment. Mean and standard deviation of 5 measurements.

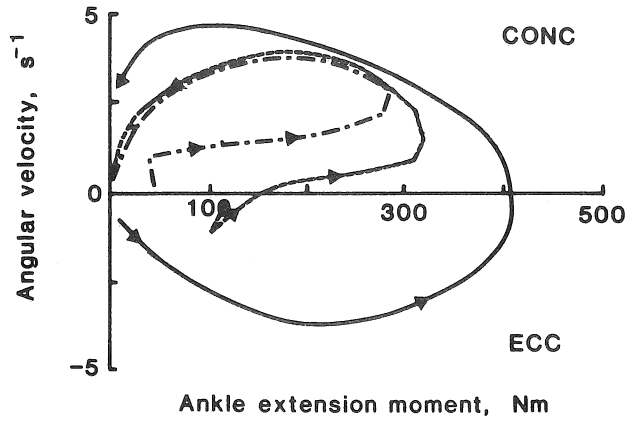

Figure 2. Relationship between ankle extension moment and angular extension velocity during SJ (-·-·-), CMJ (------) and DJ (——).

DISCUSSION

Only part of the observed stretch-enhancement of jumping performance can be attributed to strain energy storage in stretched elastic components of muscle and tendon. Additional strain energy storage was 34% of the additional potential energy gained during CMJ compared with SJ. In DJ, additional strain energy storage accounted for 43% of the additional potential energy gained in the jump.

These results suggest that mechanisms other than strain energy storage account for over half the performance enhancement that occurs as a result of prestretching the jumping muscles. Other effects of pre-stretch which may have contributed to enhanced performance in CMJ and DJ include increased EMG activity (myoelectric potentiation), higher peak angular velocities, higher peak moments (Table 1) and higher muscle moments at the onset of the concentric phase of the jump.

References

Alexander, R. McN. & Bennet-Clark, H.C., Nature 265:114-117, 1977

Bosco, C. et al. Acta Physiol Scand. 114:557-565 1982

Cavagna, G.A., J. Appl. Physiol. 29:279-282, 1970.

Cavagna, G.A. & Citterio, G., J. Physiol 239:1-14, 1974.

Cavagna, G.A. et al., J. Appl. Physiol. 24:21-32, 1968.

Komi, P.V., Scand. J. Sports Sci. 1:2-15, 1979.

Melville-Jones, G. and Watt, D.G.D., J. Physiol. 219:709-727, 1971

Norman, R.W. & Komi, P.V., Acta Physiol. Scand, 106:241-248,1979.

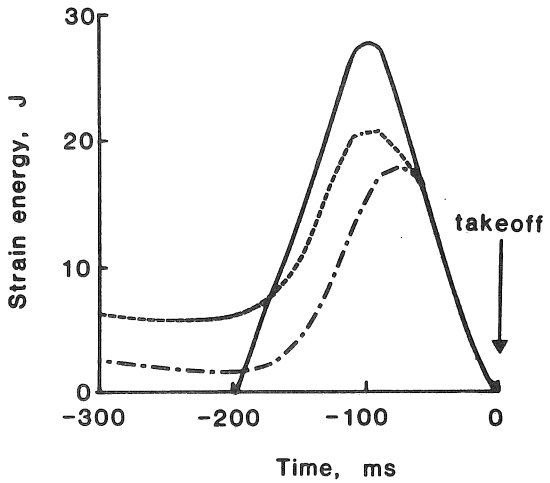

Figure 3. Elastic energy storage in the single equivalent ankle extensor muscle prior to take off during SJ (-·-·-), CMJ (--------) and DJ (——).

IN-VIVO PASSIVE RESISTIVE PROPERTIES BEYOND THE HUMAN SHOULDER COMPLEX SINUS

A.E. Engin
Department of Engineering Mechanics
The Ohio State University
Columbus, Ohio 43210, USA

S.M. Chen
Department of Engineering Mechanics
The Ohio State University
Columbus, Ohio 43210, USA

INTRODUCTION

In mathematical modeling of multisegmented articulating total-human-body, there is no doubt that the shoulder complex plays one of the most important roles. However, proper biomechanical passive resistive force data have been lacking in the literature. This paper presents statistically meaningful data on the three-dimensional passive resistive joint properties beyond the maximal voluntary shoulder complex sinus for the normal male population of ages 18 thru 32. The term "shoulder complex sinus" designates the voluntary range of extreme allowable motion of the humerus with respect to torso. Ten subjects were randomly chosen to form the sample. The sample mean and sample standard deviation were obtained in a systematic way and were expressed in functional expansion form relative to a locally-defined joint axis system.

REVIEW AND THEORY

In a recent paper (1), the senior author and his associates introduced a new kinematic data collection methodology by means of sonic emitters and data analysis technique based on selection of the "most accurate" local axis system from an over-determinate number of sonic emitters on the moving segment. This technique was further applied to collect data on the passive resistive properties of the human shoulder complex as functions of drawer displacements of the upper arm along its long bone axis (2). The methodology permits the investigation of complex three-dimensional gross body motions. By applying this technique, this paper reports statistically meaningful data on the passive resistive properties of the human shoulder complex beyond the shoulder complex sinus. We exclude the rotational influence of the upper arm along its long-bone axis; thus the passive resistive force can be expressed as $f = f(\phi, \theta)$ where ϕ and θ are the spherical coordinates with respect to the local joint axis system defined by (ϕ_n, θ_n) (see Figure 1 of the paper (by the same authors), entitled "IN-VIVO KINEMATIC PROPERTIES OF THE HUMAN SHOULDER COMPLEX" which appears in these proceedings and will be hereinafter referred as intra-proc.-ref.).

METHODOLOGY

The basic components of the data acquisition system are the sonic digitizer, the digitizer sensor assembly, and the subject restraint/positioner system which was designed so that the subject's torso can be positioned in a wide range of orientations. The force applicator is a hand-maneuvered device with a six-component transducer which measures forces and moments in three orthogonal directions. The orientation of the upper arm with respect to torso is monitored by means of an arm cuff with six sonic emitters.

The subject's upper arm was abducted or adducted in a quasi-static manner until the subject experienced discomfort or the upper arm could no longer be displaced (e.g., adduction into the torso). During the entire course of each force test (forced sweep), the subject was instructed to let his arm hang limply and not to actively (muscularly) resist the motion of the test, or stating it in a different manner, the recorded values are the passive resistive force values.

With respect to the joint axis system, these forced sweeps took place in a direction of increasing θ, and at an approximately constant-ϕ value. By appropriately positioning the subject's torso, a series of constant-ϕ sweeps were obtained. In this way the tests were performed as four sub-series with each sub-series discernible by its own experimental set-up configuration. The groupings consist of constant-ϕ sweeps in: 1) the upper-rear quadrant ($0° < \phi < 90°$), 2) the lower-rear quadrant ($90° < \phi < 180°$), 3) lower-front quadrant ($180° < \phi < 270°$) and 4) the upper-front quadrant ($270° < \phi < 360°$).

The data obtained according to the procedure briefly outlined above were analyzed as follows. First, the force and moment vectors obtained from the force applicator data were used to calculate a total moment vector with respect to the glenohumeral joint center location. Next, a moment arm vector was calculated from the center of the best-fitted sphere (described in the intra-proc.-ref.) to the point of force application. Next, the intersection of this vector with a sphere of radius equal to one meter was selected as a "normalized" point of force application. The total moment vector was then divided into components along the moment arm and perpendicular to the moment arm vector. The component along the position vector (moment arm vector) was then discarded, since it does not serve to restore the moving segment to an orientation within the voluntary shoulder complex sinus. From the remaining moment component and the normalized position vector the restoring force vector was then calculated. Since the moment arm is normalized to one meter, the magnitude of the restoring force vector is the same as that of the restoring moment vector. Note that this force vector is always tangent to the surface of the selected normal sphere.

To facilitate the statistical analysis on the restoring force (moment) data, the raw data are first curve fitted by the functional expansion:

$$f(\phi,\theta) = (C_1 + C_2\cos\phi + C_3\sin\phi)\theta + (C_4\cos^2\phi + C_5\cos\phi\sin\phi + C_6\sin^2\phi)\theta^2 + (C_7\cos^3\phi + C_8\cos^2\phi\sin\phi + (C_9\cos\phi\sin^2\phi + C_{10}\sin^3\phi)\theta^3 \quad (1)$$

North American Congress on Biomechanics
Montréal (Québec) Canada, 25-27 August 1986

Since $\theta(\theta \geq 0)$ measures how far the upper arm departs from the z-axis of the local joint axis system, and ϕ goes from 0 to 2π, we can treat θ as the radial coordinate and ϕ as the angular coordinate in the polar coordinate system (θ, ϕ). The pole is then the z-axis of the local joint axis system. Therefore, if we introduce the following coordinate transformation: $p = \theta\cos\phi$ and $q = \theta\sin\phi$; then, (p, q) can be regarded as the corresponding rectangular coordinate system.

We shall consider f as a random variable and ϕ and θ as independent variables. Therefore, by applying the mathematical expectation operator E on Eq. (1), we obtain the population mean μ_f for f as

$$\mu_f(\phi,\theta) = \{E[C_1] + E[C_2]\cos\phi + E[C_3]\sin\phi\}\theta + \{E[C_4]\cos^2\phi + E[C_5]\cos\phi\sin\phi + E[C_6]\sin^2\phi\}\theta^2 + \{E[C_7]\cos^3\phi + E[C_8]\cos^2\phi\sin\phi + E[C_9]\cos\phi\sin^2\phi + E[C_{10}]\sin^3\phi\}\theta^3 \quad (2)$$

Next, by applying the variance operator VAR on Eq. (1), we obtain the population variance σ_f^2 for f as

$$\sigma_f^2(\phi,\theta) = \{VAR[C_1] + VAR[C_2]\cos^2\phi + VAR[C_3]\sin^2\phi\}\theta^2 + \{VAR[C_4]\cos^4\phi + VAR[C_5]\cos^2\phi\sin^2\phi + VAR[C_6]\sin^4\phi\}\theta^4 + \{VAR[C_7]\cos^6\phi + VAR[C_8]\cos^4\phi\sin^2\phi + VAR[C_9]\cos^2\phi\sin^4\phi + VAR[C_{10}]\sin^6\phi\}\theta^6 \quad (3)$$

where we have utilized

$$COV(C_i, C_j) = 0 \text{ for all } 1 \leq i < j \leq 10 \quad (4)$$

since all the ten coefficients are independent.

From the sample, an estimate, $\bar{C}_i$ and $S^2_{C_i}$, for $E[C_i]$ and $VAR[C_i]$, respectively, can be obtained for the i^{th} coefficient by

$$\bar{C}_i = \frac{1}{10}\sum_{j=1}^{10}(C_i)_j \quad (5)$$

and

$$S^2_{C_i} = \frac{1}{9}\left\{\sum_{j=1}^{10}(C_i)_j^2 - \frac{1}{10}\left[\sum_{j=i}^{10}(C_i)_j\right]^2\right\} \quad (6)$$

where $(C_i)_j$ stands for the i^{th} coefficient for the force (moment) expansion function $f(\phi,\theta)$ of the j^{th} subject. Therefore, from Eq. (2), an estimate for $\mu_f(\phi,\theta)$ is:

$$\bar{f}(\phi,\theta) = (\bar{C}_1 + \bar{C}_2\cos\phi + \bar{C}_3\sin\phi)\theta + (\bar{C}_4\cos^2\phi + \bar{C}_5\cos\phi\sin\phi + \bar{C}_6\sin^2\phi)\theta^2 + (\bar{C}_7\cos^3\phi + \bar{C}_8\cos^2\phi\sin\phi + \bar{C}_9\cos\phi\sin^2\phi + \bar{C}_{10}\sin^3\phi)\theta^3 \quad (7)$$

and an unbiased estimate for $\sigma_f^2(\phi,\theta)$ from Eq. (3) is:

$$S_f^2(\phi,\theta) = (S^2_{C_1} + S^2_{C_2}\cos^2\phi + S^2_{C_3}\sin^2\phi)\theta^2 + (S^2_{C_4}\cos^4\phi + S^2_{C_5}\cos^2\phi\sin^2\phi + S^2_{C_6}\sin^4\phi)\theta^4 + (S^2_{C_7}\cos^6\phi + S^2_{C_8}\cos^4\phi\sin^2\phi + S^2_{C_9}\cos^2\phi\sin^4\phi + S^2_{C_{10}}\sin^6\phi)\theta^6. \quad (8)$$

RESULTS

As mentioned before, the force(moment) data were collected beyond the maximal voluntary sinus up to the point, which we shall call the maximal forced sinus, where the subject starts experiencing discomfort or the upper arm can no longer be displaced (e.g., adduction into the torso). Figure 1 shows a perspective view of the resistive force (moment) contours for a subject. Figure 2 shows the constant resistive force (moment) contour map of the sample mean of the force (moment) data, i.e., Eq. (7). In addition, the sample mean of the maximal voluntary sinuses and the sample mean of the maximal forced sinuses are indicated on the same figure. Results of this study can be directly incorporated into the mathematical modeling of total-human-body.

REFERENCES

1. Engin, A.E., et al. J. Biomech. Engng. 106:204-211, 1984.

2. Engin, A.E., et al. J. Biomech. Engng. 106:212-219, 1984.

ACKNOWLEDGMENT

This research was supported by the Aerospace Medical Research Laboratory of the U.S. Air Force, Wright-Patterson AFB, OH 45433, USA.

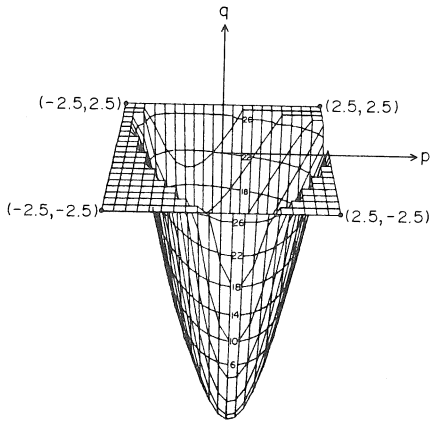

Figure 1. Perspective view of the resistive force (moment) contours for a subject.

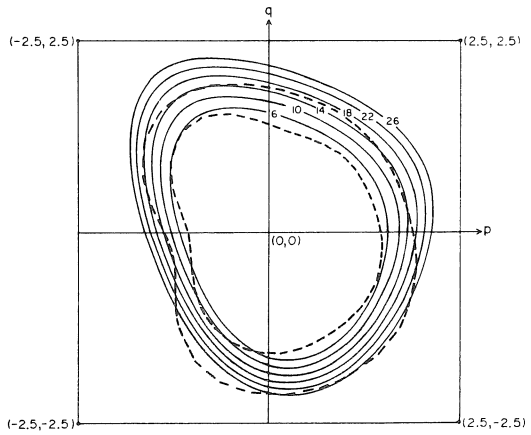

Figure 2. Mean constant resistive force (moment) contour map and mean maximal voluntary (inner dashed) and forced (outer dashed) sinuses.

FINITE ELEMENT MODEL OF ASYMMETRICAL RIB GROWTH IN SCOLIOSIS

J. Dansereau*, I.A.F. Stokes*, J.P. Laible+, M.S. Moreland*

* Department of Orthopaedics & Rehab. ; + Department of Civil & Mechanical Engineering
University of Vermont, Burlington, Vermont, 05405

INTRODUCTION: The role which is played by rib growth in spinal deformations have not been tested as a possible etiologic cause of scoliosis. It can be hypothesized that a disturbance on the side-to-side rib growth pattern may generate lateral deviation and rotation of the vertebra causing the initial instability of the spine. Clinical results from stereo radiographic reconstruction of scoliotic rib cages and spines have shown side-to-side rib asymmetry in arc and chord length measurements as well as in posterior curvature, enclosed area and extrinsic rib angulation parameters (1). This paper presents a 2-D finite element model of one rib-vertebra anatomical level to study the impact of rib asymmetrical growth on vertebral displacement in scoliosis. The different components of the model have been validated using results of reported experimental studies.

DESCRIPTION OF THE MODEL: The one anatomical level model is composed of 48 flexible beam elements (44 nodes) representing the sternum, the vertebra and two symmetrical ribs and costal-cartilages (Figure 1). The ribs are attached anteriorly to the cartilages and these last to the sternum by means of small flexible beam joint elements. Posteriorly, the costo-vertebral joints are modeled on both sides by two flexible beam elements; one attached to the lateral part of the vertebral body and the other one attached to the tip of the transverse process. The reconstructed shape of ribs T7 of a normal subject gave geometric data for rib components. Right and left sides were averaged to obtain symmetry. Costal-cartilages and sternum dimensions were also measured from the same individual. Reported data (2) provided cross-sectional area and moment of inertia distribution along the ribs and costal-cartilages. The material properties of the ribs, cartilages, sternum, vertebra and joints were derived from published data (2,3,4). The growing effect was obtained by analogy with thermal expansion by incorporating a "coefficient of thermal expansion" into the model. The amount of growth could then be controlled by varying the "temperature" on each element. Based on an experimental study (5) where rib growth of young pigs was measured, a 1 to 4 ratio between growth at the vertebral end and growth at the sternal end was imposed. To stimulate the rib growth over time, the finite element model was used iteratively allowing relocation of nodes after each step and a release of the internal stresses, representing bone remodeling and adaptation (6).

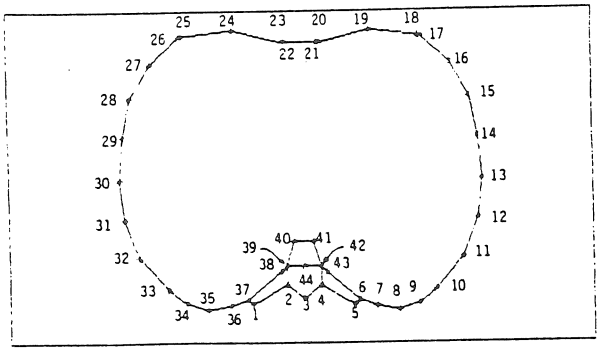

Figure 1 - Node locations of the single anatomical level finite element model.

VALIDATION OF MODEL COMPONENTS: The deformations of the ribs, costo-sternal and costo-vertebral articulations were calculated in conditions similar to reported experiments (7,8) for antero-posterior and lateral traction and/or bending loading (7.4 N). Displacement values calculated by the model components at the loading points showed agreement with the experimental results (difference within 6% to 18% or 0.3 mm to 1.3 mm).

RESULTS: Two major factors determine model response: 1) growth conditions given by the "temperature" parameter, and 2) the types of displacement constraints imposed on specific nodes. In this paper, the responses of the finite element model to two constraint conditions are presented. In the first case, the rib growth on the sternal end is two times greater on the right side than on the left side and no rotation and translation displacements on nodes 21 and 22 are allowed (sternum fixed and other

North American Congress on Biomechanics
Montréal (Québec) Canada, 25-27 August 1986

anatomical features free to move). In the second case, rib growth is imposed on the right side only (no growth on the rib posterior parts) while no translation displacement on nodes 17,21,22,26 (costo-chondral and costo-sternal junctions) and no lateral displacement on rib lateral nodes are allowed. Results are presented in Figure 2a,b.

Figure 2a shows a vertebral rotation in a similar direction to that observed in scoliosis but a lateral deviation in a non-corresponding direction. The ribs are minimally deformed but had moved a considerable distance laterally. This lateral deviation of the ribs may not be realistic because it does not take into account the constraint of the other adjacent rib levels. Figure 2b presents the results with such constraint conditions. It shows vertebral lateral deviation and vertebral rotation in similar direction to that observed in scoliosis. The model's geometry was evaluated by the same parameters used to measure rib shape of scoliotic patients (arc length, chord length, posterior curvature, enclosed area, posterior rib rotation). In 25 patients with right thoracic scoliosis, 16 have shown all 5 rib parameters following the same direction of asymmetry to that predicted by the model. The 9 other patients had equal or greater arc length and enclosed area on the opposite side to the model predictions, but posterior rib rotation, curvature and chord length parameters in agreement with the model. For a similar percentage of rib arc length difference (7.3%), the 16 patients presenting qualitative agreement with the model showed enclosed area and posterior curvature difference 2 times greater than calculated by the model. The chord length parameter differed by a factor close to 3.5 while the vertebral and posterior rib rotation were in close agreement with the model. The vertebral lateral deviation calculated by the model was smaller by a factor of 8.0, implying that the forces involved in the buckling of the spine have not been taken into account in the finite element model.

CONCLUSIONS: Results from the model indicate that a disturbance on the side-to-side rib growth pattern may have an effect on the initial instability of the spine in scoliosis.

REFERENCES:

(1) Dansereau J, et al. 9th meeting of American Society of Biomechanics, 45,1985. (2) Robert SB, Chen PH. J. Biomech. 3:527-545, 1970. (3) Andriacchi T, et al. J. Biomech. 7:497-504, 1974. (4) Sundaram SH, Fend CC. J. Biomech. 10:505-516, 1977. (5) Snellman O. Acta Orthop. Scand., Suppl. 149, 1973. (6) Hart RT, J. Biomech. Eng. 106:342-350, 1984. (7) Schultz AB, et al. J. Biomech. 7:303-309, 1974a. (8) Schultz AB, et al. J. Biomech. 7:311-318, 1974b.

ACKNOWLEDGEMENTS: Supported by Scoliosis Research Society and Institut de Recherche en Santé et en Sécurité du Travail du Québec.

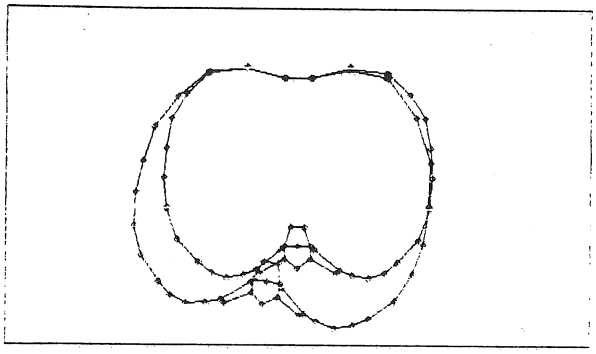

Figure 2a - Resulting configuration obtained after 20 iterations. Only the sternum is fixed.

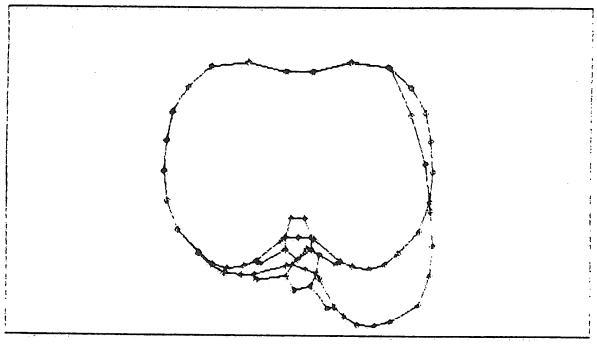

Figure 2b - Resulting configuration obtained after 20 iterations. The costo-sternal and costo-chondral junctions are fixed while only lateral constraints are applied on the lateral part of the ribs.

THE EFFECT OF LIMITED KNEE-FLEXION RANGE ON PEAK HIP JOINT TORQUES IN HUMANS TRANSFERRING FROM SITTING TO STANDING

Susan J. Fleckenstein*, R. Lee Kirby*, Donald A. MacLeod+

*Division of Physical Medicine and Rehabilitation, Department of Medicine, Dalhousie University and

+Clinical Locomotor Function Laboratory, Nova Scotia Rehabilitation Centre, Halifax, Nova Scotia, B3H 4K4 Canada

INTRODUCTION

Transfers from sitting to standing are a frequent daily activity in normal humans and are a virtual prerequisite to bipedal locomotion. For many patients with arthritis this activity is difficult and painful. Many such patients are confined to wheelchairs before they have lost the ability to walk, as they are unable to get to their feet.

We tested the hypothesis that limiting the knee-flexion range would increase the peak hip-extension torque while transferring from sitting to standing. Ten normal human volunteers were filmed (100 fps) twice while transferring to standing from sitting. With the knees flexed only 75° the peak hip-extension torque was significantly greater than with the knees flexed 105°.

REVIEW AND THEORY

Our understanding of hip joint kinematics and kinetics during transfers is limited. Kelley et al. found a peak hip-extension torque of 80 Nm just after the buttocks left the seat in 6 subjects (1). Bajd et al., studying a single healthy subject, compared hip and knee moments during a normal transfer and a slow transfer with the hips fully flexed (2) and found that the peak moments at the hip (160 Nm) did not differ.

We have observed that patients with limited knee-flexion range often throw their arms and upper bodies forward to get up, particularly if the seat is low or has no armrests. We hypothesized that limiting the knee-flexion range would significantly increase the peak hip-extension torque while transferring from sitting to standing. The object of this study was to test the hypothesis with normal subjects and to describe the altered mechanics.

METHODOLOGY

We studied 10 normal human volunteers, 5 women and 5 men, with a mean (± 1 SD) age of 25.4 (± 4.0) years. Each subject rose from an upright seated position on a padded 44-cm-high stool twice, once with the knees initially flexed 105° from full extension and once with the knees initially flexed 75° (3). The subjects could choose their foot angle and base width. They were not permitted to use their arms to apply force to the seat or their legs. Each subject practiced the movements in balanced order until comfortable with the tasks.

We used a highspeed cine camera to film the transfers at 100 frames per second from the left lateral perspective. We digitized the film on a rear projection platen beginning when the trunk started moving forward (defined as 0% of the movement) and ending when the subject had come to rest in the standing position (100%). In each frame we digitized a fixed reference point and the external auditory meatus, C7, T12, acromion, lateral epicondyle of the humerus, wrist, greater trochanter, lateral epicondyle of the femur, lateral malleolus, calcaneus and fifth metatarsophalangeal joint.

The digitized film data were filtered using a second-order Butterworth digital filter. A cutoff frequency for each digitized coordinate was determined by the procedure of Wells and Winter (4). A first-order finite difference technique was used to obtain velocities and accelerations of the coordinates as a function of time. These data, along with segment lengths and inertial parameters (5), were used to calculate the joint torques. To enable comparison among subjects, the data were normalized for time. For graphic purposes ensemble averaging was done using an interpolating spline and calculating the average and standard deviation for the 10 subjects at each 0.5% of the transfer.

Parameters derived for statistical comparison from the individual curves were the peak hip joint angular displacements, torques and torque impulses (torque . time), the timing of the peak torques and the duration of the tasks. We used matched-pairs t-tests, defining the level of significance at $p<0.05$.

RESULTS

The results are presented in the Table. Figure 1 illustrates the hip angles during the transfers. The peak hip-flexion angles with the initial knee-flexion range limited to 75° were an average of 20° greater than with the knees initially flexed 105°. The peak hip-extension torques (Fig. 2) and impulses were much greater with the knees less flexed (75°) at the initiation of the transfer than when they were more flexed (105°). There was no difference in the timing of the peak hip-extension torques, or in the magnitude or timing of the peak hip-flexion torques. Hip-flexion impulses were slightly greater with the knees initially flexed 75°. The transfers with initial knee flexion of 75° took significantly longer than transfers with initial knee flexion of 105°. In qualitatively reviewing the kinematics of transferring from sitting to standing, the forward arm and trunk movement appeared to be much greater when transferring with limited initial knee flexion range (75°).

DISCUSSION

The results support our hypothesis that limiting the initial knee-flexion range significantly increases the peak hip-extension torque while transferring from sitting to standing. The small initial hip-flexion torque is probably a reflection of the muscle action used to begin the forward movement of the upper body (1), whereas the large hip-extension torque allows the subject to stand up from the forward flexed position. Our data for hip torques with normal knee-flexion range are comparable to those of other groups (1, 2). As anticipated from clinical experience, when the initial knee-flexion range is limited, transfers were

accomplished by throwing the upper body and arms forward, the effect of which on the hip is presumably magnified by the long moment arms.

The generalizability of our study is limited by the small number, limited age range and normality of the subjects studied. The variability among our subjects was not marked, but it might have been reduced if we had normalized our results on the basis of subject height or weight. Although in this study we focused on the effects of limited knee-flexion range at the hip joint, future investigation of the effects on the shoulder joints and spine may be fruitful.

The results of our study have implications for patients with arthritis of their hip joints and limited knee-flexion range as is often the case when there is associated arthritis in the knees. If the peak torques rise in such patients to an extent similar to that of our subjects, accelerated hip joint damage may result. Our data also has implications for the design of hip replacements. Among the causes of loosening of endoprostheses, biomechanical effects have been demonstrated to play an important role.

CONCLUSIONS

In summary, we found that peak hip-extension torque increases significantly if the initial knee-flexion range is limited. With initial knee flexion of 75° our subjects accentuated the forward movement of their arms and upper bodies to aid them in standing up. We hope that these observations provide new insight into the mechanics of transfers, the effects such movements and the associated forces may have on aggravating joint disease or loosening endoprostheses, and in emphasizing the importance of preserving knee-flexion range.

References

1. Kelley, D.L. et al. Biomechanics V-B. Komi PV (ed). Univ Park Press, Baltimore, pp 127-134, 1976.
2. Bajd, T. et al. J. Biomech. 15: 1-10, 1982.
3. American Academy of Orthopaedic Surgeons, Chicago, 1965.
4. Wells, R.P. et al. Proc. Can. Soc. Biomech., Human Locomotion I, pp 92-93, 1980.
5. Dempster, W.T. et al. Am. J. Anat. 120: 33-54, 1967.

TABLE: Transfer from Sitting to Standing

Parameter	Knee Position[1] 105°	75°
Hip Joint		
Flexion		
peak angle (degrees)	115 ± 10	135 ± 8 †
peak torque (Nm)	42 ± 30	54 ± 38
timing peak torque (%)	5.8 ± 6.5	7.8 ± 3.4
torque impulse (Nm .s)	904 ± 939	1258 ± 873 *
Extension		
peak torque (Nm)	142 ± 37	253 ± 65 †
timing peak torque(%)	39.5 ± 7.6	38.6 ± 6.3
torque impulse (Nm. s)	6628 ± 2766	12228 ± 3896†
Duration of transfers (s)	1.37 ± 0.32	1.57 ± 0.16*

Values are means ± 1 SD for 10 subjects.
*=significant at the $p<0.05$ level.
†=significant at the $p<0.0001$ level.

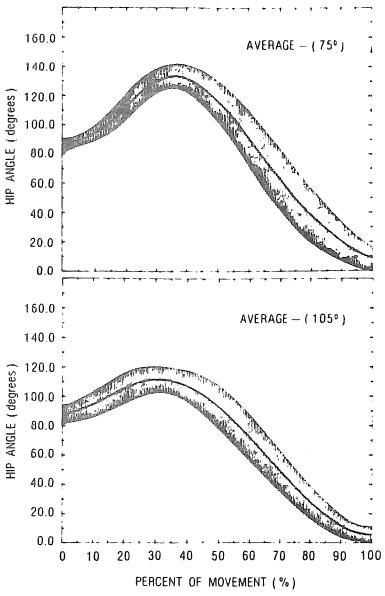

Fig 1. Joint angles at hip during transfers from sitting to standing, with knees flexed initially at 105° and 75°. 0° is full extension.

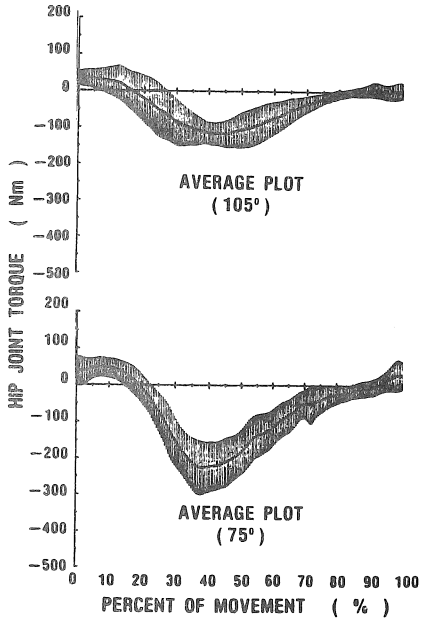

Fig 2. Hip joint torques at initial knee-flexion angles of 105° and 75° during transfers from sitting to standing. The mean values (± 1 SD at every 0.5%) for the 10 subjects are shown. Flexion torques are positive and extension torques are negative.

RELIABILITY AND APPLICATION OF A COMPUTERIZED TRIAXIAL ELECTROGONIOMETER FOR THE EVALUATION OF HEAD MOVEMENTS

F. MALOUIN and J. PREFONTAINE
Physiotherapy Section and Laboratoire de Neurobiologie
Faculty of Medicine
Laval University
Quebec, G1K 7P4

INTRODUCTION

The use of a triaxial electrogoniometer (EGM) for the evaluation of head movements offers various advantages. For instance, monitoring head position over time makes it possible to measure kinematic variables such as the duration, the speed, as well as the range of movements. Also, the instantaneous sampling of head positions in the three planes allows the description of concomitant movement patterns (simultaneous movements in the other planes) while specific voluntary movements are attempted. The analysis of such variables gives valuable guidelines when characterizing dysfunctions of head postural control and assessing the effects of treatment in patients with movement disorders. The results of a reliability study concerning the application of a computerized neck triaxial electrogoniometer system will be presented and discussed in terms of its application for the evaluation of spasmodic torticollis (ST).

METHODOLOGY

This study was carried out in seven male volunteers aged 24 to 37 (mean 30.1 ± 3.9) years with no medical history of cervical disorder. Each subject was submitted to two evaluations (test-retest) repeated 24 hours apart. Subjects were seated in an adjustable chair with a backrest allowing free motion of the head. Trunk movements were restrained by shoulder straps and the forearms attached to the arm rests to prevent hiking of the shoulders. The EGM system was composed of a helmet to which were attached three interconnected potentiometers. These potentiometers were attached to sliding rods which were in turn connected to central rings suspended 45 to 60 cm above the helmet. Two more potentiometers were mounted on these rings to measure translational movements in the sagittal and frontal planes. The EGM signals were fed to an A/D converter of an IBM-PC microprocessor and sampled at 50 Hz. The potentiometers were calibrated (zero reference) by placing the head in an upright position (defined by a level attached to the helmet). Subjects were asked to perform three repetitions of flexion-extension, rotation (left-right) and lateral flexion (left-right) movements in a random order. Concomitant movement patterns, during specific single movements were analyzed. Calculation of angular displacements (degrees), duration (s) and speed of movement (degrees/s) were made by a computer program. Mean values for these variables were calculated for each subject and the reproducibility of the repeated measurements evaluated by the Spearman rank correlation coefficient and the Wilcoxon matched-pairs signed-ranks test. Coefficients of variation were also calculated. Results from two female patients with ST, aged 14 (case 1) and 35 (case 2) years, submitted to a similar evaluation, are also compared to normal values.

RESULTS

Mean peak amplitude values for head movements, in the normal men are given in Table 1. Correlation coefficients, which ranged from 0.79 to 1.0, and the coefficients of variation ranging from 2 to 4.2% indicate very good reproducibility of the measurements. The mean peak amplitude values for head rotation, however, is significantly increased on the retest day ($p<0.01$). If the third repetitions only are compared, the increase is not significant. In Table 2, mean kinematic values are compared to values of a young dystonic patient (case 1). In this patient, all head movements were executed at least 50% faster and the range of movements was markedly decreased (except for head rotation). Despite these differences, the concomitant movement patterns, which in normals are characteristic for each head movement, were similar to normal patterns. In contrast, in case 2, disturbances were most obvious in the concomitant movement patterns. Thus, for this patient (Fig. A), the concomitant movement patterns (in frontal and sagittal planes) during head rotation were in opposite directions in comparison to the normal pattern (B). Moreover, as shown by the slopes of the angle traces rotation movements (in A) were slower from right to left. Visual inspection also indicates a greater variability between rotation movements in the patient (A) than in the normal subject (B). Lastly, head rotation to the right was less (65°) than to the left (102°) in A, while in B, the displacements to either side of the midline were more symmetrical.

DISCUSSION

Amplitude values reported for the three specific voluntary head movements are in accordance with values obtained in 40 male subjects aged 24-29, who were tested with a goniometer in a sitting position (1). The correlation coefficients are within the ranges of values reported by others with different types of goniometers (2,3). Although highly correlated ($r_s=1.0$), mean amplitude values for head rotation were shown, however, to increase with repetitions and between tests. These findings indicate a greater variability in head rotation measurements and suggest the use of the coefficient of variation to measure this variability (4). In patient 1, it was quite surprising to find that, in contrast to case 2, concomitant head movement patterns were normal despite marked differences in kinematic features. It is not sure if these discrepancies in patient 1 are related to the recent apparition of the torticollis or if it is linked to its suspected psychogenic origin (5). In the latter case, this would indicate that kinematic features of the performance can be more readily modified than the concomitant head movement patterns which may be

North American Congress on Biomechanics
Montréal (Québec) Canada, 25-27 August 1986

centrally pre-programmed like other postural and locomotor movements (6). These results indicate that this computerized triaxial neck EGM is reliable and its use for the evaluation of disturbed head movements makes it possible to characterize individual dysfunctions.

REFERENCES

1. Blanchard, R.S. et al. Bull. Univ. Minn. Hosp. 24: 470-476, 1953.
2. Defibaugh, J.J. J. Amer. Phys. Ther. Ass. 44: 163-168, 1964.
3. Leighton, J.R. Arch. Phys. Med. Rehabil. 37: 494-499, 1956.
4. Yang, J.F. et al. Arch. Phys. Med. Rehabil. 64: 417-420, 1983.
5. Tibbetts, R.W. J. Psychosom. Res. 15: 461-469, 1971.
6. Grillner, S. Physiol. Rev. 55: 247-304, 1975.

TABLE 1

Mean amplitude values obtained in normal subjects (n=7), Spearman rank correlation coefficient (r_s) and coefficient of variation for three repetitions (CV1) and for the test-retest (CV2).

Head movements	Test (degrees)	Retest (degrees)	r_s	CV1 (%)	CV2 (%)
Flex. Ext.	120.6 (11.7)	119.9 (16.9)	0.89	2	3.6
Lateral Flex.	77.2 (7.7)	80.1 (8.1)	0.79	3.3	4.1
Rotation	150.4* (18.0)	159.0 (13.9)	1.0	2.3	4.2

Values in brackets are ± 1 S.D., * $p<.01$

TABLE 2

Comparison of values for specific voluntary head movements in normal subjects (n=7) and in a dystonic patient (case 1).

	Flexion extension		Lateral flexion		Rotation	
	N	Case 1	N	Case 1	N	Case 1
Amplitude (degrees)	120.6 (11.7)	71	77.2 (7.7)	58.7	150.4 (18)	171.2
Duration (s)	48.5 (15.6)	22	36.6 (7.8)	18	34.8 (6.5)	17.5
Speed (°/s)	31.1 (7.2)	49	27.7 (6.7)	53	60.8 (13.6)	100

Values in brackets are ± 1 S.D.

ACKNOWLEDGMENTS

The authors thank D. Tardif and L. Laroche for technical assistance. This work was supported by grants from the Medical Research Council of Canada and Research funds from Laval University. J. Préfontaine was the recipient of a summer studentship from l'Institut de recherche en santé et en sécurité du travail du Québec (IRSST).

Figure: Illustration of concomitant movement patterns during head rotation. In A, a dystonic patient (case 2), and in B, a normal subject. Time base: 2s/division.

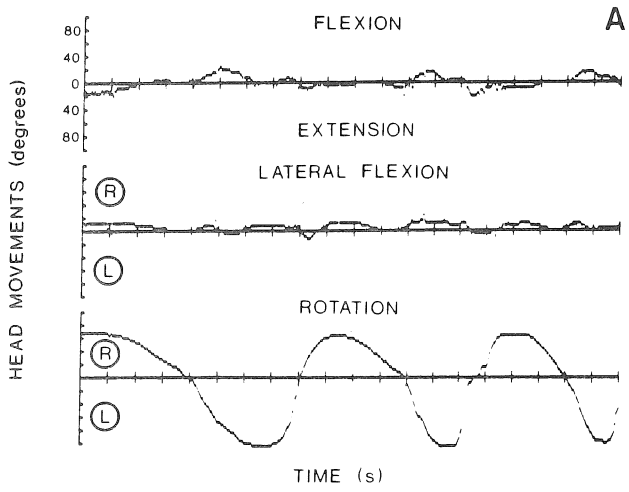

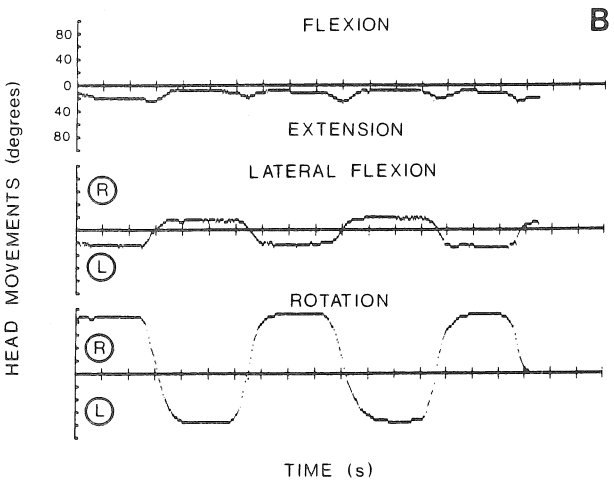

BIOMECHANICAL ASPECTS OF PRECLINICAL DESCRIPTORS OF OSTEOARTHRITIS

James Alexander, Amit Bhattacharya, Priyadarshi Patel and Stuart Brooks, Biomechanics-Ergonomics Laboratory,

Department of Environmental Health, University of Cincinnati Medical Center, Cincinnati, Ohio 45267-0056

INTRODUCTION

It has been well established by epidemiologic data that 90% of individuals at age 40 years have radiological or clinical evidence of osteoarthritis. Current clinical methods of evaluation of this ubiquitous process have been demonstrated to be inadequate in detecting preclinical disease states. There currently exists a need for an alternative method of clinical evaluation which will identify individuals or populations at risk and also detect the development of preclinical disease. The purpose of this investigation was to refine and evaluate a non-invasive in-vivo quantitative technique initially described by previous researchers (1) which would satisfy the demonstrated requirement for a screening tool for osteoarthritis.

REVIEW AND THEORY

The transmission, absorption and attenuation of energy that intakes to the skeleton due to heel strike is an important component of bone physiology and pathology (1). The body's natural shock absorption system normally attenuates and dissipates the incoming force associated with the heel strike. This process is a natural and rational mechanism which protects the vital central nervous system structures. However, functional deficiencies of the natural shock absorbers in the human skeleton, i.e. subchondral bone, cartilage, muscle and other soft tissue structures, may pre-dispose the proximal joints to increased loading. Voloshin and Wosk (1) employed a technique that registers impact accelerations in bone during walking. With the use of a low mass accelerometer, impact accelerations may be registered in several points of the skeleton such as the tibial tuberosity, medial femoral condyle, sacrum and forehead. Knowledge of the accelerometer placement site along with the foot plate force will permit a quantitative determination of a joint's functional capacity to attenuate the incoming force. Deviation from available normal values of force attenuation in various joints would thus suggest a functional abnormality of the bone, cartilage or soft tissue, i.e. the natural shock absorbers of the human skeletal system.

METHODS

The twenty-seven subjects (mean age: 50.6 yrs $\pm$ 16.8 SD) who were evaluated by the accelerometer technique were clinically classified as "normal", "osteoarthritic" or "possible osteoarthritic". The eleven subjects who had no history of knee pain, trauma, swelling or stiffness and had no evidence of knee pathology on physical examination, were assigned to the "normal" group. In addition the eleven patients who suffered from pain, trauma, swelling or stiffness in one or both knees were assigned to the "osteoarthritic" group. All eleven of these subjects were previously diagnosed by their physician as having osteoarthritis. Five subjects were assigned to the "possible osteoarthritic" group. These individuals, although asymptomatic, were identified to be at high risk for development of osteoarthritis based upon the presence of one of the following factors: history of trauma, genetic susceptibility, occupation and age. Physical examination of this group revealed no evidence of early osteoarthritic changes.

Single axis accelerometers (Entran models) were attached below and above each knee on each subject (one on the anterior tibial tubercle and another on the lateral femoral condyle). The subject was instructed and trained to walk a figure "8" pattern on a 3.66 meter by .86 meter walkway at a speed approximately 1.66 meters per second. The amplified signal was recorded on a strip chart recorder, an FM instrumentation tape recorder and sampled (at 1000 Hz) by an analog to a digital convertor which was connected to a microcomputer. The data was analyzed utilizing a series of software programs developed at the Biomechanics-Ergonomics Research Laboratory of the Department of Environmental Health, College of Medicine, University of Cincinnati. The two parameters of the accelerogram evaluated were the absolute peak to peak values of the waveform produced by the heel strike and the frequency contents within the selected waveform. The amplitude damping ratio (ADR), i.e. the ratio of the peak value of acceleration at the anterior tibial tubercle to the peak value of the lateral femoral condyle was determined for each knee. In addition, a Fast Fourier Transform (FFT) analysis of a selected acceleration waveform associated with each heel strike was conducted. The first 51 harmonics of the FFT were determined. The parameters utilized in analyzing the first 100 Hz of the FFT waveform included: the number of peaks, the value of the frequency of each peak, the decibal (dB) down value for each pair of successive peaks, and the area under the FFT curve.

RESULTS AND DISCUSSION

The ADR for the eleven normal subjects was 1.39 $\pm$ .18 SD, while the ADR for the osteoarthritic group was 1.19 $\pm$ .10, which was statistically significantly different at $p < .0001$. Such decrement in shock absorbing capacity in the diseased group was expected. The occurrence of the number of peaks in the FFT waveform, up to 100 Hz, varied with the clinical condition. One of the preclinical descriptors of osteoarthritis has been considered to be the altered material properties of subchondral bone. The altered material property manifests itself as the stiffening of subchondral bone. Therefore, under impact loading of the heel strike, the accelerogram (at the anterior tibial tubercle) obtained from the osteoarthritic patients would show higher frequency contents than those found in the normals. All eleven normal subjects demonstrated one or two peaks, while all eleven in the osteoarthritic group were

observed to have at least three distinct peaks in the high frequency range. The four subjects with mild osteoarthritis were noted to have three peaks, while four peaks were observed in the seven subjects with moderate to severe osteoarthritis. The frequency distribution of the peaks, up to 100 Hz, revealed higher frequencies in the osteoarthritic group. Comparison of the dB down for the first and second peak in the normal and eleven osteoarthritics revealed statistically significant difference at $p < .001$. A lower dB down in the osteoarthritic group implied higher (than normal) contributions by the second frequency peak in the FFT plot. The difference in the area under the FFT curve up to 100 Hz for the eleven normal and eleven osteoarthritic subjects was statistically significant at $p < .05$. The area values were higher for the osteoarthritic group than those of normals.

The effect of chronic, asymmetric, repetitive impulse loading to the subchondral bone of weight bearing joints appears to be a major factor in the development of osteoarthritis. The physiologic response of the bone to this loading results in stiffening of the subchondral bone. Spatial reorientation of the microtrabeculae, stiffening of the subchondral bone and the development of stress concentrations precede the involvement of the overlying articular cartilage in the development of osteoarthritis. The results obtained from the present study are consistent with the expected data as related to the biomechanical properties of stiffened bone, i.e. decreased shock absorbing capacity and higher frequency contents on the impact accelerogram.

The results of this clinical investigation do suggest that this quantitative non-invasive in-vivo technique for the identification of individuals or populations at risk for the development of osteoarthritis and/or the presence of preclinical disease may indeed have merit.

REFERENCE

1. Voloshin, A. and Wosk, A., "Shock absorption of meniscectomized and painful knees: A comparative in-vivo study". J. Biomed. Engr. 5: 157-160, 1983.

USE OF STATIC PRE-LOADING IN ESTIMATION OF DYNAMIC STRENGTH WITH THE KIN-COM DYNAMOMETER

V. PIETTE, C. RICHARDS and M. FILION

Neurobiology laboratory
Faculty of Medicine
Laval University
Quebec, G1K 7P4

INTRODUCTION

In the measurement of dynamic muscle strength with isokinetic dynamometers, several methodological factors interfere with the estimation of true dynamic capacity in the early part of the movement, especially at higher velocities. In studies before 1983, with the Cybex isokinetic dynamometer, forces were not recorded during the initial free acceleration phase. Moreover, once a selected speed of movement was attained, the impact torque caused by the sudden braking of the accelerating segment created oscillations in the torque-angle curves. Because of that, many investigators have discarded the first part of the torque-angle curves. These problems have been corrected by controlling acceleration at the beginning of the movement (2). However, few have emphasized the fact that dynamic forces recorded during the rise-time of muscle tension underestimate the maximal dynamic muscle capacity. This rise-time period has been attributed to several factors including the time needed to recruit motor-units and to stretch the series elastic components of muscle. To minimize the underestimation, Gransberg and Knutsson (2) have suggested to allow sufficient time to reach maximum tension before the onset of movement. They did not give any other guidelines, however, for the determination of this pre-loading. Therefore, with a Kin-Com dynamometer, we tested the effects of different static pre-loading levels on isokinetic force-angle curves obtained during maximal voluntary contractions of the knee extensors at 30°/s and 180°/s.

METHODOLOGY

The maximal static and dynamic capacity of the knee extensor muscles of 5 healthy men was evaluated with the computer-controlled Kin-Com dynamometer. First, we measured the peak rate of tension development and the force during maximal voluntary static contractions of the knee extensors at 90°, 75°, 60° and 45° of knee flexion. Two weeks later, we measured the force developed during maximal voluntary isokinetic contractions through a 90° arc at 30°/s and 180°/s, each movement permitted only after attainment of a predetermined level of the maximal static tension. These levels were set at 0%, 50% and 100% of the maximal force recorded just prior to the dynamic tests with the knee at 90°. Differences in the shape of the force-angle curves and in the angle of peak force were emphasized in the analysis. During both the static and dynamic contractions, the EMG activity in the quadriceps was recorded with surface electrodes and displayed as time-averaged rectified EMG (time constant = 20 and 200 ms) with a Grass polygraph.
Technical note: The controlled acceleration phase of the Kin-Com dynamometer is fixed and dependent on the selected speed. At speeds of 30°/s and 180°/s it covers the first 2 and 20 degrees of movement (about 75 and 150 ms) respectively.

RESULTS

The force-time curve of the knee extensors (Fig. 1) shows that 50% and 90% of the maximal static tension is reached in 80 and 475 ms respectively. The diamonds, in figure 2, show the maximal static force at 90°, 75°, 60° and 45°. The peak of the dynamic force-angle curve at 30°/s without pre-loading nearly reaches the maximal level of static force. This is not the case for the movement at 180°/s and the peak occurs later. Note that in this case the dynamometer is controlling the acceleration, and the velocity is therefore not constant, during the major part of the rise in force, as indicated by the interrupted line. Figure 3 shows force-angle curves obtained at 180°/s with 3 levels of pre-loading. The ANOVA test indicates a significant difference ($p<0.01$) between the 3 curves only in the first 15 degrees of movement: from 90° to 75°; that is when the acceleration is controlled by the dynamometer. The lack of difference later in the curves explains why the 5° shift of the angle of the peak force (from 63 ± 4.4° without pre-loading to 68 ± 3.2° with 50% pre-loading) is barely perceptible in the figure. At 30°/s the difference between the curves at the 3 levels of pre-loading (not illustrated) is significant only in the first 5 degrees of the movement and the angle of the peak force (77 ± 7°, see Fig. 2) did not change significantly with pre-loading.

DISCUSSION

In the isokinetic curves previously described in the literature, underestimation of muscular force, with free acceleration dynamometers, is manifested by two observations: a tendency for the force nurves to show the largest isometric-isokinetic difference at the beginning of the movement and a shift in the peak force angle with increasing speed of testing (4,5,7,8). With the use of acceleration control in this study, the force was recorded at the beginning of the movements. As indicated in methodology, however, the pattern of controlled acceleration of the Kin-Com dynamometer varies with the selected speed. This fact limits the force comparisons to the isokinetic range (ex: 70°-10° at 180°/s). Nevertheless, we observed a difference in the angle of peak force in the three velocities tested (0°/s, 30°/s, 180°/s). Assuming with Wickiewicz (8) that the rise time to peak tension in the muscle is relatively constant regardless of the test speed, the arc length covered in that time varies with velocity even with controlled acceleration. For example, according to the force-time curve (Fig. 1) the 80 ms delay required to reach 50% of the maximal static tension corresponds in the force-angle curves, to a displacement of 2° at 30°/s, compared to about 10°, at 180°/s.

Static pre-loading was used to eliminate part of the rise-time phase, as suggested by Gransberg and Knutsson (2). With pre-loading levels of 50% and 100%, the main effects on the force-angle curves at 180°/s (Fig. 3) are the increased amplitude of forces in the first part of the curves and a shift in the angle of the peak force closer to that observed at 0°/s and 30°/s. Because of the extent (20°) of the controlled acceleration phase, a peak that would have occurred before 70° could not have been considered. With maximal pre-loading (100%) the curve drops, in the controlled acceleration range, as expected from the force-velocity relationship. Thereafter, this curve intersects the 50% curve and decreases according to the force-angle relationship.

In conclusion, when controlled acceleration lasts as long as 20°, the use of pre-loading does not give a better estimate of the maximal dynamic capacity at 180°/s. Indeed, the curve obtained without pre-loading at this speed does not significantly underestimate the forces in the early isokinetic range (comparisons were not made in the controlled acceleration phase).

REFERENCES

1. Cavagna, G.A., et al. J. Appl. Physiol. 24: 21-32, 1968.
2. Gransberg, L., et al. Acta. Physiol. Scand. 119: 317-320, 1983.
3. Komi, P.V. Scand. J. Sports Sci. I: 2-15, 1979.
4. Moffroid, M., et al. Phys. Ther. 49: 735-746, 1969.
5. Perrine J.J., et al. Med. Sci. Sports 10: 159-166, 1978.
6. Smith, G.L. J. Biochem. 6: 79-92, 1973.
7. Thorstensson, A., et al. J. Appl. Physiol. 40: 12-16, 1976.
8. Wickiewicz, T.L. J. Appl. Physiol. 57: 435-443, 1984.

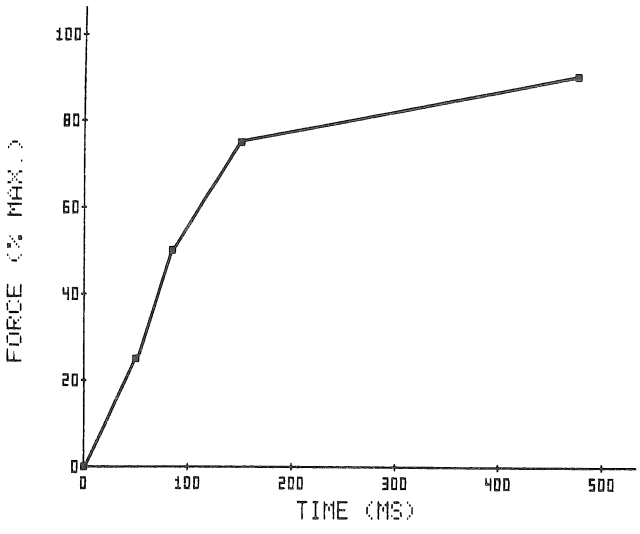

Figure 1 Normalized static force-time curve determined during maximum voluntary knee extensions (90° of knee flexion) at peak rate of tension development. Each point represents mean values for 5 subjects.

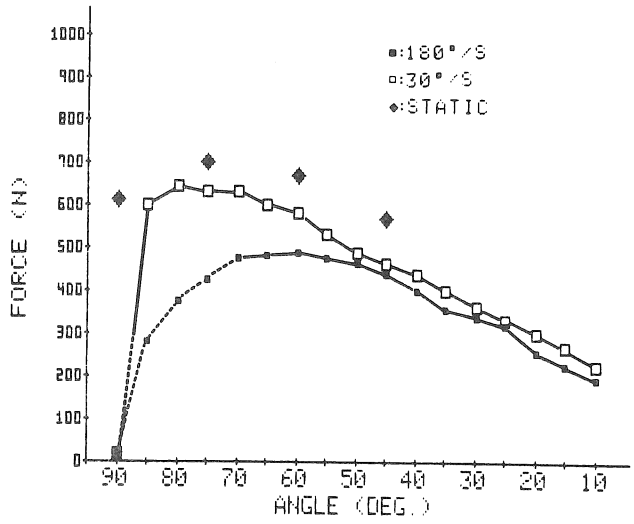

Figure 2 Comparison of force-angle curves recorded during maximal voluntary knee extensions at 0°/s (static), 30°/s and 180°/s without pre-loading. Controlled acceleration phase is indicated by interrupted line (----).

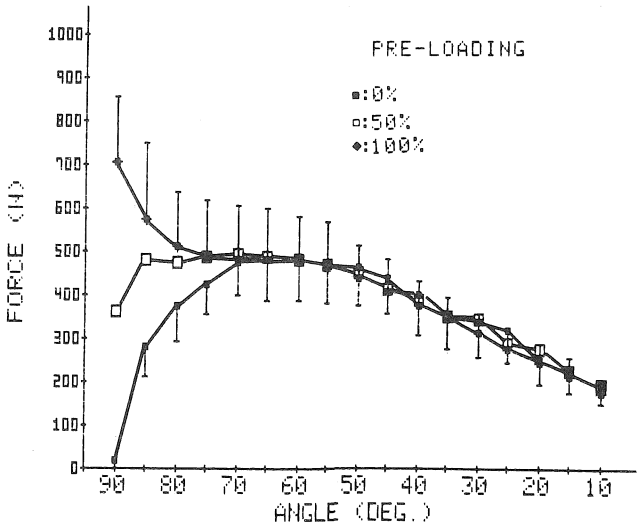

Figure 3 Force-angle curves recorded during maximal voluntary isokinetic knee extension movements at 180°/s with three different levels of pre-loading. Vertical bars indicate 1 S.D.

Acknowledgements

The authors thank Daniel Tardif and Lise Laroche for technical assistance. This work was supported by l'Institut de recherche en santé et en sécurité du travail du Québec.

MUSCLE UTILIZATION IN GAIT DETERMINED BY A PHYSIOLOGICAL CALIBRATION OF EMG

M.C. NORMAND, C.L. RICHARDS and M. FILION

Department of Physical Activity
Université du Québec à Trois-Rivières
and Neurobiology Laboratory
Faculty of Medicine
Laval University
Quebec, G1K 7P4

INTRODUCTION

The measurement of the intensity of muscle activation is an essential prerequisite to determine the functions of muscles during movements and the deficits of impaired muscles. Assuming that the intensity of muscle activation is best represented by measurements of the force generated by muscle contraction, one must admit that it is technically difficult to measure directly the force generated by muscles during complex movements. EMG measurements are, however, relatively easy to record during complex movements, but the relation between force and EMG varies with the length of the muscles and the speed of contraction. A correct measure of intensity of muscle contraction by EMG analysis must therefore take into account these two variables. The present paper reports the results of such an analysis. The EMG recorded during gait was calibrated with respect to that produced during a maximal voluntary isokinetic contraction (MVC) by the same subject, the same muscle, at the same angle and, grossly, at the same velocity. We believe the resulting curves of the percentage of muscular utilization are a useful measure of the intensity of muscle contraction. For example, they are sensitive to functional interactions of bi-articular muscles, and greatly facilitate the measure of coactivation.

REVIEW AND THEORY

Jonsson (1) stated that electromyography offers the possibility of obtaining a relative measure of the force of muscle contraction. In fact, some researchers have estimated the force or the intensity of contraction from EMG (2-7). All of these studies, except one, used the EMG produced during isometric MVC as a reference. Richards (6) used the peak EMG produced during isokinetic MVC at 30°/s as a reference to compare EMG levels in five dynamic activities. However, as emphasized by Bouisset (8), the tension developed by a muscle for a constant level of excitation depends on its length and velocity of shortening. Therefore, in order to estimate the muscular force from EMG, it is necessary to take into account muscle length and contraction velocity. The purpose of this study was to carry out such an analysis for muscle activations recorded during level walking.

METHODOLOGY

Electromyograms were taken with surface electrodes fixed to the skin over the rectus femoris (RF) and biceps femoris (BF) in 10 normal men. The mean age was 27.3, the weight 70.2 Kg and the height 176.2 cm. First, all subjects executed three knee extension and flexion movements at 30, 180 and 300°/s through a 90° arc. For each muscle and each subject we established 270 EMG reference values (90 degrees x 3 speeds). After completion of the isokinetic movements the electrodes were left in place and three footswitches were taped to the ipsilateral shoe sole. The EMG activity was then recorded during 20 gait cycles. Kinematic parameters (angular displacements and velocities) were measured by a LED system (9). The percent utilization was established as follows: for a given subject, at heel strike for example, the knee is at 172°, the angular velocity is 160°/s and the rectified time averaged EMG of the RF 200 uV; the reference value is the EMG recorded (ex: 1000 uV) at 172° during knee extension at 180°/s (the closest speed); the percentage is calculated by dividing the EMG produced during walking (200 uV) by that recorded during MVC (1000 uV); therefore the percent utilization for the RF is 20% at that specific point in the gait cycle. The operation is repeated at 5% intervals throughout the gait cycle.

RESULTS AND DISCUSSION

Figure 1 presents the curves of angular displacements of the hip (A) and knee (B), the activation of RF (C) and BF (D), the percent utilization of RF (E) and BF (F) and the coactivation of RF and BF (G) during the gait cycle. At heel strike, the percent utilization is probably required to stabilize the knee as it flexes in early stance (B and C). The highest and most variable percent utilization (15.1%) is at 40% of the gait cycle and likely related to stabilization of the knee (B) and to restraint of hip extension (A). The mean percent utilization of RF during the gait cycle was 8.5%. The peak percent utilization for BF (F) occurs at the end of the swing phase (31.1%). By comparing activation (C and D) and utilization curves (B and F), we observe that the patterns are similar except at 40% of the walking cycle where there is an increase in percent utilization which does not show on the activation curves. At this point both ends of the bi-articular muscles are sollicited at the same time. The coactivation of RF and BF during the gait cycle is given in G. In order to measure coactivation we simply superimpose the utilization curves since the later are normalized activation curves. The common area of the two curves is the measure of coactivation. The peak coactivation value (14.3%) occurs during weight bearing on a flexed knee, while the mean coactivation level during the gait cycle is 7.5%.

Acknowledgements:

We thank D. Tardif and Lise Laroche for technical assistance. This work was supported by l'Institut de recherche en santé et en sécurité du travail du Québec (IRSST).

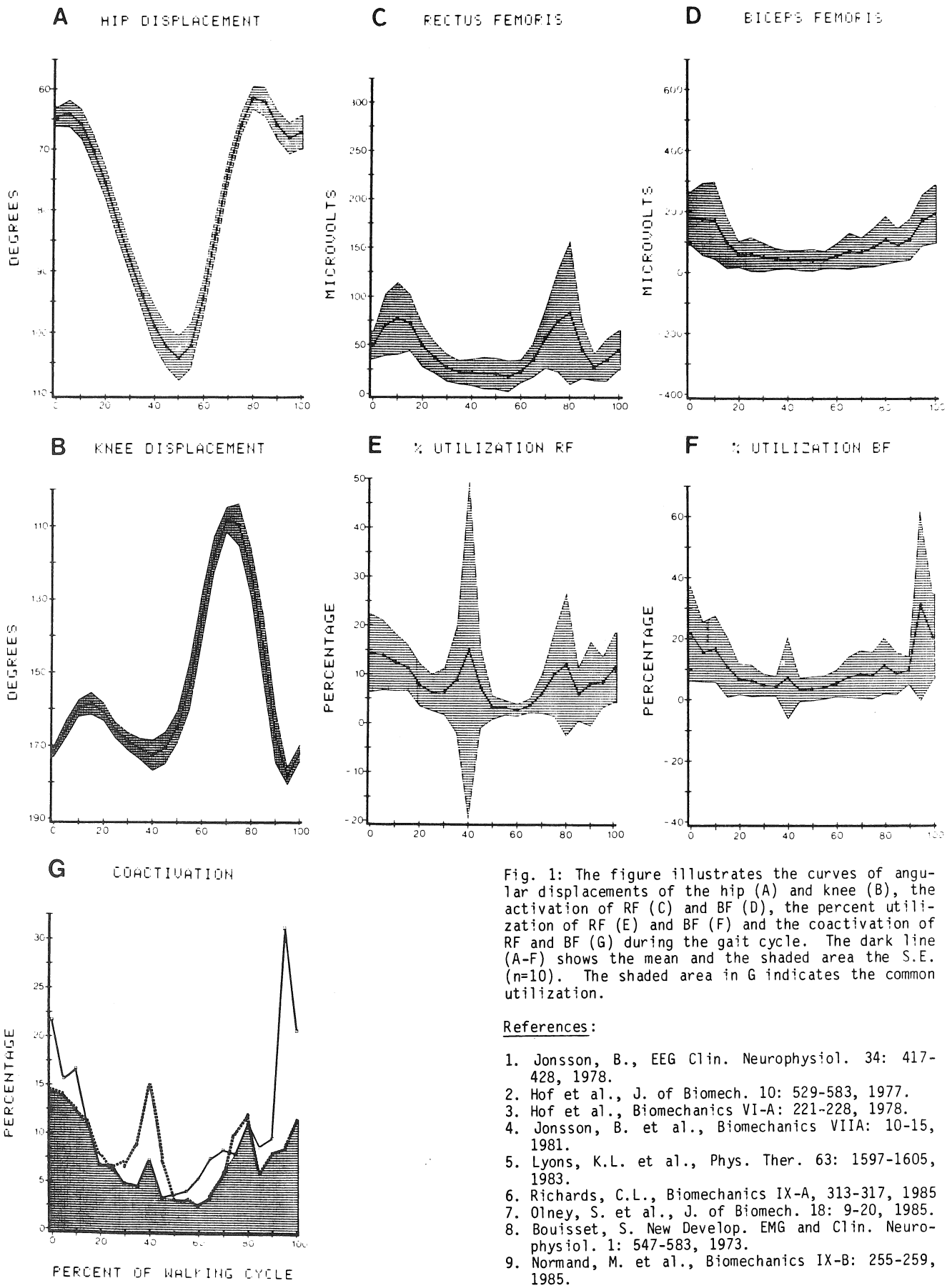

Fig. 1: The figure illustrates the curves of angular displacements of the hip (A) and knee (B), the activation of RF (C) and BF (D), the percent utilization of RF (E) and BF (F) and the coactivation of RF and BF (G) during the gait cycle. The dark line (A-F) shows the mean and the shaded area the S.E. (n=10). The shaded area in G indicates the common utilization.

References:

1. Jonsson, B., EEG Clin. Neurophysiol. 34: 417-428, 1978.
2. Hof et al., J. of Biomech. 10: 529-583, 1977.
3. Hof et al., Biomechanics VI-A: 221-228, 1978.
4. Jonsson, B. et al., Biomechanics VIIA: 10-15, 1981.
5. Lyons, K.L. et al., Phys. Ther. 63: 1597-1605, 1983.
6. Richards, C.L., Biomechanics IX-A, 313-317, 1985
7. Olney, S. et al., J. of Biomech. 18: 9-20, 1985.
8. Bouisset, S. New Develop. EMG and Clin. Neurophysiol. 1: 547-583, 1973.
9. Normand, M. et al., Biomechanics IX-B: 255-259, 1985.

BILATERAL ANALYSIS OF THE LOWER LIMBS DURING WALKING IN NORMAL INDIVIDUALS

Sylvia Õunpuu
David A. Winter

Department of Kinesiology
University of Waterloo
Waterloo, Ontario N2L 3G1

INTRODUCTION

The assumptions of symmetry in normal walking are made frequently in both the laboratory and in clinical research due to reasons such as simplification of data collection and analysis and equipment limitations. Few attempts have been made to validate these assumptions and certain problems exist concerning the normalization of signals and quantification of differences. It appears from the literature that certain aspects of gait are symmetrical while others are not. Hamill (1), for example, found that normal healthy subjects exhibit a symmetrical gait pattern with respect to ground reaction descriptors. Hannah (2), however, reported that reasonable symmetry exists in kinematic (joint angles) data of the lower limb. Chodera (3), concluded that normal walking was not symmetrical in nature after analysing foot print records. It is obvious that a clear definition of what is considered asymmetrical or not does not exist. A multifaceted study looking at both the lower limbs is needed in order to be comprehensive. Thus, the purpose of this study was to determine in normal individuals when walking whether there are systematic asymmetries in the left and right lower limbs with respect to electromyographic, kinematic and kinetic variables.

METHODS

The data aquisition was partitioned into two sections the first, EMG collection (ten subjects) and the second kinematic variable collection (four subjects). Anthropometric measurements and tests for footedness were made on each subject.

Seven lower limb muscles were selected bilaterally including the tibialis anterior (TA), medial gastrocs (MG), soleus (SOL), rectus femoris (RF), vastus lateralis (VL), medial hamstrings (MH), and the gluteus maximus(GM). A major subproblem dealt with was the normalization procedure for the EMG signals. It was decided that normalization would be completed by applying equal, known, isometric torques to each muscle pair. The contraction level selected fell within the level of activity found in the specific muscle during normal walking. Ensemble averages (4), were then represented as a percentage of the normalization factor (an average of at least three calibration trials). Subjects performed one walk an a long walkway in which 12-14 consecutive strides of EMG were collected on both sides simultaneously.

Kinematic data were collected by cine camera at 50 fps. The non-camera side was modelled using a projection at the hip level and skin markers on the medial side of the leg. Care was taken to ensure that the markers were symmetrically placed on the appropriate bony landmarks. The validity of this model was confirmed by using two cameras and comparing the results obtained from the medial side markers with those on the lateral side. Filming was done concurrently with the collection of ground reaction forces and moments from two AMTI force plates imbedded into the walkway. A total of four trials were completed.

RESULTS

Preliminary results from the EMG trials of one subject are presented. Table 1 shows the mean ensemble level of EMG across the stride in uV's, as a % of calibration contractions, plus the coefficient of variation (CV). CV is, in effect, a single measure of percentage variability over the stride (4).

Table 1: Comparison of the EMG results between right and left sides.

MUSCLE	RIGHT SIDE $\bar{X}$ (μV)	RIGHT SIDE % cal.	RIGHT SIDE CV	LEFT SIDE $\bar{X}$ (μV)	LEFT SIDE % cal.	LEFT SIDE CV
GM	24.6	19.1	51	12.6	9.1	49
MH	71.3	44.7	53	41.9	14.5	19
RF	23.0	11.0	33	61.0	18.4	51
TA	157.0	108.3	34	137.0	136.0	46
MG	105.0	44.9	49	90.6	47.3	41
SOL	78.5	40.8	26	103.0	96.0	27

Examples of bilateral relative angle, joint moment and power differences in the ankle, knee and hip were plotted and are illustrated in Figures 1, 2 and 3 respectively.

DISCUSSION

As is evident in Table 1 by the non-normalized EMG recorded in uV's, the level of activity was not symmetrical between muscle pairs. This result, however, may be confounded due to such factors as skin thickness, adipose tissue, differences in muscle bulk, etc. Normalization, to the EMG level produced by the applying the same torque, illustrated that differences still existed and in most cases there was no improvement in symmetry (as indicated by lower differences in the normalized values). The largest dif-

ferences were seen during peak levels of contraction. This finding is in agreement with the results of Arsenault and Winter (5), who found bilateral amplitude differences at the uV level and when the EMG was normalized to %MVC for the rectus femoris and soleus muscles. The CV's reported are in agreement with previous results recorded in the data base at the University of Waterloo during the past 5 years. Thus, although the EMG seems to be bilaterally phasically similar it does not appear that symmetry in normal individuals while walking can be assumed with respect to amplitude measurements.

Table 2: Summary of kinematic and kinetic results.

JOINT	ANGLE (DEGREES)		MOMENT (N.m)		POWER (W)	
	RMS	MAXDIFF	RMS	MAXDIFF	RMS	MAXDIFF
ANKLE	2.30	4.65	6.86	16.01	16.79	58.86
KNEE	9.42	14.32	11.35	28.57	19.53	57.30
HIP	6.55	12.10	5.56	9.22	9.91	19.10

As seen in Figures 2, 3 and 4 the largest right/left differences occur during the stance phase. The RMS differences (Table 2), were larger at the knee than at the ankle or hip in all of the three measures. A maximum difference of 14.3 degrees occured between the knees at push-off. During early stance, a difference of 28.57 N.m's and 57.3 W's was found in the knee moments and powers respectively. Calculations of work done (J) at push-off (Figure 3), for example, were all asymmetrical at the three joints analysed: right ankle- 150/left ankle-86, the right knee- 5/left knee- 37 and the right hip- 134/left hip- 115.

CONCLUSIONS

It is evident from the above data that the assumptions of symmetry are not valid in normal walking. Knowledge of expected differences in normal walking will aid in the analysis of pathological gait and in our understanding of the normal neural control patterns.

ACKNOWLEDGMENTS

The authors would like to acknowledge the funding of NSERC, grant #A2917 and the MRC grant #MT4343. The tecnical assistance of Mr. Paul Guy was also greatly appreciated.

REFERENCES

1. Hamill, J. et al. Med.Sci. in Sports and Exer., 15:170, 1983.
2. Hannah, R.E. et al. Arch. Phys. Med. Rehab., 65:155-158, 1984.
3. Chodera, J.D. Physiotherapy, 60:179-181, 1974.
4. Winter, D.A. Arch. Phys. Med., 65:393-398, 1984.
5. Arsenault, B. et al. Arch. Phys. Med. (in press), 1986.

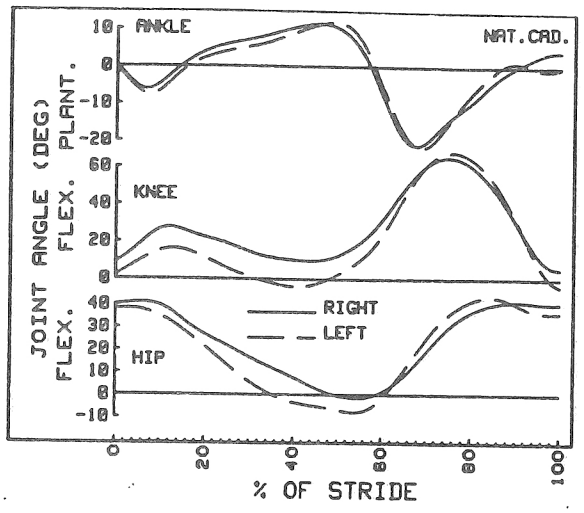

Figure 1: Comparison between right and left joint angles.

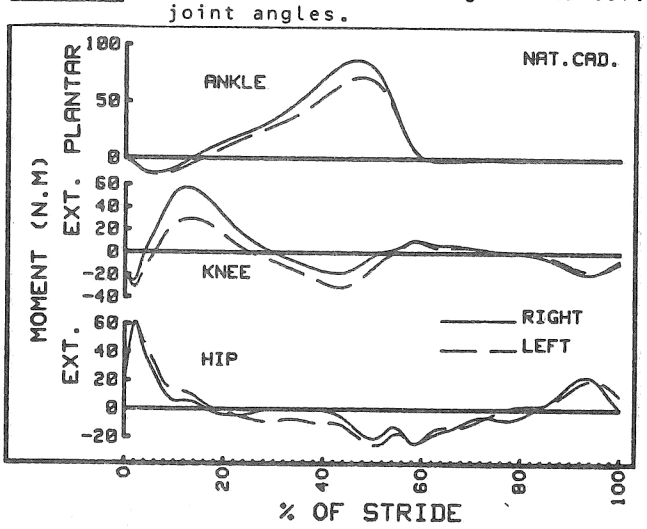

Figure 2: Comparison between right and left joint moments.

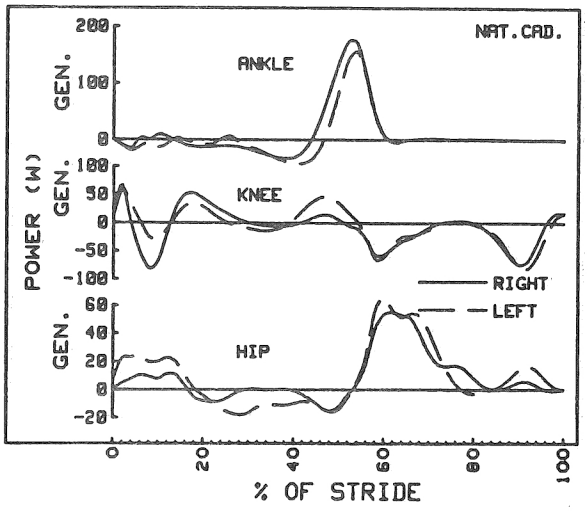

Figure 3: Comparison between right and left joint powers.

ASYMMETRY IN LOADING TIMES BETWEEN THE NATURAL AND PROSTHETIC LIMBS IN THE ABOVE-KNEE AMPUTEE

Wendy O'Connor, Physiotherapy Department, Royal Ottawa Regional Rehabilitation Centre

Ottawa, Ontario K1H 8M2

INTRODUCTION

Subjective gait analysis of the above-knee amputee suggests that the prosthetic limb is loaded slower than the natural limb. Clinically, it was felt that to improve the gait pattern, the amputee should load his prosthetic limb more rapidly. To verify this, objective measurement of vertical force patterns were taken from 14 amputees and 5 normal subjects using a hidden forceplate in the gait laboratory at our centre. The amputees were asked to walk at their natural walking speed. The normal subjects were recorded at slow, moderate and natural walking speeds. Measurements were taken from these forceplate readings to determine the time required for the limb to reach maximum weight acceptance. This data indicated that the time required for the above-knee amputee to fully load their prosthetic limb was similar to the loading time for normal subjects at similar walking speeds. Therefore, it was actually the natural limb of the above-knee amputee which was being loaded more rapidly than would be expected from the normal data at similar speeds.

REVIEW AND THEORY

A standardized subjective gait evaluation of above-knee amputees in our centre indicated an asymmetry in loading. This asymmetry has been observed by Koerner (1). A training program at our centre using a limb load monitor (6) to increase the speed of loading of the prosthetic limb showed that the amputee walking at slower speeds was loading his prosthesis slower than his natural limb.

Symmetry of lower limb motions are believed to be important in energy efficient walking (3).

It is felt clinically that the ability to load a prosthetic limb may reflect the impact of a number of factors such as prosthetic fit and comfort, residual limb pain, balance deficits or mechanical discrepancies between ability of prosthetic and natural limbs.

For these reasons, we felt that improved symmetry would likely result in improved gait.

The purpose of this pilot was to compare the speed of loading of each limb of the above-knee amputee to normal subjects at comparable walking speeds, by using vertical force patterns.

METHODOLOGY

The gait laboratory provides kinematic measurements with electrogoniometers, temporal-spatial data from footswitches, 2 video cameras and a forceplate concealed in a 10 X 5 metre hallway. Data in the lab is collected on a PDP II/34 computer.Figure 2&3.

Forceplate data included 21 runs by 14 above-knee amputees (ages 23-78 years). Sixteen of these runs were done without walking aids. Data from 5 normals was also collected at slow, moderate and natural speeds. Slow was defined as 0.3 meters/sec to .7 meters/sec, and moderate as greater than .7 m/sec to 1.0 m/sec. Each normal subject did 3 runs bilaterally at each speed.

The time to peak loading was calculated from the X axis of the vertical force patterns for all of the subjects (see figure 1). The data from the amputees was then compared to the normal subjects at comparable speeds.

RESULTS & DISCUSSION

The amputee subjects walked at varying speed, but specifically 9 runs were at the .3 to .7 m/sec "slow" speed, 9 runs were at the .71 to 1.0 m/sec "moderate" speed, and 3 were at the greater than 1.0 m/sec "natural" speed.

The groups were divided into these 3 groups to better enable us to compare peak loading at different velocities.

The data from the normal subjects showed gait velocities to be proportional to time to maximum weight acceptance. This has been confirmed by other research (6). Time required for maximum weight acceptance decreased as walking speeds increased.

The loading times for the prosthetic limbs were found to be very similar to those of the normal subjects at similar speeds. It was the natural limb loading times that were more rapid than expected.

Our normal subjects showed symmetry in loading times between right and left limbs at similar velocities.

Asymmetry in gait has been of some concern to researchers and clinicians as it may indicate higher energy expenditure and has less esthetic appeal. It may reflect factors such as pain, poor prosthetic alignment of fit, or balance deficits.

For these reasons, and as the normals showed symmetry of vertical force readings, it seems reasonable to train above-knee amputees to improve gait by improving symmetry.

Further investigations into the above-knee amputee population walking at greater than 1.0 m/sec (our sample was small - 3), may provide more information about expectations of symmetry of forces and their natural walking speeds.

References

1. Koerner, Ilse, B. Normal Human Locomotion and the Gait of the Amputee, 1976.

2. Lower Limb Prosthetics, New York University, 1980.

3. Hannah, R.E., Kinematic Symmetry of Lower Limbs, Arch Phys Med & Rehabil, Vol 65, April, 1984, pg 155-158.

4. James, Urban, Oxygen Uptake & Heart Rate During Prosthetic Walking, Scand J Rehab Med 5: 71-80, 1973.

5. Skinner, Stephan R., M.D., The Correlation Between Gait Velocity and Rate of Lower Extremity Loading, Bull of Prosth Research, Vol 18, No 1, 1981, 303-304.

6. Follows, D. et al, A Rate Dependent Limb Load Monitor, Can Med & Biol Conf., Ottawa, 1984.

ACKNOWLEDGEMENT

The assistance of the Gait Laboratory Team is acknowledged with gratitude.

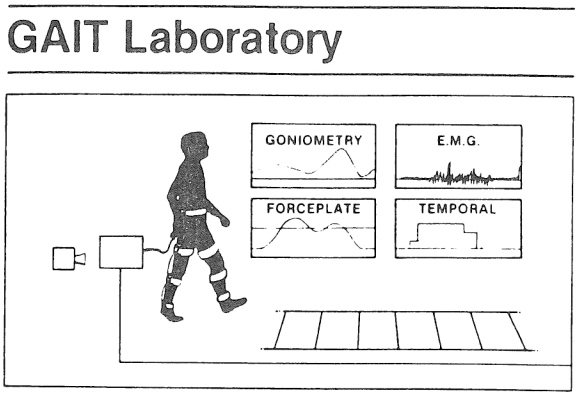

Figure #2 A graphic representation of our gait laboratory.

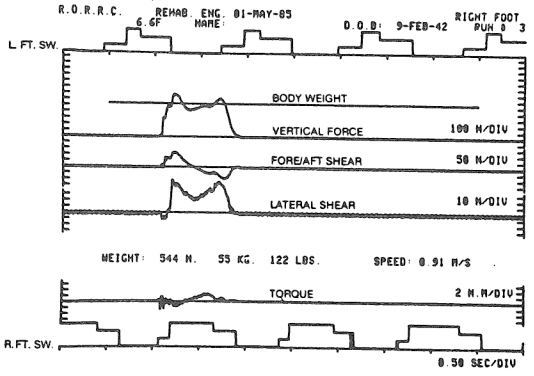

Figure #3 Force plate outputs showing vertical force, fore-aft shear, lateral shear, and torque.

Figure #1 An example of normal vertical force readings at varying velocities.

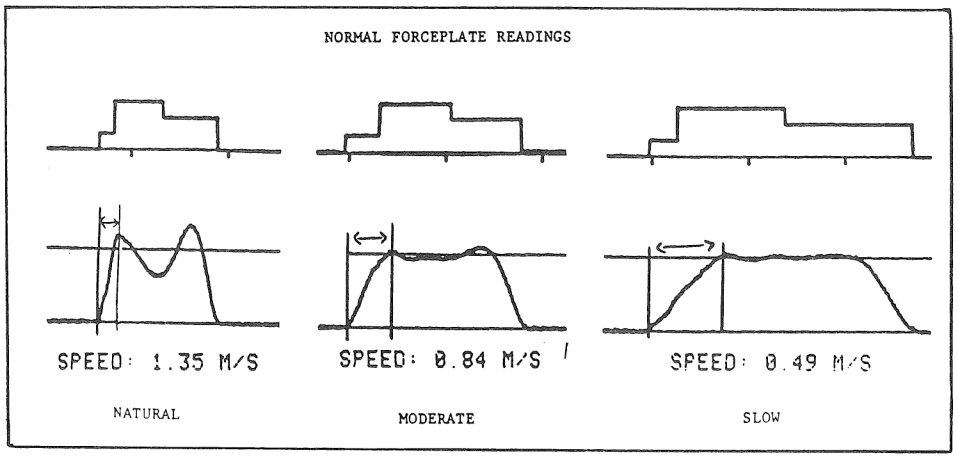

SYSTEM FOR LOCOMOTOR REHABILITATION

H. Barbeau, Ph.D., School of Physical and Occupational Therapy, McGill University

L. Finch, B.Sc. PT, School of Physical and Occupational Therapy, McGill University
M. Wainberg, B.Sc. OT, School of Physical and Occupational Therapy, McGill University

INTRODUCTION

One of the most important goals in rehabilitation is the restoration of safe near normal gait. Often even after training, some patients are still unable to walk well. Neurological gait studies demonstrate that the majority of patients are unable to support their body weight while moving forward (1). In fact, abnormal weight distribution and weight transference over the affected limb during stance, especially at slow walking speeds, is characteristic of neurological patients (2,3). We propose a new strategy based on the adult spinal animal model: a regime of progressively increasing the amount of weight supported by the patient during interactive locomotor training (4).

The purpose of this paper is to describe the progressive partial weight bearing training system developed for locomotor rehabilitation of neurological patients with impaired gait.

SYSTEM DESCRIPTION

The training system (figure 1) consists of a treadmill, a mounting frame, the external weight support (EWS) apparatus and data collection equipment. Unless otherwise indicated, the system was designed in-house.

EWS Apparatus

The patient, mechanically supported in a harness over the treadmill, is lifted by an electric motor (½ HP). The motor, on the upper frame, uses a gear box and slip gear which is manually controlled by the operator. Automotive seat belt strapping is used for lifting and attaches the motor to the force transducer (Figure 1B). The transducer, situated at the base of a double cantilever U-channel, is a Whetstone bridge type constructed of two pairs of strain gauges (Measurements Group Inc., EA-13-125BT-120) with an output of 1 volt/45 kg. The force measured by the transducer is normalized for each patient to 100 % of body weight and training levels are determined accordingly. The force transducer system is then connected by automotive seatbelt strapping via pillow blocks mounted on the tranverse beam to the patient's harness. The harness was conceived to support the patient in a vertical position without interfering with respiration or lower limb movement. Comfort was of prime importance with particular attention to the shoulder and lower pelvic regions. This custom designed harness supports the patient about the pelvis and lower abdomen with 10 cm wide mountaineering padding and strapping. The major points of attachment employ quick-eject parachute latches. In case of emergency, it is possible to remove the patient from the apparatus and harness within 15 seconds.

Data Collection

Kinematic and electromyographic recordings are made of a series of walking trials at specific EWS levels and treadmill speeds. Each training session is of 1 hour duration.

A recording of EWS, foot floor contact (footswitches (Tapeswitch Systems of America) placed bilaterally beneath the heel, head of the 5th metartarsal, and the great toe) and EMG is shown in Figure 2. It can be noted in the raw EMG trace a high signal-to-noise ratio at a high pass of 10 Hz and the absence of crosstalk or movement artifact during treadmill locomotion. The interlimb (bilateral footswitch pattern) and intralimb (ipsilateral footswitch and EMGs) coordinations are typical of normal gait. In the EWS, the two peaks seen in each gait cycle correspond to the double support phases. With reflective markers affixed to specific anatomical landmarks, movement in the sagittal plane is videotaped (60 fps, exposure time 0.002 s). Identical time codes (Skotel Time Code Generator, TCG-80N) are recorded on videotape and on FM magnetic tape (with EMG, footswitches and EWS) to allow synchronization of this data and correlation of mechanical events with muscle activity. Data processing and analysis is performed off-line using interactive computer programmes (Digital PDP 11/34).

DISCUSSION

Conventional locomotor rehabilitation approaches have limitations, one of which is the inability to train simultaneously the three required components of locomotion: posture, balance and stepping. Consequently, rehabilitation outcomes are not always as desired, particularly in neurological patients. This system permits the development of a novel training strategy, via progressive grading of weight support during locomotion as well as the possibility of training simultaneously the three components of locomotion. Furthermore, the experimenter, interacting with the patient, is able to focus on specific aspects of gait by altering training parameters (treadmill speed, EWS) and more importantly, intervening directly during walking. Interactive locomotor training facilitates the treatment of postural instability and balance through a partial to full weight bearing progression. In combination with treadmill stimulation, this training also facilitates stepping and encourages smooth forward progression. In addition, other modalities such as cutaneous stimulation (5), stretching (6), electrical stimulation (7), and biofeedback (8) can also be incorporated. Preliminary studies on the effect of partial weight bearing on normal gait (9) and the applicability of progressive partial weight bearing treadmill training in patients with

incomplete spinal cord injuries (10) have been performed.

We are in the process of validating this treatment strategy in patients with neurologically impaired gait. These findings may form the basis from which this approach can also be applied in the treatment of neurological and orthopaedic patients in the early stages of recovery.

REFERENCES

1. Chin, P.L., et al. Studies in hemiplegic gait. IN Advance in Stroke Therapy, Rose, F.C. (Ed.). New York, Raven Press, 197-211, 1982.
2. Carlsoo, S., et al. Scand J. Rehab. Med. 6:166-179, 1974.
3. Mizrahi, J., et al. Med. Biol. Eng. Comput. 20:628-634, 1982.
4. Rossignol, S., et al. IN Development and Plasticity of Mammalian Spinal Cord, Spoletto (In press), 1986.
5. Rossignol, S., et al. State dependent responses during locomotion. IN Muscle Receptors and Movement, 1981, Taylor, A., Prochazka, A. (Eds.). New York, MacMillan, 389-402.
6. Sapega, A.A., et al. Phys. Sports Med. 9-57-65, 1981.
7. Vodovnik, L. CRC Crit. Rev. Bioeng. 6:63-102, 1981.
8. Binder-MacLeod, S.A. Biofeedback in Stroke Rehabilitation. IN Biofeedback Principles and Practice for Clinicians, Basmajian, J.V. (Ed.). London, Williams and Wilkins, 73-89, 1983.
9. Finch, L., Barbeau, H. Can. J. Neurol. Sci. 12:183, 1985.
10. Wainberg, M., Barbeau, H. Can. J. Neurol. Sci. 12:183, 1985.

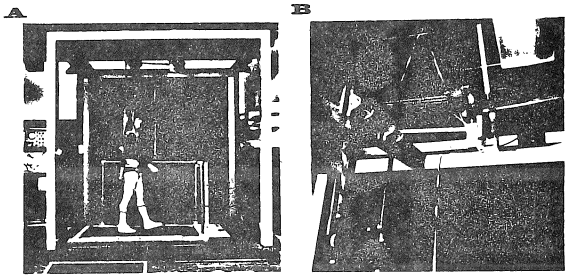

Figure 1. Figure 1A is a lateral view of the complete system. The subject is mechanically supported in a harness while walking on a treadmill. Figure 1B shows the transducer used to determine the amount of EWS provided.

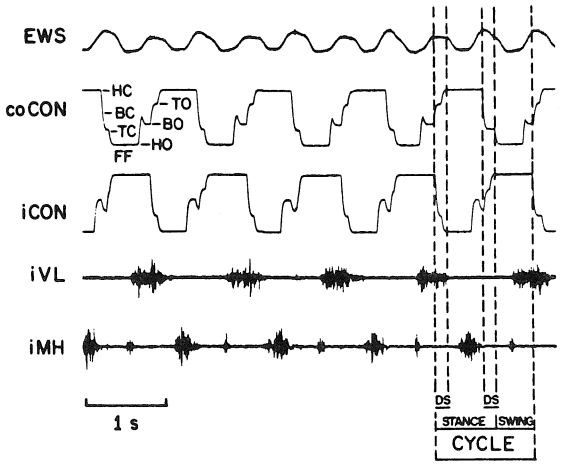

Figure 2. Figure 2 illustrates the EWS, the contralateral and ipsilateral footswitches and the EMG activity of the knee extensor Vastus lateralis (iVL) and the knee flexor Semitendinosus (iST) of a normal subject walking at a comfortable speed (.85 $m.s.^{-1}$) on a treadmill with 30% EWS. The critical events of a gait cycle are HC - heel contact, BC - ball contact, FF - foot flat, HO - heel off, BO - ball off, and TO - toe off. The phases of a gait cycle of the ipsilateral limb are DS-double support, stance, swing, and total cycle duration.

KINEMATIC ANALYSIS OF GAIT PATTERNS IN UNOPERATED CHILDREN WITH SPASTIC DIPLEGIA

O. Huk, H. Labelle, M. Duhaime, P. Allard
Centre de Recherche Pédiatrique, Hôpital Sainte-Justine,
Montréal, Québec, H3T 1C5

INTRODUCTION

The gait pattern of the cerebral palsied child with spastic diplegia is most typically described as "crouch gait" (1). However, not all spastic diplegic children have the classical crouch gait pattern. In fact, several combinations in postural attitudes of the lower extremity exist depending on the simultaneous joint interactions of the ankle, knee and hip. These postural combinations have been qualitatively and clinically described (2). A review of the literature, however, fails to reveal any scientifically conducted studies classifying the spastic diplegic gait patterns by means of quantitative data. A long term study at our gait laboratory has been undertaken to identify a standardized data base of specific gait patterns in spastic diplegia. This paper reports the kinematic results of a preliminary retrospective pilot study undertaken to investigate if indeed distinct gait patterns could be identified. Analysis of joint angular displacement data identified 4 such patterns.

REVIEW AND THEORY

As a result of a primary central nervous system lesion, with limited selective motor control and unmasking of primitive locomotor patterns, the gait of the spastic diplegic child is complex to evaluate. The predictive weakness of clinical evaluation in cerebral palsy gait and the often erroneous surgical procedures planned solely on the basis of clinical observation was noted by Phelps as early as 1932 (3). The lack of correlation between clinical evaluation and gait performance is also well known (4,5).

Sutherland et al. (1), are perhaps the first to demonstrate one of the gait patterns of the diplegic child, namely, the crouch gait. The joint angular displacement data reported in this work reveals excess stance knee flexion and ankle dorsiflexion. This study, however, focuses on a selected group of 4 patients all of whom had previous Achilles tendon lengthening procedures. Simon et al. (6) describe the kinematics, kinetics and EMG profiles of spastic cerebral palsied children with genu recurvatum. Two different types of genu recurvatum are identified, an early and late stance phase. This study includes a heterogenous group of 15 patients with a major proportion having had previous surgical interventions.

The vast heterogeneity of patient groups as well as the specificity of focus in each study precludes a comprehensive synopsis of the gait abnormalities in spastic diplegia. These problematic issues have brought to light the need for objective and quantitative classification of gait patterns in a homogenous group of unoperated spastic diplegic children to serve as a reference baseline in the management of the diplegic gait disorders.

METHODOLOGY

Walking films of 16 spastic diplegic children of average age 7 years (± 4 years) were analysed for this study. The inclusion criteria were no previous surgery of the lower limbs and ability to walk without ambulatory aids. The clinical evaluations of the children were obtained from their medical dossiers.

Each child was filmed walking barefoot and wearing underpants. Adhesive markers were used to identify 6 anatomical landmarks on the lateral aspect of each side of the lower limb and trunk. Each child was instructed to walk at natural cadence on an elevated walkeway 10 meters in length. A Hycam II high speed camera was used to film the sagittal plane motion at a rate of 100 frames/sec.. The films were projected by a variable speed projector onto a Houston digitizing table.

A single representative stride was digitized for each side of the body to obtain the body marker coordinates for each frame. The digitized coordinates were transmitted via a graphic terminal to a PDP 11-23 microcomputer for kinematic analysis. The calculated sagittal plane joint angular displacement data included the degree of ankle dorsiflexion/plantarflexion and the degree of knee and hip flexion/extension. Percent stance was also calculated for each stride digitized.

Final group identification was based on the division of joint angular displacement curves according to similarities in curve trends.

All angular curves belonging to the same group were ensemble averaged at 5% intervals and represented as a function of 100% stride. The averaged angular curves are compared to curves constructed from normative adult joint angular displacement data reported by Winter (7). An adult sagittal plane angular pattern is established by 2 years of age (8,9) and as normative data for children is not well established, it was felt justified to use normal adult values for comparison.

RESULTS AND DISCUSSION

Four major gait patterns were identified. Limb symmetry was seen in 14 of 16 patients. The average percent stance for the entire group of patients was 66% ± 5%. There were no significant differences in percent stance between groups.

Group 1 (Fig. 1) consists of 13/32 limbs (41%) and is characterized by excess plantarflexion and excess knee and hip flexion throughout the entire stride period. At the beginning of each stride, weight was accepted by the metatarsal heads with the foot in an equinus position. Rather than the usual plantarflexion movement which follows weight acceptance, the ankle in this group of children moves into progressive dorsiflexion in an attempt to

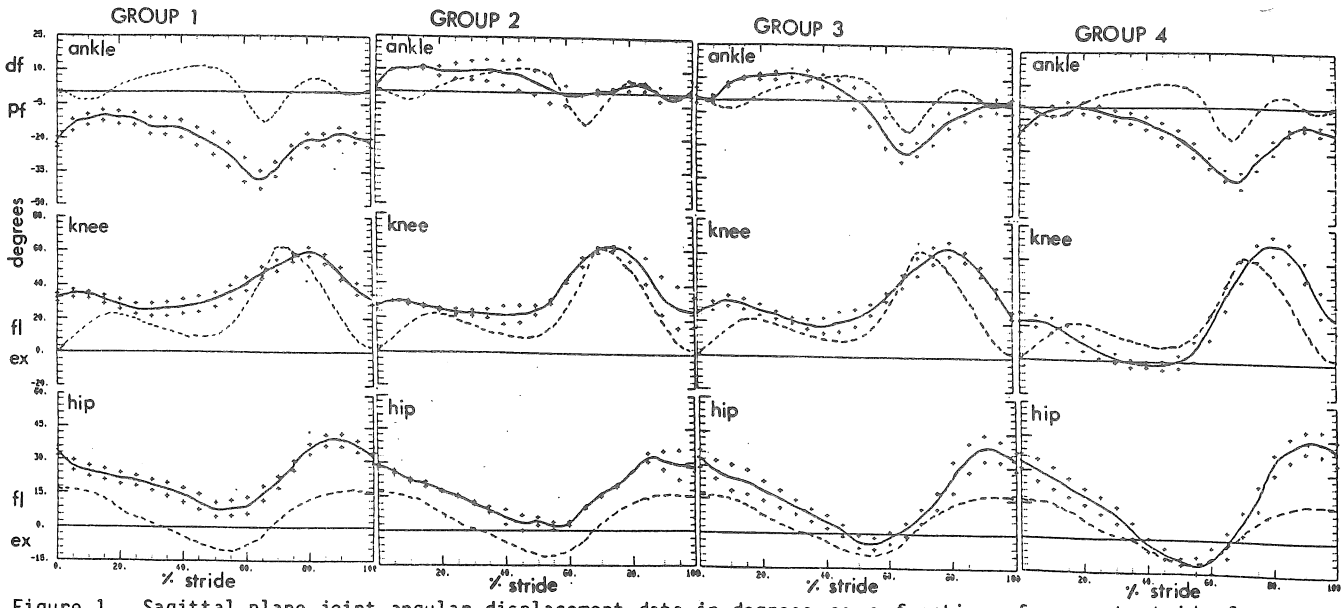

Figure 1. Sagittal-plane joint angular displacement data in degrees as a function of percent stride for group 1, 2, 3 and 4. Group curves represented as ensemble average ± 1 S.D. (continuous traces) are compared to normal (interrupted traces). Abbreviations: df: dorsiflexion, pf: plantarflexion, fl: flexion, ex: extension.

touch the heel to the ground. Weight acceptance is invariably initiated in excess knee flexion. Knee flexion is excessive and the amplitude is dampened throughout stride. On clinical examination, these children belong to a group that have an important degree of spasticity of the entire lower limb and fixed ankle contractures. This is most likely the group of children who Sutherland et al. (1) describe as those whose gait will deteriorate into one of progressive crouch should they succumb to Achilles tendon lengthening procedures.

Group 2 consists of 4/32 limbs (12%) and is characterized by excess stance dorsiflexion and inadequate swing plantarflexion. There is excess knee and hip flexion throughout entire stride. The patients in this group correspond to the typical crouch gait walkers described by Sutherland. However, in contrast to Sutherland's group, these children have never had any surgical procedures to weaken their plantarflexors. Interestingly enough, physical examination of both diplegics in this group reveals significant spasticity of the hips and knees without ankle spasticity. In fact, both patients demonstrated poor plantarflexor strength to explain the flat-footed nature of their gait. It appears therefore, that the development of a crouch gait in spastic diplegia is not necessarily preceded by Achilles tendon lengthening procedures and that a certain group of spastic children, have inherent plantarflexion weakness.

Group 3 consists of 5/32 limbs (16%) and is characterized by excess stance dorsiflexion, excess swing plantarflexion and exess knee and hip flexion throughout stride. On physical examination, all limbs are described as having significant ankle spasticity, making it difficult to manipulate into dorsiflexion. Yet during the dynamic walking situation, excess dorsiflexion is manifest during stance. The lack of correlation between the joint angular displacement data and physical examination for this group illustrates the often weak predictive value of a static examination in assessing dynamic gait abnormalities.

Group 4 is represented by 10/32 limbs (31%) and is characterized by excess ankle plantarflexion throughout stride, stance phase hyperextension of the knee (genu recurvatum) and excess hip flexion. At weight acceptance the knee is in excess flexion and then hyperextends into the remaining stance phase. This group of patients appears to closely resemble the first group of patients with genu recurvatum described by Simon et al. (6) whose genu is caused by excess calf muscle activity. Indeed, clinical evaluation of all patients in our group revealed significant ankle spasticity with fixed ankle contractures. Simon's kinetic and EMG evaluation reveals excess plantarflexion activity secondary to an increasing dorsiflexion ankle moment which is responsible for early stance arrest of forward tibial motion yet unabated forward advancement of the femur and trunk producing hyperextension about the knee.

CONCLUSION

The gait patterns of 16 unoperated spastic diplegic children were analyzed using high-speed cinematography and computer data analysis. Sagittal plane joint angular displacement data identified four distinct patterns depending on the simultaneous positions of the ankle, knee and hip. Such a classification is envisioned as one which will allow for easier categorization of the diplegic child's troubled gait and permit objective verification of the results of orthopedic or surgical treatment.

References

1. Sutherland, D.H., et al. Orthop. Clin. North Am. 9:143-154,1978.
2. Perry, J. Clin. Orthop. 102:18-31, 1974.
3. Phelps, W.M. J. Bone Joint Surg. 14:773,1932.
4. Perry, J., et al. J. Bone Joint Surg. 56A:511-521, 1974.
5. Perry, J., et al. J. Bone Joint Surg. 58A: 201-208, 1976.
6. Simon, S.R., et al. J. Bone Joint Surg. 60A:882-894, 1978.
7. Winter, D.A. Biomechanics of Human Movement, Wiley-Interscience Publication, 159-176,1979.
8. Burnett, C.N., et al. Dev. Med. Child Neurol. 13:207-215, 1971.
9. Sutherland, D.H., et al. J. Bone Joint Surg. 62A:336-353, 1980.

HIGH-RESOLUTION REAL-TIME MOVEMENT ANALYSIS AT 100 Hz

with Stroboscopic TV-camera and Video-Digital Coordinate Converter

E.H. Furnée

Movement Studies Lab. Signal Processing Dept.
Faculty of Applied Physics Delft University of Technology
PO Box 5046 2600 GA Delft the Netherlands

INTRODUCTION

In human or animal movement data acquisition and analysis, photographic methods such as high-speed film with subsequent manual digitizing for computer analysis, tend for reasons of convenience, longer data series and rapid turnover, to be augmented or replaced by opto-electronic methods. These provide automatic position measurement of contrasting landmarks attached to the subject in motion, be it in sports, bio-medicine, rehabilitation or ergonomics.
Real-time video-digital coordinate conversion has since the earliest prototype (1) established a position measuring interface between tv-cameras and computers.

This paper reports recent improvements in temporal and spatial resolution by specially developed high-speed stroboscopic tv-cameras based on a solid-state image sensor. This permits application in relaxed ambient light conditions.The geometric linearity and stability of the matrix sensor contributes to the high resolution, which the system attains by the estimation in real time of the centroid coordinates of individual markers.

REVIEW AND THEORY

Early versions of real-time video-digital coordinate conversion systems (1, 2, 3), subsequent developments and a commercial product from other sources (4,5,6,7,8), other systems (9,10,11) or recent developments (12,13,14), as well as numerous clinical and research applications by this and other authors have shown the potential of tv-based automatic movement data acquisition of non-wired reflecting body markers, observed by multiple cameras for 3-D reconstruction. Due to standard principles of tv-scanning, position digitizing of bright spots in the 2-D tv-image is essentially a fast counting operation. Above-threshold video pulses trigger instant read-out of binary modulo-n counters for line number (vertical) and column number (horizontal coordinate). As reported in (13), the multiple coordinate data of individual marker contours are reduced to single, high-precision pairs by calculation of each markers' geometric centroid.This occurs in real time with arithmetic hardware and microprocessor implemented inside the measuring instrument (an early approach with large markers, albeit averaging of coordinates, and performed off-line with video processing of film data, was reported in (10)). The real-time, high-resolution data reduction has allowed use as a host computer of modest PC's, with limited disc storage and standard data bus interface. The video-based movement analysis system has thus become transportable outside dedicated laboratories.

A logical next step is the facility for extracting markers' images in conditions of brighter ambient light or in daylight. This entails new effort at the systems' front end.

METHODOLOGY

Existing systems use retro-reflective markers (Scotch 3M 7610) illuminated by rings of LED's centered around the camera lens. We report an optimal arrangement with separately directed LED-rings, where the radiation angle diagram of the LED's and the scatter diagram of the reflecting markers are considered. This provides equal-amplitude marker images across the cameras' field of view, and along a large distance range from the camera, so to permit uniform setting of video threshold.

Obviously, existing systems use the LED illumination in a strobed flash mode, in synchrony with the tv scan rate, so providing crisply defined images of the moving markers. This alone does not much improve the contrast ratio of marker images against background, so ambient light was subject to restrictions. Although a synchronous rotary shutter can be

used in front of the tv-camera (6), for reasons of size, robustness and image quality, we prefer an all-electronic shuttering system without components in the optical path.

Based on the frame-transfer matrix image sensor (Philips NXA 1010) we developed a non-standard tv-camera with a dual purpose:
1. stroboscopic in the sense that it is only sensitive (an image is only retained) during the LED light flash, and insensitive (no image) to the scene in ambient light between the stroboscopic LED flashes.
2. high-speed, to provide a sample frequency of at least 100 images frames per second, for faithful sampling of fast motion components.

Our method for realizing the stroboscopic camera feature with a marketplace sensor is to apply additional pulse sequences, preceding the regular shift patterns for frame transfer and clocked video output. The CCD sensor structures being amenable to higher shift frequencies has enables us to raise the image rate to 100 Hz at present.

RESULTS AND DISCUSSION

The spatial resolution has improved to 1:32.000 of (2-D) field-of-view dimensions. This basic resolution of output data is a meaningful figure of merit because measurement noise has been considerably reduced, to a standard deviation of better than 1:10.000 for stationary markers. This performance is equaled for small linear marker displacement. It is due to the features of centroid calculation, geometric sensor stability and the profitable tight coupling of the CCD shift pulse patterns with the coordinate converter clocks. Note that this sensors' matrix defition is 312 lines by 604 columns.
As pointed out in (15), the low noise plus a higher sample rate are of special benefit, where derivation of speed and acceleration is of prime interest, as in many applications.

The stroboscopic sensitivity feature of the tv-camera means an aperture time of .5 ms with a 10 ms image repetition period. This entails a 20-fold increase in marker contrast under the synchronous LED light strobes with respect to the scene under ambient illumination. In a pilot experiment, markers stood out clearly at 30 m in outside daylight of 2.000 lux, holding promise of field applications in sports and ergonomics.

The high-speed capability, with sampling rate at least 100 Hz, as advocated by some authors (16), adapts the system to analysis of rapid phenomena like heel strike or fast disturbances in normal or impaired gait.

Software and clinical and research applications are discussed in relevant literature.

CONCLUSIONS

Concentrating at the sensor front end of the real-time centroid-processing, multi-marker video-digital movement acquisition system has upgraded spatial and temporal resolution and provides marker contrast for outdoor use.

References

1. Furnée E.H.(1967) Hybrid instrumentation in prosthetic res.Dig 7th ICMBE Stockholm
2. Furnée E.H.(1970) Graphic input computers by tv camera. Abstr 5th IMEKO Versailles
3. Furnée E.H. et al(1974) Autom.analysis of stepping movemt.cats. J.Physiol.240,3-4P
4. Jarrett M.O.et al(1974) Quantit.analysis locom, w, tv, Abstr World C,ISPO Montreux
5. Paul J.P.(1978) Kinetic meas. systems & biomech. data. J.Human Mov.St. 4,179-190
6. Andrews B.J. et al(1981) Strathclyde tv/computersyst. Comp.i.Medic. 25-28 aug 81
7. Bruegger W. ea(1978) Comp.-aided tracking bodymotion w.CCD sensor.J.MBEC 16,207-210
8. VICON trade litt. Oxford Medical Syst. UK
9. Waas, R.C.(1969) Digital optical scanning syst.f.kinematic anal.PhD Case Western Res
10. Winter D.A. ea(1972) TV-computer an.kinemat.human gait.Comp.Biomed.Res.5,498-504
11. Cheng I-S. et al(1975) Simple comp.-TV interface f.gait anal. IEEE-BME, 259-260
12. Taylor K.D. et al(1982) Automatic motion measur.syst.gait anal.J.Biomech.15,505/16
13. Furnée E.H.(1984) Intell.movemt.measurmt. dev's. Proc.Sup 40-53 8th ETAN Int.Symp. Control o.Human Extremities, Dubrovnik YU
14. Ferrigno G. et al(1985) Digit.hardw.syst. movemt.anal.realtime TV.IEEE-BME, 943/49
15. Lanshammar H.(1982) Precision limits f. derivatives fr.noisy data.J.Biomec.459/70
16. Baumann J.U. et al(1984) Gait childr. w. spastic dipl: importance higher frequency resolution. 4th ESB, Abstr J.Biomech, 457

FUNCTIONAL ANALYSIS OF HIP RESECTION ARTHROPLASTY

Tylkowski, C.M., Chase, J., Petty, R.W., G. Miller, Gait Analysis Laboratory

University of Florida, Department of Orthopaedic Surgery, Box J-246 JHMHC, Gainesville, FL 32610.

Introduction

Hip resection arthroplasty, i.e. excision of the proximal femur, either as a primary surgical procedure, or as a consequence of failed total hip arthroplasty, is performed for incapacitating hip pain (4,8). Changes in the gait patterns related to these procedures as well as the increased energy cost of walking have not been fully categorized. In this study kinematic, kinetic and oxygen consumption data were collected for 8 patients in three different groups to categorize the compensatory mechanism of gait and the metabolic consequences of these compensations. In addition this information was compared to a patient satisfaction index as well as radiographic examinations to further define this distinctive population.

Review and Theory

Hip resection arthroplasty is used as a primary procedure for incapacitating hip disease or as a secondary procedure to salvage a hip after removal of a failed implant. The clinical literature has documented differences among these two groups regarding functional success and patient satisfaction (4,8). There have been no studies to date which categorize the compensatory mechanisms these two groups utilize, their similarities and/or differences. The energy cost of walking has not been defined, although it is known that gait patterns with a high oxygen cost are poorly tolerated (1,2,6).

Methodology

Hospital records of 54 patients having undergone hip resection arthroplasty were reviewed and 40 patients could be contacted. Eighteen patients were unable to ambulate for reasons beside their hip. Group I included unilateral primary resection arthroplasty patients (age ave 27y). Group II included bilateral primary resection arthroplasty patients (age ave 29.5y). Group III included those with unilateral secondary resection arthroplasties (age ave 51y).

Four out of five patients in Group I could walk well enough to perform the study and one refused. Three out of five patients in Group II could perform the study and one refused. Only four of twelve patients in Group II could walk well enough to perform the study and one refused. Eight patients were therefore included in the study.

Each patient had fasted prior to the morning study. Joint range of motion and manual muscle testing was performed on each patient. Kinematic data was collected by filming each walk with three Redlake synchronized movie cameras operating at 50 frames per second. After processing the patient landmarks were digitized by a Graf-pen digitizer to the minicomputer. Kinetic data was collected using an AMTI (Cambridge, MA) force plate. Dynamic electromyographic data was collected by surface electrodes to skin mounted preamplifiers and sent to the final amplifiers by a light trailing cable. All data was collected on, synchronized by, and processed by a Dec PDP11/34A minicomputer. Kinematic, kinetic, and dynamic electromyographic data were syndronized and collected simultaneously (3,5,7) with oxygen consumption. Oxygen use was monitored and averaged over one minute intervals using a Water's Oxygen Analyzer (Rochester, MN) (9).

The free walking speed, a slower and a faster speed were recorded for each patient. Two representative walks were recorded at each speed. Steady state oxygen consumption was documented at each speed prior to recording the walk. Aerobic functioning was monitored by pulse and respiratory rate.

Computer processing yielded gait parameters of velocity, cadence, step lengths, stride, and time spent in single and double limb stance. Simultaneous EMG, medial/lateral, fore/aft, and vertical ground reaction forces were plotted. The joint and segment motions were calculated and displayed graphically and by three view stick figure representations.

Results and Discussion

Table I included the gait parameters and their statistical significance.

Table I Gait Parameters

	Group I Ave	(S.D.)	p	Group II Ave	(S.D.)	p
Velocity(m/sec)	1.01	(0.04)	.01	1.03	(0.2)	.09
Cadence(step/min)	97.2	(5.5)	.01	98.8	(22)	0.2
Stride (m)	1.23	(0.02)	.01	1.23	(0.04)	.02
Step (R)(m)	0.58	(0.04)	.01	0.63	(0.04)	.05
Step (O)(m)	0.66	(0.08)	.05	0.61	(0.01)	.01
% SLS (R)	31.4	(1.6)	.01	37.5	(6.6)	0.4
% SLS (O)	39.5	(1.4)	.7	33.5	(3.8)	0.1
Age	27	(7)		33	(5.6)	

	Group III Ave	(S.D.)	p	Normal
Velocity(m/sec)	0.82	(0.18)	.01	1.51
Cadence(step/min)	102.	(9.6)	.06	116
Stride (m)	0.92	(0.07)	.01	1.56
Step (R) (m)	0.47	(0.06)	.01	0.78
Step (O) (m)	0.48	(0.06)	.01	0.78
% SLS (R)	29.6	(7.4)	.08	39
% SLS (O)	39.6	(1.5)	.7	39
Age	51.3	(10.5)		

SLS = single limb stance
R = resected
O = opposite (Group II O = R)

The kinematic data of group I showed increased posterior pelvic tilt and pelvic obliquity and transverse rotational motions which were opposite in direction compared to normal. The involved hip showed decreased flexion through out the gait cycle. Flexion of the involved knee and ankle were normal; however, the normal side hip, knee and ankle (dorsal) flexion were increased. Free speed walking was reduced 17% with a 34% increase in energy consumption (fig 1).

The kinematic data of Group II showed increased posterior pelvic tilt and symmetrically increased pelvic obliquity and transverse rotational motions which were opposite in direction compared to normal. There was symmetrically decreased hip flexion in all phases of the gait cycle. Knee and ankle motion were symmetrically normal. Free speed walking was reduced 17% with a 54% increase in energy consumption (fig. 1).

The kinematic data of Group III showed increased posterior pelvic tilt and pelvic obliquity was opposite in direction and decreased in amplitude. Transverse pelvic rotation was normal. The involved hip showed decreased flexion in weight acceptance and early SLS but increased in the last half of SLS and weight release. Flexion of the involved knee was increased in SLS but ankle motion was normal. Normal hip and knee flexion were increased in SLS and weight release, ankle motion was normal. Free speed walking was reduced 32% with a 42% increase in energy consumption (fig. 1).

The vertical, medial/lateral and fore/aft ground reaction forces were near normal. The dynamic electromyograms showed persistent activity of the involved hip abductors and extensors through all of stance phase.

Conclusions

Significantly, only 15% of patients having this procedure were able to walk. All groups walked with similar compensatory mechanisms. Gait parameters (Table I) were unique for each group. All groups had a decreased free walking speed with an increased energy consumption. Significantly Group I, the primary resection arthroplasties, used less energy and walked faster than Group III, the secondary resection arthroplasties. The bilateral primary resection arthroplasty patients, Group II, walked at the same velocity as the unilaterals but consumed the greatest amount of energy.

The patients with secondary resection arthroplasties walked at one-half the velocity and twice the consumed energy compared to the other groups. This is attributable to their greater average age and generalized muscle weakness apparently, but not to any major differences in the compensatory patterns utilized (1,2,6).

Funded by a grant from the Orthopaedic Research and Education Foundation --- Zimmer Research Award.

BIBLIOGRAPHY

1. Fisher, S.V., and Gullickson, G.: Energy Cost of Ambulation in Health and Disability: A Literature Review. Arch. Phys. Med. Rehab., 59:121-133, 1978.
2. James U: Oxygen Uptake and Heart Rate during Prosthetic Walking in Healthy Male Unilateral Above-Knee Amputees. Scand. J. Rehab. Med., 5:71-80, 1973.
3. Mansour, J.M., Lesh, M.D., Nowak, M.D., and Simon, S.R.: A Three-Dimensional Multi-Segmental Analysis of the Energetics of Normal and Pathological Human Gait. J. Biomech. Vol. 15, No. 1:51-59, 1982.
4. Petty, W. and Goldsmith, S.: Resection Arthroplasty Following Infected Total Hip Arthroplasty. J. Bone Joint Surg. Vol 62A, No. 6, September, 1980.
5. Simon, S.R., Nuzzo, R.M. and Koskinen, M.F.: A comprehensive Clinical System for Four Dimensional Motion Analysis. Bull. Hospital. Joint Dis., 38(1):41-44, 1977.
6. Takahashi, K., Laughman, R.K., Chao, E.Y. and Sim, F.H.: Functional Performance of Patients with Custom Bone and Joint Prostheses at the Hip and Knee. Trans. Orthop. Res. Soc., 7:130, 1982.
7. Tylkowski, C.M., Simon, S.R., Mansour, J.M.: Internal Rotation Gait in Spastic Cerebral Palsy. In the Hip Society: The Hip: Proceedings of the Tenth Open Scientific Meeting of the Hip Society, 1982, CV Mosby, 1982
8. Vatopoulos, P.K., Diacompoulos, G.J., Demeris, Ch.S., Gorgolis, J. and Papathanassion, B.T.: Girdlestone's Operation: A follow-Up Study. Acta Orthop. Scand. 47:3240328, 1976.
9. Webb, P., and Troutman, S.: An Instrument for Continuous Measurement of Oxygen Consumption. Journal of Applied Physiology, Vol. 28:867-871, June, 1970.

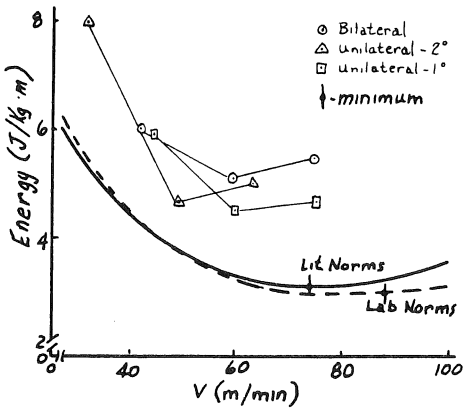

Figure 1 - Energy vs. Velocity

CHANGE IN ADULT ACQUIRED HEMIPLEGIC GAIT PATTERN FOLLOWING SURGICAL CORRECTION OF EQUINUS

R. Sherman, M.D., M. Pinzur, M.D., P. DiMonte-Levine, R.P.T. and J. Trimble, Ph.D.

from The Pathokinesiology Laboratory of Loyola University Medical Center and Hines VA Hospital

INTRODUCTION

Surgical correction of adult hemiplegic gait disorders by combination of tendon lengthening, transfer and release has been performed with increasing frequency over the past decade. Keenan, et. al.[1] have determined balance as the best predictor of eventual independent walking following stroke or brain injury. We have previously reported a consistent pattern of deformity in this patient population.[2] This premise that acquired gait disorders in adult hemiplegic patients are the result of a complex pattern of neurological abnormalities, as opposed to a series of random deformities, provided the impetus for this study. The goals of this study were twofold: (1) to evaluate the impact of the correction of ankle equinus on gait pattern in a series of adult hemiplegic patients, and (2) to evaluate the relationship of the dynamic deformities at the hip, knee and ankle in this complex patient problem.

METHODS

Twenty-seven adult acquired hemiplegic patients underwent multiple factor gait analysis before and after motor balancing surgery to correct spastic equinovarus. Surgery combined tendo-Achilles lengthening, lateral transfer of the tibialis anterior, percutaneous toe flexor release and lengthening of those flexors that exhibited out-of-phase electrical activity as determined by pre-operative walking electromyography.

Dynamic walking electrogoniometric analysis of the hip, knee and ankle joints was accomplished with the Orthopaedic Systems, Inc. (Berkely, California) electrogoniometer. Temporal monitoring of gait was accomplished concomitantly with the ultrasonic gait monitor.[3] The data was obtained by having each patient walk along a flat 25 foot linoleum walkway at a self-selected velocity. Angle measurements for the hip, knee and ankle joints were taken at reproducible points in the gait cycle corresponding to heel points in the gait cycle corresponding to heel strike, mid-stance, toe-off and mid-swing phases of gait. The data presented is an average derived from sampling from each individual patient.

RESULTS

Dynamic electrogoniometric data is depicted in the following figures. Positive numerical values represent hip and knee flexion and ankle dorsiflexion.

The dynamic deformity of early stance phase ankle equinus was accompanied by decreased knee flexion, progressing to knee hyperextension in the more severely neurologically involved patients and increased hip flexion. This deformity remained consistent through stance phase of gait and only seemed to vary with the severity of the central neurological involvement. When comparing the study population pre- and post-operative electrogoniometric data, we observed a correction of the gross deviations from the normal electrogoniometric pattern. The pattern of deformity persisted following surgery, but the energy wasting gross deviations were markedly improved, as depicted in the above stick figure data.

DISCUSSION

The major deformity pattern in adult acquired hemiplegic gait appears to be early stance phase ankle equinus combined with decreased knee flexion. This basic pattern persists throughout stance phase and into swing phase of gait. This pattern was consistent throughout the study group with increasing deformity in the most severely involved patients. In the surgically treated group, correction of the equinus deformity at the ankle made a major impact on the abnormal gait pattern. While not fully correcting the related dynamic abnormalities at the hip and knee, the improvement in the pattern of gait was significant.

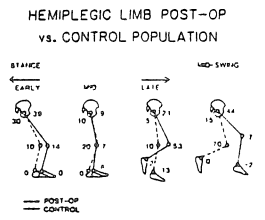

Figure 1.

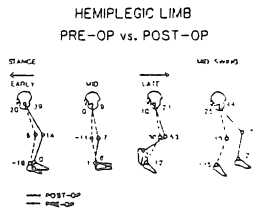

Figure 2.

References

1. Keenan, et. al.: Clin. Ortho., Vol. 182, 1984.
2. Sherman, Pinzur, et. al.: Proceedings Ortho. Res. Soc., 1985.
3. Pinzur, et. al.: Journal of Rehab. Engineering, 21:2, July 1984.

CHANGE IN ADULT HEMIPLEGIC GAIT PATTERN FOLLOWING SURGICAL CORRECTION OF EQUINUS

R. Sherman, M.D., M. Pinzur, M.D., P. DiMonte-Levine, R.P.T. and J. Trimble, Ph.D.

The Pathokinesiology Labortory
of
Loyola University Medical Center
and
Hines V.A. Hospital

Twenty-seven adult acquired spastic hemiplegic patients had gait analysis before and after motor balancing surgery. Pre-operatively, early stance was characterized by ankle equinus, decreased knee flexion and increased hip flexion. All were at least one year post neurological insult at the time of surgery. Post-operative dynamic electrogoniometry was performed at least one year post-surgery. The abnormal gait patterns present pre-operatively were corrected in each of the patients tested as compared to both their uninvolved side and the normal control population of our laboratory. Results of this dynamic study suggest that spastic equinus is the major deforming force in adult acquired hemiplegic gait. Control or correction of this deformity may be the key factor in improving abnormal gait in this population.

ANALYSIS OF CANINE GAIT WITH FORCE PLATFORMS FOLLOWING ANTERIOR CRUCIATE LIGAMENT REPAIR: A PILOT STUDY

Meller, B.T.; Manley, M.T.; Hurley, P.; Yoshia, S. The Cleveland Clinic Foundation, Department of Musculoskeletal Research, Cleveland, Ohio 44106.

INTRODUCTION:

The canine model is widely accepted for studies involving knee surgery. Techniques for reconstructing torn anterior cruciate ligaments (ACL's) have been evaluated in dogs. Evaluation is based almost exclusively on examination of the articular surfaces, histological sections and mechanical test data from ligaments in the knees following sacrifice. These examinations however, give no quantitative information on the clinical degree of function in the operated limb, i.e. the amount of body weight carried on that limb. This paper outlines a method of analyzing canine gait using force platforms (1) and a video-recording system. The method provides quantitative data on the percent of body weight carried by each limb correlated with visual gait data. It can be used for repeated, non-invasive assessment of surgical treatments.

REVIEW AND THEORY:

In order to assess the degree to which ACL reconstruction has improved function in humans, a gait analysis can be performed (2),(3),(4). Similarly, in a dog model, functional effects of ACL reconstruction can be studied using standard force platforms. The dog, a quadruped, is a sensitive model for evaluating knee surgery since it is able to walk on three limbs and effectively reduce the load on an operated leg. Without force data, it is difficult to observe the degree to which a dog may be reducing the load on an operated limb. This attempt to unload an operated limb is easily discernable by studying the force platform data.

Of particular interest is the difference between the magnitudes of the vertical forces carried by the operated hind leg and the non-operated hind leg. Further, it is of interest to examine mechanisms of unloading the reconstructed knee: whether load is increased on the non-operated hind limb, or perhaps more load is carried by one or both of the fore limbs.

METHODOLOGY:

Subject dogs ranging in weight from 13-25 kg were tested. Force data were collected using two force platforms recessed into a wooden walkway 1.2 m wide and 4.9 m long. Both plates were covered with individual sheets of plywood to afford better traction for the dogs.

A 60 Hz video-recording system allowed analysis of gait patterns and verification of acceptable data acquisition runs. The system was composed of two cameras, one positioned directly behind the dogs oriented in the direction of the walkway and the second positioned two meters from the force platforms oriented to show a lateral view of the platforms. The following criteria were established to verify a data run:

1. Dog leashes must remain slack.
2. Each paw must strike at least one plate cleanly; any strike at the border of a plate nullifies the run.
3. Dogs must maintain a constant pace across the force plates.
4. Dogs must face in the direction of motion at all times.

Three verified gait tests were collected for each dog.The video-recording system provided a split-screen image of the motion in which the images from both cameras could be viewed simultaneously. This image was used to correlate specific paw strikes with the force data collected from the platforms.

RESULTS:

Data on five control dogs and three test dogs were recorded. Test dogs had undergone surgical repair of ACL's in one hind leg. All three were tested eighteen months after surgery.

Loads on limbs are presented as a percent of total body weight. Figure 1 shows the difference between the magnitudes of the loads carried by each hind leg in a given dog. Figure 2 shows the difference between fore legs. Finally, figure 3 compares the difference between hind legs to the difference between fore legs in each dog.

DISCUSSION:

The difference between the magnitudes of the loads carried by each hind limb of a given dog in percent of body weight ranged from 16-38% in the test dogs while in control dogs it ranged from 1-8%. Further, this percent difference in the operated dogs correlated with the visual appearance of their gait. In figure 1, the dog with the greatest difference (6) showed a more pronounced limp than the dog with the smallest difference (8). As expected, the operated hind limb carried a smaller load than the non-operated hind limb in each test dog.

The loads carried by the non-operated hind limbs were not significantly larger than the corresponding limbs of control dogs (figure 1). However, with the great difference in load bearing between the operated and non-operated hind legs of the test dogs, one might expect the fore limbs to perhaps carry a larger load. The load bearing on fore limbs does not reveal any substantial increase to compensate for decreased loading in operated hind limbs (fig. 2). Also, the difference in loading between both fore paws in all dogs tested shows no significant difference between the two groups (fig. 2). The difference was 4.6% in control dogs and 3.7% in dogs with reconstructed ACL's.

The final graph (fig. 3) combines the first two graphs to compare the absolute load differential between the fore limbs of each dog to the absolute load differential between the hind limbs of each dog. This graph illustrates, again, that the test dogs do not compensate for decreased loading on operated hind limbs by altering the magnitude of the loads carried on the fore limbs.

CONCLUSIONS:

The dog is a sensitive model for the study of ACL reconstruction. Analysis of canine gait using force platforms and a video recording system correlate loading patterns on dog limbs with operative treatment. This system of analyzing the model allows repeated, non-invasive assessment of operative procedures for ACL reconstruction.

REFERENCES:

1. Ramey, M.R. Force Plate Designs and Applications. Journal of Bone and Joint Surgery Jul;57(5):613-6, 1975.
2. Gronley, J.K., et al. Gait Analysis Techniques. Rancho Los Amigos Hospital Gait Laboratory. Physical Therapy Dec;64(12):1831-8, 1984.
3. Laughman, R.K., et al. Objective Clinical Evaluation of Function. Gait Analysis. Phys. Therapy Dec; 64(12):1839-45, 1984.
4. Winter, D.A. Biomechanics of Human Movement. Milsum, J.H. (ed.). John Wiley and Sons, Toronto, 1979.

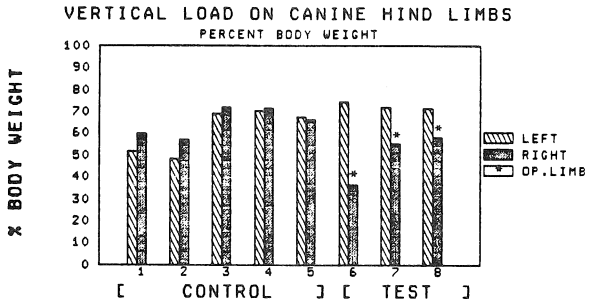

Figure 1. The difference between the magnitudes of the loads carried by each hind leg in control dogs (1-5) and ACL-repair dogs (6-8). The difference ranged from 1-8% in control dogs and from 13-38% in test dogs.

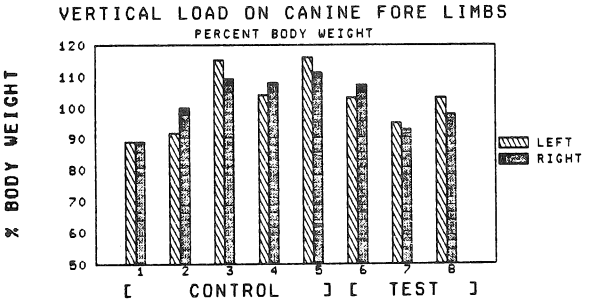

Figure 2. The difference between the magnitudes of the loads carried by each fore leg in control dogs (1-5) and ACL-repair dogs (6-8). Test dogs show no alteration in fore-limb loading (compared to control dogs) to compensate for changes in the magnitudes of hind-limb loading.

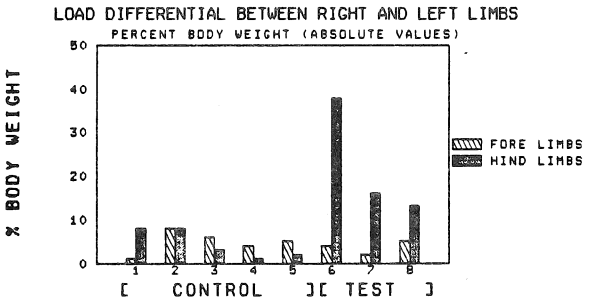

Figure 3. The absolute load differential between fore limbs shows no significant difference between controls (1-5) and test dogs (6-8). The differential between hind limbs is larger for the test dogs than for the control dogs.

GAIT OF PATIENTS WITH TOTAL KNEE REPLACEMENTS (TKR)

U.P. Wyss
Clinical Mechanics Group
Queen's University
Kingston, Ontario, K7L 3N6

S.J. Olney, I. McBride
School of Rehabilitation Therapy
Queen's University
Kingston, Ontario, K7L 3N6

T.D.V. Cooke
Department of Surgery (Orthopaedics)
Queen's University
Kingston, Ontario, K7L 3N6

INTRODUCTION

It is necessary to evaluate the success of total knee replacements statically and dynamically. Radiographs are used for the static assessment, and gait analysis evaluates the success of TKRs dynamically. One purpose of this study was to investigate TKRs that were inserted with different operating techniques. One technique is based on standard instruments, while the other technique relies on a special cutting jig (2) for accurate alignment and placement of the prostheses. The other purposes of the study were to analyse the knee motion after joint replacements and to assess the feasibility of a larger study.

REVIEW AND THEORY

Andriacchi et al and Prodromos et al (1,3) have analysed gait of patients with different TKRs. They found the best results with cruciate retaining prostheses. They indicated that this was not so obvious during level walking, but it became clearer by going upstairs. They also found that the adductor moment does not always correlate with the alignment of the hip, knee and ankle, which indicates that a part of the malalignment can be compensated during gait. It is preferable, however, to correct the alignment during implantation, so that the conditions are optimal for an ideal load distribution on the medial and lateral condyles with a minimal adductor moment. The instruments currently used are not ideal for a correct alignment and placement of TKRs. A new cutting guide system that incorporates features for accurate placement and alignment was developed at Queen's (2) and is used on a routine basis. It is believed that a more accurate alignment and placement of a prosthesis will enable the subject to walk more closely to normal. The aim of this pilot study was to evaluate gait of patients with TKRs by using different inserting instruments. The results from the pilot study were used to plan a larger study focussing on the same topic.

METHODOLOGY

Seven subjects, four female and three male, were selected for this study. Five were fitted with a PCA knee of which four were fitted with the new cutting guide, and the other two subjects were fitted conventionally with Townley knees. Both, the Townley and the PCA knee retain the posterior cruciate ligament. Therefore, they were considered as part of the same group of knee implants for this study. Except for one patient, all had osteoarthritis. The mean age was 68 (55-70) and the mean weight was 768 N (589 N - 1070 N). All patients walked barefoot at their comfortable speed on a level surface, and went up and down two standard size steps representing a stairway. The kinematics were recorded from the side for a two-dimensional analysis. The force reaction forces were recorded with a force platform simultaneously. Five muscles, soleus, tibialis anterior, vastus medialis, vastus lateralis, and the medial hamstrings, were instrumented with EMG electrodes. The same walking and stair climbing experiments were repeated in this configuration for the collection of the EMG. The alignment of the prosthesis was evaluated by using Standardized Radiography (4) and the success of the operation was scored with the Insall scoring method.

The relative angles, the segment angles and the energies were calculated for both sides, while the moments and the powers were only calculated for the side facing the camera. The linear envelope EMG of all five muscles were recorded and the patterns were compared with those of normal subjects.

RESULTS

The small number of subjects in this study did not allow a statistical analysis. Nevertheless, the analysis of the data showed interesting results, that partly determined the format of a larger study.

EMG. The differences between the linear envelope EMGs of different subjects were quite significant. The EMG curves did also deviate considerably from normal EMG patterns. The peak activity in normals could be seen as a peak in subjects as well, but it was not always the highest peak. The medial hamstrings showed, in some patients, very high activities just after foot contact. This might be a reflex to prevent full extension. It was observed in a number of subjects that they felt unstable in full extension and therefore prevented it from occurring by higher hamstring activity. The subjects would have collapsed without reaction from the knee extensor apparatus, which could be observed in higher activity of the vastus medialis and lateralis. The irregularities in the vastus medialis were more obvious than in the vastus lateralis. It is possible that this is related to the degree to which the vastus medialis pulls the patella medially in order to prevent the patella from subluxing laterally. Only the anlysis of a larger number of subjects can provide answers to which extent the EMG patterns are related to placement and alignment of prostheses.

Kinematics & Kinetics. All kinematic and kinetic data represent an average of two steps. Figure 1 shows the range of knee flexion for the good side and the TKR side. The mean values with -2 standard deviation values are from data of normal subjects for the same age group. It shows that this subject Group did not have a flexion range within -2 standard deviations for the affected side, but five out of seven were within the limits for the good side. It cannot be said by this small number of subjects that the

knee replacements that were inserted by using the new cutting jig showed better results. The analysis of the standardized radiographs for this group did show, however, a slightly better alignment when the jig was used. This finding was confirmed by a larger study currently in progress. The curves of the moments, energies and powers, show similar characteristics as those of the EMG; more irregularities than for normals. This correlates well with a lower efficiency during walking. The necessity for stabilization requires more antagonistic muscle action which prevents a smooth 'flow' during walking and requires more energy.

The walking speed is generally considered as a rough indicator of a persons' gait condition. It is interesting to observe that there is no correlation between the walking speed and the Insall score as shown in Figure 2. This clearly indicates that patient satisfaction does not reflect measureable parameters only. Pain reduction seems to overwrite other parameters considerably. It demonstrates that a passive evaluation, such as an Insall score, must be complemented by a dynamic evaluation. A better dynamic performance will most likely yield a better long-term success and will minimize the side effects on other joints due to pathological gait patterns at the knee.

The stair climbing experiments did not show conclusive patterns for this group. This was largely due to the fact that some patients could only go up or down one step at a time, which is a different pattern that cannot be compared with normal stair climbing activity. It was, however, obvious that stair climbing adds stress and magnifies irregularities.

DISCUSSION

In order to evaluate gait patterns with respect to alignment and placement of prostheses, it is necessary to evaluate a considerable number of gait parameters, before it is possible to come to significant conclusions. A single parameter might show a tendency, but it is only possible to prove a hypothesis if a cluster of parameters looking at the same effect correlates well. A simple yet meaningful presentation of gait data is certainly needed (5).

This study shows that it is feasible to study alignment and placement of knee prostheses with respect to gait. The chosen methods, however, must be expanded for the three-dimensional analysis. Medio-lateral malalignment will show larger changes of the gait parameters in the frontal plane than in the walking plane. The evaluation of the adductor moment as shown by Prodromos et al (3) is impossible without frontal data as well. The influence of placement and alignment to gait can be further evaluated by analysing gait before and after surgery. A larger number of subjects divided into subgroups, however, is necessary for a statistical analysis.

ACKNOWLEDGMENTS

Financial support from the Dean's MRC Fund and the Ontario Ministry of Health is gratefully acknowledged.

REFERENCES

1. Andriacchi, T.P., et al. JBJS 64-A:1328-1335, 1982.
2. Cooke, T.D.V., et al. J. Biomed. Eng. 7:45-50, 1985
3. Prodromos, C.C., et al. JBJS 67-A:1188-1194, 1985.
4. Wevers, H.W., et al. J. Biomed. Eng. 4:319-324, 1982.
5. Wyss, U.P. Int. Series in Biomech. X: In press.

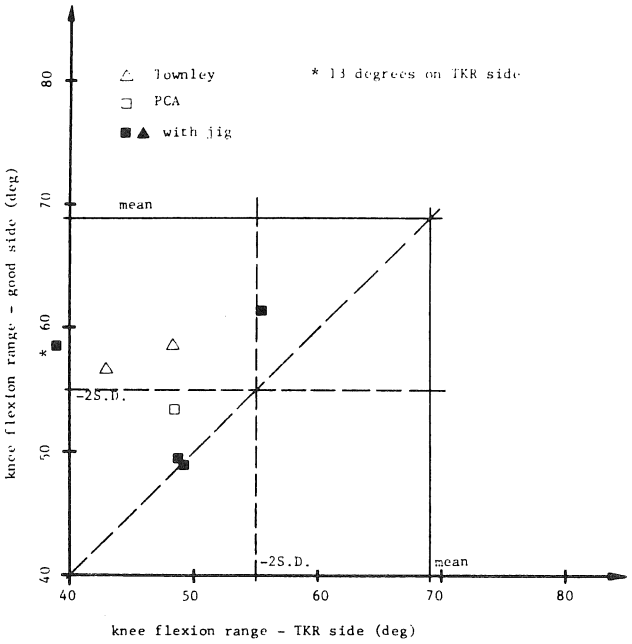

Fig. 1. Total knee flexion range for the good side and the total knee side.

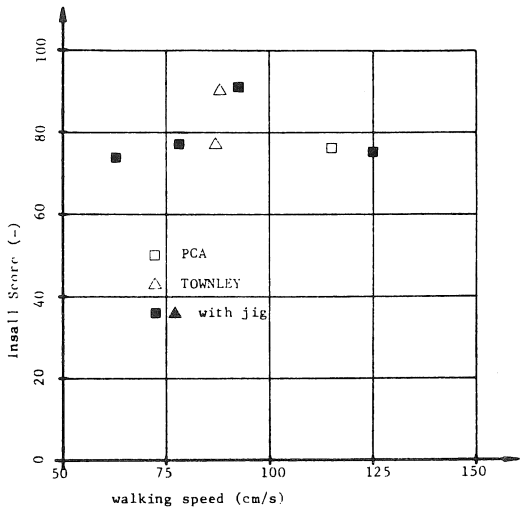

Fig. 2. The relationship between the Insall score and walking speed.

EFFECTS OF PROXIMAL TIBIAL OSTEOTOMY ON KNEE JOINT LOADING

B. Cairns, S. Naumann*, P. Tepperman**, V. Kekosz**
Hugh MacMillan Medical Centre, and *Institute of Biomedical Engineering
**Physical Medicine and Rehabilitation Department, University of Toronto

INTRODUCTION

Primary osteoarthritis of the knee is of unknown etiology. It commonly affects the medial compartment more than the lateral compartment of the knee leading to progressive varus deformity. The major presenting complaints are pain and stiffness. It is often associated with patellofemoral osteoarthritis in which the degenerative changes commonly found in the femoral-tibial joint are also present in the patellofemoral compartment. Surgical intervention is indicated when the patient is significantly limited in daily activities. The accepted surgical approach for medial compartment osteoarthritis of the knee is a valgus high tibial osteotomy designed to decrease compressive forces on the medial compartment. This may be combined with a Maquet procedure to decompress the patello-femoral compartment.

A set of 3-foot anteroposterior roentgenograms in which the patient is fully weightbearing is used to determine the degree of correction. A wedge is removed that is 1 mm wide at its base for each degree of total change desired at the knee.

REVIEW AND THEORY

Surgical success has largely been documented in terms of decreased pain, increased knee stability and improved walking tolerance. The objective determination of an optimal degree or range of valgus has been based upon both static[1,2] and dynamic[3,4,5] assessments. Static assessments, in which a radiograph of the patient standing on one leg is used, are meant to provide an estimate of the knee joint loading that occurs in mid-stance. Dynamic assessments have taken one of two forms. Either changes in the knee valgus/varus angle have been correlated with both clinical and gait laboratory measurements or a mathematical model has been used to estimate the forces internal to the knee and hence the load distribution across the knee during walking. No single study exists in which the above approaches have been systematically combined pre- and postoperatively to determine the results of this procedure, the ability to predict outcome based upon a preoperative assessment, and the secondary effects of this procedure on the hip, ankle and foot. This paper describes methods used to determine biomechanical changes resulting from high tibial osteotomy and discusses preliminary results.

METHOD

Gait Assessment: Nine reflective markers are placed on each lower limb of the subject to identify the relative rotations of the limb segments. Four video cameras that can detect infra-red light reflected from the markers (VICON) are positioned along one side of a 12-metre long walkway so that each marker is viewed. A force platform (Kistler) is used to record ground reaction forces. Electromyographic activity of six muscles via surface electrodes is recorded together with foot-floor contact patterns. Data is collected for 5 runs per side.

External Model: A plane for each limb segment is defined by having at least 3 markers associated with it. Each joint of the lower limb is modeled as a sequence of three single axis rotary joints to obtain the three angular degrees of freedom for that joint. A fixed coordinate frame is embedded in each link and the rotation of each segment is obtained relative to a fixed laboratory frame. These rotations are then used to obtain the intermediate transformations between the segments from which the actual joint angles may be obtained. Once the joint trajectories have been computed, the dynamics of the leg are then modeled as a sequence of four rigid links connected by three rotary joints. The model is used in an iterative Newton-Euler formulation to compute the joint torques based on the joint angles and ground reaction forces. Inertia, acceleration and gravitational effects are accounted for[6].

Internal Model: The method for estimating in vivo joint forces is based upon a model developed by Harrington (1983). Assumptions made are that: (i) no co-contraction of muscle groups acting about the joint can occur; (ii) muscles spanning the knee are grouped into units that have a single function represented by single lines of force action; (iii) the tibial plateau is a plane at right angles to the long axis of the tibia; (iv) all externally applied shear load is taken up by cruciate ligaments and muscles and only those ligaments that tend to oppose instantaneous external forces will resist these forces at any instant in time; (v) medial and lateral joint compartment loads act at predefined points.

Muscle forces, ligament forces, the resultant joint force acting on the tibial plateau and its location are obtained by equating the external and internal model force and moment equations.

Subject Material: Twenty-one subjects have been seen preoperatively. Of these, 18 have had proximal tibial osteotomies. Eleven subjects have been seen 3-to-6 months postoperative, and 3 have been seen for a second examination 6 months postoperatively. The results of 8 subjects (5 men, 3 women) are presented here. Five of the 8 subjects also underwent a Maquet procedure. The mean age of these 8 subjects was 58 years (36 to 75 years) and the mean weight and height were 93.5 Kg. (69 Kg to 132 Kg) and 166.4 cm (150 to 177 cm) respectively.

RESULTS

The average of 5 runs per side together with the standard deviation for each parameter were calculated. Examples of the data are shown in Figures 1 and 2. Figure 1 is a display of knee valgus/varus joint angle and torque time histories for one subject during the stance phase. Figure 2 illustrates the joint load during stance and the

percentage of joint load acting on the medial compartment of the tibial plateau.

Parameters determined include the maximum joint load acting on the tibial plateau normalized by body weight (max JL/BW), the percentage time during the gait cycle at which this maximum occurred (% GC), the percentage of the average joint load acting on the medial compartment (% MED JL), the speed of walking (SM/S), and the change in valgus/varus knee angle (VAR). Table 1 summarizes these results. All changes in Table 1 between preoperative and postoperative values were significant at a level of $p<.01$ using a two-sided t-test. In calculating the pre- and postoperative change in speed, the results of one subject were not used. This subject had her knee overcorrected to a valgus angle of 20 degrees. She had no pain but could not balance properly. As a result her speed decreased from a mean value of 0.94 m/s to 0.29 m/s.

	PREOPERATIVE		POSTOPERATIVE	
	MEAN	STD.DEV	MEAN	STD.DEV
max JL/BW	2.485	0.774	1.740	0.297
% GC	17.4	7.4	29.3	12.7
% MED JL	85.69	8.42	68.94	16.68
S (m/s)	0.801	0.208	0.896	0.174
VARUS (degrees)	8.00	3.30	-9.25	4.55

Table 1: Summary of Results

DISCUSSION

The results indicate that the method of determining joint loading through static analysis is likely to be inaccurate. This method requires the subject to be x-rayed while standing on one foot to approximate mid-stance and hence the phase of maximum joint loading. Our results show that while maximum joint loading occurred at 29% of the gait cycle postoperatively, preoperatively it occurred at 17% of the gait cycle. Changes in start and end of the single support phases remained relatively unchanged.

This study should determine whether an optimal degree or range of valgus exists that will provide the most functional gait pattern with a concomitant reduction and relocation of compressive stress in the medial femoral tibial compartment. Confirmation of this will require the construction of a jig that will permit the surgeon to more accurately determine and remove a wedge of the required size from the tibia.

REFERENCES

1. Kettlekamp et al, J.B.J.S., 58-A; 952-960, 1976.
2. Insall et al, J.B.J.S., 56-A; 1397-1405, 1974.
3. Johnson et al, J.B.J.S., 62-B; 346-349, 1980.
4. Harrington, J.B.J.S., 65-A; 247-259, 1983.
5. Prodomos et al, J.B.J.S., 67-A; 1188-1194, 1985.
6. Apkarian et al, J. Biomech. (submitted).
7. Kettlekamp and Chao, Clin. Orthop., 83; 202-213, 1972.

ACKNOWLEDGEMENTS

The authors gratefully acknowledge the financial assistance of the National Health Research and Development Programme of Health and Welfare, Canada, and of the Physicians of Ontario through the P.S.I. Foundation. The assistance of Dr. I. Harrington in implementing the internal model, and the efforts of Drs. A. Gross and M. Milner are appreciated.

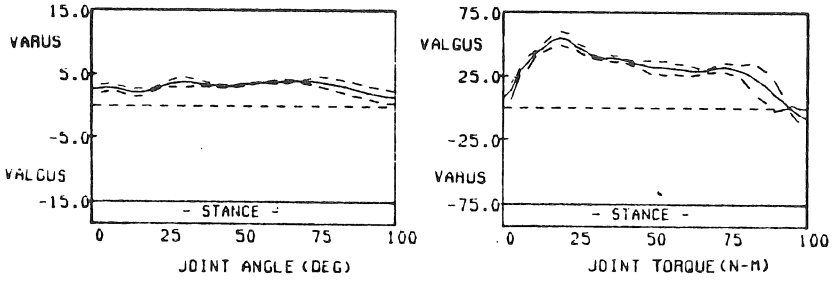

FIGURE 1: VARUS/VALGUS JOINT ANGLE AND JOINT TORQUE VERSUS PERCENT OF STANCE.

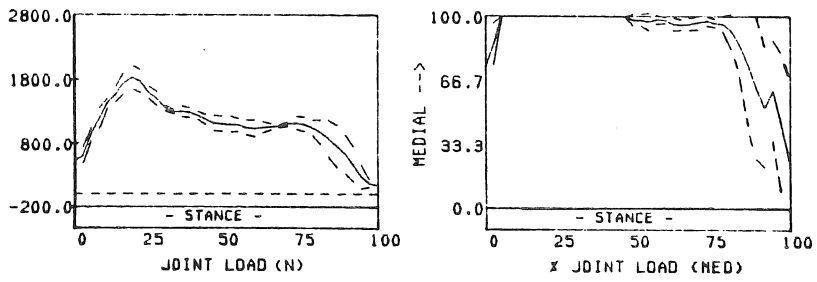

FIGURE 2: JOINT LOAD AND PERCENT OF JOINT LOAD ACTING ON THE MEDIAL COMPARTMENT VERSUS PERCENT OF STANCE.

BIOMECHANICAL ASSESSMENT OF THE RESULTS OF KNEE SURGERY

Michael W. Whittle and Rosalind J. Jefferson
University of Oxford
Oxford Orthopaedic Engineering Centre
Headington, Oxford, England

INTRODUCTION

Assessment by clinical means alone of the results of surgery to the knee may fail to identify shortcomings in the surgical procedure. Both to the patient and to the surgeon, the relief of pain is much more important than the restoration to normal of the biomechanics of the joint. However, the long term success of the surgery may well depend upon the magnitude and direction of the forces transmitted through the joint. Malalignment of the knee in the coronal plane may produce high abduction or adduction moments, which in turn lead to high forces in the ligaments and across the articular surfaces.

METHOD

During the period of the study, the majority of patients admitted to the Nuffield Orthopaedic Centre, Oxford, for surgery to correct a varus or valgus deformity of the knee have been asked to participate. A preoperative assessment of knee function was performed, followed by a postoperative assessment at least six months after surgery. The decision as to whether the patient would receive a total or unicompartmental knee replacement, or a high tibial osteotomy, was made on clinical grounds, and was not influenced by their participation in the trial. The trial is not yet complete; at the time of writing 37 patients have entered the study.

Assessment was made using the Vicon three-dimensional television/computer system illustrated in Figure 1, using four television cameras and two Kistler force platforms interfaced to a DEC PDP 11/23 minicomputer, to study both legs at the same time. The patient undressed, put on a swimming costume, anthropometric measurements were taken and retro-reflective markers were stuck over 13 anatomical landmarks on the pelvis and both legs. These showed up as bright spots to the television cameras, using stroboscopic illumination. The computer determined the positions of these points in the television images every 20 msec, and a calibration procedure enabled their positions in three-dimensional space to be determined to an accuracy of 3-4mm. Data were recorded with the patient standing, and during four walks at free speed. The total time spent by the patient in the laboratory was about 40 minutes. Processing the data, including interpretation, took approximately four hours.

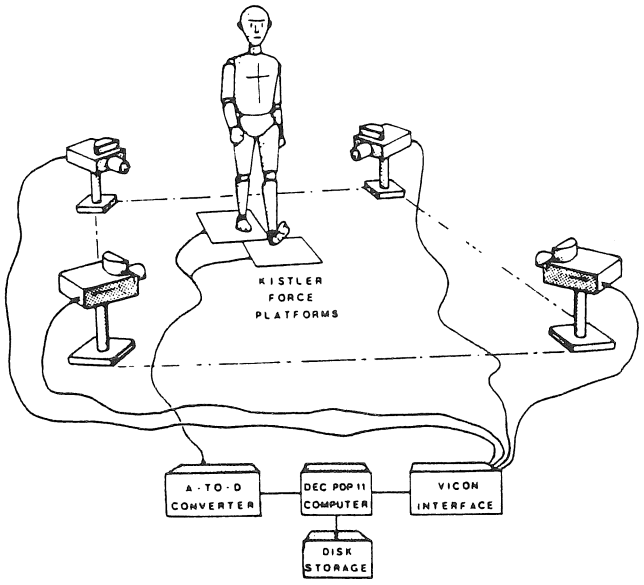

Figure 1: The three-dimensional measurement system.

A number of corrections were applied to the data during processing, to overcome some of the practical problems inherent in this type of study. Missing parts of a marker trajectory (such as when the arm masked a hip marker) were filled in by interpolation, and the coordinate system was adjusted to base it on the patient's plane of progression. The patient was not informed of the presence of the force platforms, and sometimes failed to achieve a complete single step on each platform. If repeating the walk several times with different starting positions failed to correct this, the force platform outputs were processed to reapportion the data appropriately between the two feet.

The standing data were processed to measure the knee angle in the sagittal and coronal planes, and to obtain further anthropometry.

The data from the four walks were combined, except where it was obvious that a walk was not typical. The mean walking velocity was obtained from the trajectory of the two hip markers, and the cadence was determined from the cyclical repetition of the leg marker positions. Stride length was calculated from velocity and cadence. All subsequent processing was based on the length of gait cycle. Plots of the knee angles and external moments in the sagittal and coronal planes (the 'knee-C-G') were used as the main basis for comparing the biomechanics of the knee before and after surgery.

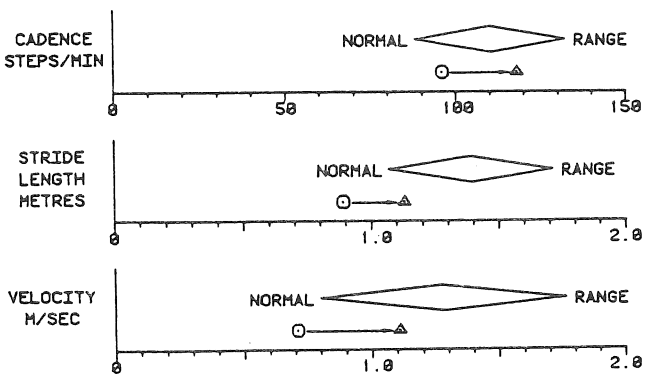

Figure 2: Mrs. SP: General gait parameters.

North American Congress on Biomechanics
Montréal (Québec) Canada, 25-27 August 1986

RESULTS

This study is not yet complete, and only illustrative results will be given.

Mrs. SP is a 71 year old lady who had suffered from osteoarthrosis of the right knee, with increasing pain and varus deformity, for about 5 years. Since the lateral compartment of the knee was well preserved, she was treated by medial unicompartmental knee replacement using the Oxford Meniscal Knee. The standing data showed a change in the right knee angle from 9° hyperextension to 1° of flexion and from 3° of varus to a neutral alignment. The general gait parameters (cadence, stride length and velocity) all showed an improvement, as illustrated in Figure 2, which also gives the normal ranges for our laboratory.

Figure 3 shows the knee angles and external moments in the sagittal and coronal planes, before and after surgery. The stance phase occupies approximately the first 60% of the cycle. The sagittal plane angle showed a reduced excursion before surgery, and an almost normal pattern afterwards. The coronal plane angle during the stance phase showed correction to neutral of the preoperative adduction (varus) angulation. The coronal plane angle during the swing phase is subject to measurement errors, and should be disregarded. The sagittal plane moment pattern was corrected from a pathological 'extension only' to the normal biphasic pattern, although the magnitude of the moments was small. The adduction moment in the coronal plane was slightly raised prior to surgery, and was normal afterwards.

Mr. CR is a 60 year old man who injured his right knee playing football in 1944. Over the last few years his knee has become increasingly painful with osteoarthrosis and a varus deformity. He was treated by high tibial osteotomy. The standing knee angles changed from 7° to 16° of flexion, and from 10° of varus to 4° of valgus.The general gait parameters showed a small reduction in cadence and velocity.

Figure 4 shows the knee angles and moments before and after surgery. A small flexion deformity was present, with an associated 'flexion only' moment pattern, both before and after surgery. In the coronal plane the preoperative varus angulation during the stance phase was slightly overcorrected, and and the pathologically high adduction moment before surgery was reduced to an abnormally low moment.

DISCUSSION

It is essential that objective assessment is used wherever possible to examine the outcome of a surgical procedure. Patients with a varus or valgus deformity of the knee may be treated conservatively, or by one of several operations, of which the three examined in the present study are the most common. While the clinical results of these procedures have been studied in some detail, only recently have methods become available to study the biomechanics of the joint during walking. Information of this type should help the surgeon to make the decision as to which type of treatment to offer.

The two examples given show the type of information which can be provided by the measurement system at present. They also illustrate the differing results, in biomechanical terms, that can be obtained from different procedures, although it would be unwise to draw any conclusions about the merits of different operations from only two cases, and without considering clinical factors such as pain. By studying sufficient numbers of patients, it is hoped to learn those factors which indicate the best procedure for an individual patient. In order for this type of measurement to be useful clinically, the data need to have some prognostic value, and this will only be the case when sufficient numbers of patients have been assessed.

It would be naive to think that the methods described here represent the ultimate in biomechanical measurement. At present, the patient is only studied when walking under carefully controlled conditions, and measurements of joint angles and moments are made in only two planes. However, such measurements represent a useful starting point in the process of making available information which cannot either be seen by the surgeon or felt by the patient.

CONCLUSIONS

Objective biomechanical assessment of knee joint function is a valuable technique in clinical research. It enables the outcome of different surgical procedures to be compared, and it is hoped that eventually it will provide a more scientific basis for the choice of treatment for individual patients.

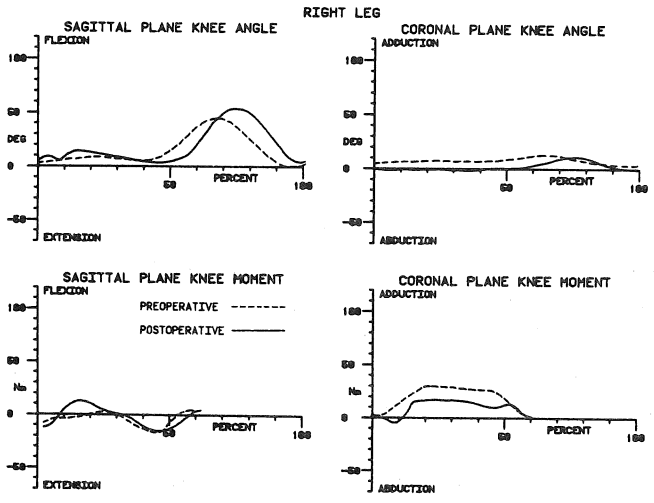

Figure 3: Mrs. SP: Knee angles and moments.

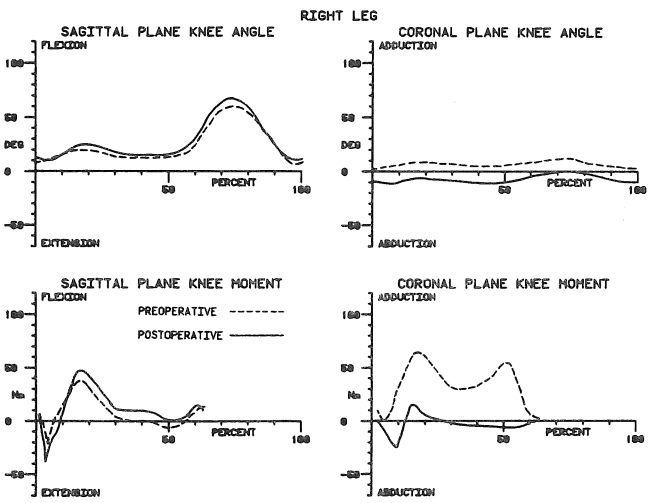

Figure 4: Mr. CR: Knee angles and moments.

BIOMECHANICAL CORRELATES WITH RUNNING ECONOMY IN ELITE DISTANCE RUNNERS

Keith R. Williams
Human Performance Laboratory
University of California
Davis, CA 95616

Peter R. Cavanagh
Biomechanics Laboratory
The Pennsylvania State University
University Park, PA 16802

INTRODUCTION

While a great deal of information is available concerning the biomechanics of running for the novice and the well-trained recreational or collegiate runner (4), there are only limited data available concerning running mechanics at the elite level (1). World ranking lists are often separated by very small margins as evidenced by the 2% bracket that contained the world top 13 marathon runners in 1985. The possibility of being able to make adjustments to an athlete's mechanics in order to improve running economy ($\dot{V}0_2$ at a given submaximal speed of running) and performance is an intriguing one but, at present, little evidence exists on which to base the rationale for change. At the same time few elite athletes are likely to be receptive to making arbitrary changes to their running style without convincing evidence that it is likely to enhance their running potential. The present study provides some initial information concerning the relationships of running mechanics at the elite level with running economy.

METHODS

Data were obtained for thirteen elite male distance runners who participated in a running camp at the United States Olympic Training Center. All runners had been actively competing at a high level prior to the experimental sessions and typically raced distances from 1500 m to the marathon. In order to evaluate the runners at a speed appropriate to their abilities, the target pace for all measurements was set a 5.96 m/sec (4:30 min/mile).

Ground reaction force data were collected using an AMTI force platform on-line to a microcomputer, and data from the support phases for each foot were analyzed to yield measures of peak forces and impulses for each of three force components. These data were then averaged to provide characteristic measures for each subject. Impulse measures were used to calculate changes in horizontal and vertical velocity during support. Kinematic data were obtained using two LOCAM cameras while subjects ran on a treadmill. A side view camera operating at 150 fps was used to provide measures of trunk angle, vertical oscillation, and linear and angular kinematics of lower extremity movements. Two cycles of running were analyzed for each subject and averaged. A front view camera operating at 50 fps provided measures of stride width, based on 20 successive foot strikes, and wrist motion in a frontal plane, averaged over four cycles. Various anthropometric measures for the lower extremity were also obtained. During the same running camp submaximal oxygen consumption ($VO_{2submax}$) data was collected by a physiology group during overground running at four individually determined paces ranging between approximately 5 and 6 m/sec. $VO_{2submax}$ data (ml/kg/min) for the test pace were predicted from regression equations derived for each subject from these data.

RESULTS

Table 1 lists mean values for selected kinematic and kinetic variables. Eight of the runners showed midfoot strike patterns and five were rearfoot strikers. Figure 1 illustrates differences in knee-ankle angle-angle diagrams between two runners in the sample, a rearfoot striker and a midfoot striker. The midfoot striker shows a more plantar flexed position at foot strike. Maximal vertical forces averaged more than 3BW (FZ2) and most of the midfoot strikers showed initial vertical peaks (FZ1-a) feature often not present at slower speeds in midfoot strikers (2). Several of the runners showed very large initial force peaks (up to 3.6BW in training shoes and over 4BW in racing shoes), as illustrated for one subject in Figure 2. The mean change in horizontal velocity (DELV Horiz.) during the braking phase of support represented 5% of the target pace and showed a wide range among subjects from -0.21 to -0.38 m/s.

Lower extremity angles showed relatively large values for maximal thigh flexion and extension and for knee flexion during swing than have been previously reported (3). This is to be expected because of the faster pace used in the present study. Mean trunk angles varied from 7.5 to 13.1 degrees, indicating that all of the runners exhibited some amount of forward lean. A negative value for step width indicates that a runners crossed over the midline during support - that is they placed the right foot to the left of the midline and vice versa. Ten of the subjects showed this pattern for at least one of their feet.

Correlations between $VO_{2submax}$ and the various biomechanical variables were, in general, moderate to low. Of the ground reaction force variables the highest correlations were with support time (r=0.49) and peak force pushing medially on the foot during support (r=0.50). Some of the kinematic variables gave somewhat higher correlations, such as correlations of 0.53 with maximal thigh extension, 0.56 with knee angle at toe off, 0.46 with maximal plantar flexion velocity, and -0.64 with horizontal heel velocity at contact. These correlations indicate that, in general, lower oxygen consumption was associated with a longer support time, greater maximal thigh extension, less knee extension at toe off, a greater maximal plantar flexion velocity, and a greater horizontal heel velocity at contact. The anthropometric variables related to body size showed the highest correlations with $VO_{2submax}$. Leg length, pelvic width, and foot length showed correlations from -0.55 to -0.68 with $VO_{2submax}$. The correlation with body weight was -0.39. Thus the large values of these measurements tended to exist in the more economical runners.

DISCUSSION

The biomechanical variables compared with economy in the present study were the relatively simple kinematic and kinetic measures that can be obtained quickly from film or video and force platform analysis. It must be recognized that the sample size in the present study was small, with the implications that the results may not apply to other samples and that the correlations may be somewhat unstable. Yet within these limitations, the lack of a relationship between oxygen uptake and measures traditionally thought to be important - such as vertical oscillation and the braking impulse during ground contact - implies that the biomechanical correlates of economy in elite runners may be at a level of complexity greater than that used in the present study. Obvious candidates for future study are the storage and release of mechanical energy and the transfer of energy between segments of the body. It should also be noted that it is unlikely that any one variable is likely to correlate highly with $VO_{2submax}$ in a group of subjects. It is more likely that a number of factors each contribute a small amount to the variance in $VO_{2submax}$. Some of the runners showed relatively extreme values or unusual patterns for isolated measures compared to the typical response. At present it is not possible to distinguish whether these factors contribute to making the runner less efficient than he would otherwise be, or in fact represent the means by which the individual has optimized his performance to suit his own anatomical and physiological makeup.

References

1. Cavanagh, P.R. et al. Int. J. Sport Biomech., 1(1):36-62,1985.
2. Cavanagh, P.R. et al. J. Biomech., 15(5):397-406, 1980.
3. Elliott, B.C. et al. Can. J. Appl. Sport Sci., 5(4):203-207, 1980.
4. Williams, K.R., Ex. and Sport Sci. Rev. 13:380-442, 1985.

TABLE 1. BIOMECHANICAL MEASURES OF RUNNING STYLE

	Mean	SD	Units
FZ1	2.9	0.5	BW
FZ2	3.2	0.2	BW
Contact Time	162.8	9.3	ms (20N threshold)
Dec. Horiz. Vel.	-0.29	0.05	m/s
Chg. Vert. Vel.	1.58	0.13	m/s
Trunk Ang.	10.2	1.9	deg
Max. Thigh Ext.	-32.9	3.7	deg
Max. Plant. Flex.	58.6	6.7	deg
Max. Knee Flex.	134.4	7.8	deg
Max. Pl. Flex. Vel.	-12.4	45.8	rad/s
Step Length	191.7	10.4	cm
Step Width	-2.1	3.6	cm

ACKNOWLEDGEMENTS

This work was partially supported by the United States Olympic Committee. The authors would like to thank Jack Daniels and Pat Bradley who collected the oxygen uptake values used in this study.

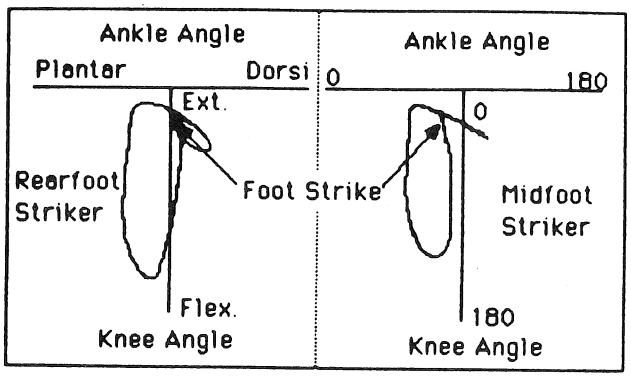

Figure 1. Knee-ankle angle-angle diagram for a rear- and a mid-foot striker. Notice the difference in plantar flexion angle at foot strike.

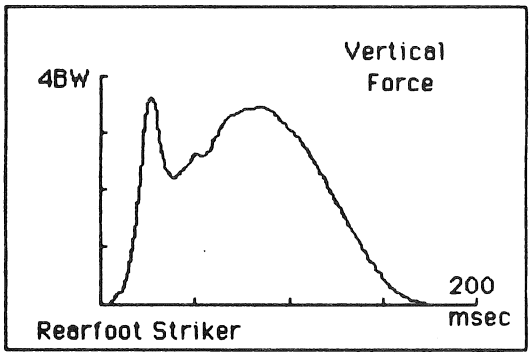

Figure 2. Vertical ground reaction force for a rearfoot striker showing a large initial force peak.

MUSCULAR AND "MECHANICAL" MOMENTS OF FORCE IN SWING MOTION*

Elizabeth M. Roberts

Lin, Jia Ling
Department of Physical Education and Dance
University of Wisconsin-Madison, WI 53706

Robert P. Moorman

Introduction

The influence of the mechanical moments of force about the knee joint on the motion of the shank-foot segment during swing in running was studied under normal conditions and under two conditions of simulated loss of knee muscular moment. The purpose was to illucidate the role of these "mechanical" moments of force in controlling the motion of the shank-foot segment through its interaction with the thigh. The results indicate that the shank-foot mechanical moments are acting in opposition to muscular moments throughout most of the swing and may perhaps be thought of as being controlled by the muscular moments. When knee muscular moments are lost the remaining mechanical moments are unrestrained and their influence on segment motion is clarified.

Review & Theory

In previous work on the component mechanics of the swinging limb in running, Phillips et. al. (1983) suggested that non-muscular intersegmental reactions play a substantial role in knee flexion and extension. They related the increase in speed of the shank-foot during knee extension, for example, to the decrease in speed of the thigh. Putnam (1983) on the other hand made a reverse interpretation concluding that the decrease in thigh angular velocity, in a punt was merely "__ a result of the influence of the shank's angular motion of the thigh.", (p693). Putnam's conclusions were based on a component analysis of the moments acting on the two segments. The interpretations of Phillips et. al. were based on a comparison between components under observed conditions with those under simulated conditions when the muscular moment at the knee was mathematically set to zero. In the latter analysis the motion of the thigh segment in addition to that of the shank-foot was permitted to change from its observed behavior thereby causing interactions of the thigh on the shank that were different from normal. A simulation in which the motion of the thigh was not permitted to change in comparison to when it was permitted to change could throw further light on the mechanisms of free segment limb control, a topic of considerable significance in many animal motion studies. That was the purpose of this work.

Methodology

Cinematographic records of 5 Masters runners over age 60 years and 3 young adult middle distance runners (20-25 years) were taken at 200 fps at the outdoor track. Subjects were asked to run at a near maximum speed. Two of the subjects, one young adult and one Masters runner were selected for simulation analysis. Running speeds were 9.26 $m.s^{-1}$ and 5.92 $m.s^{-1}$ respectively. Segment centers of mass (Dempster 1955) and angles of inclination were calculated from digitized end points and curve fitted by digital filtering. Linear and angular velocities and accelerations of the thigh and combined shank-foot segment were derived. Horizontal and vertical forces, muscular torques, "mechanical" torques and total torques at the hip and knee were calculated.

The first simulation isolated the influence of the knee muscular moment (M_1) on the shank by constraining the thigh to its normal motion. The equation for the summation of torques about the center of gravity of the shank-foot was written as a function of the shank-foot angular acceleration ($\ddot{\theta}_1$), angular velocity ($\dot{\theta}_1$) and angle (θ_1). The linear accelerations of the knee were used as input data and M_1 was set equal to zero. The remaining second order differential equation was solved numerically for $\theta_1\dot{\theta}_1\ddot{\theta}_1$.

The second simulation examined the influence of M_1 on both segments by allowing the thigh to vary and constraining the hip to its normal motion (Phillips et al). The moment equations for the thigh and shank-foot were written as functions of the thigh angular acceleration $\ddot{\theta}_2$, angular velocity $\dot{\theta}_2$, angle θ_2 and $\theta_1\dot{\theta}_1\ddot{\theta}_1$. The linear accelerations at the hip and the hip muscular moment (M_2) were used as input data. M_1 was set to zero and the observed data were used for the initial values at the beginning of each simulation. The simulations were initiated at several different points.

Results and Discussion

The observed data on the shank-foot segment directly calculated from film and normalized in time, Fig. 1, illustrate that the total moments of force ($I_1\ddot{\theta}_1$) are composed of "mechanical" moments of force ($M_{x1}+My_1$) and the muscular moment of force (M_1). The "mechanical" moments are produced by joint forces which in the observed motion include forces produced by the muscles but in the simulations are only bone on bone forces. Throughout most of the observed swing the mechanical moments are in opposition to the muscular moment, M_1, with the latter dominating. Total moments are therefore in the direction of the muscular moments for the most part. There are two notable exceptions - 1) at the very beginning, from zero to 10% of swing, when knee flexion and shank-foot backward rotation are being initiated, and 2) from approximately 40% to 48% of swing where shank forward rotation begins at 40% and the reversal of knee flexion to knee extension occurs at 44%. For these periods both knee muscular and mechanical moments are in phase and it is at these times that major shank angular velocities of flexion and extension respectively are being developed. Shortly afterward, at 12% and 55% respectively, total moment $I_1\ddot{\theta}_1$ reverses and shank angular speed begins to decrease. It should be noted however that knee muscular and mechanical moments are not in phase near the end of swing where knee extension reverses to flexion (93% of swing) prior to touchdown. During the period just preceeding final knee reversal (74% to 92%) both muscular and mechanical moments are larger than at any other time and of opposite sign. The muscular moment prevails.

When the muscular moment is lost first from the shank-foot only (first simulation) and second from both the shank-foot and thigh (2nd simulation) mechanical moments are unopposed in their action of the shank-foot segment. They do not, however retain their original pattern (Fig 2) since a com-

ponent of the joint forces involved in "mechanical" moments was originally provided by the muscle. In both simulations when M_1 is eliminated at 0% the mechanical flexor moment at the beginning of swing (zero to 10%) is greater than it was in the observed motion thus even though the flexor moment of the muscle is gone, the total flexor moment ($I_1 \ddot{\theta}_1$) is still appreciable and knee flexion is initiated. Following the first 10% of swing mechanical moments are less negative (flexor) than normal until 28% and 20% for the 1st and 2nd simulations respectively. They then become positive (extensor) much sooner than normal.

Once the muscular moment is eliminated the mechanical moments become more closely associated with the motion of the distal end of the thigh which retained its normal motion in the first simulation but was no longer "held in check" in the 2nd simulation. With the zero time cut-off of M_1 the remaining knee flexor and extensor moments were clearly present but were not sufficient to provide the same velocity of flexion (especially in simulation 1) or to initiate extension. In addition their timing was changed toward that of the thigh velocity increase rather than to the timing of M_1. Since thigh motion is exaggerated in the 2nd simulation when the opposing moment from M_1 is missing the mechanical moments are similarly exaggerated.

M_1 was also set to zero at 40% of the swing at a time when the velocity of the shank-foot segment was zero but knee flexion had not quite ceased. The discontinuities in the simulation moments in Fig. 2 indicate this point. Here again the magnitude and timing of the mechanical moments are shifted toward velocity changes in the thigh. When the mechanical moments become negative in simulation one they remain negative much longer than normal. With the initially low velocity the change in position of the shank-foot was small and the segment stayed close to the rear horizontal. Thus with the thigh motion normal the associated mechanical moments were not adequate to produce the normal motion. In the second simulation where thigh motion was exaggerated the extensor influence was greater and the flexor influence less such that knee extension exceeded normal. This is in agreement with Phillips et. al.

In summary, the first simulation tends to clarify the mechanical influence of the thigh on the shank under normal circumstances while the 2nd simulation tends to amplify those effects. In light of the present data the suggestions of both Phillips et. al. and Putnam have validity in that thigh moments, both muscular and mechanical, influence the shank, and shank moments influence the thigh. Internal moments alone would have such effects. However the thigh can be subject to external inputs and there are still questions regarding the extent to which external moments at a given point in time influence the behavior of the shank, not only in a run but perhaps more dramatically in a kick. Further study is needed to clarify this point.

References

1. Phillips, S.J. et al. J. Biomech. 16:411-417,1983.
2. Putnam, C.A. Biomechanics VIIIB. Human Kinetics Pub. pp 688-694, 1983.

*Supported in part by the Research Committee of the Graduate School, University of Wisconsin-Madison (Grant #101-1527).

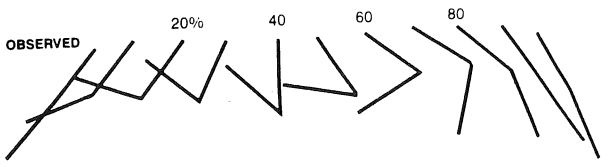

Fig. 1a. Swing limb in running; % time.

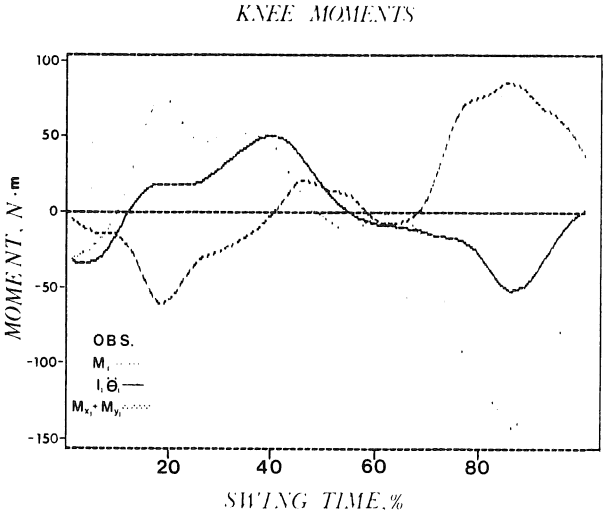

Fig. 1b. Moment components acting on shank for observed swing. Muscular moment, M_1; "mechanical" moments, $M_{x1}+M_{y1}$; total moments, $I_1\ddot{\theta}_1$. Positive moments are extensor.

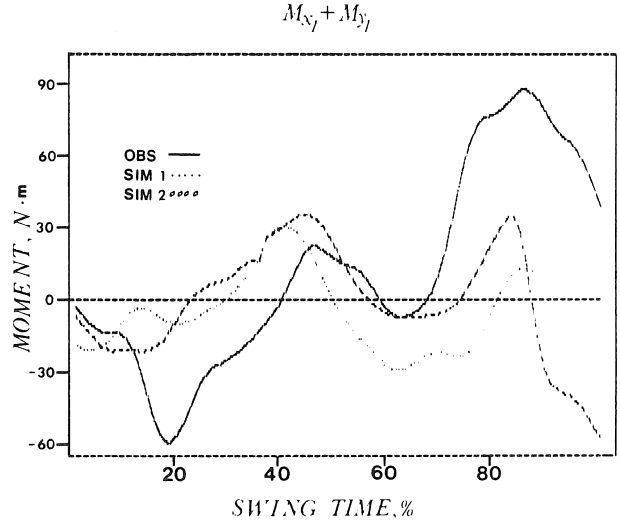

Fig. 2 "Mechanical" moments acting on shank. Observed, obs.; stimulated loss of M_1 on shank, sim. 1; simulated loss of M_1 on shank & thigh, sim. 2. Positive moments are extensor.

AN EMPIRICAL MODEL TO CALCULATE THE EFFECTS OF WIND AND ALTITUDE ON THE TIMES OF 100 METER SPRINT RACES

J. Dapena and M.E. Feltner
Department of Physical Education
Indiana University
Bloomington, IN 47405

INTRODUCTION

Air density and the prevailing wind at the site of a race affect the air resistance force encountered by the sprinters, and consequently the time of the race, thus making it difficult to compare the true values of sprinting performances achieved under diverse wind and altitude conditions. This paper describes the development of a new model for the adjustment of the effects of wind and altitude on the times of 100 meter sprint races. The model can be considered a further refinement of the models of Hill (1), Garcia & Garcia (2), and Heidenstrom (3). It was developed in three stages: the first stage involved the generation of an initial model that eliminated some of the most questionable assumptions of previous models; in the second stage, the model was evaluated using statistical information from world-class sprinting races; in the final stage, the model was modified by adjusting the value of a key parameter until the results produced by the model fit with the statistical data.

THEORY

The air resistance force exerted on a sprinter can be calculated using a standard equation:

$$F_A = 1/2\ C_D\ d\ A\ v_r^2 \quad (1)$$

where C_D is the drag coefficient of the sprinter, d is the air density, A is the frontal area, and v_r is the velocity of the air relative to the sprinter. Data from world weather records were used to produce an equation that calculated air density at any altitude H:

$$d_H = 1.175\ (1 + 0.95\ 10^{-5}\ H - 1.00\ 10^{-9}\ H^2)\ e^{-0.000125H} \quad (2)$$

The frontal area may be assumed to be directly proportional to total body area (A_b):

$$A = K_A\ A_b \quad (3)$$

where K_A is a proportionality constant, and A_b can be estimated from the mass (m, in kg) and the standing height (h, in m) of an individual (4):

$$A_b = 0.217\ h^{0.725}\ m^{0.425} \quad (4)$$

Data from the literature led to initial estimates for K_A and C_D: K_A=0.24; C_D=0.99. For convenience, eqs. (1), (3), and (4) were combined into one:

$$F_A = K\ d_H\ h^{0.725}\ m^{0.425}\ v_r^2 \quad (5)$$

where $K = 1/2\ 0.217\ C_D\ K_A$. The value of this constant in our initial model was K=0.02578.

METHODOLOGY

Nine male sprinters were filmed during two competitive 100 meter races. There was no wind during the filmed races. The film data were used to calculate displacement, velocity, and acceleration values for each subject. The net propulsive force F_R exerted on each of the subjects at each instant of the race was calculated from the acceleration. The air resistance force F_A was calculated using eqs. (2) and (5). The value of F_P, the ground propulsive force, was subsequently calculated as the sum of the magnitudes of F_R and F_A. Fig. 1 shows plots of F_P, F_A, and F_R versus running speed, for a typical subject (for normalization purposes, all force values were divided by the mass of the subject). Up to the instant of attainment of maximum speed, the graph of F_P vs. velocity could be modeled quite well in all cases by two straight lines, but the reductions in propulsive force and in velocity due to fatigue in the later stages of the race posed a problem. To solve it, a plot was drawn for each subject showing the differences between the actual and the fitted values of the propulsive ground force, versus time. In the early stages of the race, the graph fluctuated around zero, but after maximum velocity it showed increasingly negative values. This later part of the graph could be modeled with reasonable accuracy by a straight line that intersected the abscissae axis at the time of maximum velocity. Thus, three linear functions could be used to predict the propulsive ground force of any of the athletes in our sample at any instant, knowing the velocity of the athlete at that instant and the time elapsed since the start of the race. The three functions were defined by a total of six coefficients (K1 through K6). Two more coefficients, K7 and K8, defined the reaction time and the position of the athlete at the start of the race, respectively. Regression was used to find eight equations that permitted the calculation of K1 through K8 for any athlete (including athletes not in our sample) from his race time. The coefficients could then be used to simulate a whole race in any conditions of wind and altitude using Euler's method with an integration step of 0.01 s. This permitted the calculation of the time that the athlete would have achieved in any set of wind and altitude conditions, knowing the time of the athlete in another set of wind and altitude conditions.

MODEL EVALUATION AND MODIFICATION

Wind-aided races will generally produce better times than wind-hindered races. Consequently, the wind readings of the best 100 race times ever recorded should be expected to include a disproportionately large number of wind-aided values. The adjustment of race times to compensate for different air conditions should make the times of wind-aided races deteriorate, and it should improve the times of the wind-hindered races. This would bring more wind-hindered races into the corrected list of the top 100, and it would eliminate some of the wind-aided races, thus leading to a more balanced combination of wind-aided and wind-hindered races. An underadjustment of the race times should be expected to leave an excessive number of wind-aided races in the list of the top 100; a proper adjustment should lead to the same distribution of wind-aided and wind-hindered races as in the general population of all track and field meets; an overadjustment should lead to an excessive number of wind-hindered races. This rationale was used to evaluate the model and to introduce modifications into it. The wind readings reported by Track & Field News between 1975 and 1985 yielded an average wind of +1.11 m/s for races held in the United States, and +0.14 m/s for races held in Europe. The reasons for this difference were not clear, but it

could be attributed to differences in meet organization and/or stadium design. We then compiled a listing of the top 100 times ever recorded, regardless of wind conditions. Both the American and the European races in this list had more positive average wind values than the average race. This was not surprising, and it reflected the fact that the more wind-aided races have a greater probability of making it into the list of the top 100 uncorrected races. A new listing was then compiled after correcting the times of races using our initial model. As expected, the corrections made part of the wind-aided races drop out of the list of the top 100, and brought in more wind-hindered races. However, the races in the corrected top 100 list had more negative average wind values than the average race, indicating that our initial model overadjusted for the effects of air resistance. This was attributed to an excessive value for constant K of eq. (5). It was then assumed that the proper value of K would be the one that would produce an unbiased value for the average wind reading in the list of the top 100 corrected times. To find the optimum value of K, a major part of the model development process was repeated. This was done twice, using K=0.018 and K=0.010. The differences between the average wind readings of the adjusted races and the expected unbiased values were calculated, and plotted against the respective K values (Fig. 2). The plots indicated that a K value of approximately 0.0098 (American races) or 0.0124 (European races) would minimize the wind discrepancies. The average of these values (K=0.0111) was chosen for the final model. The process of model development was repeated once more, using K=0.0111. The curves in Fig. 3 show the effects of wind and altitude on the time of a 10.00 s race according to this final model.

DISCUSSION

We were surprised that the adjustments predicted by our final model were much smaller than those predicted by the previous models and by the initial form of our own model. The accuracy of our final model ultimately relied on the test that compared the average wind reading of all races with the average wind reading of the races included in the list of the top 100 adjusted times. The validity of this test was based on two main assumptions: (a) that the average wind of the meets where performances of intrinsically high value are achieved is not different from the average wind of other meets; and (b) that there are few errors in the official wind readings. The first assumption appeared to be quite solid: it would not make much sense that the organizers of the best competitions would consistently make the sprinters run into headwinds. The second assumption was more difficult to assess, but apart from a few isolated instances, we had no reason to doubt the competence of officials in general, or the accuracy of the wind gauges. Consequently, we accepted the validity of our final model. The fact that the values of K obtained using wind data from European races and from American races were not very different from each other further supported the validity of the time adjustments predicted by our final model.

References

1. Hill, A.V. Proc. Roy. Soc. L. B, 102:380-385, 1928.
2. Garcia, J.M. et al. Atlet. Español, 18(12):30-32, 1971.
3. Heidenstrom, P. Australasian T&F, Nov.:19-22, 1980.
4. Vaughan, C.L. et al. J. Hum. Movem. Stud., 3:207-213, 1977.

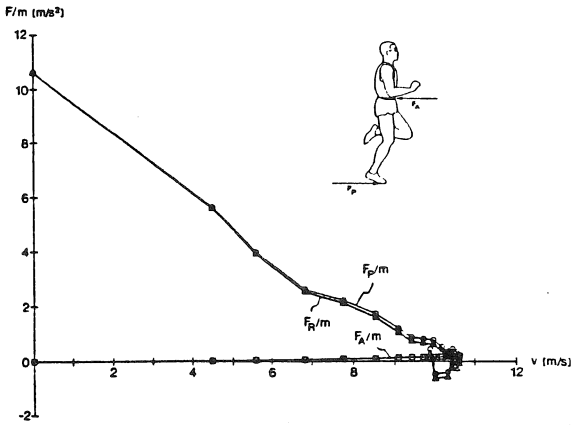

Figure 1. Plots of F_P, F_A, and F_R, vs. time, for a typical subject.

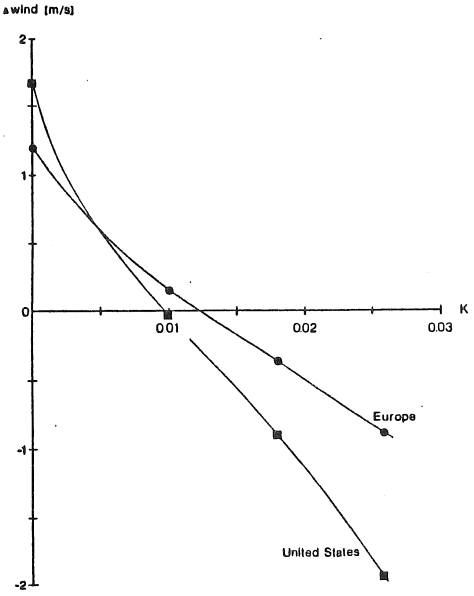

Figure 2. Differences between the average wind of the American and European races in the list of the top 100 races, and the average wind of all American and European races (wind of top 100 - wind of average race), vs. K.

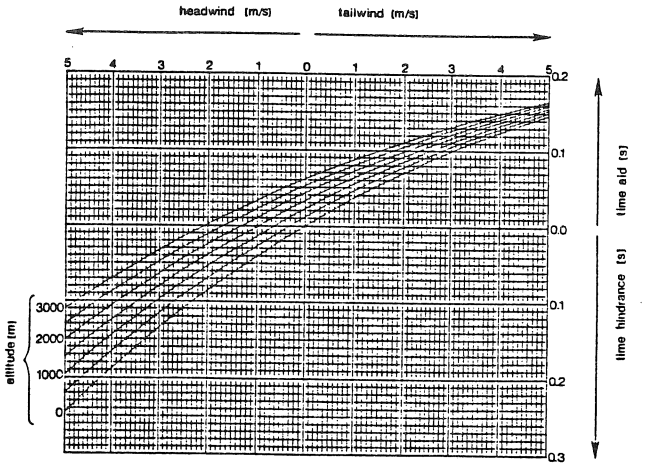

Figure 3. Wind and altitude corrections predicted by the final model (K=0.0111).

IDENTIFICATION OF SKATEBOARD RIDER CONTROL STRATEGIES

M. Hubbard, H. Fujikawa
Department of Mechanical Engineering
University of California
Davis, CA 95616

INTRODUCTION

Dynamic equations for the skateboard are used together with Linear-Quadratic control theory to identify the feedback law used by a rider in control of the skateboard in a tracking task. A numberical optimization procedure yields the control law which gives the best fit between experiment and computer simulated dynamic behavior.

REVIEW AND THEORY

As the number of injuries increases as a result of skateboard accidents [1], it becomes urgently necessary to solve the mechanism of human control and stability of the skateboard.

Two previous studies [2,3] have been made of skateboard dynamics and control. Hubbard [2] investigated the natural lateral dynamics and stability of the skateboard in the absence of rider control. Examining two simple models, it was found that the speed of the venicle is an important parameter and that the uncontrolled vehicle is unstable. This is unfortunate for an inexperienced rider because of the dangers of operation of the venicle at nigh speed. In a second study [3] the dynamical equations describing the controlled system in a tracking task were deduced. The performance index for the tracking task was assumed to be an integral of quadratic forms in the state and the control. Experimental results from a professional rider were presented which strongly supported the hypothesis that the human functions as an optimal controller in the skateboard tracking and balancing task.

In this paper, the optimal vehicle behavior when manipulated by an experienced skateboard rider is discussed in further detail. Two sets of state equations are presented, which result in fourth or firth order dynamic models according to the choice of the control variable. Under certain conditions simple proportional feedback control of rider tilt angle or tilt angular velocity can stabilize roll motion of the vehicle. Therefore, we can select either the board tilt angle or the tilt angular velocity as the control variable. If tilt angle is selected as the control variable, the system model may be written in first order vector-matrix state equation form with four state variables, ($\bar{x} = [\phi, \dot{\phi}, \theta, x]^T$). When tilt angular velocity is chosen as the control, however, the system has a five-dimensional state vector ($\bar{x} = [\phi, \dot{\phi}, \theta, x, \gamma]^T$) where, ϕ is the rider tilt angle, θ is the yaw angle of the board center-line, x is the position deviation from a desired track, and γ is the board tilt angle. Figures 1 and 2 show these coordinates in front and top views, respectively. The equations of motion may be found in [2] and [3] but are omitted here for brevity.

It is believed that an experienced skateboard rider controls a board nearly optimally. Thus for the tracking task, a linear quadratic performance index is assumed.

$$PI = \int_0^\infty \bar{x}^T Q \bar{x} + u^2/r \, dt$$

Using system identification techniques, the exact set of feedback gains actually implemented by the rider is found. This is accomplisned by first identifying the particular set of weighting matrices in the quadratic performance index which minimizes the mean squared residual between experimental data and simulation results. The residual selected as a measure of similarity between experimental and simulation data was

$$Res = \int_0^\infty \left\{ (\phi_e - \phi_s)^2 + (x_e - x_s)^2 + (\gamma_e - \gamma_s)^2 \right\} dt$$

where the subscripts e and s correspond to experimental and simulation, respectively. A related approach has been taken by Levinson [4] and Lancraft and Kleinman [5] in the analysis of optimal control model for a human operator.

RESULTS

The optimal performance index and the feedback gains which minimize the weighted residual between experimental data and simulation results are calculated for four cases; diagonal and nondiagonal state weighting matrix Q for both 4th and 5th order models. The calculations are done using the program CTRLC. Figure 3 shows the decrease of the performance index versus iteration number for the four cases. Figure 4 shows the predicted time response for a turning maneuver compared with the experimentally measured dynamic behavior for the same maneuver. Agreement in the board and rider angles ϕ and γ is good, but the agreement is less good in lateral position deviation x.

DISCUSSION

It is found that the weighted residual for 5th order model is considerably smaller than that for the 4th order model. This means that the rider likely controls tilt angular velocity rather than tilt angle to optimize the vehicle control. Also it is found that the weighted residual for nondiagonal Q is somewhat smaller than that for a diagonal Q using both 4th and 5th order models. Thus it is concluded that the rider regards the error of tilt angle and deviation from desired track as important factors but that cross products of these variables are important as well.

References

1. Jacobs, R. A. and Keller, E. L., "Skateboard Accidents", Pediatrics, Vol. 59, pp. 939-942, (1977).

2. Hubbard, M., "Lateral Dynamics and Stability of the Skateboard", J. of Applied Mechanics, Vol. 46, pp. 931-936, (1979).

3. Hubbard, M., "Human Control of the Skateboard", J. of Biomechanics, Vol. 13, pp. 745-754, (1980).

4. Levinson, W. H., "A Quasi-Newton Procedure for Identifying Pilot-Related Parameters of the Optimal Control Model", Proceedings of the 17th Annual Conference on Manual Control, Los Angeles, 1981.

5. Lancraft, R. E. and Kleinman, D. L., "On the Identification of Parameters in the Optimal Control Model", Proceedings of the 15th Annual Conference on Manual Control, Dayton, OH, 1979.

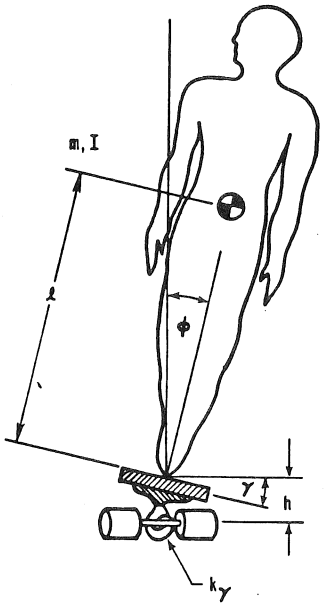

Figure 1. Rear view of skateboard-rider system which is controlled through the board tilt angle γ.

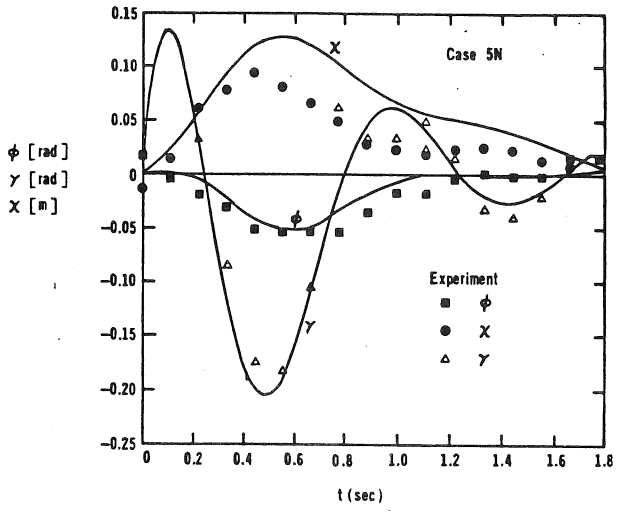

Figure 4. Experimental turning data and trajectories predicted by simulation using minimum residual feedback gains in Case 5N.

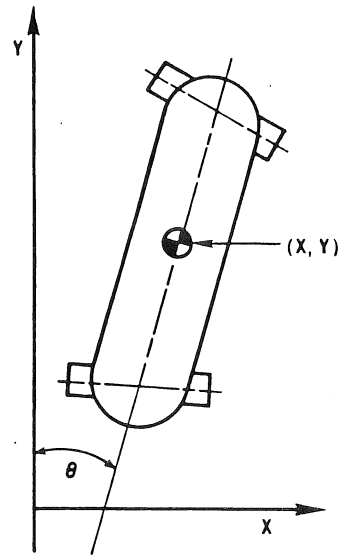

Figure 2. Top view of skateboard and definition of tracking tasks.

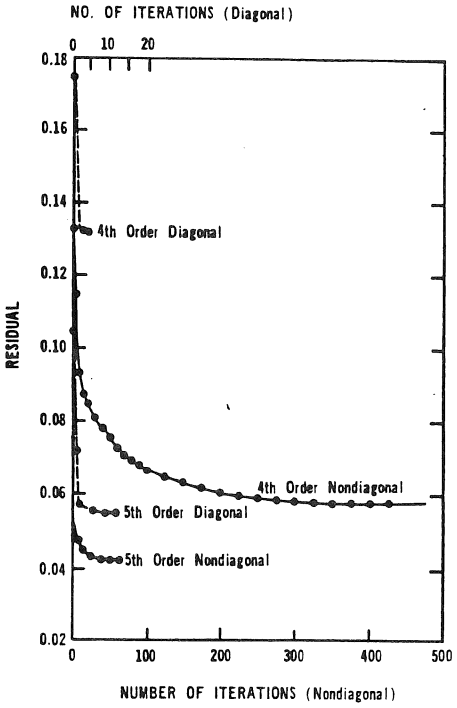

Figure 3. Residual versus iteration number for four cases.

MEASUREMENTS OF THE ROTATIONAL FRICTION OF COURT SHOES ON AN OAK HARDWOOD PLAYING SURFACE

G.A. Valiant
NIKE Sport Research Lab
9000 SW Nimbus Ave.
Beaverton, OR 97005

L.B. Cooper
T. McGuirk

NIKE Sport Research Laboratory

INTRODUCTION

A physical test is described that is capable of measuring the rotational traction characteristics of different combinations of athletic shoes and playing surfaces. Examples of the use of the device to measure resistance to rotation in different court shoes are presented. Findings are compared to results from measurements made as a subject pivoted on a force platform while wearing the test shoes. A linear relationship was found between free moment of rotation and normal load, and suggestions concerning the use of this relationship to quantify traction characteristics of sport shoes are made.

REVIEW AND THEORY

It is generally assumed that low resistance to rotation about a vertical axis passing through the forefoot is desired in order to protect an athlete's knee joint from high rotary forces that can be transmitted to the leg if the shoe is not free to rotate on the playing surface. This is particularily true in sports performed on natural or artificial turf while wearing cleated shoes (Torg and Quedenfeld, 1974), but this requirement is also a consideration in court sports.

METHODOLOGY

A traction testing device was constructed to evaluate the rotational friction characteristics of athletic shoes. The device incorporates a 6 degree of freedom force measuring platform. A footform is inserted into a test shoe such that the anterior 44% of the outsole rests flat on the test surface. A steel shaft supported by an external frame is pinned to the footform in the location corresponding to the 1st and 2nd metatarsal heads. The shaft can be loaded with a stack of steel weights. A rotary actuator spins the shaft through 125 degrees, thereby rotating the shoe on the playing surface. The force platform measures the vertical force acting against the playing surface and the free moment of rotation about a vertical axis passing through the forefoot region of the shoe.

Six different court shoes were tested in a counter-clockwise direction at 3 different normal loads on an oak hardwood floor surface. Tests were also made with a sport sock covering the footform. The shoes were tested in a random order, and for each shoe, the normal load and the trial number were randomly presented. Two to four trials were conducted for each combination of conditions.

In addition to these measurements, the free moment of rotation and the vertical ground reaction force were measured while a 655 N subject performed 180 degree pivots wearing the 6 different shoes and balanced on one leg on a force platform covered with the same oak hardwood surface. These rotations were also counter-clockwise.

RESULTS

An example of the free moment measured by the traction testing device is shown in Figure 1. The torque (Mz) attained a value of 20 N-m within 200 ms after initiation of movement. Figure 2 contains the mean value of torque for each of the 7 conditions, measured at 3 different normal loads. The torque increases linearly with normal load. The dashed portion of the straight lines represents an extrapolation of Mz to an unloaded condition. These dashed lines meet the ordinate between 1 and 4 N-m.

An example of the free moment and the vertical reaction force measured while a subject pivoted in a shoe is shown in Figure 3. Before movement of the shoe occurs, a moment is generated in the opposite direction as the subject develops sufficient angular momentum with the upper body to complete the 180 degree spin. The normal load fluctuates about body weight during the rotation, decreasing at the initiation of the spin, and then increasing in the later stages as the rotation comes to an end. The vertical force is observed to be decreased by about 10% at the time of peak torque.

The mean Mz values measured while a subject pivoted in each shoe condition are plotted in Figure 2 at a normal load equal to 0.9 BW. The range of values are 3 to 6 N-m lower than the interpolated values from the traction testing device at a corresponding normal load, as shown by the shaded boxes in Figure 2.

In Figure 4 the shoe conditions are ranked in ascending order according to the rotational resistance measured at the 597 N load. The rotational resistance measured when a subject pivoted on a force platform in each of the conditions is also shown in Figure 4. Except for shoe #3, the order of ranking of the shoe conditions is exactly the same.

DISCUSSION

Repeat measures of rotational resistance of different shoe outsoles made by the traction testing device described in this paper were within 5% of each other for all but one of the shoes. Due to the dependence on the nature and condition of the interacting surfaces, the characterization

of frictional forces is largely an empirical process. As such, the determination of friction forces with an accuracy of better than 5% is often difficult.

A nonzero value for Mz is determined for zero normal loads. This value may be a reflection of the friction in the bearings that support the shaft and thus offer resistance to rotation about a vertical axis. These extrapolated values for torque range between 1 - 4 N-m, which is close to the amount that the free moment values measured by the traction testing device exceed the measures made when a subject pivots in the same shoes on a force platform. By making a correction in the free moment results to account for bearing resistance, the two measures used to evaluate the turning resistance of the different shoes become very close.

It appears that the described traction testing device has merit in the evaluation of turning resistance. With this device, it is easier to maintain constant testing conditions. Tests at different normal loads can easily be made. There is less fluctuation in the normal loading when compared to subject initiated pivots. Turning motions from different sports can be closely simulated under many different conditions without the fear of subject injury. Although not discussed in this paper, the same device can also be used to make translational friction measurements.

Due to the linearity of the data in Figure 2, the slope of the line relating free moment to normal load may be used to characterize a shoe's resistance to rotation. If some variable which had units of length were used to multiply the normal load variable along the absicca, then the slope becomes a dimensionless quantity that characterizes rotational resistance in much the same way that static and kinetic coefficients characterize translational friction. A possible candidate for such a variable could be the radius of the outsole measured from the point about which the shoe rotates.

The shoes tested in this study did not differ very much in their rotational friction characteristics. The outsoles of all of the shoes were made of a similar rubber compound, except for shoe #2, which had a PU outsole. The outsole tread pattern in the forefoot of shoes #1 - 4 was a concentric circle pattern. Outsoles for shoes #5 and 6 had a herringbone-type pattern with shoe #6 also having a small circular patch in the forefoot. It is likely that the material out of which an outsole is composed has the greatest effect on friction. The large difference in friction when comparing the rubber outsoles and the sport sock support this contention. Thus, the concentric circle patterns of the 1st four shoes result in only a small decrease in the rotational resistance.

REFERENCES

Rheinstein et al. Medicine Sci. Sport and Exercise, 10(4): 282-288, 1978

Schlaepfer et al. Biomechanical Aspects of Sport Shoes and Playing Surfaces, 153-160, 1983

Torg et al. Research Quart, 42(2): 203-211, 1974

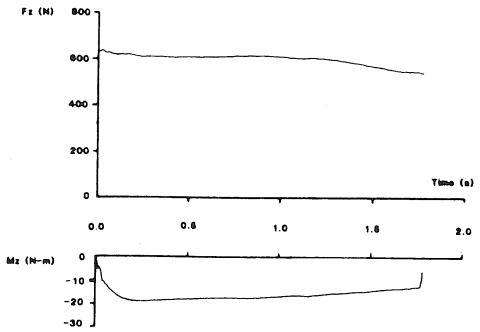

Figure 1. Free moment of rotation and normal force measured on shoe #5 at 597 N.

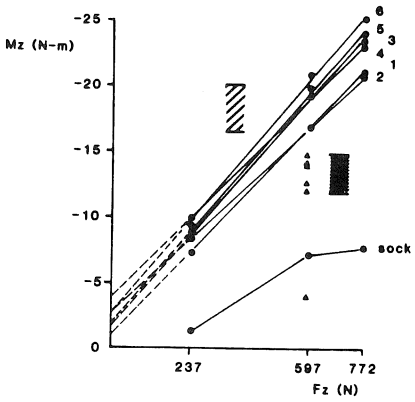

Figure 2. Mean values for Mz as a function of Fz measured on the traction tester.

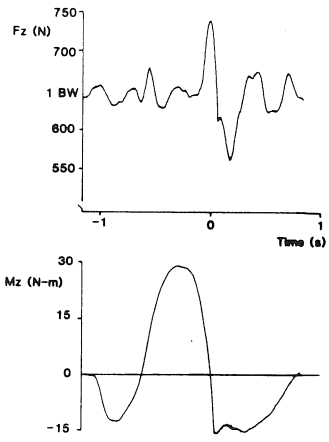

Figure 3. Example of Mz and Fz during a pivot on the force platform in shoe #5.

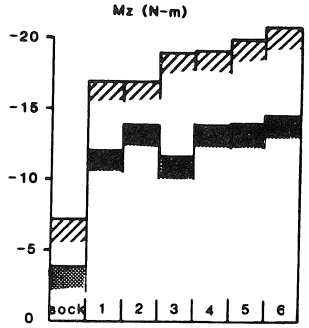

Figure 4. Mz of different shoes determined by a pivot on the force platform and by the traction ester with a load of 597 N.

THE USE OF AUGMENTED FEEDBACK TO MODIFY PEDALLING MECHANICS

DAVID J. SANDERSON AND PETER R. CAVANAGH

BIOMECHANICS LABORATORY, THE PENNSYLVANIA STATE UNIVERSITY, UNIVERSITY PARK, PA 16802

INTRODUCTION

On-line computer representation of forces applied to the pedals were used to train a group of cyclists to modify their pattern of force application. Eight cyclists were instructed to minimize the forces applied to the pedals during a 90-degree recovery segment beginning at a crank angle of 225 degrees after top dead center. The subjects rode for 32 minutes each day for 10 days. During these training rides, four cyclists were given feedback on only their pedalling rate, while four other cyclists were presented with feedback on their patterns of force application during the recovery segment as well as cadence. At the end of the training period, the experimental group showed significantly reduced recovery forces. Analysis of the pedalling mechanics of each individual showed that, while there was considerable variation in their response to the training, performance of a complex task can be modified by feedback of a biomechanical nature.

REVIEW AND THEORY

To use feedback of a biomechanical variable to modify a complex movement requires that the movement pattern be readily measured and controlled in the laboratory without major compromises to the actual event. Also required is the necessary equipment to measure the biomechanical variable continuously as the individual performs. Cycling is a good example of a skilled movement which statisfies these requirements primarily because of the limited degrees of freedom of movement available to the cyclist and also because of the reasonable similarity between steady-rate road riding and riding in a laboratory.

Typically, experiments on cycling have been done by modifying the bicycle and assuming that the cyclist can adjust to these modifications. As a motor skill, however, cycling provides a good opportunity to assess the efficacy of providing feedback to a subject arising from his pattern of motion. The feedback can be used to modify the pattern of motion and perhaps to enhance performance. However, there are a series of questions which arise from this theme. First, can feedback of real-time biomechanical data be implemented usefully? Second, if so, can the pattern of motion of cycling be modified?

The objective of this study was to attempt to train subjects to modify their pattern of force application to the pedals while riding at a steady power output. This was to be achieved by recording the pedal forces in real-time and using those forces to modify a graphic image visible to the riders in the experimental group but not to the riders in a control group. The systematic reduction of the time during which the feedback was visible would test whether the task could be assimilated via kinesthetic learning and retained after the feedback had been removed (as in the actual sporting event).

METHODOLOGY

The subjects were requested to modify the application of forces to the pedal during a 90-degree sector of the recovery phase while they rode at 60 RPM at a power output of 112 Watts. The sector of interest began at 225 degrees after top dead center (TDC) and extended to 315 degrees after TDC. The subjects (n=8) were volunteer males with an average age of 29 years. Each subject was assigned randomly to one of two groups: an experimental group and a control group. Each group had four members.

The apparatus used in this study was based on a 57.5 cm bicycle frame (Masi) mounted on a rigid platform. The crank was instrumented such that TDC for the right crank and continuous crank position could be recorded as an analog signal. Force measuring pedals were used to monitor left and right pedal angle relative to the crank, and left and right shear and normal components of the force applied to the pedals. The data were sampled by a 12-bit analog-to-digital converter at a sample rate of 100 Hz.

The visual feedback consisted of a graphics image, in the shape of a vertical bar, processed on the basis of the force applied to the pedals during recovery. The force data were sampled for five consecutive cycles. During the sixth cycle the program computed the mean resultant force applied by each leg during the 90-degree sector of the recovery phase. The average of the left and right legs was then computed and used to determine the height of the vertical bar which was then presented to the riders. These same data were collected for the control group, but there was no presentation of the image to them.

Each of the riding sessions lasted 32 minutes and were conducted over 10 days. Because it was important that the riders not become dependent upon the computer generated feedback, the time during which the feedback was visible was reduced gradually according to a fixed schedule which resulted in progressively less feedback over the 10 day period. Pre-test values were determined at the beginning of the first taining ride. Post-test values were recorded at the end of the last training ride and then again after a seven-day interval. During this interval the subject did no cycling.

RESULTS AND DISCUSSION

Figure 1 presents the mean of the left and right leg for each group over the complete training period. Statistical analysis indicated that the experimental group reduced the pedal forces significantly over the 10 days while the control group showed no significant reduction in pedal force. There was not a significant difference over the seven-day post-test interval between post-test 1 and post-test 2. There were no significant differences between the left and right legs.

These results indicated that the riders of the experimental group had successfully learned the new pattern of force application. That is, they were able to reduce the mean force during the 90-degree recovery sector. Further, they were able to maintain this in the post-test 1 without feedback and seven days later in the post-test 2. Thus, the augmented feedback served to assist the experimental group to idenfify

kinesthetic variables that were used to control the new pattern of force application. The control group subjects were unable to identify the same variables. It was notable that due to intragroup variation there were no significant statistical differences between the two groups even though the differences in the means were rather large.

Hobart and Vorro (1) and Landa (2) have shown that kinematic changes resulting from the acquisition of a novel motor skill occur within the very first few trials. The present data agree very well with these published works. It seemed that the biomechanical variable being used for feedback contained sufficient information that the desired response was relatively easy to identify. It would not be appropriate to conclude, however, that the new motor pattern had been completely incorporated and that subsequent days of rehearsal were totally unnecessary.

For the training procedures to have been considered successful, in biomechanical terms, it was necessary that the pattern of force application over the whole cycle be considered appropriate. The data presented in Figure 2 show this to be the case. The control group showed that they were able to reduce the pedal forces to only a limited extent in the sector of interest, whereas the experimental group showed a marked decrease in force in this region. The reduction in the force applied during the first 180 degrees of the pedal cycling for both groups was a function of the need to maintain a constant cadence and power output. The reduction in force in the recovery phase allowed the propulsion forces to be reduced. Thus, the cyclists in the experimental group were applying less overall force to achieve the same task after the training period.

The selection of which particular biomechanical variable to manipulate (zero recovery force) was made partially on what seemed appropriate in biomechanical terms and partially on the software/hardware capabilities of the system. Thus, the question of whether reduced pedal forces in the 90-degree sector of the recovery phase would truly result in better cycling economy remains unanswered. However, this project has provided a powerful training tool to help design an experiment to examine this and other such questions quantitatively. For example, an experimental group of cyclists can now be accurately trained to reproduce various non-standard force or motion patterns, and measurement of their metabolic costs could be compared to a similar control group to ascertain the overall desirability of these new patterns.

CONCLUSIONS

The data presented here illustrate the nature of the changes made by the experimental group in their pedalling mechanics. The experimental group reduced the recovery forces to a larger extent than the control group and specifically made these changes in the region of interest. Thus, in spite of the lack of specific information on timing, the visual feedback assisted the riders in the experimental group to focus on a region of interest and further augmented their kinesthetic learning and enabled them to retain this pedalling skill. The visual feedback contained enough implicit information to allow the experimental group as a whole to focus on the sector of concern, and in general to retain their skill even after the removal of the feedback.

REFERENCES

1. Hobart, J.R. & Vorro, D.J. Electromyographic analysis of intermittent modification during the acquisition of a novel throwing skill. In R.C. Nelson and C.A. Morehouse (Eds.), Biomechanics IV. International Series on Sport Science. Volume I, University Park Press, Baltimore, pp. 559-566, 1974.

2. Landa, J. Analysis of skill acquisition on a novel throwing task in terms of biomechanical factors. Journal of Human Movement Studies, 5, 52-60, 1979.

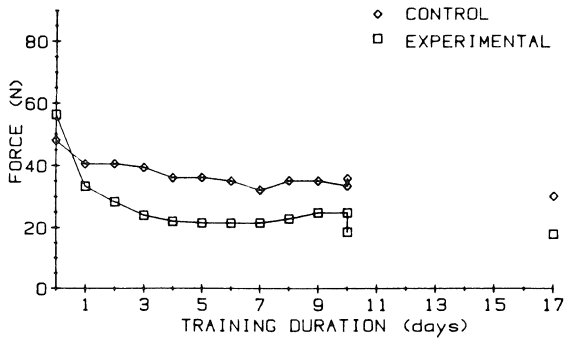

Figure 1. Mean resultant forces in the recovery segment averaged over the left and right legs for the control and experimental group over the whole testing period. The pre-test scores are plotted as day 0, the post-test 1 as the last connected point and post-test 2 are on day 17.

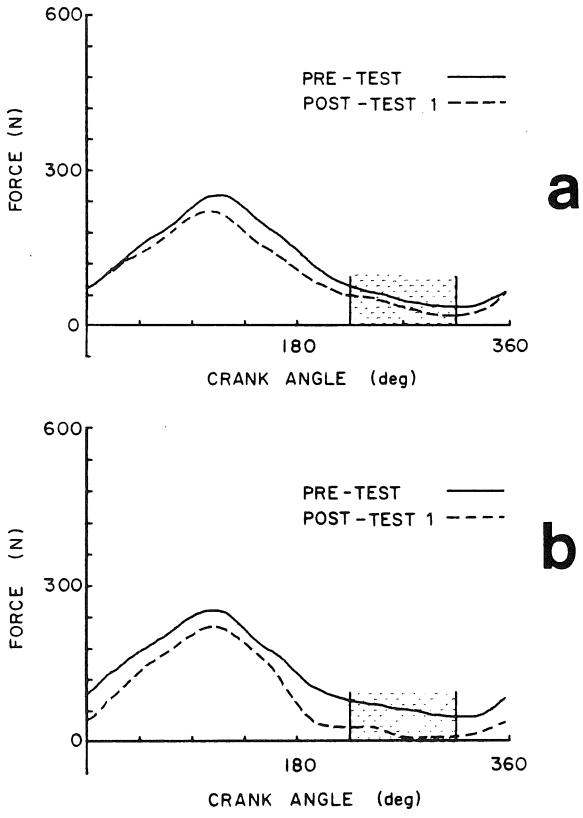

Figure 2. The resultant force crank-angle curves for (a) the control group and (b) the experimental group. For both groups, the pre-test and post-test 1 plots are presented.

THE KINEMATICS OF UPHILL AND DOWNHILL WALKING

J C WALL and J CHARTERIS*

School of Physiotherapy
Dalhousie University
Halifax, Nova Scotia
CANADA

*Department of Human Movement Studies
Rhodes University
Grahamstown
South Africa

INTRODUCTION

Although slopes are an everyday obstacle to walking, surprisingly few studies have looked at the locomotor changes that occur when people move from level to grade walking. A very extensive literature exists in which physiologists have manipulated the walking gradient while focussing on the determination of general equations for efficiency, or economy, or quantification of internal and external work, heat exchanges, energy flow between segments and the like. Some work by electromyographers has provided information relating to the 'firing' sequences of various muscle groups with gradient changes. To further an understanding of the adaptations to the temporal and angular gait kinematics gradient walking have been investigated and are the subject of this paper.

METHOD

Fifteen male and fifteen female subjects, all healthy young adults, were each walked on a motorized treadmill at five gradients; -20%, -10%, level, +10% and +20%, in order to study changes in the temporal and angular kinematics during uphill and downhill walking. The subjects were habituated (Charteris and Taves, 1978; Wall and Charteris, 1980, 1981) to treadmill walking at each of these grades. The subject's preferred walking speeds on each gradient were determined. The sequence of grades was randomized for each subject at each practice session and during the recording session.

The temporal patterns of foot/treadmill belt contact were measured using footswitches similar to those described elsewhere (Wall and Charteris, 1980). The signals from these footswitches were recorded on a strip-chart recorder, with respect to time. The chart recording was placed on a sonic digitizer plate and using this device the X-Y co-ordinates of the points of make and break of contact of each footswitch were entered into a microcomputer for processing and storage.

Five consecutive strides were analysed at each grade for each subject. The preferred walking speeds relative to stature ("relative speeds", in units statures.s^{-1}) were calculated, as were the means and standard deviations of stride time, stride length and velocity.

Five male and five female subjects were randomly selected from the group for a cinematographic study of the angular kinematics. Each of the subjects was filmed at 64 fps for four strides at each of the grades. During filming an event marker on the recorder was activated so that the two analysis techniques were synchronised. Activity clothing was worn by each of the subjects, enabling visible markers to be placed over hip, knee and ankle joints. The film was projected normally onto a viewing screen which incorporated a sonic digitizer. Using the digitizer pen, the X-Y co-ordinates of the joint markers were transferred to a minicomputer for storage and processing.
One stride was analysed at each grade for each subject. The analysis was carried out using data from all the frames exposed during the stride, measures being taken at intervals of 0.0156s. From these data the computer calculated the joint angles at 1% intervals of each stride.

RESULTS

The subjects in this study chose to adapt to increasing positive or negative gradients by marginally reducing their speeds, even when the absolute angulations of slope are as small as 6^{o} and 12^{o} from the horizontal. The extent of preferred speed reductions with increased positive or negative slope are practically indentical on either side of the level condition for each sex and virtually the same in extent between sexes. In the present study under all conditions the female group chose relative speeds (statures.s^{-1}) marginally faster than their male counterparts.

With increasing uphill slope under "preferred speed" conditions it was found that stride time increased and that an increasing percentage of stride time was spent in contact, at a rate of approximately 1% per 5^{o} incline. There was a decreasing percentage of stride time spent in single support (and therefore in swing) and an increasing percentage of stride time was spent in double support. Marginally slower speeds were selected as the incline increased from 0% to +10% gradient. Thereafter the rate at which preferred speed dropped increased. At + 10% gradient preferred speed was reduced by less than 4% of its level grade value, while at + 20% gradient it was reduced by less than 9% of its level grade value. The onset of heel-strike was later and the duration of toe contact longer.

With increasingly downhill slope under "preferred" speed conditions it was found that the temporal phases of the gait cycle were unaffected when compared to level walking. Cycle (stride) time decreased with decline walking (at a rate of 1% for every 5% gradient) in the range of grades investigated. Heel rise occurred earlier in the cycle and there was a shorter duration of toe contact.

When the thigh/knee interactions through the whole range of gradients from -20% to +20% are compared against the 0% standard, the downhill cyclogram is seen clearly as one of excessive knee flexion to cushion the impact of foot-contact as the quadriceps muscles, resisting gravity, have negative work done on them. During recovery the thigh is maximally flexed about half as much as in level walking.

Again, compared against the level walking standard, the uphill pattern is very different in overall form. Here the chief characteristic is one of excessive knee and thigh flexion at foot contact, a depressed cushioning reflected by an increase in knee flexion in early support (first 10% of cycle) and later, during swing, a relatively excessive flexion of both thigh and knee. It is the "compass" spread of the thighs in uphill walking and the greater extent of knee flexion for the first 40% and last 20% of cycle that characterises the uphill thigh/knee cyclogram.

DISCUSSION

This investigation was designed to study the kinematic effects of grade walking under conditions which were as natural as possible, and therefore of greater applicability to every-day settings. Thus the subjects were permitted a free choice of walking speeds. Strictly applied, our findings are relevant to kinematic variables at these non-controlled and variable "preferred speeds". A limitation of this design is that one cannot precisely ascribe what the component of speed differences is under the two conditions of positive and negative gradients. However the effect of this limitation was very slight: physiological and kinematic data routinely collected in our laboratories lends assurance to our view that the effects of uncontrolled speed in the present study were minimal. For instance, in a subject of 1.7m stature, walking at a velocity of 1.45 m/s the predicted VO_2 would be 15.29 ml/kg/min. whereas at 1.41 m/s predicted VO_2 would be 14.80 ml/kg/min; a small effect given usual expectations of a 5% or more intra-subject day-to-day coefficient of variation with respect to measures of locomotor economy. Our subjects chose to walk at marginally slower speeds as the gradient increased either positively or negatively. We are assured that the kinematic differences here reported can, for all practical purposes, be ascribed to differences in gradient not in walking speed. Certainly what is lost in precision of speed-control is more than compensated for, in our view, by the importance of our observation of the effect, on preferred-speed, of moderate (10% = 5.7 deg^0, 20% = 11.3^0) changes in gradient. These slight reductions in speed may be taken as unconscious expressions of perceived comfort.

Of major interest, in the context of our focal concern on the adaptive behaviour of pedestrians accommodating to slopes, was our finding that in a group of healthy young adults, all thoroughly habituated to treadmill walking and allowed free choice of speed with changing gradient, only very slight speed-adjustments were in fact made.

REFERENCES

Charteris, J. and Taves, C.

The process of habituation to treadmill walking. A kinematic analysis. Perceptual and Motor Skills 47: 659-666, 1978

Wall, J C and Charteris, J.

The process of habituation to treadmill walking at different velocities. Ergonomics 23 425-435, 1980

Wall, J.C. and Charteris, J.

A kinematic study of long-term habituation to treadmill walking. Ergonomics 24 : 531-542, 1981

ELECTROMYOGRAPHIC PATTERNS DURING VISUALLY PERTURBED GAIT

Andrew W. Smith
David A. Winter

Department of Kinesiology
University of Waterloo
Waterloo, Ontario N2L 3G1

INTRODUCTION

Normal human gait patterns result from a complex interaction not only between various elements within each individual, but between the individual and the environment as well. Vision, along with proprioceptive and vestibular inputs, provide the necessary feedback which shapes the observed gait patterns. The electromyogram (EMG), although variable within and between subjects, does provide a valuable estimate of the so-called "normal" neural drive to gait. It is reasonable, then, to consider alterations in EMG profiles due to systematic visual perturbations within subjects as being an indication of the influence of vision on gait. The purpose of the present study was to document EMG patterns while walking under five conditions of visual perturbation.

METHODOLOGY

Four female university students were subjects in this study. EMG data collection and analyses employed in this paper have been in use for ten years in the Gait Laboratory of the University of Waterloo and have been previously cited (2). Bipolar silver-silver chloride surface electrodes were used to gather data from the following seven muscles on each leg: gluteus maximus, rectus femoris, vastus lateralis, medial hamstrings, tibialis anterior, medial gastrocnemius, and soleus. Subjects walked in a straight line over a distance of approximately 15 m.

A normal trial and five perturbed conditions were collected for each subject. The perturbed conditions were: no exproprioception (1) (i.e., no view of one's own body), no central vision, no peripheral vision, and two trials with closed eyes, the second of which introduced a 10 s delay between the occlusion of sight and the initiation of walking. Subjects walked to a metronome set at the cadence of their normal trial. Thus, each subject was her own control. The number of strides of usable data ranged from 4 to 10 strides per leg for the four subjects.

Ensemble averages (EA) were calculated from the linear envelope (LE) EMG data. This technique involves normalizing each stride (i.e., heel contact to heel contact) to 100% of stride and calculating a mean and standard deviation at each 2% interval of the strides. Use of this technique allowed for comparison between conditions within each subject. In order to facilitate within-condition comparisons, the percent root mean square (%RMS) difference was calculated between any two stride LEs, or between the EA and each stride LE within the same trial. As well, each LE within any perturbed condition was compared to the EA of the control trial. These analyses were conducted in order to investigate the specific nature of the known variability of EMG with respect to this particular problem.

RESULTS AND DISCUSSION

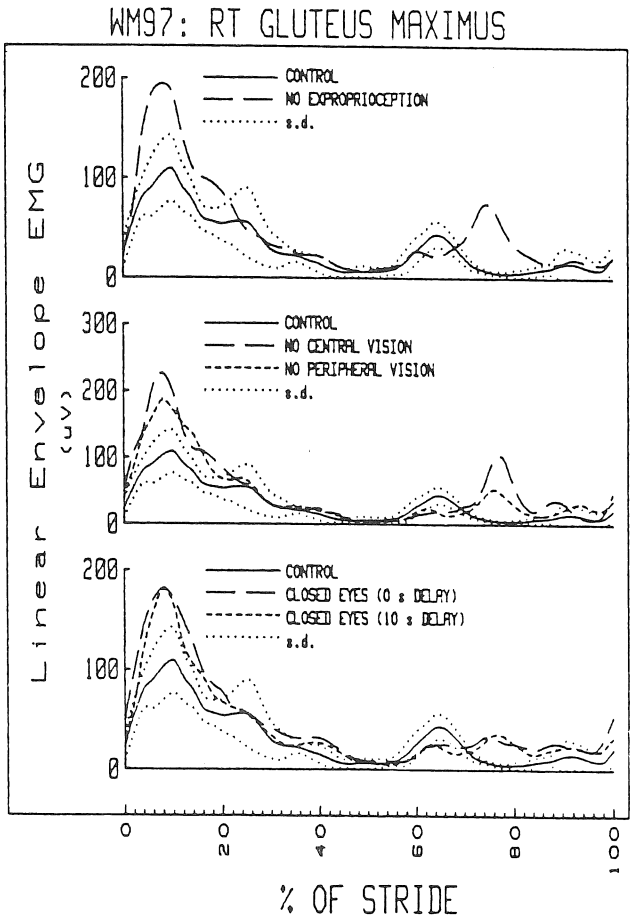

Figure 1: Linear Envelope EMG (EA)

Right gluteus maximus EMG patterns: Control EA vs perturbed EAs (WM97)

The analysis of these data was based on the tabular results of the %RMS analysis as well as visual assessment of the plotted EAs. Since the entire analysis procedure produced 56 EA plots and 336 tables of %RMS data, only

one example of each is included here (Figure 1 and Table 1).

General Trends

From a visual inspection of the plotted EAs, it was clear that, in general, most of the perturbed EAs were not noticeably different from that of the control trial. However, the means of the EAs as well as peak values showed certain trends. Two of the subjects (WM97 & WM98) showed a tendency for more activity in the left leg in the control trial. These two subjects showed different trends in the perturbed conditions in spite of a similar bias toward higher activity in that leg. For WM97, there was an overall increase in right leg activity and a decrease in the left leg. On the other hand, WM98 showed a clear increase in the dominant leg's EMG level and no real trend in the right leg.

Neither leg showed greater activity for the third subject (WM99). This lack of a dominant leg extended to the perturbed trials for this particular subject. Overall, for WM99, there was a slight decrease in activity across the five conditions.

A fourth subject (WL01) demonstrated a proximal muscle bias in one leg and a distal bias in the other in the control trial. With respect to the perturbed trials, in most cases, the proximal muscles demonstrated a trend toward increased activity, while the distal muscles remained largely unchanged. No muscle was consistent in all conditions, although several had similar responses in at least three of the five perturbed trials. This was true for both legs.

Specific Differences

In general, the %RMS analysis supported what the plotted EAs revealed in terms of the trend of change in the EMG levels. Taking WM97 as an example, the average %RMS difference between stride LEs within the control trial for all muscles ranged between 25% and 40%. When each stride LE within a given perturbation was compared to the control EA, the differences ranged from 20% to over 100%, averaging in the 35% to 50% area, depending on the muscle. Referring to Table 1, in the within-condition analysis, the column "A" lists the LE vs EA comparison for each stride, while the columns "B1" through "B8" contain the inter-stride LE comparisons, i.e., "B3" refers to the comparison between one LE and the subsequent third LE. In the between-condition analysis, these data show that the 7th stride LE demonstrated the largest deviation from the control EA (115%) while the smallest difference occurred with stride 4 (56%), which is still larger than the values in the within-condition analysis (column "A").

In order to ascertain whether the %RMS differences were due to random variations over the stride or due to a bias, mean differences were calculated between each perturbed stride LE and the control trial EA. With no bias, the %RMS averaged about 30%. If the plot revealed an obvious decrease or increase in the EMG activity, the %RMS would be somewhat higher than 30% and the average mean difference would be less than 0 (decrease) or more than 0 (increase).

Table 1: %RMS ANALYSIS

RMS Analysis for WM97 Right Gluteus Maximus: No Exproprioception (strides=9)

WITHIN-CONDITION ANALYSIS (%RMS)

S	A	B1	B2	B3	B4	B5	B6	B7	B8
1	23	30	41	32	26	40	33	26	40
2	31	37	38	28	43	43	36	46	
3	27	35	32	40	59	38	30		
4	24	38	42	52	36	33			
5	18	40	41	23	33				
6	29	41	40	37					
7	32	33	43						
8	20	27							
9	29								

S = stride number
A = compares S to trial ensemble average
Bn = compares S to stride S+n

BETWEEN-CONDITION ANALYSIS (%RMS)
Perturbed LE vs Control EA

S = 1	2	3	4	5	6	7	8	9
93	108	71	56	84	87	115	77	57

OBSERVATIONS

From these data, it can be seen that two general observations can be made with respect to the influence of vision on EMG in gait. First, it appears that subjects not only exhibit different bias patterns in the muscles of the lower extremity during normal walking, but as well, they demonstrate characteristically different patterns of change in EMG activity under various visual conditions. Second, in light of the lack of noticeable differences in the data, it is likely that the alterations in human gait resulting from visual perturbations are quite subtle. The normally high variability in EMG probably masks the role vision plays in gait rather effectively. Measures with less inherent variability, such as joint torques and powers, might provide more clear evidence of the effect vision has on human locomotion.

References

(1) Lee, D.N. Scand. J. Psych. 18:224-230, 1977.
(2) Winter, D.A. Arch. Phys. Med. 65:393-398, 1984.

The authors acknowledge the financial support of MRC Grant MT4343 and NSERC Grant A2917, and the technical assistance of Mr. Paul Guy.

THE GAIT OF PACERS

B. D. Wilson, R. J. Neal,and S. Groenendyk*
Departments of Human Movement Studies and Veterinary Surgery*
University of Queensland, Brisbane, Australia.

INTRODUCTION

A number of studies have been conducted to characterise the gait of Standardbred pacers during racing, at different pacing speeds and on different speed tracks. The relationship between conformation and pacing gait has also been investigated. All pacers studied were three or more years of age and were in training for weekly racing. Animals were filmed while pacing in full harness along the home straight on a flat allweather track surface. Digital analysis of high speed cine film for a single stride cycle was used to determine stride length and timing characteristics of gait. Correlations for length and timing measures between consecutive strides were above r = 0.94 for length measures and above r = 0.92 for timing measures, except for near double support (r = 0.85), indicating a consistency of stride characteristics over consecutive strides.

STUDY 1

Twenty pacers were studied under race conditions to describe the gait of the pacer, and to determine whether differences in selected gait kinematics exist for lap or stage of the race, for low or high order finishing pacers. ANOVA on lap by finish order wass used on each of the length and timing variables to distinguish between groups. Cluster analysis (1) was used to describe the movement sequence and timing of variables. Stride lengths of the order of 6.7 m and stride times of 450 ms were recorded for pacing speeds of 15 m/s. The double support period of stance increased with the stage of the race while pacing speed decreased marginally for low order pacers and increased for high order finishers. High order pacers appear to have greater stance and stride lengths than do low order finishers. Pacers could be seperated into low order and high order groups on the basis of their movement patterns. High order pacers exhibited greater ranges of limb motion than did low order finishers.

STUDY 2

Sixteen pacers were studied pacing at four different nominated speeds, 2:20, 2:10, 2:05 (min:sec) and fastest pace, to determine factors which contribute to pacing speed. A deterministic model is proposed in which pacing speed is a function of stride length and timing variables (Figure 1). For a 22% increase in pacing speed the following changes in gait were observed: A 13% increase in stride length; a 26% increase in flight distance; an 8% increase in stride frequency; 35% and 16% increases in contact and lift off single support times; and a 23% decrease in the period of double support. Stance length and flight time remained relatively constant over the different pacing speeds. Variables which best discriminated between pacing speeds were flight length and double support time. At near maximal speed animals paced at increased speeds with an increased stride length (Figure 2). This increase in speed was attributed to an increased flight length with little difference in flight times.

STUDY 3

A further study compared the gait of the 16 pacers on a slow track with that of 17 pacers on a fast track for a similar range of nominated speeds. ANCOVA on stride length and timing variables, with pacing speed a covariate within pacing speeds, was used to determine if differences existed between gaits on different tracks. On the slow track pacing speeds ranged from 9.4 to 16 m/s while stride length ranged from 5.1 to 7.8 m and stride frequency ranged from 1.8 to 2.4 Hz. On the fast track, pacing speeds ranged from 7.9 to 16.9 m/s while stride length ranged from 4.2 to 6.8 m and stride frequency ranged from 2.0 to 2.6 Hz. Similar pacing speeds were achieved on the fast track with shorter stride lengths and higher stride frequencies than on the slow track (Figure 3). Flight length was shorter and double support times were less as a percentage of stride time, on the fast compared to the slow track. The decrease in the double support as a percentage of stride time is consistent with an increase in the efficiency of movement as each limb makes its own contribution to the energy storage and propulsion of gait.

STUDY 4

In the final study in this series, the standing conformation of 29 pacers was measured directly and by digital analysis of saggital plane photographs of the standing animal. Of 23 measures used to define standing conformation, only 10 could be reliably determined on a seperate test occasion. Canonical correlation analysis was used to determine the relationship between standing conformation and gait kinematics. Results indicate that animals with functionally long fore limbs, as predicted from high scores on the conformation variables of wither height, shoulder height, and fore pastern length, were able to achieve long flight lengths and thus were likely to be able to pace at higher speeds than their short limbed counterparts.

These studies were completed with the financial assistance of the Australian Equine Research Foundation.

References

1. Wilson, B. D. and Howard, A. Movement pattern recognition in the description and classification of the backstroke swim start. J. Human Mvt. Studies 9:71-80.

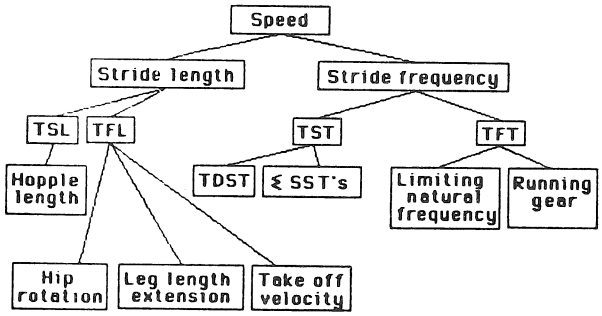

Figure 1. Deterministic model of factors contributing to pacing speed.

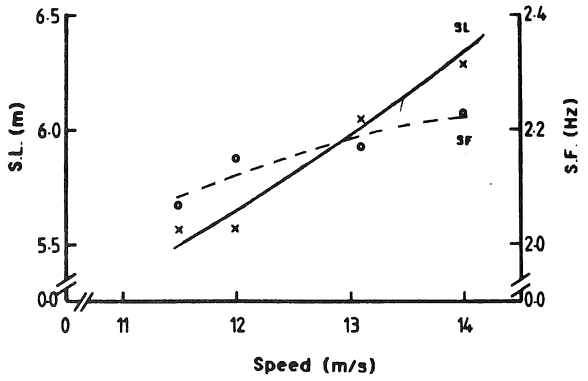

Figure 2. Mean stride length and mean stride frequency at selected pacing speeds.

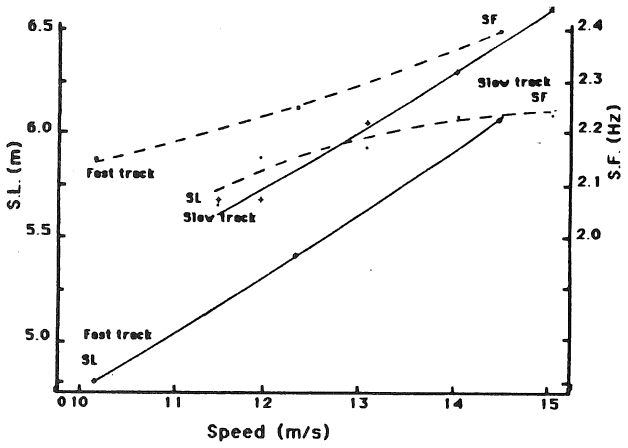

Figure 3. Mean stride length and mean stride frequency at selected pacing speeds on slow and fast tracks.

A PRELIMINARY STUDY OF THE TEMPORAL GAIT KINEMATICS OF AFRICAN OCCUPATIONAL HEADLOAD CARRIERS

J CHARTERIS, P A SCOTT AND J C WALL*

Department of Human Movement Studies
Rhodes University, Grahamstown

*School of Physiotherapy
Dalhousie University, Halifax,
Nova Scotia, Canada

INTRODUCTION

Head-loading is very widespread in the industrially developing countries of Africa, particularly among women, as a means of heavy load transporting. It's roots, however, are to be found in economy of effort, not cultural or ethnic tradition, for head-loading of one form or another is commonly practiced in Tibet, Nepal, the high Andes, Papua and across Africa, and, as Datta and Ramanathan (1971) have shown, it is one of the least energy expensive forms of load carriage, ahead of backpacking, back- and head-sling (Sherpa) loading, the shoulder yoke method, and bi-manual load carrying, which may surprise ergonomists working from within the perspective of the highly industrialised countries (see Wisner, 1985). Clearly millenia of arduous load bearing has resulted in this near-universal adoption of the least fatiguing feasible method of carrying akward loads. The efficiency of walking depends, in part at least, on the magnitude of the rise and fall of the centre of mass with each step and on the smoothness of the transition of this motion (Saunders et al., 1953). The greater the deviation from the normal movement of the centre of mass the less efficient will be the walk. This being the case, one would anticipate that the added burden of carrying a load would make this criterion even more critical. The fact that head-load carrying has been found to be physiologically efficient implies that the walking pattern should not be greatly different from normal. This paper reports the preliminary results of a study being undertaken in the Department of Human Movement Studies at Rhodes University to investigate the temporal gait kinematics of habitual head-load carriers in order to determine the extent of differences, if any, between the walking patterns in loaded and unloaded conditions.

METHODS

Four female occupational wood carriers walked both with and without head-loads along a walkway some 20m in length. In the loaded condition a bundle of firewood, 40% of body mass in weight and of an overall length equivalent to 160% of body stature, was carried on the head. Such a load is heavy and awkward but is typical of those carried by these women. Each subject traversed the walkway several times at walking speeds spanning the range from slow to fast for both the loaded and unloaded conditions. During each traverse data were obtained from footswitches which provided information on the parts of each foot in contact with the ground. The data from these footswitches were transmitted via a telemetry system (B and L Engineering) to a polygraph pen recorder. This instrument also recorded the signals from optical switches set at either end of the central 6m of the walkway over which data from the footswitches were collected. These signals allowed for the calculation of mean overall walking velocity. The data were reduced from the recording and input to a microcomputer for processing, analysis and storage.

RESULTS

The results of this study show that the gait pattern adopted by the head-load carriers was one of "minced" steps characterised by shorter cycle times and therfore higher cadences, and shorter stride lengths. When the duration of the phases within the stride were considered it was found that in the unloaded condition the patterns were as expected from normal populations from other studies. However, in the loaded condition although the trends expected with walking speed were maintained, the absolute contact times were unaffected. Because the raw contacts were unchanged and the head loaded cycle times were always shorter, it follows that under the loaded condition contact, in relative terms, was always longer as a percentage of stride time.

Thus the "minced" stepping pattern under headload is one in which swing time is not only shorter with the shorter step, but faster relative to the cycle as a whole. The reduced swing-to-support ratio under headload shows the basic overall pattern difference: in headload walking the mechanism is one in which the less stable single support phase is reduced, absolutely and relatively, and the more stable double support phases are increased. Since overall contact time is absolutely the same and relatively longer and single support is shorter it follows that the double support phases are absolutely and relatively longer.

Breakdown of the sequence of foot-to-floor contacts revealed how the "mincing" gait pattern was composed. At all speeds of headload walking the shock-absorbing phase, from heel-strike to foot-flat was significantly less than in unloaded walking: the same small pre-tibial muscles, working against a superincumbent load considerably closer to their maximal capacity, being less effective in cushioning the impact of heel-strike. Thus, in an absolute and relative sense with respect to total contact time, the braking mechanism becomes less effective under headloading; the foot-slap being earlier and sharper. However, one positive effect of this is that a greater surface area, that of the whole foot, is earlier posed to the walking surface, increasing stability and dissipating foot-floor pressure.

The foot flat phase (with at least heel and ball of foot in contact with the ground) was always relatively longer as a percentage of contact in the headload condition. This is especially significant since heel-rise occurs relatively earlier in the loaded condition. This earlier heel-rise implies that greater propulsive thrust is

required to move walker plus load, and that plantar thrust from the triceps surae may well cause an earlier than normal disengaging of the heel. It must be remembered that heel rise does not of itself mean that calf muscle propulsion (concentric contraction) is the cause; for the heel may disengage passively. However, the step is shorter under headload, so that the centre of mass is not far forward of the rear leg at this time, which argues against a passive heel-rise. It is more likely that heel-rise is absolutely and relatively earlier under headloading because of a greater eccentric priming of the triceps surae.

CONCLUSION

These preliminary results indicate that headload walking is a pattern in which there is a longer double support phase, a short quick swing phase and a smaller, faster, more "mincing" pace than is seen in the unloaded condition at the same overground velocities of walking. Under headloading the foot slaps down earlier than under normal walking conditions. The period of foot-flat between the "braking" and "propulsive" phases at each end of the contact period is longer under headloading. All these phenomena help to explain how balance is maintained and heavy loads are sustained by headload carriers.

The adaptations of headload carriers are complex and involve significant differences from normal walking; but these are always differences of degree, not of kind: patterns are accentuated or attenuated but not reversed or obliterated. Although the differences between normal and headload walking have been stressed, given the nature of the burden being moved in this study (both awkward to balance and heavy to bear), it is quite remarkable how "natural" the headload pattern is; and how stable the normal pattern of human locomotion is to be so little disrupted.

REFERENCES

Datta, S.R. and Ramanathan, N.L. Ergonomic comparison of seven modes of carrying loads on the horizontal plane. Eronomics 28: 269-278, 1971.

Saunders, J.B.de C.M, Inman, V.T. and Eberhart, M.S. The major determinants in normal and pathological gait. J Bone Jnt Surg 35-A: 543-558, 1953.

Wisner, A. Ergonomics in industrially developing countries. Ergonomics 28: 1213-1224, 1985.

ACKNOWLEDGEMENTS

The authors would like to acknowledge the financial support provided by Rhodes University in the form of a visiting fellowship to J.C.W.

A COMPARISON BETWEEN FORWARD AND BACKWARD WALKING

B.T. Bates and S.T. McCaw
Biomechanics/Sports Medicine Laboratory
University of Oregon
Eugene, OR 97403, USA

INTRODUCTION

Recently backward locomotion has been suggested as an alternate form of training and a rehabilitative modality. If backward locomotion can be of value in these areas, then the mechanics of this form of gait need to be understood. The purpose of this pilot study was to describe the temporal and kinematic differences between walking forward and backward on both level terrain and uphill. The results indicate that some differences do exist and that backward locomotion is not simply a reverse pattern of forward motion. The observed differences appear to support the use of backward locomotion as a viable training aid and/or rehabilitative modality.

REVIEW AND THEORY

Traditionally, backward locomotion has been associated with sports played on a field or court or eccentric individuals interested in having their name in the Guinness Book of World Records. In sports such as basketball, football and tennis, short spurts of backward running are often part of a defensive maneuver. Some of the more interesting records include a 4 hr 7 min 54 s marathon by Scott Weilend and a 6 min 7.1 s mile and 133.5 km 24 hr walk by Donald Davis (McWhirter, 1984).

The use of backward locomotion as a training and rehabilitative modality has not yet received wide spread recognition. Most clinical support for its effectiveness is anecdotal. Some of the areas where it appears to be effective include post surgical knee rehabilitation, groin and hamstring injuries, low back pains and ankle sprains. In addition, claims have been made that it improves overall muscle balance and forms a stronger foundation thereby lessening the chances of injury.

METHODOLOGY

Two males volunteered as subjects. Four conditions were chosen for evaluation: forward level (FL), backward level (BL), forward uphill (FU), and backward uphill (BU). All testing was done on a treadmill to optimize film image size and control walking speed and grade. The grade used for the uphill conditions was 10^{o}. A walking speed (1.34 ms^{-1}) that could be comfortably maintained for all conditions was selected and each subject practiced walking on the treadmill for all conditions until he felt comfortable. Subjects were then filmed (75 Hz) from the side for a minimum of five complete strides and three consecutive steps were identified for analysis. Six anatomical landmarks were identified and digitized on the side of the body nearest the camera. The assumption was made that right vs. left side differences would be less than errors resulting from estimating landmark locations on the opposite side of the body.

Temporal and kinematic data describing trunk orientation as well as hip, knee and ankle joint angles were calculated for individual trials and then averaged for each subject condition. Since both subjects performed in a very similar manner only mean values are presented.

RESULTS AND DISCUSSION

Mean segment and joint angle values for selected positions are given in Table 1. Graphic comparisons of representative trials for selected conditions are presented in Figure 1. For all conditions, trunk movements were minimal with ranges of 4.6 to 5.2^{o}. The movement patterns were opposite resulting in a mirrored image of each other. Both forward conditions began with a slight backward rotation (2.0^{o}) followed by a larger forward rotation (4.6^{o}) and concluded with a second backward rotation (2.4^{o}). The FU condition always resulted in greater forward lean. The trunk positions for backward walking were always greater and behind the vertical most of the time. The actions consisted of a forward (2.4^{o}), backward (5.2^{o}) and second forward rotation (1.8^{o}). The BU condition exhibited slightly greater backward lean values.

The dominant movement patterns for the hip joint were opposite for forward and backward walking but similar for the level and uphill conditions. The forward stance phase consisted of extensor movement (47.7^{o} and 80.3%) with a reversal of direction (9.9^{o} and 19.7%) just prior to toe-off. Backward travel was characterized by a minimal amount of hip extension upon impact followed by hip flexion (28.8^{o} for 85.3%). The pattern was similar for BU but with considerably less flexion (16.6^{o} for 86.4%). Backward locomotion produced a mirrored image of forward travel with a reduced range of motion which was exaggerated in the uphill condition (34.8 vs. 67.6%).

Evaluation of ankle joint movements also showed opposite actions resulting in a similar mirrored image between the forward and backward conditions. FL walking was characterized by minimal plantarflexion following touchdown (1.3^{o} and 15.5%), a long period of dorsiflexion (12.0^{o} and 53.8%), and extensive plantarflexion just prior to take-off (26.8^{o} and 30.7%). The corresponding FU values were 4.2^{o} and 13.2%, 12.2^{o} and 32.2%, and 36.4^{o} and 54.6%. The backward patterns consisted of considerable dorsiflexion followed by a long period of plantarflexion and a second period of dorsiflexion during the final part of push-off. BL and BU values were quite similar and averaged 18.3^{o} and 12.8%, 25.9^{o} and 55.5%, and 11.6^{o} and 18.6%, respectively.

The greatest observed differences between the two forms of locomotion were observed for the knee joint. The forward pattern is well documented and consisted of a load accepting flexor period (17.4^{o} and 23.1%) followed by extension (22.4^{o} and 45.1%) and a second flexor period (43.6^{o} and 31.8%) prior to toe-off. Backward locomotion, on the other hand, consisted of the single extensor phase. The range of motion values for the first two phases of forward walking were 24.9 and 24.8^{o} for FL and FU, respectively. The corresponding values for backward

Table 1. Mean Segment and Joint Angle Values for Selected Positions

Segment/ Joint	Condition	Touch-down	Min	Max	Take-Off
Trunk	FL	88.3	86.0	90.6	88.2
	BL	93.5	89.8	95.0	92.6
	FU	85.8	83.0	87.6	85.2
	BU	93.4	91.7	96.8	95.6
Hip	FL	152.0	151.8	196.0	186.2
	BL	181.6	159.6	188.4	159.6
	FU	141.6	141.1	192.3	182.3
	BU	178.6	166.2	182.8	166.2
Knee	FL	177.5	157.2*	179.2	133.9
	BL	131.2	131.2	179.8	179.8
	FU	169.0	154.4*	182.1	140.0
	BU	121.2	121.2	178.2	178.2
Ankle	FL	94.7	84.0	110.2	110.2
	BL	93.2	73.2	97.8	85.8
	FU	87.8	79.8	116.2	116.2
	BU	87.6	71.0	99.8	88.5

All values given in degrees. FL = forward level, BL = backward level, FU = forward uphill, BU = backward uphill. *First minimum value within stance phase.

travel were 48.6 and 57.0^{o} .

Although no magnitude values were reported, the patterns of motion presented by Thorstensson (1) are similar to those presented in this study. Previous values reported by Bates et al. (2) for running also showed similar patterns but different magnitudes due to speed differences. Hip and knee joint range of motion values reported were 34.3 and 16.5^{o} and 30.7 and 40.7^{o} for forward and backward running, respectively.

CONCLUSIONS

Several important findings relative to the use of backward locomotion for training and/or rehabilitation were identified. First, there is a reduced range of motion at the hip joint and an increased range of motion at the knee joint. Second, the eccentric flexion phase of knee activity immediately following impact is eliminated resulting in continuous hip flexion with knee extension throughout the entire support period eliminating the possibilty of utilizing elastic energy stored in the muscle. Third, maximum knee extension occurs late in the support period when the hip is maximally flexed resulting in a greater stretch of the hamstring muscles. Finally, the foot strike pattern for backward walking is always toe-heel altering the impact force characteristics. These findings appear to support the use of backward locomotion as a viable training and/or rehabilitative modality.

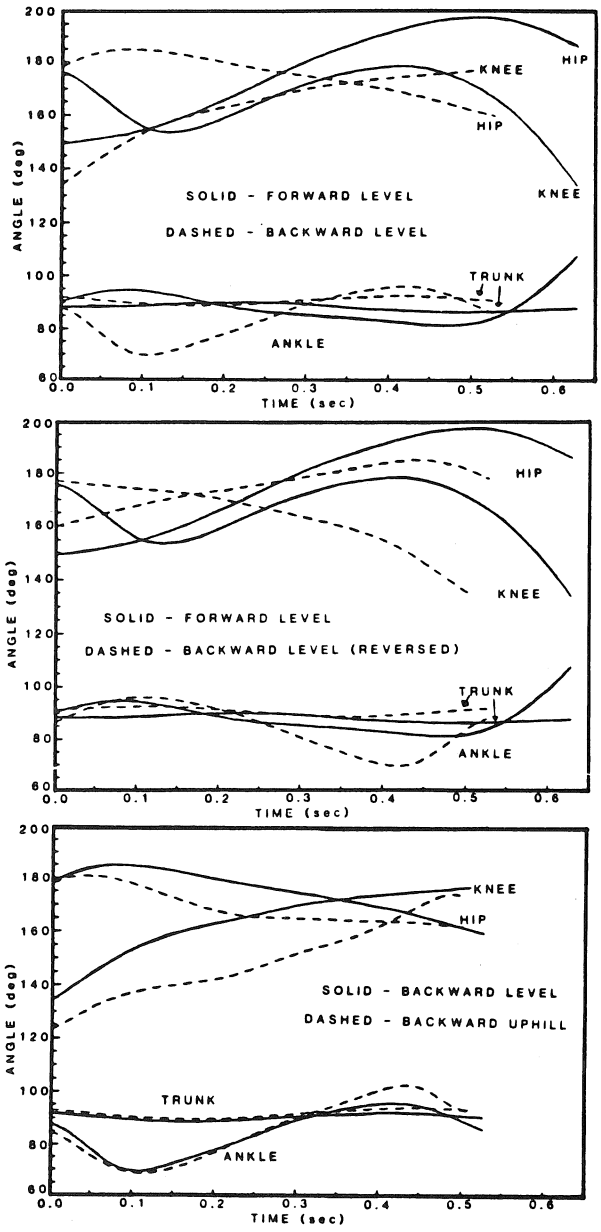

Figure 1. Representative segment positions and joint angle data for selected conditions.

References

1. McWhirter, N. Guinness Book of World Records, 1984.
2. Thorstensson, A. How is the Locomotor Program Modified to Produce Backward Walking? Experimental Brain Research (In Press).
3. Bates, B.T., et al. A Comparsion Between Forward and Backward Running. Olympic Scientific Conference Proceedings (In Press).

Index List of Contributors

* Bold characters refer to pagination of volume II

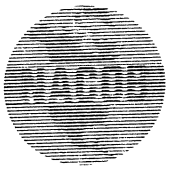

* Bold characters refer to pagination of volume II

* Bold characters refer to pagination of volume II

List of Exhibitors

Advanced Mechanical Technology, Inc.
141 California Street
Newton, MA
USA 02158
(617) 964-2042

Chattecx Corporation
101 Memorial Dr.
P.O. Box 4287
Chattanooga, TN
USA 37405
(615) 870-2281

Holt, Rinehart and Winston
of Canada Ltd
55 Horner Avenue
Toronto, Ontario
Canada M8Z 4X6
(416) 255-4491

Intertechonology, Inc.
3675 Blvd. des Sources, Suite 105
Dollard-des-Ormeaux, Québec
Canada H9B 2T6
(514) 683-0930

Kistler Instrument Corporation
75 John Glenn tr.
Amherst, NY
USA 14120
(716) 691-5100

The Langer Biomechanics Group Inc.
21 E. Industry Court
Deer Park, NY
USA 11729
(516) 667-1200

Northern Digital
415 Phillip Street
Waterloo, Ontario
Canada N2L 3X2
(519) 884-5142

Oxford Metrics, Inc.
14206 Carlson Circle
Tampa, FLA
USA 33625-2803

Selspine AB
Selective Electronic, Inc.
1233 Chicago Road
Troy, MI
USA 48083

Extraneous Activities

ISB Council Meeting

Working group on the definitions, terms and conventions for use in research of humain gait (Joint effort of CSB and ISB).

Acknowledgements

The Organizing Committee of the North American Congress on Biomechanics acknowledges the generous support of the following institutions:

DÉPARTEMENT D'ÉDUCATION PHYSIQUE
UNIVERSITÉ DE MONTRÉAL

CANADIAN HOWMEDICA, LTD

NATIONAL SCIENCES AND ENGINEERING
RESEARCH COUNCIL OF CANADA

EMPLOYMENT AND IMMIGRATION CANADA